Copyright Warning & Restrictions

The copyright law of the United States (Title 17, United States Code) governs the making of photocopies or other reproductions of copyrighted material.

Under certain conditions specified in the law, libraries and archives are authorized to furnish a photocopy or other reproduction. One of these specified conditions is that the photocopy or reproduction is not to be "used for any purpose other than private study, scholarship, or research." If a, user makes a request for, or later uses, a photocopy or reproduction for purposes in excess of "fair use" that user may be liable for copyright infringement,

This institution reserves the right to refuse to accept a copying order if, in its judgment, fulfillment of the order would involve violation of copyright law.

Please Note: The author retains the copyright while the New Jersey Institute of Technology reserves the right to distribute this thesis or dissertation

Printing note: If you do not wish to print this page, then select "Pages from: first page # to: last page #" on the print dialog screen

ABSTRACT

ACCOUNTING FOR MIDBLOCK PEDESTRIAN ACTIVITY IN THE HCM 2010 URBAN STREET SEGMENT ANALYSIS

by
Albert Forde

The Urban Street segment analysis Chapter of the 2010 Highway Capacity Manual (HCM 2010) provides a methodology for analyzing automobile performance on signalized roadway segments within an urban roadway network. The methodology involves applying a platoon dispersion model to: a) predict the vehicle arrival flow profiles at a downstream signalized intersection; b) use the predicted arrivals to compute the proportion of vehicle arrivals on green; and c) subsequently estimate the delay, travel speed and Level of Service (LOS) under which the segment operates. Vehicles arriving during the red interval at a signalized intersection generally accumulate and form a platoon. When the signal turns green, the platoon of vehicles is discharged from the upstream intersection to the downstream intersection. As vehicle speeds fluctuate, the platoon will disperse before it arrives at the downstream intersection. This is called *Platoon dispersion.* Notwithstanding its importance and application in evaluating the performance of urban roadway segments, the predictive ability of the HCM 2010 platoon dispersion model under friction and non-friction traffic conditions has not been evaluated. Friction traffic conditions include midblock pedestrian activity, on-street parking activity, and medium to high truck volume. Furthermore, one key limitation of the methodology for evaluating automobile performance on urban street segment is that it does not account for the delay incurred by platoon vehicles due to pedestrian activity at midblock (or mid-

segment) crosswalks Therefore, the first objective of this research is to evaluate the predictive performance of the HCM 2010 platoon dispersion model under friction and non-friction traffic conditions using field data collected at four urban street segments. The second and primary objective is to develop an integrated deterministic-probabilistic (stochastic) model that estimates the delay incurred by platoon vehicles due to midblock pedestrian activity on urban street segments.

Results of the statistical model evaluation show statistically significant difference between the observed and predicted proportion of arrivals on green under traffic. The results, however, show no statistically significant difference between the observed and predicted proportion of vehicle arrivals on under no traffic friction condition. In addition, the developed delay model was validated using field measured data. Results of the statistical validation show the developed midblock delay model performs well when compared to delays measured in the field. Sensitivity analysis is also performed to study the relationship between midblock delay and certain model parameters and variables. The model parameters are increased and decreased by 50% of their baseline values.

ACCOUNTING FOR MIDBLOCK PEDESTRIAN ACTIVITY IN THE HCM 2010 URBAN STREET SEGMENT ANALYSIS

by
Albert Forde

A Dissertation
Submitted to the Faculty of
New Jersey Institute of Technology
In Partial Fulfillment of the Requirements for the Degree of
Doctor of Philosophy in Transportation

John A. Reif, Jr. Department of Civil and Environment Engineering

May 2015

APPROVAL PAGE

ACCOUNTING FOR MIDBLOCK PEDESTRIAN ACTIVITY IN THE HCM 2010 URBAN STREET SEGMENT ANALYSIS

Albert Forde

Dr. Janice Daniel, Dissertation Advisor — Date
Associate Professor of Civil and Environmental Engineering, NJIT

Dr. Steven Chien, Committee Member — Date
Professor of Civil and Environmental Engineering, NJIT

Dr. Ronfang Liu, Committee Member — Date
Associate Professor of Civil and Environmental Engineering, NJIT

Dr. Athanassios Bladikas Committee Member — Date
Associate Professor of Mechanical and Industrial Engineering, NJIT

Dr. Jian Yang, Committee Member — Date
Associate Professor of Management Science and Information Systems, Rutgers

BIOGRAPHICAL SKETCH

Author: Albert Forde

Degree: Doctor of Philosophy

Date: May 2015

Undergraduate and Graduate Education:

- Doctor of Philosophy in Transportation
  New Jersey Institute of Technology, Newark, New Jersey, 2015

- Master of Science in Transportation
  New Jersey Institute of Technology, Newark, New Jersey, 2009

- Bachelor of Science in Civil Engineering
  Fourah Bay College, University of Sierra Leone, Sierra Leone, West Africa, 2005

Major: Transportation

Presentation:

Forde, A. and Daniel, J., Evaluating the HCM 2010 Platoon Dispersion Model for Midblock Friction and Non-Friction Traffic Conditions. *Transportation Research Board* 94th Annual Meeting, Washington, D.C., 2015.

This dissertation is dedicated to my dad (R.I.P), who inspired me to study engineering

ACKNOWLEDGMENT

I thank my dissertation advisor, Dr. Janice Daniel, for her dedication, insight, motivation and guidance. I also thank her for her confidence in me to achieve a PhD. I'd also like to thank my dissertation committee members: Dr. Athanassios Bladikas, Dr. Steven Chien, Dr. Rongfang Liu, and Dr. Jian Yang. To my fellow graduate students, thank you for walking with me on this journey, Yang He and Yuanyuan Fan. Without the support of my family, I would never have pursued and completed a doctorate. My parents, Prince (R.I.P) and Maya, my sister Nyanda , my brothers Lawrence and Arthur, thank you so much for your love and encouragement. I also appreciate support from the New Jersey Institute of Technology.

TABLE OF CONTENTS

TABLE OF CONTENTS
(Continued)

TABLE OF CONTENTS
(Continued)

CHAPTER **Page**

TABLE OF CONTENTS
(Continued)

CHAPTER **Page**

LIST OF TABLES

LIST OF TABLES
(Continued)

LIST OF TABLES
(Continued)

LIST OF FIGURES

LIST OF FIGURES
(Continued)

LIST OF FIGURES
(Continued)

LIST OF FIGURES
(Continued)

LIST OF FIGURES
(Continued)

LIST OF FIGURES
(Continued)

CHAPTER 1

INTRODUCTION

1.1 Background

The Urban Street Segment Analysis Chapter of the 2010 Highway Capacity Manual (HCM 2010) describes four methodologies for evaluating the performance of an urban street segment. Each methodology addresses one possible travel mode within the street right-of-way. The four travel modes include: Automobile mode, Transit mode, Pedestrian mode, and Bicycle mode. The methodology on automobile mode evaluates urban street segment performance from the motorist`s perspective. The methodology involves estimating three performance measures for a segment travel direction. These performance measures include: Travel speed, Stop rate, and Automobile traveler perception scores. The methodology on pedestrian mode evaluates urban street segment performance in terms of its service to pedestrians. The methodology estimates three performance measures: pedestrian travel speed, average pedestrian space, and pedestrian Level of Service (LOS) scores for the link and segment. The Bicycle mode methodology evaluates the performance of urban street facility in terms of its service to bicyclists. The methodology is applied through series of three steps that culminate in the determination of the facility LOS. The steps include determining: bicycle travel speed, bicycle LOS score, and bicycle LOS. The Transit mode methodology evaluates the performance of an urban street facility in terms of its service to transit passengers.

The performance measures described above can be used to assess the performance of urban street segments, and provide insights on where improvements can be made to improve roadway operation. A key improvement to the 2010 HCM urban street segment methodology on automobile mode is the use of a platoon dispersion model to predict arrival flow profiles, and subsequently determining the control delay at a downstream signalized intersection and Level of Service (LOS) under which the segment operates. Vehicles arriving during the red interval at a signalized intersection generally accumulate and form a platoon. When the signal turns green, the platoon of vehicles is discharged from the upstream intersection to the downstream intersection. As vehicle speeds fluctuate, the platoon will disperse before it arrives at the downstream intersection. This is called *Platoon dispersion.* A key component of the HCM 2010 platoon dispersion model is a segment running time equation. The HCM 2010 segment running time equation, in its present form, estimates the running time based on the segment`s operational and geometric characteristics. The equation incorporates a component that accounts for other delays, d_{other}, which is described in the HCM 2010 as delay due to other sources along the segment(e.g. curb parking, pedestrian activity etc.) in s/veh . The manual, however, does provide specific values to adjust the segment running time for such delays. These delay values cannot be easily measured or estimated by users of the model. In addition to the platoon dispersion model, the HCM 2010 Urban Street analysis methodology also applies the segment running time in estimating the average segment travel speed. The HCM 2010 considers travel speed as a key measure of performance on urban street segment.

1.2 Urban Street Segment Defined

The 2010 HCM Urban Street Segment methodology builds on the methodology used in the HCM 2000. The term "urban street", as used in the HCM 2000, refers to urban arterials and collectors, including those in downtown areas. The HCM 2010 expands on this definition stating that an urban street is separated into individual elements that are physically adjacent and operate as a single entity for the purpose of serving travelers. Two elements are commonly found on urban street system: A *point* which represents the boundary between links and is represented by an intersection or ramp terminal, and a *link* which represents a length of roadway between two points. A link and its boundary intersection are referred to as a *segment.* Urban streets are also referred to as arterials or roads that primarily serve longer through trips; providing access to commercial and industrial land uses. Urban streets which are collectors provide both land access and traffic circulation within residential, commercial, and industrial areas. The access function of collector streets is more important than its importance on arterials, and unlike arterials, the operation of collector streets is not always dominated by traffic signals. Urban streets which are downtown streets are signalized facilities that often resemble arterials. In addition to moving through traffic, downtown streets also provide access to local business for passenger cars, transit buses, trucks, and parking vehicles (HCM 2000).

1.3 Overview of the HCM 2010 Urban Street Segment Analysis

The HCM 2000 presents a methodology for assessing mobility on an urban street and provides the basis for the HCM 2010 methodology. The degree of mobility is assessed in

terms of average travel speed for the through traffic movements. The average travel speed is then used as a service measure to determine the LOS. According to the Manual (2000), average travel speed is the basic service measure for urban streets performance. Significant changes occurred between the HCM 2000 and the HCM 2010 Urban Street Segment methodology. In both methodologies, travel speed is a function of the sum of segment running time and the control delay of through movements at signalized intersections. The HCM 2010 includes terms in the travel speed estimation to account for mid-block delays. In computing the control delay, a critical characteristic that must be quantified is the quality of the platoon progression. In the HCM 2000, the parameter that described this characteristic was the Arrival Type (AT). The HCM 2000 defines six types of platoon arrival flow, with Arrival Type 1 as the worst condition and Arrival Type 6 as the best condition. Arrival Type 1 is characterized by a dense platoon of more than 80 percent of the lane group volume arriving at the start of the red phase.. Arrival Type 6 is reserved for exceptional progression quality on routes with near ideal characteristics. It represents dense platoons progressing over several closely spaced intersections with minimal or negligible side street entries.

While the HCM 2000 uses Arrival Types to characterize platoon arrival flow, the HCM 2010 applies a platoon dispersion model to predict platoon arrival flow profiles at downstream signalized intersections. This is a key improvement made to the HCM 2000 and presented in HCM 2010. The 2010 urban street methodology considers the downstream platoon flow profile as a combination of three upstream traffic movements; cross-street right turn, major-street through, and cross-street left turn. These three arrival flow profiles are added to produce the combined platoon arrival flow profile. The arrival

flow profile is then used to compute the proportion of vehicle arrivals during the green phase. The Manual (2010), estimates the proportion of arrivals on green when the upstream intersection is signalized and coordinated with the downstream intersection. Otherwise, the proportion of vehicle arrivals is computed as the effective green to cycle length ratio. Once the proportion of arrivals on green is computed, the delay and LOS are subsequently estimated.

The HCM Urban Street methodology tries to capture the level of detail in estimating platoon arrivals on green as has been used in several simulation models. Two of these simulation models include TRANSYT-7F and CORSIM. TRANSYT-7F (**TRA**ffic **N**etwork **S**tud**Y** **T**ool) version 7F is a traffic software tool used primarily for signal timing design and optimization. It combines a detailed optimization process with a detailed macroscopic simulation model including platoon dispersion, queue spillback, and actuated control simulation. The platoon dispersion model used in TRANSYT-7F forms the basis for the platoon dispersion model adopted for use in the HCM 2010 Urban Streets methodology The ***COR***ridor ***SIM***ulation program which forms the core component of the simulation and modeling tool suite, Traffic Software Integrated System (TSIS), is an integration of two microscopic simulation model; NETSIM (***NET***work ***SIM***ulation) and FRESIM (**FRE**eway **SIM**ulation). NETSIM represents traffic on urban streets and FRESM represents traffic on freeways. As a microscopic simulation model, CORSIM does not have an explicit platoon dispersion model but simulates individual vehicle and driver behavior within a traffic stream. It simulates traffic operations based on a one second time step. That is, each vehicle is considered a distinct object which is moved each second.

1.4 Significance of Research

Urban streets typically serve multiple travel modes, in particular the automobile, pedestrian, bicycle, and transit modes. Travelers associated with each of these modes perceive the service provided to them by the urban street in different ways (HCM 2010). This research focuses on both the automobile and pedestrian modes. The methodology on automobile mode, as described previously, evaluates urban street segment performance from the motorist`s perspective. The methodology involves estimating the following performance measures for a segment travel direction: travel speed, stop rate, and automobile traveler perception score. The methodology on pedestrian mode evaluates urban street segment performance in terms of its service to pedestrian. The methodology estimates the following performance measures: pedestrian travel speed, average pedestrian space, and pedestrian level of service scores for the link and segment.

Several studies have been conducted on pedestrian activities at upstream signalized intersections and at midblock crosswalks on urban street segments. Gates et al (2006) conducted a study on pedestrian walking speeds for timing of pedestrian clearance intervals at several sites including but not limited to signal-controlled intersections with pedestrian signals (including two midblock crossings) and three un-signalized. Rastogi et al. (2011) conducted a parametric study of pedestrian walking speeds at midblock crossings based on certain factors, including but not limited to traffic volume, width of roadway, gender, age, pedestrian group size. In addition to studying pedestrian activities on urban street segments, other studies have been conducted on delay incurred by through vehicles traveling along a street segment. Bonneson (1998) developed a deterministic model for estimating the delays to major-street though drivers due to vehicles turning from the outside

through traffic lane on the major street. This maneuver can be in the form of a left or right-turn from the major street into a driveway. A modified form of the Bonneson(1998) model is incorporated into the HCM 2010 automobile methodology.

All of the studies described above, including the HCM 2010 methodology on automobile mode, do not account for the impact of pedestrian crossings at midblock crosswalks on platoon vehicles on urban street segment. Therefore, the significance of this research, is it primary goal of account for the impact of midblock pedestrian activity on platoon vehicles in the HCM 2010 methodology on automobile mode.

1.5 Problem Statement

In modeling platoon movement on urban streets/arterials, platoon dispersion models try to estimate the dispersion of a platoon as it travels to a downstream intersection from an upstream signalized intersection. These models typically estimate the arrival profile of vehicles at downstream intersections based on an upstream vehicle discharge profile and an average traffic-stream space-mean speed. Several studies have been conducted to study platoon dispersion. One of the first platoon dispersion models was a kinematic model developed by Pacey (1956).The model assumes that if the speeds of vehicles within a traffic stream are normally distributed, then the dispersion of the corresponding platoons can be described by the difference in speed of the vehicles. This phenomenon is called the *Diffusion Theory.* Robertson (1967)**,** also developed a recursive relationship to describe the dispersion of traffic. This relationship forms the core of the TRANSYT software, which is commonly known as TRANSYT-7F in North America. Robertson`s

platoon dispersion model has become a universal standard model and has been incorporated into other traffic-simulation software.

Platoon dispersion models typically model the movement of vehicles from an upstream intersection to a downstream intersection without external interruptions. However, in many urban areas, the dispersion of the platoon can be impacted by mid-block delays and stops. The HCM (2010) identifies the following as sources of mid-block delays:

- Vehicles turning from the segment into an access point approach,
- Pedestrians crossing at a mid-segment crosswalk,
- Vehicles maneuvering into or out of an on-street parking space,
- Double-parked vehicles blocking a lane, and
- Vehicles in a dropped lane that are merging into the adjacent lane.

Friction conditions, such as curb parking (on-street parking activity), transit bus operation, pedestrian mid-block crossings, and bicycles increase segment running time, consequently lowering the segment`s average travel speeds.. Another mode of transportation that interacts with automobiles is truck. Trucks are classified as heavy vehicles; they are longer and move much slower than other automobiles. Unlike on-street parking and mid-block pedestrian activities, trucks do not interrupt platoon movements at mid-segment. Rather, they interact with other vehicles within the traffic stream as they travel along the segment. On principal urban arterials with moderate to high truck volume, this interaction can be significant especially when a large proportion of the leading vehicles in the platoons are truck. Their slow movements increase the platoon arrival time and consequently increase the segment running time. On-street parking

activity interferences on urban street segments are typically due to platoon vehicles slowing to execute a parking maneuver, or parked vehicles pulling off from parking spaces. The HCM specifies a value of 18 seconds for the mean duration of parking maneuver in estimating the parking adjustment factor used in determining the saturation flow rate at the downstream intersection. As on-street parking intensity increase, the platoon arrival time and segment running time also increase the delay.

The interactions described above do impact platoon dispersion and arrival flow profiles at a downstream signalized intersection. The HCM 2010 methodology for evaluating the performance of automobile traffic traveling along an urban street segment does not provide an approach for evaluating urban street segments for some these factors or traffic conditions. This inability in the methodology is considered a limitation. A key limitation of the methodology for applying the platoon dispersion model and also for estimating the segment average travel speed is that it does not account for the impact on platoons due to mid-block pedestrian activity. In addition, despite its importance and application, the HCM 2010 platoon dispersion model has not been extensively studied to evaluate its ability to effectively predict vehicle arrival profiles at a downstream signal. For these reasons, there is a need to extensively evaluate the HCM 2010 platoon dispersion model; improve the HCM 2010 platoon dispersion model and segment average travel speed equation by incorporating into the segment running time equation develop a model that estimates the delay incurred by platoon vehicles due to pedestrian activity at midblock crosswalks on urban street segments.

1.6 Research Objectives and Scope of Work

The first objective of this research is to extensively evaluate the performance of the HCM 2010 platoon dispersion model under both friction and non-friction traffic conditions. The second objective is to develop an integrated deterministic-stochastic midblock delay model that estimates the delay incur by platoon vehicles due to midblock pedestrian activity on urban street segments. To achieve the research objectives, the following tasks were performed:

- Collected discharge and arrival flow data at four urban street segments under friction and non-friction conditions.
- Used the field data to determine the proportion of vehicle arrivals on green.
- Applied the HCM 2010 platoon dispersion model and procedure to estimate the proportion of arrivals on green using the geometric and operational characteristics observed at each site.
- Performed statistical analyses to determine significant differences between the field observed and the HCM 2010 estimated proportion of arrivals on green.
- Developed an integrated deterministic-stochastic midblock delay model
- Collected data on midblock pedestrian activity at two urban street segments in downtown Newark, New Jersey.
- Validated the developed midblock delay model using the field measured variables and parameters.
- Performed sensitivity analysis by varying certain parameters and analyze their relationship with midblock delay.

1.7 Organization of the Dissertation

This Dissertation is organized in seven chapters. Chapter 1 provides background information about platoon dispersion and the HCM 2010 platoon dispersion model and its application. The Chapter also provides brief information on the Urban Street Segment

analysis. The Chapter further presents the problem statement, the research objectives, and the scope of work that was performed. Chapter 2 presents a detailed review of some of the studies on platoon dispersion. It also reviews the urban street segment methodology used in the HCM 2010. The Chapter also reviews several studies on pedestrian activity on urban street segments with midblock and non-midblock crosswalks. The final section in this chapter discuses technique used in model validation. Chapter 3 describes the methodology for achieving the research objectives. The Chapter includes the theoretical models and description of the statistical approaches used in the research. Chapter 4 describes the field data collection sites and the techniques used in collecting data in the field. In Chapter 5, a detailed analysis of the data is presented and the results of both regression analysis used in the model development and the midblock delay model are presented and discussed. Chapter 6 provides the results of sensitivity analyses performed by varying certain parameters and analyze their impact on midblock delay. Chapter 7 presents the conclusion based on the results obtained this research, and the future research to be conducted to address some of the limitations of this research.

CHAPTER 2

LITERATURE REVIEW

2.1 Introduction

This chapter presents a review of several studies that have been conducted on platoon dispersion. The chapter is divided into three sections: Section 2.2 presents a review of the platoon dispersion models. This section is further divided into several subsections: Subsection 2.2.1 reviews studies that have calibrated and evaluated platoon dispersion models; Subsection 2.2.2 discusses the calibration of the Recurrence platoon dispersion model; Subsection 2.2.3 presents factors that impact platoon dispersion and degradation on urban street segments; Subsection 2.2.4 presents a detailed review of the 2010 Highway capacity Manual platoon dispersion model; in Subsection 2.2.5, application of the 2010 Highway Capacity Manual platoon dispersion model is presented; Subsection 2.2.6 presents the limitations of the 2010 HCM Urban Street methodology; Subsection 2.2.7 presents details of the procedure of the HCM 2010 arrival flow profile prediction. Section 2.3 describes the development and verification of a model that estimates the delay incurred by major-street through vehicles due to a vehicle turning right on to access point from a major street**.** Section 2.4 presents a review of pedestrian activity on urban street segments, including midblock crosswalks. The section is divided into different subsections: Subsection 2.3.1 discusses the Gap-Acceptance Theory of Pedestrian Crossing Behavior on urban street crosswalks; Subsection 3.3.2 reviews several research studies on pedestrian walking speeds on urban street segments.

2.2 Platoon Dispersion Models

One of the first platoon dispersion models was a kinematic model developed by Pacey (1956).In this unpublished report**,** the model assumes that if the speeds of vehicles within a traffic stream are normally distributed, then the dispersion of the corresponding platoons can be described by the difference in speed of the vehicles. This phenomenon is considered the *Diffusion Theory*. Pacey`s platoon dispersion model is shown as follows:

$$q_d(j) = \sum_{i=1}^{j} q_0(i)\, f(j-i) \tag{2.1}$$

$$f(T) = \frac{x}{T^2 s\sqrt{(2\pi}} \exp\left[\frac{-(a/T - \bar{v}}{2s^2}\right] \tag{2.2}$$

Equation 2.2 is the probability distribution function of journey time $f(j-i)$.

Where T is the journey time and x is the distance along the road, $\bar{v}$ is the mean speed and s is the standard deviation.

Robertson (1967), also developed a recursive relationship to describe the dispersion of traffic. This relationship forms the core of the TRANSYT software, which is commonly known as TRANSYT-7F in North America. Robertson`s platoon dispersion model has become a universal standard model and has been incorporated into other traffic-simula0tion software including, SATURN, TRAFLO, and SCOOT. According to Rakha and Farzaneh (2005), Robertson`s model is used mainly because of the simplicity of applying its recursive formulation**.** The general form of the recurrence platoon dispersion model is shown below in Equation 2.3

$$q'_{a/s,j} = Fq'_{s,i} + (1-F)q'_{a/s,j-1} \quad (2.3)$$

with

$$j = i + t' \quad (2.4)$$

where:

$q'_{a/s,j}$ = arrival flow rate in time step j at a downstream intersection from upstream source s (veh/step)

$q'_{s,i}$ = departure flow rate in time step i at upstream source s (veh/step)

F = smoothing factor;

j = time step associated with platoon arrival time t';

t' = platoon arrival time

The smoothing factor, used in Equation 2.3, as developed by Robertson is given in Equation 2.5

$$F = \frac{1}{1+\alpha\beta T_t'} \quad (2.5)$$

Where α and β are the platoon dispersion coefficient and platoon arrival time coefficient, respectively. These coefficients have values of 0.5 and 0.8 respectively. The upstream flow source s in Equation 2.3 can include the left turn, through or right-turn movements at the upstream intersection. The upstream source s can also be the combined set of right turn or left turn movements at access points between the upstream and downstream intersections.

Geroliminis and Skabordonis (2005), proposed an analytical methodology for predicting platoon arrival profiles and queue length along signalized arterials. A two-step Markov decision process (MDP) was used to model traffic between successive traffic signals. Modeling of traffic dynamics was done on the basis of the kinematic wave theory. The Markov decision process formulation can be used to predict arrival profiles several signals downstream from a known starting flow. Queue lengths and travel times can be estimated and predicted respectively using this modeling technique. A one-step recursive formulation was used to model traffic behavior between successive signals. The formulation was defined by considering a system in state i at time t with the property that, given the present state, the future does not depend on the past. The state of the system at time $t+1$ is then predicted from the state at time t. The arrival of vehicles at downstream signalized intersection ($i+1$) were considered a function f of the departures of vehicles from upstream signalized intersection i. Sequentially, the departures of vehicles from the downstream intersection were considered a function h of the arrivals at this intersection ($i+1$). The process was expressed mathematically as shown in Equation 2.6.

$$q_{i+1,j}^{in}(t') = h[q_{i,j}^{out}(t)] \tag{2.6}$$

$$q_{i+1,j}^{out}(t') = h[q_{i+1,j}^{in}(t')] \tag{2.7}$$

where:

$q_{i+1,j}^{in}(t')$ = arrival flow at signal $i+1$ at time t from signal i during cycle j,

$q_{i,j}^{out}(t)$ = departing flow from signal i at time t during cycle j,

t = arrival time of a vehicle at the downstream signal traveling at free-flow speed,

h =signal filter function.

$$t' = t + \frac{L}{u_f} \tag{2.8}$$

where

L = signal spacing,

u_f =free-flow, and

f =platoon dispersion function

As stated above, platoon dispersion was modeled using the kinematic wave theory proposed by Ligthhill and Whitham (1955) and Richards (1956) known as the LWR theory. According to the LWR theory, a functional relationship exists between the traffic flow (q) and the traffic density (k). This relationship could be used to describe the speed at which a change in traffic flow propagates either downstream or upstream from an origin point. The proposed methodology estimates the average platoon ratio and non-uniform platoon profile for any concave $q-k$ relationship. Single platoon analysis was done based on the conservation law of flow. The flow of vehicles decreased with the distance from the intersection stop line. The total number of vehicles (N_{tot}) departing from the intersection stop line was calculated using the following equation:

$$N_{tot} = q_0 . t_0 . \tag{2.9}$$

Where q_0 the initial platoon flow and t_0 is the width at the intersection stop line. The platoon width t_i at distance L_i (distance between the stop line and section of the

trajectory of the last vehicle with the ith interface) was estimated using the following equation.

$$t_i = t_0 + L_i\left(\frac{1}{u_0} - \frac{1}{u_f}\right) \tag{2.10}$$

Where u_0 and u_i are the free-flow speed and speed of the group of vehicles between the ith and the $(i+1)$ interface respectively.

2.2.1 Calibration and Evaluation of Platoon Dispersion Models

Several studies have been conducted to calibrate and evaluate the various platoon dispersion models. The majority of these studies used a best fit statistical regression approach to calibrate the appropriate parameters. The following literature is a review of some of the calibration and evaluation techniques that have been used.

Grace and Potts (1964), carried out a theoretical investigation of Pacey`s kinematic model to emphasize its application in coordinating traffic signals. The basic assumption of the speed of cars being normally distribution was considered. It was considered that the parameters of this distribution were related to a diffusion constant that measured the dispersion of the platoon. The rate of platoon dispersion was found to be directly proportional to the diffusion constant. The dimensionless diffusion constant as is shown as follows

$$\alpha = \frac{\sigma}{m} \tag{2.11}$$

Where σ is the variation in car speeds (standard deviation of speeds in ft/s or mph), and m is the average car speed (ft/s or mph). In addition, analytical and numerical solutions of the model were presented using assumed initial flow conditions. In concluding, several aspects of the model and its application were discussed.

Herman, Potts and Rothery (1964), studied the behavior of traffic leaving a signalized intersection by applying Pacey`s (1956) kinematic model (diffusion theory). The objective of the study was to test the kinematic model of traffic platoon behavior, and to test the theoretical results obtained by Grace and Potts (1964). The experiments involved selecting two observation stations A and B located 757ft and 2142ft from the stop line of an upstream intersection, respectively. At each of the two locations, vehicle arrival times were recorded simultaneously on magnetic tapes coordinated with a Traffic Data Acquisition System (TDAS). These arrival times were later converted to digital data for computer use. The switches at each location were placed 35ft apart from to form a speed trap. The speed distributions were computed by the ratio of the width of speed traps to the difference in arrival times at the end of the 35ft speed traps. The mean speed and standard deviation were found to be (57.9ft/s, 10.2ft/s) and (56.1ft/s, 10.0ft/s) at points A and B, respectively.

Seddon(1971, 1972), examined the kinematic wave theory, diffusion theory, and the Recurrence relationship with the aim of comparing and validating their capability and

effectiveness in predicting platoon dispersion. To assess the methodology used and assumptions made in each of the three approaches, field observation and computer simulation were used to obtain the following data at two sites in England: a) the vehicular flow in increments of time at the stop line and at a number of observation points along the road; b) the relationship between speed and flow with concentration (density); and c) details of the position, speed and acceleration of every vehicle in each platoon for the entire time it was within the section of road being considered. In part one of three of the analysis, the kinematic wave theory as presented by Lighthill and Witham (1955) was examined. The theory assumes the existence of waves within a traffic stream if there is a fundamental relationship between: i) the flow q (which is the number of vehicles passing a given point in unit time); ii) the concentration (density) k (which is the number of vehicles per unit length of road segment); and iii) the distance x along the road. The speed of wave c is the slope of the tangent to the flow-density ($q-k$) curve. In other words, the speed of wave is the ratio of the change in flow to the change in density at the downstream and upstream locations, respectively. Change in form of kinematic waves is due mainly to the wave speed being dependent on the flow. To mathematically obtain the gradient of the flow-density curve, eight attempts were made to fit curves to the data obtained at the sites. The final calibrated flow-density equation based on the collected data was obtained from a log-linear regression of velocity with concentration as shown in Equation 2.12.

$$q = 17.119ke^{-6.2379K} \tag{2.12}$$

In part two of his analysis, Seddon (1971), examined the Diffusion theory presented by Pacey (1956) to predict platoon dispersion, as shown above in Equations 2.11 and 2.12. According to the Diffusion theory, changes in the shape of a platoon of vehicles released from a traffic signal is due to differences in speed between the vehicles in the platoon. It is also assumed that there is no interference with overtaking and that vehicles proceed at constant speeds irrespective of the number, or distribution of vehicles on a road/street segment. This assumption is likely in free flowing traffic conditions. It is, however, unlikely in congested condition such as on urban streets. The analysis involved collecting data for two sites in England. The first site was a three-lane dual-carriageway with 10 to 15 percent of trucks and buses in the peak hour and relative freedom for overtaking. The second site was a two-way road with 2 to 3 percent trucks and buses in peak hour and restriction for overtaking. To fit Pacey`s method to the collected data, a computer program was written and run. The flow pattern assumed for the stop line was those obtained from the observation, and was adjusted to exclude vehicles turning from the major street(s). The predicted flow patterns at five points were compared with those observed by calculating the sum of squares of the differences in each interval. The diffusion constant (standard deviation/mean speed) were found to be 0.19 and 0.18 for the two sites, which were compared with 0.21 and 0.25 used by Pacey.

In concluding his three-part analysis, Seddon (1972), examined Robertson`s (1967) recurrence platoon dispersion model as shown above in Equation 2.3. The model predicts the proportion of vehicles in a platoon arriving at a downstream intersection at a specified time after departing from an upstream intersection. The analysis involved collecting data at the same sites stated above. Flow patterns were obtained for the stop

line (at upstream intersection) and five points along the road segments. Additional data on composition (proportion based on vehicle type), lane occupancy, turning movements, the startup time (which is the time for the first few vehicles to get into motion), and cross the stop line, overtaking were also obtained. According to Robertson, the smoothing factor equation has the following functional form:

$$F = \frac{1}{1 + as^{/}} \tag{2.13}$$

Where a is a constant (taken as 0.5 by Robertson), and $s^{/}$ is the average arrival time of the leading vehicles in the platoon. A further analysis of the smoothing factor is shown in the subsequent literature. Based on the observed data collected at the two sites, the values for a were found to be 0.395 and 0.629, respectively. These values are different from the one obtained by Robertson.

Seddon (1972), applied Robertson`s recurrence platoon dispersion model and Pacey (1956) diffusion model to derive the delay/difference-of-offset relationship for a link. To achieve his objective, it was considered necessary to predict the number of vehicles arriving at the end of the link in each of the N increments of the cycle. Seddon went further by transforming Robertson`s recurrence model by applying the geometric distribution of journey time. The transformed Robertson`s recurrence model is shown in Equation 2.14.

$$q_d(j) = \sum_{i=1}^{j-t} q_0(i) F (1-F)^{j-t-i} \tag{2.14}$$

Where, $F(1-F)^{j-t-1}$ is a geometric distribution probability function, and it is the probability that a vehicle passing the first point in the *ith* interval will pass the second point downstream in the *jth* interval. A relationship between the smoothing factor and the average increase in platoon running time due to dispersion was derived by taking into consideration the geometric distribution which forms the basis of Robertson`s platoon dispersion model. The distribution describes the probability of vehicles arriving at a downstream intersection during a particular time step. The smoothing factor equation was formulated thus:

$$F = \frac{1}{1+s^{/}} \tag{2.15}$$

where:

$s^{/}$ = the average increase in platoon running time in steps;

$t_R^{/}$ = average segment running time;

The average segment running time is sum of the average increase in platoon running time and the platoon arrival time $t^{/}$. That is,

$$t_R^{/} = s + t^{/} \tag{2.16}$$

According to Robertson (1967)**,** the platoon arrival time ($t^{/}$) could be estimated as a proportion of the average segment running time ($t_R^{/}$). This was confirmed by Seddon (1972). Therefore,

$$t' = \beta t'_R \tag{2.17}$$

Where β was found to be 0.8.Re-arranging Equation 2.15 with respect to Equation 2.16 and Equation 2.17, the smoothing factor equation becomes

$$F = \frac{1}{1 + 0.25t} \tag{2.18}$$

Applying the collected data to the transformed recurrence model and the Pacey transformed normal distribution model, it was concluded that because both models resulted in almost equally good fits, the distribution of journey time is not important and not the principle influence on accurately predicting platoon dispersion.

Tracz (1975), presented a methodology for predicting platoon dispersion based on rectangular distribution of journey time. The following data were obtained for two sites using filming techniques: a) the flow in increments of time at the stop-line and at a number of observation points along a road; and b) the distribution of journey times for vehicles leaving traffic signals at the same observation points. A sampling technique was then used to derive the journey –time distribution for a typical platoon. The journey-time data was obtained for observation points at 60m (197ft), 200m(656ft), 300m(984ft), and 400m(1312ft) from the stop lines. The means, standard deviations and coefficient of

variations were calculated from the observed data. These parameters were used to derive the following theoretical distribution: a) transformed normal; b) normal; c) geometric; and d) rectangular. The platoon dispersion based on rectangular distribution of journey time was predicted using Equation 2.13. In comparing the methods of predicting platoon dispersion, theoretically, the transformed normal was considered the most applicable. But since the differences in predicted platoon dispersion using transformed normal, geometric and rectangular distributions were found to be insignificant, it was concluded that the choice of distribution in platoon prediction is not important.

$$q_2(i+t_1) = F_d * \sum_{i-t_2+1}^{i} q_0(i) \tag{2.19}$$

where:

$q_2(i+t_1)$ is the flow in the $(i+t_1)^{ith}$ time interval of the predicted platoon, $q_0(i)$ is the flow in the ith time interval of the initial platoon.

$$F_d = \frac{1}{1+a_d t_j} \tag{2.20}$$

With F_d the dispersion factor, a_d is a coefficient whose value was optimized, and t_j the journey time.

Rouphail (1983), developed an analytical solution to the recursive platoon dispersion formula used in the TRANSYT model. The objectives of the study were: a) develop a close-form solution to the platoon dispersion algorithms in the TRANSYT-type models b) investigate the time dependency impacts of the algorithm on the predicted flow rates ,and c) explore potential uses of the analytical expressions developed in the study for signal-coordination schemes.

Denney R.W. (1989), analyzed platoon dispersion modeling techniques (Kinematic wave Theory, Diffusion Theory and the Recurrence Model) so as to present a new mechanism suggested by these models. To test the mechanism, field travel time data were collected using filming technique. The travel distributions of the field data were compared with those obtained from the microscopic TEXAS model for intersection traffic with the aim of validating the use of this model to simulate data. Input data for the TEXAS model were created to replicate the geometrics and operational features of the test site. The demand was set to be in excess of the operational capacity of the signal just as with the field site, so that the platoon size would be dictated by the length of the effective time rather than by upstream arrival distribution. Using the empirical field data, the mechanism was shown to provide accurate platoon dispersion modeling. When compared with the diffusion model, it was shown to have almost similar results. While a comparison with the recurrence model showed improved results.

2.2.2 Calibration of the Recurrence Platoon Dispersion Model Coefficients for Various Traffic Conditions using Field and/or Simulation Data

The previous section includes a review of several studies that have evaluated and/or calibrated the various forms of platoon dispersion models. This section presents a review of studies that have specifically calibrated Robertson`s recurrence platoon dispersion

model coefficients considering various geometric and operational features using field data, simulation data, or both.

Robertson (1969), developed a method for predicting platoon dispersion by conducting field study at four sites in West London. The sites were selected considering various physical characteristics such as single lane flow with heavy parking and very restricted overtaking; multi-lane roadways with no parking and relatively free over taking. Traffic leaving an upstream signal was studied by stationing four observers downstream with the first observer stationed just beyond the signal and 300ft, 600ft, 1000ft, respectively. To obtain a wide range of inflow conditions, the study was carried on various times of the day. At each station, the passing time of every vehicle was recorded. A total of over 700 platoons were recorded during the entire field study. To analyze the results obtained, platoons were grouped into one of four categories according to the average approach flow measured over a five minute period. A further analysis of the observations using the recurrence model obtained a platoon dispersal pattern of an average platoon of traffic. The smoothing factor (F), for the best fit between the actual and calculated platoon patterns was found to be:

$$F = \frac{1}{1+0.5t} \tag{2.21}$$

Rumsey and Hartley (1972), developed a method for predicting vehicle arrivals at a downstream intersection using simulation model. A simulation program was written to model traffic flow through two fixed-time, signal-controlled intersection. Arrivals at the

upstream intersection were considered to follow a Poisson distribution (random arrivals); while the arrivals at the downstream intersection were due to traffic platoons leaving the upstream intersection. No traffic from the side street was generated into the link. The analysis involved assigning a vehicle travel time to every vehicle leaving the upstream intersection based on either the Pacey (1956) or Robertson (1969) travel time distribution. A vehicle was deemed to have arrived at the downstream intersection after this time had elapsed. The program determined the mean queue length and mean delay experienced by vehicles passing through the downstream intersection.

McCoy et al. (1983), carried out a research with the objective of developing a definite description of the definite description of the relationship between the appropriate values of alpha and beta under varying roadway condition. For this research, the model coefficients were calibrated for passenger cars under low friction traffic conditions. A typical low friction roadway comprise of the following geometric and operational attributes: a) 12 ft. lane width; b) sub-urban high-type arterial; c) No parking; d) divided; 5) turning provisions. These attributes were considered in selecting the sites for data collection. Platoon dispersion studies were conducted on six arterial streets at four locations over a distance of 1000ft downstream from the source signal. The six sites were on two- way two- lane streets and two-way four lane divided streets. To collect data, four observers were stationed from the source intersection. The first observer was stationed at a point immediately from the intersection. Subsequent observers were stationed 300ft, 600ft and 1000ft, respectively. At each station, the arrival time of each vehicle was recorded by pressing a switch connected to a 20-pen recorder. The passenger-car flow pattern for nearly1700 platoons was analyzed. Platoon sizes ranged from 5 to 38 vehicles.

Finally, the TRANSYT platoon dispersion model was applied to the average platoon(total number of vehicles discharged during the observation period/ number of observation intervals) flow pattern at the first observation point to predict the average platoon pattern flow pattern at each of the other three downstream points. This was achieved by varying alpha and Beta in increments of 0.01 over ranges of 0.01-1.00 and 0.5-1.00, respectively. The combination of α and β values that minimized the sum of squares of the differences between the observed and predicted average platoon flow patterns was selected as the best-fit for the study.

Axhausen and Korling (1987), measured Robertson`s platoon dispersion factors as used in the TRANSYT model. The first part of this study involved analyzing the sensitivity of the TRANSYT results to various platoon dispersion coefficients. A real network of traffic signal nodes was used with peak evening traffic data. The flow rate was assumed to be 1800vph. Link speeds varied between 30km/hr (19mph) and 60km/hr (37mph). The results obtained were summarized and plotted. The second part of the research involved conducting a pilot study for the calibration of alpha and beta for various traffic conditions such as: a) number of lanes available; b) slope; c) parking activity (number and intensity of parking maneuvers along the link); d) crossing pedestrian downstream (intensity of Jay walking); and e) flow conditions at the stop line (disturbances by narrow lanes, crossing pedestrians, and turning vehicles blocking the lane). The study was conducted at eight sites in Germany. Two hand held computers were used to record all passing vehicles with an accuracy of 0.1 second. At each site, observation was done for three consecutive 10-min. periods during the afternoon peak hour by observers stationed at the upstream intersection stopline,120m(394ft),and

250m(820ft) downstream. All data collected were further analyzed and calculated using an IBM-XT. According to Wikipedia, IBM-XT was IBM's successor to the original IBM Personal Computer, equipped with a hard drive, and was released as IBM Machine Type number 5160 on March 8, 1983.For calibration; the data were aggregated into 4-second intervals. The results of all measurements were presented. The mean alpha value from the entire sites was found to be 0.37. This value is close to the default value (0.35) proposed by TRANSYT/8, but different from that proposed by TRANSYT/7F, which is 0.5.

Manar and Bass (1996), demonstrated that platoon dispersion not only depends on external friction caused by elements such as parking, pedestrian traffic, insufficient lane widths and turning movements; but also on the internal friction between vehicles in the platoon such as lane change, merge and traffic volume. The methodology involved collecting data at eight different site locations within a 3-year period based on the external friction caused by elements such as parking, pedestrian traffic and inadequate lane widths described in the TRANSYT-7F User Guide (1995). Five sites were selected to represent low friction suburban type arterials, two sites representing well designed arterials near central business districts (CBD), and one site representing an urban CBD. To study platoon dispersion under varying traffic conditions, observations were carried out before, during and after peak hour periods. The passing times of vehicles, which are the elapse times between vehicles passing a point, were obtained at a minimum of two control points by using portable microcomputers and video cameras. The platoons at different control points were simulated using Robertson`s platoon dispersion model. The platoon dispersion factor (α) and travel time factor (β) were calibrated simultaneous. The platoon dispersion factor was increased from 0 to 1 with a step of 0.01 while the

travel time factor was kept constant. Subsequently, β was varied between 0.5 and 1, and α recalibrated. A parabolic model relating α and v/s was proposed as shown in Equation 2.22 below. The internal friction is represented as the ratio of volume to saturation flow at the stop line.

$$\alpha = f_e . \frac{v}{s} . \left(1 - \frac{v}{s}\right) \tag{2.22}$$

where:

f_e = external friction factor
v =traffic volume, and
s = saturation flow
The functional form of this model satisfies the following limiting conditions,

$\alpha \to 0$ When $v/s \to 0$
$\alpha \to 0$ When $v/s \to 1$
α , reaches a maximum when $v/s \approx 0.5$

Wasson J. et al. (1999), presented a procedure for quantifying the percentage of vehicles arriving at a downstream signalized intersection using field data, simulation(CORSIM) data, and theoretical model(Robertson`s dispersion model).Data were collected at several sites at least 5000ft between signalized intersection so that the downstream intersection would not impact the platoon. Also, to minimize the impact of merging and diverging vehicles on the platoon, sites with minimum number of side streets and driveways were selected. The data collection included the use of two Hewlett Packard 48 GX Scientific calculators to record observations. The calculators used by both

upstream and downstream observers were programmed the same. One of the calculators was used to record the signal transition times and the other was used to record downstream arrival time for every vehicle. For a particular site, the start of data collection involved recording and displaying a reference time using two pre-programmed keys. The signal observer used three pre-programmed keys to collect information about the intersection (i.e., start of green, end of green, and vehicle count). Further analysis involved using CORSIM to run simulation for different combination of travel speed and initial platoon discharge rates to replicate observed field data conditions. Initial platoon discharge rates were obtained by setting the main street traffic in oversaturated condition and the signal time to the required length. Vehicle arrival times at downstream distances at 500ft intervals were obtained by extracting vehicle positions from the CORSIM animation file.

Finally, computer spread sheet was used to predict the percentage of vehicles arrivals based on the Robertson platoon dispersion model. With the use of spread sheet, the average arterial speed, initial platoon size and the platoon dispersion coefficients could be varied. The coefficients used included but not limited to those suggested by McCoy et al. (1983).After a careful analysis, it was concluded that the platoon dispersion predicted by the theoretical Robertson model was much greater than the field data or CORSIM simulation. Platoon dispersion was found to be directly proportional to the product of the two platoon dispersion coefficients. CORSIM simulation demonstrated an overall platoon dispersion similar to the field data. However, it was found to introduce more dispersion than the observed field data.

Yu (2000), presented a technique that can be used to calibrate the TRANSYT platoon parameters. The technique is based on statistical analysis of link travel time distribution. A mathematical relationship between the average link travel time and its standard deviation (σ^2) and the platoon dispersion parameters was established. The basic properties of the geometric distribution were applied to the arrival flow equation as presented by Seddon (1972),which resulted to three equations for calibrating the travel time factor(β),platoon dispersion factor(α) and smoothing factor (F) as shown below in Equations 2.23, 2.24 and 2.25.

$$\beta = \frac{1}{1+\alpha} \tag{2.23}$$

$$\alpha = \frac{\sqrt{1+4\sigma^2-1}}{2t_a+1-\sqrt{1+4\sigma^2}} \tag{2.24}$$

$$F = \frac{\sqrt{1+4\sigma^2-1}}{2\sigma^2} \tag{2.25}$$

Two scenarios of TRANSYT`s implementation were examined using data collected on two links on the same streets. Link 1 and Link 2 were measured to be 320m (1050ft) and 560m (1837ft). To test the first scenario, α, β, F were calibrated using the proposed calibration technique. Because TRANSYT uses a fixed value for β, and users are restricted from inputting the value of β; the actual values of β and F used by TRANSYT were found to be different from the calibrated values. TRANSYT only permits the input of α, which doesn't secure the accuracy of the platoon dispersion predictions. The second scenario was designed based on the limitation of the first

scenario. The scenario was set up such that TRANSYT used the calibrated F instead of the calibrated α. The calibrated F was set as a fixed value, while the α value was calculated inversely by using $\beta = 0.8$. Using such technique, a different value of α is inputted into TRANSYT but will ensure the use of calibrated value of F by TRANSYT. Finally, several methods for revising TRANSYT were recommended. The first method is to permit users input the values of α and β. The second method is to permit users to input the values β and F. The third method of revising the TRANSYT is to allow users to input the average link travel time and its standard deviation directly. The research also attempted to validate the assumption in the TRANSYT User Guide, that streets or links with similar traffic and roadway conditions should use the same platoon dispersion factor. To examine such assumption, field travel time data were collected from two links of different lengths on the same street.

Bonneson et al. (2010) developed a procedure for predicting the arrival flow profile for an intersection approach. The profile describes the variation in flow rate during the average signal cycle as it would be measured at a specified point downstream of a signalized intersection. The procedure consists of a platoon dispersion model, a mid-segment arrival flow profile, and a platoon decay model. The arrival flow profile at a downstream intersection was considered as representing the aggregation of two arrival flow profiles. One profile is the platoon arrival flow that describes platoon arrival from the upstream signalized intersection. The other profile is the mid-segment arrival flow profile that describes random arrivals from mid-segment access points. Calibration data were collected at 10 urban study sites during the mid-afternoon and evening peak traffic periods. Three hours of traffic operation were videotaped at each site. A 15-min sample

of data was extracted from each 1-hr video tape for a total of thirty 15-min samples from the 10-sites. The collected data consisted of: a) the time each vehicle crossed a reference mark on the pavement; b) its manner of entry to the segment, and c) the vehicle`s classification and color. Each vehicle was tracked between a pair of upstream and downstream marks. The running time for each tracked vehicle was added to obtain a total running time for each cycle and site. The total running time was divided into the partial segment length to estimate the cycle running speed. A total of 5883 through vehicles were tracked along partial segments during the thirty 15-min time periods. To calibrate the platoon dispersion model, through vehicles were defined as vehicles that entered the segment as through vehicles and crossed the downstream reference mark as through vehicles. Vehicles that entered and exited at an access point were excluded from the analysis. Platoon dispersion model coefficients (α and β) were obtained using a non-linear regression analysis. The dispersion coefficient (α) for a set of sites ranged from 0.13 and 0.36, while the platoon arrival time coefficient (β) ranged from 0.84 and 0.95.

2.2.3 Factors that Impact Platoon Dispersion and Platoon Degradation

Platoon dispersion along an urban street segment or arterial can be impacted by several factors such as: a) Length of segment/arterial; b) the level of driveway activity along the segment; c) the segment cross-section. The Highway Capacity Manual (2010) illustrates the platoon dispersion process by comparing the platoon dispersion profile of three traffic movements (cross-street right turn, major-street through, and cross-street left turn). The profiles are represented as three x-y plots. In the first plot, the major- street through illustrates a dense platoon as it departs the upstream intersection. However, when the platoon reaches the downstream intersection it has spread out over time and has lower

peak flow rate. The amount of platoon dispersion typically increases with increasing segment length. For very long segments, the platoon structure degrades and arrivals become uniform throughout the cycle.

Furthermore, platoon degradation can be the result of significant access point activity along the segment. Streets with frequent active access point intersections tend to have more vehicles leave the platoon (i.e., turn from the segment at an access point) and enter the segment after the platoon passes (i.e., turn into the segment at an access point). Both activities result in significant platoon decay. Platoon decay tends to have more impact on platoon degradation than platoon dispersion on streets with very busy access points.

2.2.4 The 2010 Highway Capacity Manual Platoon Dispersion Model

The Highway Capacity Manual (2010) describes a model for predicting the extent of platoon dispersion as a function of the segment running time. The functional form of the model was originally developed by Robertson. It is based on the division of the signal cycle into an integer number of intervals, each with an equal duration called time steps. Input to the model is the flow profile for a specified traffic movement discharging from an upstream signalized intersection, as defined in terms of the flow rate for each time step. Output measures from the model include: a) the arrival time of the leading vehicles in the platoon to a specified downstream intersection; and b) the flow rate for each time step at this intersection.

In general, the arrival flow profile has lower peak flow rate than the discharge flow profile due to the dispersion of the platoon as it travels downstream. Also, for similar reasons, the arrival flow profile is spread out over a longer period of time than the

discharge flow profile. The dispersion rate is considered to be directly proportional to the segment running time. Hence, the rate of dispersion increases with increasing segment running time, as may be caused by access point activity, on-street parking maneuvers, and other mid-segment delay sources. The general form of the Highway Capacity Manual platoon dispersion model is the recurrence model. But the HCM 2010 incorporates a different smoothing factor below in Equation 3.6. In addition to the smoothing factor, the 2010 HCM platoon dispersion model incorporates the platoon arrival time model. The model estimates the time of arrival of the leading vehicle platoon arrival time at the downstream intersection after departing from the upstream intersection.

2.2.5 Application of the 2010 Highway Capacity Manual Platoon Dispersion Model

The 2010 HCM applies the platoon dispersion model in evaluating automobile performance on urban street segments. The process involves several steps. Firstly, the proportion of vehicles arriving during the effective green time at the downstream intersection is computed using Equation 2.30. This equation only applies when the upstream intersection is signalized and coordinated with the downstream intersection. Otherwise, the proportion of vehicle arrivals is computed as the effective green to cycle length ratio. After computing the proportion of vehicle arrivals, the next steps in the performance evaluation involve: a) determining the signal phase; b) determining the through delay; c) determining the through stop rate; d) determining the travel speed; e) determining the spatial stop; f) determining the level of service (LOS); g) Determining the automobile traveler perception score. Each of these steps is described in detail in the

2010 HCM. The step by step computation can be intensive and therefore requires the use of software is recommended.

2.2.6 Limitations of the 2010 HCM Urban Street Methodology

The 2010 HCM provides a methodology for evaluating the performance of automobile traffic traveling along an urban street segment. However, the methodology doesn't provide an approach for evaluating urban street segments under varying traffic conditions. This inability in the methodology is considered a limitation. Some of the limitations are shown below:

- The methodology doesn't account for on-street parking activity along the link;
- The methodology also doesn't account for significant grade along the link;
- The methodology doesn't address the effect of stops incurred by segment through vehicles due to vehicles turning from the segment into an access point.
- The methodology doesn't address cross- street congestion blocking through traffic.

2.2.7 The 2010 HCM Arrival Flow Profile Prediction Procedure

As stated previously, the arrival flow profile is used to compute the proportion of vehicles arriving during green by comparing the profile with the downstream signal timing and phase sequence. The procedure for predicting the arrival flow profile is discussed in this section.

Tarnoff and Parsonson (1981), confirmed the validity of the combined techniques used in the TRANSYT-7F software to estimate platoon arrival flow profiles for signal system evaluation. The arrival flow profile at a downstream intersection is considered as an aggregate of two arrival flow profiles: a) the platoon arrival flow from the upstream

signalized intersection; and b) the mid-segment access points that describes random arrivals from mid-segment access points.

Bonneson et al. (2010), considered the platoon flow profile as a combination of three traffic movements; cross-street right turn, major-street through, and cross-street left turn. The platoon dispersion model uses the discharge flow profile to estimate the downstream arrival flow profile for each traffic movement. Finally, these three arrival flow profiles are added to produce the combined platoon arrival flow profile. The validity of this combination technique was confirmed by Tarnoff and Parsonson(1981) using the TRANSYT-7F by distributing the mid-segment inflow (i.e., a combination of flow profile for all access point points) uniformly among all time steps. The aggregated arrival flow profile is computed by adding the flow rates in the arrival flow profile and the mid-segment arrival flow profile on a time step –by-time step basis. The effect of decay is modeled using the origin-destination matrix, where the combined access point activity is represented as one volume assigned to mid-segment origins and destinations.

Tarnoff and Parsonson (1981), investigated this approach to estimating the mid-segment arrival flow profile to determine whether the periodic arrival of platoons at un-signalized access points tended to meter access point vehicle entry such that the use of uniform mid-segment arrival flow profile led to inaccuracies. After a careful investigation, it was found that for typical access point volumes more refined approach for modeling the mid-segment arrival profile did not improve the accuracy of the aggregated arrival flow profile. Figure 2.1 shows the arrival flow profiles at a downstream intersection on an urban street segment for three upstream movements: through, left turn, and right turn.

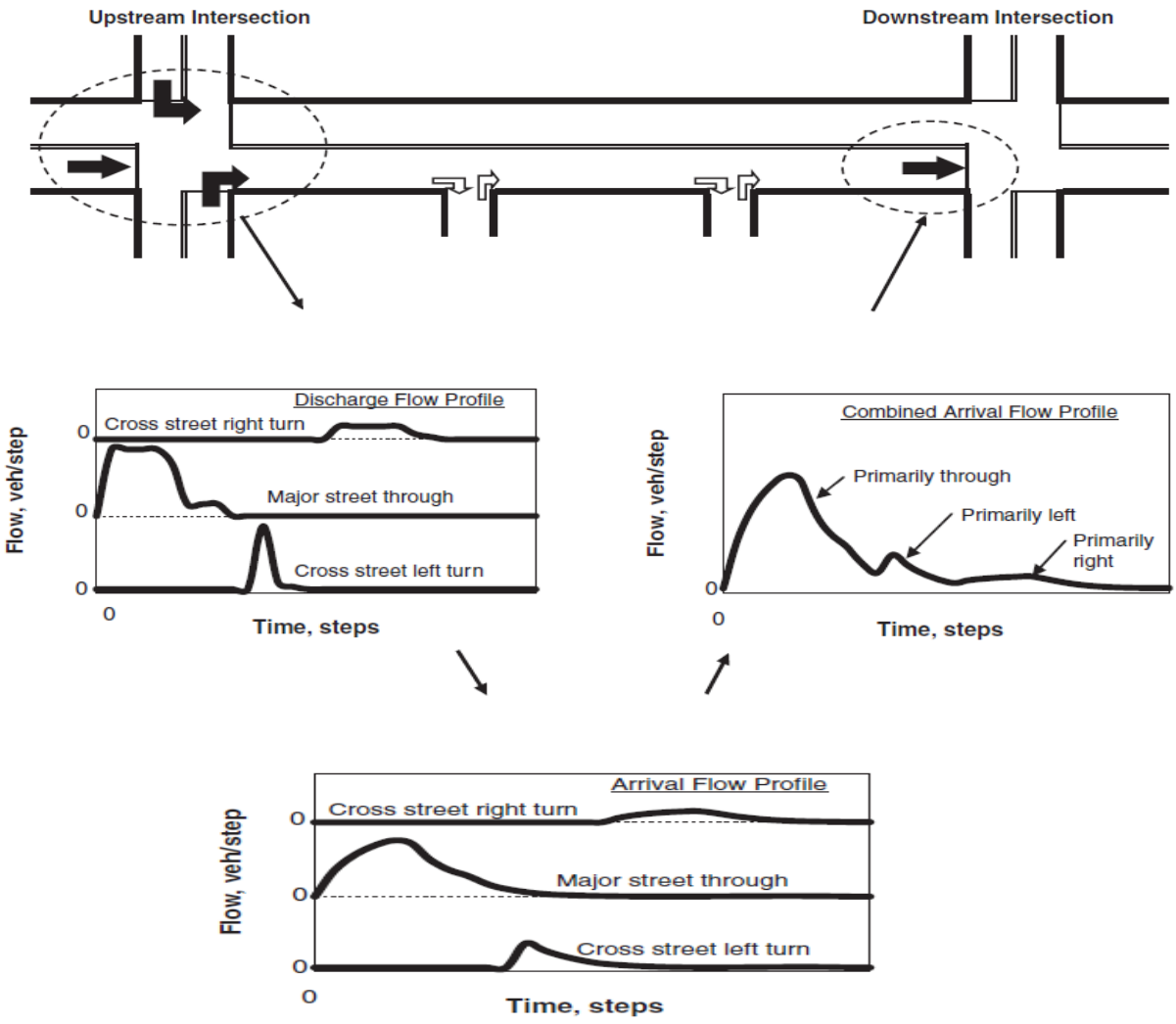

Figure 2.1 Arrival flow profiles on urban street segment.
Source: Bonneson et al. (2010)

Seddon (1972), derived a relationship between the segment running time ($T_r^{`}$), average increase in platoon arrival time ($u^{'}$) and the platoon arrival time ($t^{'}$). He defined the segment running time as follows:

$$T_r^{`} = u^{'} + t^{'} \tag{2.26}$$

Seddon(1972), further defined u' as the increase in platoon running time due to platoon dispersion. The u' value accounts for the difference in arrival times of the following vehicles in the platoon relative to the leading vehicle. Bonneson et al (2010), presents a figure to illustrate this relationship as shown in Figure 2.2 below. The Figure shows a discharge flow profile for a platoon during green at an upstream signalized intersection, and the corresponding arrival flow profile at a downstream signalized intersection. As shown, the arrival profile is spread out due to dispersion of the platoon.

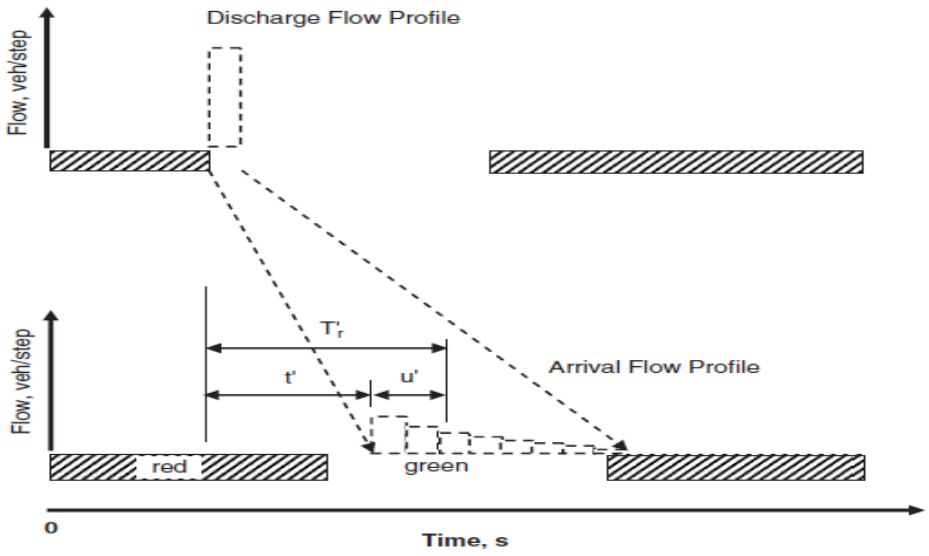

Figure 2.2 Relationship between segment running time and platoon arrival time.
Source: Bonesson et al (2010)

2.3 Major-Street through Vehicle Delay

Bonneson (1998), developed a deterministic model for estimating the delays to major-street though drivers due to vehicles turning from the outside through traffic lane on the major street. This maneuver can be in the form of a left or right-turn from the major street into a driveway. Either maneuver can cause significant delay to the following through

vehicles when a bay or an exclusive turn lane is not provided. The model was developed for passenger car stream; however, it can be extended to mixed traffic streams through modification of selected input parameters. The model development did not include assumption on the number of through lanes on the major street or the distribution of its flow rates to these lanes. However, it was assumed that the distribution of headways in the outside through lanes is assumed to follow the shifted negative exponential distribution. The delay process was modeled using a time-space representation of traffic flow along the major-street. The trajectory of the right-turn and following through vehicles are sequentially evaluated to determine the average through vehicle delay. The right turn vehicle trajectory initiates the stopping (or slowing) wave in the outside through lane. The next through vehicle may have to slow to avoid the right turn vehicle if it is closely following this vehicle. A second, third, fourth, etc. though vehicle may have to slow to maintain a minimum following distance between it and its trajectory, as originally precipitated by the right-turn maneuver. The delay is initiated by the arrival of a right-turn vehicle and ends with the arrival of a subsequent right-turn vehicle. Any through vehicle between these two right turn vehicles may be delayed.

The delay to the first and subsequent through vehicle is modeled assuming each vehicle on the major-street has the same running speed (free-flow speed). Any through vehicle that delayed by a right-turn vehicle will decelerate from this speed and then accelerate back to it. The rates of deceleration and acceleration were assumed to be constant. As the right-turning driver approaches the turn location, he/she begins to decelerate from the running speed to the desired speed. The right turning driver is assumed to reach the turn speed at the start of the turn radius and then maintain this speed

throughout the turn until he/she fully clears the outside through lane of the major-street seconds later. This clearance time is the time from the start of the turn until the back of the vehicle clears the outside through lane. The clearance time is based on the turn speed, the radius of the travel path, and the length of the turning vehicle. The following through vehicle will be delayed by this right-turning vehicle if its headway is sufficiently short as to require braking. Therefore, the maximum headway that will be associated with delay is defined as the time required by the turning vehicle to decelerate to the right-turn speed and then clear the outside through lane. If the following through vehicle has headway less than the maximum headway associated with the delay, then the driver will initiate braking at the "critical decision point" and decelerate to a speed sufficient to maintain the minimum headway between vehicles. Once the minimum speed of the first delayed through vehicle is determined, it can be used to estimate the first through vehicle delay. This delay represents the added travel time due to the deceleration and acceleration process that stems from the right-turn vehicle slowing in the outside through lane. The second and subsequent through vehicle will be delayed by the right-turn vehicle in an indirect manner due to the wave of the slowing that propagates backward in the through traffic stream. The delays to each subsequent through vehicle is less than or equal to that of the preceding vehicle.

2.3.1 Model Verification and Analysis

This subsection describes the model verification and examination. The research, however, did not validate the model using field data. The model verification involved comparing the proposed model with the findings of other researchers as well as a comparison of it to the TRAF/NETSIM model. Two approaches were used to provide

some foundation for the accuracy of the model predictions. In the first approach the delays predicted by the model compared with other research. The results show that model was in agreement with the delays obtained in other research. The results also show the delays reported by Stover et al. (1970) were lower than those reported by other researchers and the developed model.

The second approach in the model verification was to compare the developed with the TRAF/NETSIM (1995) simulation model. TRAF/NETSIM can be described as a stochastic, microscopic simulation model. It uses a car–following logic to move individual vehicles along the simulated street and additional queue-discharge logic at signalized intersection approaches. The through delay comparison between TRAF/NETSIM and the proposed model was conducted by establishing a hypothetical street segment with a single driveway at about the middle of the segment. The segment was 400 m in length, had two through lanes in each direction, a free-flow speed of 18meters/second, and was bounded at each end by a signalized intersection. Flow rates on the major-street ranged from 500 to 800 veh/hr/lane; the portion of right-turns ranged from 0.0 to 0.2 of the major-street flow rate. The simulation runs with no right-turns were used to identify the through delay due to the density of the traffic stream as predicted by TRAF/NETSIM. This density-based delay subtracted from the through delays reported by TRAF/NETSIM to obtain the delays due to right-turn activity. The simulated and estimated delays were compared using a diagonal plot. The plot showed clustering around the diagonal line(the line of perfect agreement) suggesting that the proposed model was able predict the delays incurred by major-street through divers with reasonable accuracy.

In addition to the model verification, the model was analyzed by performing a sensitivity analysis to explore the relationship between several model variables and through vehicle delays. Specially, four variables were analyzed: outside through lane flow rate; portion of right-turn in the outside lane, right-turn speed, and major-street running speed. The results show through vehicle delay increases in an exponential manner with lane flow-rate. The through vehicle delay also increases with decreasing in turn speed. The delay per right-turn vehicles decreases as the portion of right-turn vehicle increases. This decrease in delay relates to the smaller number of through vehicle that would be following each right-turn vehicle when the portion of right-turn vehicles is large.

The study concluded that while the average delay to through vehicles may appear relatively small, the total delay incurred by the through stream can be quite large. This large total delay was a direct result of the large number of through vehicles in a typical traffic stream. Therefore, in the context of improving overall operations at an un-signalized intersection, it may be appropriate to consider first those geometric improvements that could reduce right-turn related delays to the major-street through movement.

2.4 Midblock Pedestrian Activity

2.4.1 Gap-Acceptance Theory of Pedestrian Crossing Behavior

The theory of gap-acceptance of pedestrian crossing behavior states that each pedestrian has a critical gap in which to cross a roadway (Palamarthy et al., 1994). On arriving at the curb, the pedestrian checks if the current traffic gap is greater than the critical gap and

decides whether to accept the traffic gap. If the current gap is rejected, the next gap will be considered and so on. This process continues until the pedestrian accepts a traffic gap or gives up entirely and decides not to cross. The critical gap consists of two parts: The required crossing time and a safety margin. The safety margin is the difference between the time a pedestrian crosses the traffic and the time the next vehicle arrives at the crossing point. Therefore, the theory indicates that pedestrian crossing behavior is governed largely by three components: Supply of gaps, crossing time, and safety margin.

2.4.1.1 Supply of Traffic Gaps. The supply of traffic gaps is the key determinant of pedestrian quality of service for street crossing at midblock. A study by Baltes and Chu (2003) used variables that influence the supply of traffic gap as potential determinants of pedestrian quality of service for midblock crossings. The supply of traffic gaps was determined by traffic volume and its patterns. Traffic patterns indicated both the spatial and temporal distributions of traffic. In addition, six major variables were determined to influence traffic patterns: signal cycle, signal spacing, turning movements, crossing features, median treatment, and directional distribution of traffic. The research determined that three of these variables (cycle length, signal spacing, and turning movements) influence traffic patterns through their effects on the platooning of traffic. Typically, when there is low traffic volume, the supply of traffic gaps is ample. As a result, there is little difficulty for pedestrian to wait for a suitable gap and cross the street. Conversely, when traffic volume is high, the supply of traffic gaps depends on traffic platooning.

2.4.1.2 Crossing Time. Baltes and Chu (2003), determined the pedestrian crossing time by the distance to be crossed, the walking speed of the pedestrian, and whether the

median treatment allowed the pedestrian to cross the street in two stages. In situations where median treatments allow the pedestrian to make a two-stage crossing, more traffic gaps become acceptable because the required crossing time is cut in half. Walking speed determines how much time a pedestrian takes to cover a given distance. According to Coffin and Morral(1995) and Hoxin and Rubenstein(1994), personal attributes such as age are good indicators of walking speed. Median treatments, crossing location, group size of pedestrian, and trip purpose also influence walking speed. According to Bowman and Vecellio(1994), the average walking speed is higher for roadways with two-way left turn lanes than for undivided roadways, and pedestrians tend to walk faster at midblock locations than at signalized intersections.

2.4.1.3 Safety Margin. Safety margin is the difference between the time a pedestrian crosses the traffic and the time the next vehicle arrives at the crossing point. Didietro and King (1970) and Harrell and Bereska (1992), state that the size of the safety margin is determined largely by certain personal attributes such as age and gender. Landis et al. (2001) determined that safety margin may depend on other variables, including whether the pedestrian is walking or standing still before stepping into the street. Furthermore, according to Palamarthy et al. (1994), the safety margin may depend on the expected delays before the next available gap. Finally, pedestrians` choice of safety margin and perception of crossing quality of service could be influenced by traffic speed at midblock locations and the presence of large vehicles in the traffic.

2.4.2 Pedestrian Walking Speed

Baltes and Chu (2003), developed a methodology for determining the level of service for pedestrians crossing streets at mid-block locations. The methodology provides a measure of effective that indicates perceived quality of service in crossing roadways at mid-block crossings. One of the study objectives was to determine what variables were correlated with pedestrians` perceived quality of service for midblock crossings. The research defined midblock as roadway section between two consecutive intersections regardless of signalization. Data were collected at 20 mid-block locations in Tampa and 13 in and around St. Petersburg, Florida. A total of 96 participants took part in the data collection, ranging in age from 18 to 77, and 68% were women while 32% were men. The data collection involved instructing three participants to approach the curb and observe traffic conditions for 3mins. When observing traffic conditions, participants were instructed to continuously scan the roadway segment by looking left, then right, and then cross the street as many times as they could during the allotted 3 min. Once the 3 min observation window closed, participants were asked to record their perceptions of crossing difficulty on survey forms. A total of 767 observations were recorded during the 3 days of data collection.

Bowman and Vecellio (1994), carried out a research to study pedestrian walking speeds at medians located on unlimited-access urban arterials. Pedestrian crossing behavior was obtained at selected intersections and mid-block segments in Atlanta, Georgia; Pheonix, Arizona; and Los Angeles-Pasadena, California, using video cameras that had time-imaging capabilities to a hundredth of a second. Pedestrian walking speed data were recorded for three age categories: less than 18 years, age 18 to 60, and older

than 60 years. Pedestrian age was estimated from video tapes. The results show that pedestrian walking speed for the age 18 to 60 year group was significantly higher than that of the over 60 year group for both signalized intersection and midblock locations. Both age groups had significantly higher walking speeds at midblock locations than at signalized intersections. This may indicate that pedestrians feel somewhat protested at signalized intersections and do not feel the same urgency to cross as they do at midblock locations. Table 2.1 shows the average pedestrian walking speeds by age group and location type.

Table 2.1 Pedestrian Walking Speeds

	Average Walking Speed(f/s)	
Age	Midblock	Intersection
18-60	4.65	3.93
>60	4.46	3.4

KnoBlauch et al. (1996), conducted series of field study to quantify the walking speed and start-up time of pedestrian of various ages under different conditions. Sixteen crosswalks at signal-controlled intersections in four urban areas (Richmond,Virginia; Washington, D.C.; Baltimore, Maryland; and Buffalo, New York) were selected. Study sites were selected to allow for a minimum of 26 to 30 pedestrian over 65 years of age to be observed during an 8-hr data collection period. Data were collected on a subject of pedestrians who appeared to be 65 years of age or older and a control group of pedestrians under age 65 years were collected. To verify the accuracy and reliability of the age-estimation abilities of the observers, several field verification were done. First,

the age-estimation accuracy of several observers was measured; then correlations between the estimates of all other observers were determined. The actual data collection procedure involved measuring pedestrian crossing times using a hand –held digital electronic stopwatch. The watch was started as the subject (pedestrian) stepped off the curb and stopped when the pedestrian on the opposite curb after crossing. At sites with a pedestrian signal, pedestrian signal, pedestrian start-up times were also measured. A total of 7,123 pedestrians were observed. Included were 3,458 pedestrians under 65 years of age and 3,665 pedestrians 65 and over. The results show a mean walking speed for younger pedestrian is 4.95 ft/s; and 4.11 ft/s for older pedestrians. The 15^{th} percentile speeds were 4.09 and 3.19 ft/s for younger and older pedestrians, respectively. Additional, the mean and 15^{th} percentile start-up times for young and older pedestrian was measured. Start-up times were measured only at locations with a pedestrian signal. The start-up time was defined as elapsed time from the onset of a walking signal to the moment when a pedestrian steps off the curb and starts to cross. The data indicate that younger pedestrians have identical mean start-up times of 1.93 sec whether alone or in a group. Older pedestrians had nearly identical start-up time of 2.5 s when alone and 2.43 s in a group.

Fitzpatrick et al. (2006), summarized the findings of the TCRP-08-NCHRP 3-71 project and compared those findings with other researches. In one of their comparisons, they analyzed the findings by Knoblanch et al. (1996) as discussed previously, and the TCRP-NCHRP on pedestrian walking speeds. The TCR-NCHRP study collected data at 42 study sites in seven states (Arizona, California, Maryland, Oregon, Texas, Utah and Washington). The study sites were chosen in an effort to distribute the different types of

crossing treatments in certain region. The field studies included nine different types of pedestrian crossing treatments (half signals, Hawk beacon, midblock pedestrian traffic control signal, passively activated overhead yellow flashing beacon, overhead flashing beacon activated by pushing button, pedestrian crossing flags, high-visibility markings and signs, in-street pedestrian crossing sign, and pedestrian median refuge Island.). During data collection reduction, technicians assigned pedestrian to one of the following age category as shown Table 2.2. A total of 3,155 pedestrians were recorded during the study. Of this number, 81% (2,552 pedestrians) were observed as "Walking". The remaining 19% of the pedestrians (603) were observed to be running, both walking and running during the crossing, or using some form of assistance (e.g., skates, bike). Also, not included in the analyses were 107 walking pedestrians whose age could not be estimated.

Table 2.2 Walking Speed by Age Groups Knoblauch et al.(1996) and TCRP-NCHRP Studies

Walking Speed, ft/s						
	Knoblauch			TCRP/NCHRP		
Age Group	Number of Points	15th Percentile	50th Percentile	Number of Points	15th Percentile	50th Percentile
Younger	2.081	4.02	4.79	2,335	3.77	4.74
Older	2.378	3.1	3.94	106	3.03	4.25
All	4.459	3.53	4.34	2,441	3.7	4.72

Gates et al. (2006), recommended walking speeds for timing of pedestrian clearance intervals based on characteristics of pedestrian population. Pedestrian crossing data were collected at 10 intersections in Madison, Wisconsin and one intersection is

Milwaukee, Wisconsin during the summer of 2004 and 2005. The sites included eight signal-controlled intersections with pedestrian signals (including two midblock crossings) and three un-signalized intersections (including one four-way stop controlled intersection, one two-way stop controlled intersection, and one uncontrolled midblock crossing). Pedestrian crossing data were measured in the field either by an inconspicuously positioned human or a video camera. In either case, a stop watch was used to measure pedestrian crossing times, which were recorded on data collection form. The video camera provided the advantage of allowing for every crossing event to be measured. Crossing times for individuals and groups of pedestrians were observed at each of the intersection. The data collectors also recorded the following characteristics for each pedestrian crossings; Gender, age group, group size, and pedestrian signal indication (signalized intersections only). A total of 1,947 pedestrian crossings from 11 intersections were analyzed to determine the effect of age and disability, traffic control condition, group size and gender on walking speeds. The results show age had the most significant effect of all factors. Pedestrian over the age of 65 were the slowest of all age groups with mean and 15^{th} percentile walking speeds of 3.81 and 3.02 ft/s, respectively. Traffic control condition also had a statistically significant effect on walking speeds. Pedestrian were determined to walk fastest under the DW (Don't Walk) and FDW (Flashing Don't Walk) signal indication; 05 – 0.6 ft/s faster than those who began under the "Walk" indication. Group size also affected walking speed. Groups of pedestrians crossed at speeds that were on average 0.4 to 0.6 ft/s slower than individual crossers.

Rastogi et al. (2011), conducted a parametric study of pedestrian walking speeds at midblock crossings. The research team used video recording method to collect

pedestrian flow data. A camera was fixed in an elevated position, and recording was carried out for 60 minutes duration between 10 am and 12 noon and/or 4 pm to 6 pm. Pedestrian speeds were computed based on the time taken by a pedestrian to cross the roadway between two opposite curbs on an undivided roadway and between the curb and the median on a divided roadway. Pedestrian speeds were recorded based on certain factors, including but not limited to: traffic volume, width of roadway, gender, age, pedestrian group size. The result show pedestrian speed initially increased with increased with increased in traffic volume up to 2000 passenger car units per hour(pcu/h), and thereafter became almost constant. The average crossing speeds of pedestrian groups of different sizes were computed on the basis of the time difference between the entry of the first pedestrian in a group on a marked section and the exit of the last pedestrian of the group from the section. The results also show male pedestrians walk faster than female pedestrians, with average crossing speeds of 4 f/s and 3.64 f/s, respectively. Pedestrian crossing speeds were found to reduce with increase in age. Finally, pedestrian crossing speeds were found to reduce with increase in the size of the pedestrian group

2.5 Model Validation

Montgomery and Peck (1992), in their second edition book titled *Introduction to Linear Regression Analysis* present a detailed methodology for validating regression models. Regression models are used for prediction or estimation, data description, parameter estimation, and control. Most often the user of the regression differs from the model developer; therefore, before the model is released to the user, it is necessary to assess its validity. In statistics, there is distinction between model *adequacy checking* and model

validation. Model adequacy checking includes testing for lack of fit, residual analysis, searching for high-leverage or overly influential observations, and other internal analysis that investigate the fit of the regression model to the available data.

Model validation, however, is aimed at determining if the model will function successfully in its intended operating environment. In developing regression models, it is sometimes tempting to conclude that a model that fits the data will perform successfully in its final application. This is not always the case. For instance, a model may have been developed primarily for predicting new observations. There is no assurance that the equation that provides the best fit to existing data will be a good predictor. Factors that were unknown during the model development may significantly affect the new observations, rending the predictions almost obsolete. Additionally, the correlative structure between the repressor may differ in the model-development and prediction data. This may result in poor predictive performance of the model.

2.5.1 Model Validation Techniques

There are three procedures for validity regression models

- Analysis of the model coefficients and predicted values including comparisons with prior experience, physical theory, and other analytical models or simulation results.
- Collection of fresh data with which to investigate the model`s predictive performance.
- Data splitting; that is, setting aside some of the original data and using these observations to investigate the model`s predictive performance

2.4.1.1 Qualitative Techniques. Qualitative techniques, also known as subjective, visual or informal techniques on some other occasions, are typically performed on the basis of visual comparison of the predicted and observed data in various graphs and plots. It is

generally accepted and fairly reliable means to evaluate model performance and identify problems. However, the downside of this approach is also obvious: its result is also qualitative and fuzzy. That is also the reason it is necessary to employ quantitative techniques to provide complementary information. According to Ni et al. (2004), qualitative techniques generally include, but not limited to the following:

- Series plot, where values of the target variable are plotted against their observation number (e.g., time-series or space-series).
- Contour plot, where a curve links all the points in x-y space having the same z value in a x-y-z coordinate system. For example, a density contour may visualize congested regions in time-space domain if the density for congestion is properly defined.
- Surface plot, where data points are graphed in a three-dimensional space. This plot contains the most detailed information and can be reduced to the previous two plots by cutting the surface.
- Diagonal plot, where observed values are plotted against predicted values and an ideal fit would be a 45 degree line. Sometimes a transformation might be necessary to stretch or squeeze data points so that they are aligned evenly along the line.
- Histogram, where the frequency of errors is displayed and a favorable outcome generally a bell shape with most errors centered around 0.

2.4.1.2 Quantitative Technique. Quantitative techniques, also known as objective, numerical or formal techniques on some other occasions, quantify the difference between the observed and simulated. Quantitative validation techniques include, but not limited to

- Goodness-of-fit measures
- Hypothesis testing and confidence intervals

Goodness-of-Fit Measures: A number of goodness-of-fit measures can be used to evaluate the overall performance of the measures of performance (MOPs). Two frequently used goodness-of-fit measures are the root-mean-square error (RMSE) and the

root-mean-square percent error (RMSPE). These statistics quantify the overall error of the MOPs. Percent error measure provides information on the magnitude of the error relative to the average measurement. The two measures as presented by Toledo and Koutsopoulos (2004) are given below:

Suppose there are two processes X (the predicted or measured) and Y (the observed): $X_1, X_2, \ldots, X_n$ and $Y_1, Y_2, \ldots, Y_n$, where n is the sample size. Let residuals Z be the paired difference between the two processes: $Z_i = Y_i - X_i$, $i = 1, 2, ..., n$. In addition to the RMSE and RMSPE, another measure that provides information on the relative error is Theil`s inequality coefficient (e). Theil (1961), presents the inequality coefficient as follows:

$$e = \frac{\sqrt{\frac{1}{N}\sum_{i=1}^{n}(Z_i)^2}}{\sqrt{\frac{1}{N}\sum_{i=1}^{n}(Y_i)^2} + \sqrt{\frac{1}{N}\sum_{i=1}^{n}(X_i)^2}} \tag{2.27}$$

where:

e is bounded by $0 \leq e \leq 1$.

If e=0, it implies perfect fit between the predicted and measured values. If e=1, it implies the worst possible fit. Theil`s inequality coefficient may be decomposed to three proportions of inequality: the bias(e^M), variance(e^S), and covariance(e^C) proportions, which are, respectively, given by:

$$e^M = \frac{\left(\overline{Y} - \overline{X}\right)^2}{\frac{1}{n}\sum_{i=1}^{n} Z_i^2} \tag{2.28}$$

$$e^S = \frac{\left(s_Y - s_X\right)^2}{\frac{1}{n}\sum_{i=1}^{n} Z_i^2} \tag{2.29}$$

$$e^C = \frac{2(1-\rho)s_Y\, s_X}{\frac{1}{n}\sum_{i=1}^{n} Z_i^2} \tag{2.30}$$

Where $\overline{Y}, \overline{X}$, s_Y, s_X are the sample means and standard deviations of the observed and predicted values, respectively, and ρ is the correlation between the two sets of measurements. The bias proportion reflects the systematic error. The variance proportion indicates how well the model replicates the variability in the observed data. These two proportions should be as small as possible. The covariance proportion measures the remaining error and therefore should be close to one. If the different measurements are taken from non-stationary processes, the proportions can be viewed only as indicators of the sources of error.

Rouphail et al. (1997) conducted a study with the objective of validating the generalized delay model for vehicle-actuated traffic signals using both TRAF-NETSIM simulation and field data. The generalized delay model was developed to account for the limitations of the 1994 HCM delay equation. The simulation study methodology involved a comparison of the delay from four different vehicle-actuated traffic signal designs. An intersection with ideal traffic (no turning or heavy vehicles) and geometry of 3.6 m wide lanes, and two lanes on each approach was used in the analysis. Mean headways, start-up

lost times, and free-flow speeds of 1.9 s, 2.5 s, 37 mph, respectively, were used as base conditions in all simulation run. And for these base conditions, the minimum and maximum green times were set at 10 s and 50 s., respectively, for each phase. The cycle length was limited to 98 s. Four levels of traffic volume were used, ranging from 400 to 1600 vph for the cross street and 500 to 2000 vph for the main street. Furthermore, four different vehicle-actuated signal timing strategies were simulated for a total of 64 different study conditions (4x4x4). Each of the 64 conditions was simulated for ten 15-min periods (i.e. T=0.25hr) for consistency with the 1994 HCM procedure. This resulted in 640 NETSIM runs. To compare the delay values estimated by NETSIM with those estimated by the generalized delay model, the traffic volumes, average queue discharge headway, and average signal timings generated by NETSIM were used as input values in the generalized delay model. Saturation flow rates were computed as inverse of headway. According to the results, the study concluded it was evident that the delay computed using the generalized delay model was consistent with NETSIM delay.

In addition to the simulation study, the research team also conducted a field study at three sites in North Carolina. The HCM methodology was followed in the collection of the data at all sites. Data were collected on a cycle-to-cycle basis and aggregated to 15 min blocks during the data reduction. The data collected included signal timing data, traffic demand data, and stopped delay. These data were collected both manually and by video recording. The delay from the HCM delay model and the generalized model was compared with delays observed in the field. The result shows that both models predicted nearly identical delays; however, both models slightly under predicted delays observed in the field. Also, when compared with the HCM`s, the mean squared error for the

generalized delay model was much closer to the mean squared error value observed in the field. The study concluded that the generalized model was a better predictor of observed delays.

Oh et al. (2003), carried out a study aimed at validating the individual crash models intended for use in the Interactive Highway Safety Design Model (IHSDM). The Federal Highway Administration sponsored the development of the IHSDM, which is roadway design and resign software that estimates the safety effects of alternative designs. The validation methodology included: a) Internal Model Validation; b) External Model validation. Internal model validation, as applied in this research, focused on the ability of the intersection crash models to explain the underlying phenomenon. External validation, on the other hand, was concerned with the model`s ability to predict crashes over time and space. External validation is focused on the goodness of fit (GOF) of statistical models to independent data. The research applied several GOF measures to assess the model`s performance. They include:

a) Pearson product moment correlation coefficients between observed and predicted crashes, usually denoted by r, is a measure of the linear association between two variables, Y_1 and Y_2, that have been measured on interval or ratio scales and is given by:

$$r_{12} = \frac{\sum (Y_{i1} - \overline{Y}_1)(Y_{i2} - \overline{Y_2})}{\left[\sum (Y_{i1} - \overline{Y_1}) \sum (Y_{i2} - \overline{Y_2})^2\right]^{1/2}} \tag{2.31}$$

Where, $\overline{Y}$ is the mean of Y_i observations. Theoretically, a model that predicts observed data perfectly will produce a straight-line plot between the observed and predicted values, correlation coefficients of exactly 1.

b) Mean Prediction bias (MPB): provides a measure of the magnitude and direction of the average model bias in comparison with validation data. The smaller the absolute value of average prediction bias is, the better the model does at predicting the observed data. A positive MPB indicates that a model over predicts crashes, on average, while a negative MPB indicates systematic under prediction of crashes, on average. The MPB is given by:

$$\text{MPB} = \frac{\sum_{i=1}^{n} (Y_i - Y_i)}{n} \tag{2.32}$$

Where *n* is the validation data sample size, and Y is the fitted value of *Y*.

c) Mean Absolute Deviation (MAD): provides a measure of the average mis-prediction of the model. It differs from MPB in that positive and negative prediction errors do not cancel. A value close to 0 suggests that, on average, the model predicts the observation data well. MAD is given by:

$$\text{MAD} = \frac{\sum_{i=1}^{n} \left| Y_i - Y_i \right|}{n} \tag{2.33}$$

Where *n* is the validation data sample size.

d) Mean Squared Prediction Error (MSPE) and the Mean Squared Error (MSE): is the sum of the squared differences between observed and predicted crash frequencies divided by the sample size. MSPE is typically used to assess the error associated with s validation or external data set and is given by:

$$\text{MSPE} = \frac{\sum_{i=1}^{n} (Y_i - Y_i)^2}{n_2} \tag{2.34}$$

where, n_2, is the validation data sample size. MSE is the sum of the squared differences between observed and predicted crash frequencies divided by sample size minus the number of model parameters:

$$\text{MSE} = \frac{\sum_{i=1}^{n} (Y_i - Y_i)^2}{n_1 - p} \tag{2.35}$$

where: n_1 is the estimation data sample size, and p is the number of degrees of freedom.

In his dissertation research, Byun (2009), conducted field study with the goal of developing a better understanding of the impact of rain and congested conditions on traffic flow, speed, and capacity. Several speed-flow models were calibrated using data collected at different sites in New Jersey, under varying traffic and weather conditions. In addition to calibrating the speed-flow models, the validation of two selected models was

performed. The model was considered to be "suspect" if the ratio of MSPR and MSE was greater than the critical value determined by the F-distribution F(0.05, n , n^*), where n is the number of cases in the data set for the speed-flow model and n^* is the number of cases in the validation data. For one of the models selected for validation, the MSE and MSPR were found to be 20.4 and 37.18, respectively. This gave a ratio of 1.02. The critical F value was found to be 1.16. This shows that the MSPR does not differ greatly from the MSE for model-building data. This was considered a reasonably indicator of the model`s predictive ability.

CHAPTER 3

METHODOLOGY

3.1 Introduction

This chapter presents the methodology of this research. The methodology is presented in two sections. Section 3.2 presents a method for evaluating the 2010 Highway Capacity Manual platoon dispersion model in estimating the proportion of vehicle arrivals on green at downstream signalized intersections on urban street segments with both friction and non-friction traffic conditions. The model evaluation involves measuring the proportion of arrivals on green obtained at several urban street segments sites and comparing these measured proportions with those predicted using the 2010 HCM procedure. Several statistical tests are then performed to assess how well the model performs under both traffic conditions. Section 3.3 of this methodology accounts for midblock pedestrian activities on urban street segments, including the modification of the HCM segment running time equation by developing a midblock delay model that estimates the delay incurred by platoon vehicles due to midblock pedestrian activities on urban street segments. The final subsection of this methodology presents how the developed midblock delay model can be applied in computing the segment travel speed, a key measure of performance, and subsequently the level of service at which the segment operates.

3.2 Evaluation of the HCM 2010 Platoon Dispersion Model

The first part of the research methodology is to evaluate the performance of the HCM 2010 platoon dispersion model. This is achieved by comparing measured proportion of arrivals on green with those predicted using the 2010 HCM procedure. The first step in estimating the HCM 2010 proportion of arrivals is to compute of the arrival flow profiles at a downstream signalized intersection. The following Figure 3.1 and subsections provide the step by step approach for estimating components used to estimate the arrival flow profile and the proportion of arrivals on green.

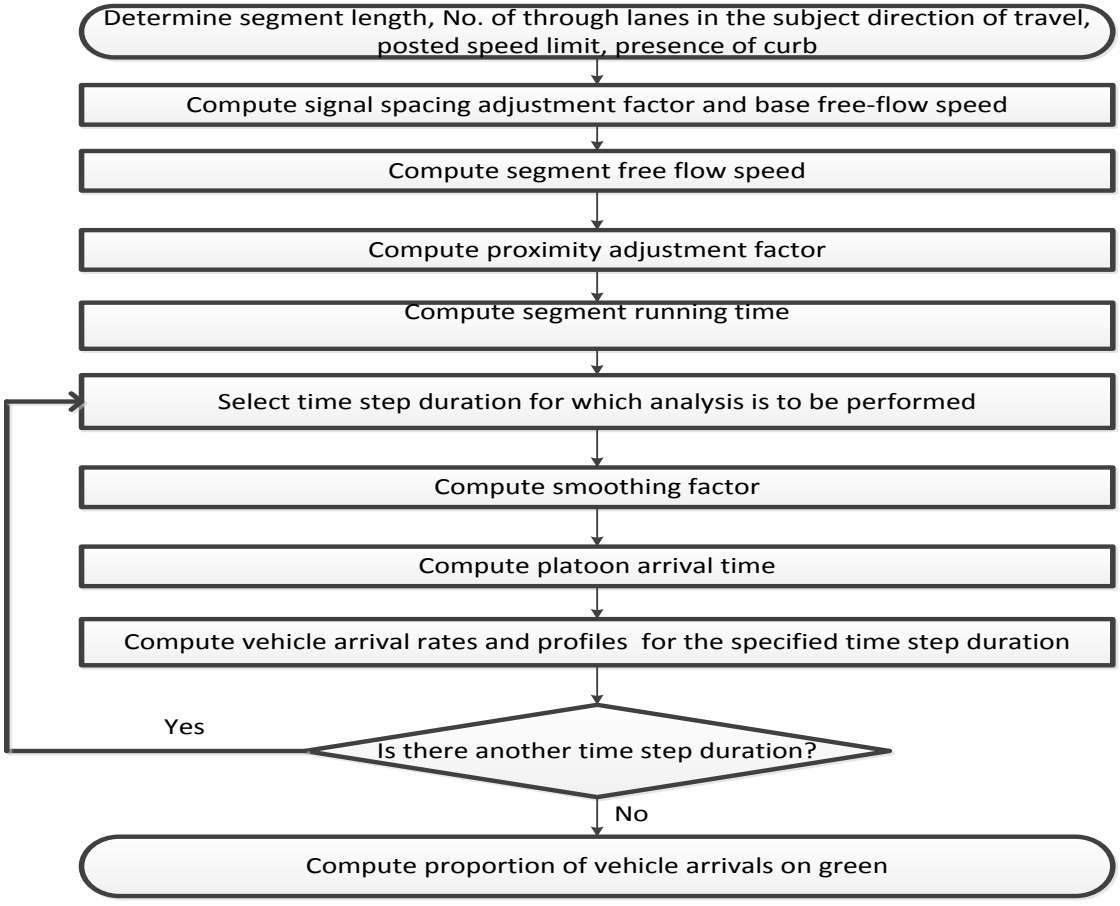

Figure 3.1 Procedure to compute the 2010 HCM vehicle arrival flow profiles and proportion of arrivals on green.

3.2.1 Computation of the Segment Running Time

The 2010 HCM computes the segment running time by taking into consideration the control type at the upstream intersection, the free flow speed, vehicle proximity, and various mid-segment delay sources. The segment running time is shown as follows:

$$t_R = \frac{6.0 - l_1}{0.0025L} f_x + \frac{3,600L}{5,280S_f} f_v + \sum_{i=1}^{N_{ap}} d_{ap,i} + d_{other} \quad (3.1)$$

where:

t_R = Segment running time(s);

l_1 = Start- up lost time (2.0 for signal control);

f_v = Vehicle proximity adjustment factor (f_v = 1.0 for no mid-segment access point);

f_x = 1.0(for signal control);

L = segment length (ft);

S_f = free flow speed (mph);

f_x = control- type adjustment factor, (f_x =1.00 for signal control);

$d_{ap,i}$ = delay due to left and right turns from the street into access point intersection i (s/veh);

N_{ap} = number of influential access point approaches along the segment= $N_{ap,s}$ + $p_{ap,lt} N_{ap,o}$

$N_{ap,s}$ = number of access point approaches along the right side in the subject direction of travel (points);

$N_{ap,o}$ = number of access point approaches on the right side in the opposing direction of travel (points)

$p_{ap,lt}$ = proportion of $N_{ap,o}$ that can be accessed by a left-turn from the subject direction of travel; and

d_{other} = delay due to other sources along the segment (e.g., curb parking, pedestrians, etc.)(s/veh)

The vehicle proximity adjustment factor (f_v) used in Equation 3.1 adjusts the free –flow running time to account for the effect of density due to increase in volume. With an increase in segment volume, the proximity adjustment factor results in increase in

running time and a subsequent decrease in speed. The vehicle proximity adjustment factor (f_v) is computed as follows:

$$f_v = \frac{2}{1+\left(1-\frac{v_m}{52.8 N_{th} S_f}\right)^{0.21}} \tag{3.2}$$

where:

f_v = proximity adjustment factor;
v_m = mid-segment demand flow rate (veh/h);
N_{th} = number of through lanes on the on the segment in the subject direction of travel (ln);
S_f = free-flow speed (mph)

The 2010 HCM defines the free flow speed (S_f) as the average running speed of vehicles traveling within the segment under low-volume conditions. There are several geometric conditions that impact the free flow speed of a roadway, such as speed limit, median type, curb presence, and segment length. The free flow speed is computed based on the base free flow speed and the signal spacing adjustment factor. The free flow speed is computed as follows:

$$S_f = S_{fo} f_L \tag{3.3}$$

where:

S_f = free flow speed (mph);
S_{fo} = base free flow speed;
f_L = adjustment for signal spacing;

The base free flow speed is the free flow speed on longer segments. It accounts for the influence of speed limit, access point density, median type and the presence of curb. The 2010 HCM computes the base free flow speed as follows:

$$S_{fo} = S_o + f_{cs} + f_A \tag{3.4}$$

Where:

S_{fo} = base free flow speed (mph);
S_o = speed constant (mph);
f_{cs} = adjustment factor for cross section (mph);
f_A = adjustment for access points (mph);

The speed constant and adjustment factors in Equation 3.4 are provided in Exhibit 17-11 of the 2010 HCM. The signal spacing adjustment factor (f_L) in Equation 3.3, adjusts the free flow speed based on the spacing between the upstream and downstream signalized intersections. According to the 2010 HCM, the segment length influences a driver`s choice of free-flow speed. It is stated that longer segments have higher free flow speeds. The signal spacing adjustment factor is computed as follows:

$$f_L = 1.02 - 4.7\frac{S_{fo} - 19.5}{\max(L_s, 400)} \leq 1.0 \quad (3.5)$$

Where:

f_L = signal spacing adjustment factor;
S_{fo} = base free-flow speed (mph); and
L_s = distance between adjacent signalized intersection (ft)

3.2.2 Computation of the Smoothing Factor

To estimate the arrival flow profile requires estimating platoon dispersion as vehicles travel from an upstream intersection to a downstream intersection. The smoothing factor is a value between 0 and 1 that describes the probability of a vehicle arriving at a downstream intersection during a specified time step after departing the upstream signalized intersection. The smoothing factor is a function of the segment running time. A decrease in segment running time tends to increase the smoothing factor and vice versa. Seddon (1972) derived a relationship between the smoothing factor and the average increase in platoon running time due to dispersion by taking into consideration the geometric distribution function which is the probability that a vehicle passing a point at the upstream during a time interval will also pass a point at the downstream intersection in the same time interval. The 2010 HCM smoothing factor is derived as a function of the segment running time and time step duration. It is shown as follows:

$$F = \frac{1}{1 + 0.138 t_R / d_t + 0.315 / d_t} \quad (3.6)$$

where:

t_R = Segment running time(s);
d_t = time step duration(s)

3.2.3 Computation of the Platoon Arrival Time

The smoothing factor is then used in the 2010 HCM platoon dispersion model to estimate the platoon arrival time. The platoon arrival time model estimates the platoon arrival time at the downstream signalized intersection after departing from the upstream signalized intersection. The estimated segment running time and smoothing factor are used to estimate the platoon arrival time. The functional form of the platoon arrival time model as presented by Bonneson et al. (2010) and incorporated into the 2010 HCM, is shown as follows:

$$t_p{}' = \frac{t_R}{d_t} - \frac{1}{F} + 1.25 \quad (3.7)$$

where:

$t_p{}'$ = platoon arrival time (step);
t_R = Segment running time(s);
F = predicted smoothing factor.

3.2.4 The Computation of Vehicle Arrival Flow Rates

The estimated smoothing factor and platoon arrival time are then used in the recurrence model to estimate the vehicle arrival flow rates. The recurrence model predicts the arrival flow rate during each time step at a specified location within a roadway segment. The functional form of the 2010 HCM platoon dispersion model is the recurrence model developed by Robertson (1969) based on data collected by others (Hillier and Rothery, 1967). The key differences between the 2010 HCM platoon dispersion model and the platoon dispersion model developed by Robertson (1969) are: the HCM 2010 platoon dispersion model uses a different smoothing factor equation and also provides a platoon arrival time equation for estimating the arrival time of the platoon at the downstream signal. The recurrence model as presented in 2010 HCM is shown as follows:

$$q'_{a/s,j} = Fq'_{s,i} + (1-F)q'_{a/s,j-1} \tag{3.8}$$

$$j = i + t'_p \tag{3.9}$$

where:

$q'_{a/s,j}$ = arrival flow rate in time step j at a downstream intersection from upstream source s (veh/step);

$q'_{s,i}$ = departure flow rate in time step i at upstream source s (veh/step);

F = smoothing factor;

j = time step associated with platoon arrival time t'_p;

t'_p = platoon arrival time.

In computing the platoon arrival flow profiles at a downstream signalized intersection, Equations 3.7 and 3.8 are applied in two steps. The first step involves predicting the platoon arrival time using Equation 3.7. This gives the arrival time of the leading vehicle of the platoon at the specified downstream location. Once the platoon arrival time is computed, the second step involves computing the vehicle arrival flow rate(veh/time step) using the recurrence model in Equation 3.8. The recurrence model uses a discrete iterative technique. The model states that the predicted downstream flow in the first time step *j* is equal to the upstream flow in the first time step *i* multiplied by the smoothing factor F, and the predicted downstream flow in the second time step *j*+1 is equal to the upstream flow in the second time step plus the left over flow in the first time step, all multiplied by the smoothing factor (Denny, 1989). This process of computing the vehicle arrival flow is iterative. It is repeated until all the vehicle arrival flows are computed. This gives an arrival flow profile of all the vehicles in a platoon. Bonneson et al. (2010) illustrates the phenomenon of discharge and arrival flow profiles as shown in Figure 3.2. The figure shows a typical discharge flow profile of a platoon from an upstream signalized intersection and the corresponding arrival flow profile at the downstream signalized intersection. As shown, the discharge rates for the first few vehicles in the platoon are smaller compared to other vehicles and not uniform for each time step. This is because of the startup lost time experienced by those vehicles after the onset of green. The discharge headways for those vehicles are larger than for those vehicles at the rear of the platoon which has the effect of reducing the number of vehicles crossing the stop line during a specified interval (time step). The discharge flow profile for the vehicles in the end of the platoon are not impacted by startup lost time and shows

a uniform discharge flow at the saturation flow rate (vph). The saturation flow rate is the maximum number of vehicles that can cross the stop line during a specified time step. It is achieved once saturation headway is reached. Once the platoon has discharged from the upstream, and dispersed while traveling along the segment, its arrival flow profile as shown in the figure is not as uniform; it spreads out due to platoon dispersion.

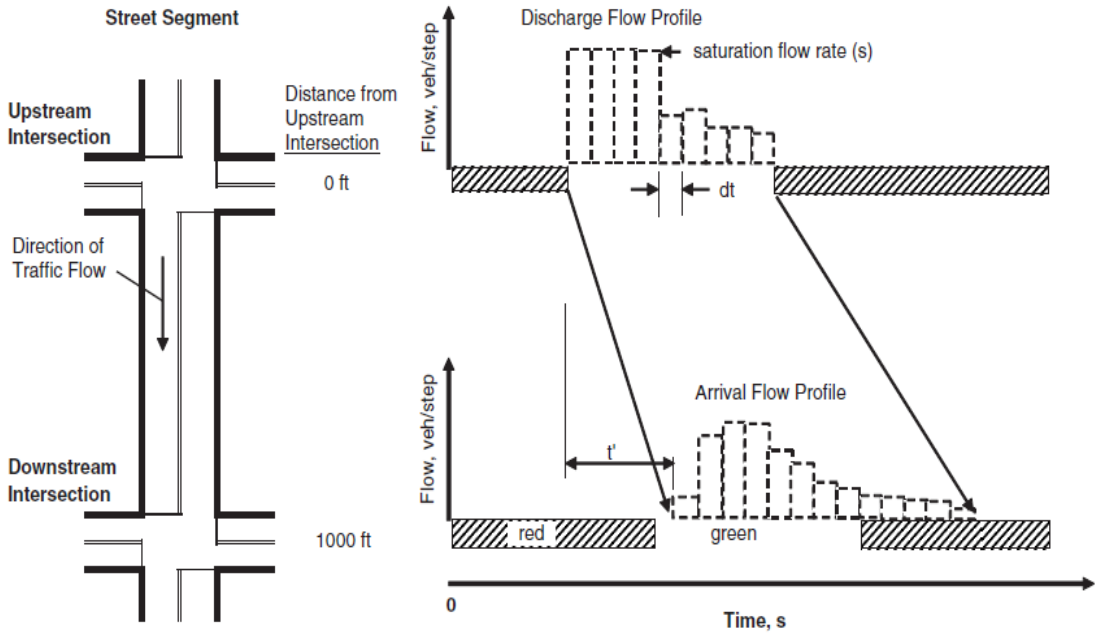

Figure 3.2 Platoon discharge and arrival flow profiles.

Source: Bonesson et al (2010)

3.2.5 Computation of the 2010 HCM Proportion of Arrivals on Green

Once the arrival flow profiles are computed, the next step is to compute the proportion of vehicle arrivals on green. The 2010 HCM Urban Street methodology for computing the proportion of arrivals includes the steps previously discussed and summarized and

presented in Figure 3.1. The 2010 HCM computes the proportion of arrivals on green using the following equation:

$$P = \frac{n_g}{q_d C} \tag{3.10}$$

where:

P =Proportion of vehicles arriving during the green indication;
n_g =arrival count during green (veh);
q_d = arrival flow rate for downstream lane group (veh/s);
C = cycle length(s);

n_g in Equation 3.10 is computed by summing the arrival flow rates for each time step (or interval) that occurs during the effective green period. The arrival flow rate (q_d) is computed as the ratio of the total number of vehicle arrivals (veh) during the cycle to the duration of the cycle.

3.3 Midblock Pedestrian Activity on Urban Street Segments

This section of the methodology presents the development of an integrated deterministic and stochastic (probability) model that estimates the delay incurred by platoon vehicles due to pedestrian activity at midblock crosswalks on urban street segments. In addition to the developing the midblock delay model, a subsection is presented to discuss the application of the developed model in computing the segment travel speed, a key measure of performance of an urban street segment.

3.3.1 Development of Midblock Pedestrian Delay Model

The methodology for accounting for midblock pedestrian activity in the HCM 2010 Urban Street Analysis Chapter involves modifying the HCM 2010 segment running time equation, a key component of the HCM 2010 platoon dispersion model and the segment travel speed equation. The midblock delay model development approach is presented in two parts: the first part develops a deterministic model that estimates delay to platoon vehicles during a midblock interference. This approach is similar to a model development approach presented by Bonneson (1998), and presented in the 2010 HCM. The model developed by Bonneson (1998), estimates the delay to through vehicles due to right-turn activity from the major street onto an access point.

The second part of the development of the midblock delay model involves incorporating a Poisson probability model into the deterministic delay model. The deterministic part of model estimates the delay to vehicles assuming there is a midblock interference. The probability model calculates the probability of a number of midblock interference occurring at a midblock pedestrian crosswalk based on the flow of vehicular and pedestrian traffics.

The midblock delay process is modeled based on a time-space representation of traffic flow along the segment. The trajectories of the leading platoon vehicle and following platoon vehicles are sequentially evaluated to determine the midblock delay. An interference is initiated by a pedestrian entering the cross walk. The leading platoon vehicle may have to slow and/or come to full stop to avoid colliding with the crossing pedestrian(s). A second, third and fourth, etc. following platoon vehicle may also have to slow or stop to maintain a minimum following distance between it and the vehicle ahead.

The delay incurred by each platoon vehicle is computed as the time lag in its trajectory from the start of the midblock interference. The modeling technique used in this research is based partly on driver and pedestrian behavior as observed in the field. Therefore reasonable assumptions are made based on the field observations.

3.3.1.1 Assumptions and Limitations. Pedestrians crossing at midblock crosswalks on urban street segments often interrupt the flow of traffic and consequently delaying vehicles. Vehicles are delayed because they have to reduce speed and, sometimes come to a full stop to avoid a collision with pedestrian(s). This delay can be several seconds in duration for the first few vehicles but will tend to decrease for the following platoon vehicles as the need for speed diminishes. For the midblock delay model development, the following assumptions and limitations are presented:

- The model is developed for passenger car streams; however, it can be extended to mixed traffic streams through modifications of selected input parameters.

- Vehicles are assumed to travel at the free flow speed. Vehicles that are delayed by pedestrian crossings at midblock will decelerate from this speed and then accelerate back to it. The assumption of a constant for all vehicles is consistent with the speed-volume relationship shown in the HCM 1994, for flow rates less than 1000 pcphpl.

- Flow conditions in the subject lane(s) are assumed to be uncongested with an average flow rate of 1000vphpls or less. This assumption will insure that each event is independent of any preceding event. At flow rates above 1000vphpl, speed reductions and subsequent delays due to density-related vehicle interaction will exceed the delays due to midblock pedestrian crossings.

- Vehicles are assumed to have constant deceleration and acceleration rates.

- The volume to capacity ratio is approximately equal to one at the upstream signalized intersection. Therefore, there is a stable queue discharge during the entire duration of the green time. The discharge headway therefore tends towards a constant value known as the *saturation headway*. The platoon size is therefore consistent for each cycle.

- It is assumed that the driver of the leading platoon vehicle sees the pedestrian/pedestrians already inside or as they enter the crosswalk. Hence, the start of an interference and delay process.

- Pedestrians always have the Right-of-Way.

- Pedestrian arrivals and crossings at midblock crosswalks follow a Poisson distribution. This assumption may change or vary depending on the pedestrian volume.

***Step 1**: Compute the Platoon Size.* The first step in the midblock delay model development is determining the platoon size (veh) discharging from the upstream signalized intersection during each cycle. The platoon size is based on the duration of the effective green time per phase, the start-up lost time and the saturation headway. Therefore, it is possible to model the amount of green time required to discharge a platoon of vehicles as follows:

$$T_g = l_1 + nh \tag{3.11}$$

Rearranging Equation 3.11 gives the platoon size as follows:

$$n = \frac{T_g - l_1}{h}$$

where:

T_g = Green time at upstream signal, sec/phase
l_1 = start-up lost time, s
n = platoon size, vehs
h =saturation headway, s/veh

Step 2: *Compute Delay to the Leading Platoon Vehicle.* At the start of a midblock interference, the leading vehicle of a platoon will decelerate from its free flow speed to slow down and/or come to a complete stop; and then accelerate to that speed after the interference ends. Therefore, the model is developed based on two scenarios.

In scenario 1, the interference starts when the pedestrian has already entered the crosswalk, assumed to be mid-way of the lane(s) in the study direction. In this scenario, the leading vehicle of the platoon slows down but does not come to a full stop during the interference. The driver of the leading platoon vehicle will be delayed by pedestrians if his/her headway is sufficiently short as to require braking to avoid hitting a pedestrian(s). If the driver of the leading platoon vehicle has headway less than this critical headway, then he/she will initiate braking at the 'critical decision point' and decelerates to a safe speed sufficient to avoid colliding with the pedestrian(s).

In scenario 2, the interference starts as the pedestrian(s) enters the crosswalk. In this scenario, the leading vehicle of the platoon comes to a full stop because it will take longer time for the pedestrian(s) to cross the segment. The driver perceives an unsafe distance and therefore initiates braking and comes to a full stop.

The following parts of this section present a derivation of the deterministic midblock delay models for both scenario1 and scenario 2. The model is derived based on the delay incurred by the leading and following platoon vehicles. At the onset of a midblock interference, the driver of the leading platoon vehicle initiates braking and decelerates from the free-flow speed (initial speed) to a minimum speed (final speed) so as to avoid colliding with crossing pedestrian(s). From basic physics equation of rectilinear motion and assuming constant deceleration and acceleration rates, the final

speed of the leading vehicle after the start of interference and the driver initiate braking, is given as follows:

$$s_m^2 = 1.47 s_f^2 + 2(-r_d)\,\mathrm{D}_d \tag{3.12}$$

where:

s_m = final vehicle speed, ft / s

s_f = initial vehicle speed (assumed to be the free flow speed), mi / h

r_d = deceleration rate (assumed negative for deceleration), ft / s^2

D_d =deceleration distance (practical stopping distance), ft

Rearranging Equation 3.12 gives

$$D_d = \frac{1.47 s_f^2 - s_m^2}{2 r_d} \tag{3.13}$$

Once the interference ends, the driver will start to accelerate from its final speed back to the free-flow speed. Therefore the free-flow speed in Equation 3.12 becomes the final speed, while the final vehicle speed during the interference becomes the initial speed. Hence,

$$1.47 s_f^2 = s_m^2 + 2 r_a D_a \tag{3.14}$$

where:

r_a = acceleration, ft / s^2

D_a =acceleration distance, ft

Rearranging Equation 3.14 gives the distance during acceleration is given as follows:

$$D_a = \frac{1.47 s_f^2 - s_m^2}{2 r_a} \tag{3.15}$$

The total distance associated with a delay, D_T, is obtained by summing Equations 3.13 and Equation 3.15. This gives:

$$D_T = \frac{1.47 s_f^2 - s_m^2}{2} \left(\frac{1}{r_d} + \frac{1}{r_a} \right) \tag{3.16}$$

D_T in Equation 3.16 is related to the free-flow speed s_f and delay time based on scenario 1, $d_{scenario1}$. Therefore, rearranging Equation 3.16 gives the total delay incurred by the leading platoon vehicle based on scenario 1 as follows:

$$d_{scenario1} = \frac{1.47 s_f^2 - s_m^2}{2 s_f} \left(\frac{1}{r_d} + \frac{1}{r_a} \right) \tag{3.17}$$

If the leading platoon vehicle slows down but does not come to a full stop, then the driver reduces his/her speed from the free-flow speed to a minimum speed to avoid colliding with the pedestrian(s). The time associated with this minimum speed is based on the time for the pedestrian(s) to cross one-half the width of the crosswalk in the study direction as assumed in scenario 1. This minimum speed (final speed) during interference is computed as the free-flow speed less the speed attained based on deceleration. The minimum speed is given as follows:

For two-lane urban street segment:

$$s_m = 1.47 s_f - r_d \left(\frac{3 L_w}{8 s_{ped}} \right) \tag{3.18}$$

For four-lane (two lanes in each direction) urban street segment:

$$s_m = 1.47 s_f - r_d \left(\frac{3L_w}{16 s_{ped}} \right) \tag{3.19}$$

where:

S_{ped} =average pedestrian walking speed (ft/s),

L_w = length of crosswalk (ft)

The steps in computing the average pedestrian walking distances $3L_w/8$ and $3L_w/16$, and the average pedestrian walking speed in Equations 3.18 and Equation 3.19 are discussed later in this section.

In scenario 2, the driver of the leading platoon vehicle decelerates and comes to a full stop because the interference starts just as the pedestrian(s) enters the crosswalk. In this scenario, the walking time is longer compared to the walking time in scenario 1, wherein the pedestrian(s) was already midway through the length of the crosswalk in the study direction. Therefore, because the leading platoon vehicle comes to a full stop, the final speed (minimum speed) during interference is zero. Therefore Equation 3.13 and 3.15 become Equation 3.20 and 3.21, respectively as shown below:

$$D_d = \frac{s_f^2}{2r_d} \tag{3.20}$$

$$D_a = \frac{s_f^2}{2r_a} \tag{3.21}$$

Therefore, the total distance associated with delay, D_T, is obtained by summing the deceleration distance in Equations 3.20 and the acceleration distance in Equation 3.21. This gives:

$$D_T = \frac{s_f^2}{2}\left(\frac{1}{r_d} + \frac{1}{r_a}\right) \tag{3.22}$$

D_T in Equation 3.22, is related to the free-flow speed s_f and delay time in scenario 2, $d_{scenario2}$. Therefore, rearranging Equation 3.22 gives the following:

For two-lane urban street segment:

$$d_{scenario2} = \frac{1.47S_f}{2}\left(\frac{1}{r_d} + \frac{1}{r_a}\right) + \left(\frac{3L_W}{4S_{Ped}} - \frac{1.47S_f}{r_d}\right) \tag{3.23}$$

For four-lane (two lanes in each direction) urban street segment:

$$d_{scenario2} = \frac{1.47S_f}{2}\left(\frac{1}{r_d}+\frac{1}{r_a}\right)+\left(\frac{3L_W}{8S_{Ped}}-\frac{1.47S_f}{r_d}\right) \quad (3.24)$$

where $\frac{3L_W}{4S_{Ped}} \geq \frac{1.47S_f}{r_d}$ and $\frac{3L_W}{8S_{Ped}} \geq \frac{1.47S_f}{r_d}$

The second component in Equation 3.23 and 3.24 represents the amount of time the leading platoon vehicle will be delayed after coming to a full stop for the pedestrian(s) to clear the crosswalk. It is the difference between the pedestrian walking time and the time from the start of interference to the vehicle coming to a full stop (i.e., the time for the leading platoon vehicle to decelerate to a stop). All variables are as previous defined. The steps in computing the average pedestrian walking distances $3L_w/4$ and $3L_w/8$, and the average pedestrian walking speed in Equations 3.23 and Equation 3.24 are discussed later in this section.

The average pedestrian walking distances discussed above are computed based on the field observations of the pedestrian walking distances during interference and a reasonable assumption based on scenario 1. those However, there is a New Jersey State law that mandates drivers to stop and remain stopped until pedestrian cross a specified distance of when crossing within a crosswalk. The New Jersey State Law on pedestrian crossing within a marked crosswalk states "…*the driver of a vehicle shall stop and remain stopped to all allow a pedestrian to cross the roadway within a marked*

crosswalk, when the pedestrian is upon, or within one lane of, the half of the roadway, upon which the vehicle is traveling or onto which it is turning. ***Half of roadway*** *means all traffic lanes conveying traffic in one direction of travel"*. Based on this law, the delay incurred by platoon vehicles in midblock crosswalks on urban street segments is increased because vehicles must stop for longer time than what was observed in the field. Therefore for scenario 1, in which it is assumed the pedestrian or group of pedestrians is already in the crosswalk in the study direction before the interference, the delay to the leading platoon vehicle is given as follows:

$$d_{scenario1} = \frac{1.47 s_f^2 - s_m^2}{2 s_f} \left(\frac{1}{r_d} + \frac{1}{r_a} \right) \tag{3.25}$$

If the leading platoon vehicle slows down but does not come to a full stop, then the driver reduces his/her speed from the free-flow speed to a minimum speed. The time associated with this minimum speed is based on the time for the pedestrian(s) to cross one-half the critical length of the midblock crosswalk. The critical length of the midblock crosswalk is the longest distance vehicles are required to be stopped for a pedestrian or group of pedestrians to cross. According to the New Jersey State Law, the average walking distance in crosswalks on two- lane urban street segments is one-half the critical length (i.e. the actual length) of the crosswalk. The average walking distance on four -lane urban street segment is one-half the length of the critical distance. The critical walking distance on four-lane urban street segment is three-fourth the actual length of the

crosswalk. Therefore, for scenario 1, the minimum speed of the leading platoon vehicle during interference is given as follows:

For two-lane urban street segment:

$$s_m = 1.47 s_f - r_d \left(\frac{L_w}{2 s_{ped}} \right) \tag{3.26}$$

For four-lane (two lanes in each direction) urban street segment:

$$s_m = 1.47 s_f - r_d \left(\frac{3 L_w}{8 s_{ped}} \right) \tag{3.27}$$

All variables are as previous defined. The steps in computing the average pedestrian walking distances $L_w/2$ and $3L_w/8$, and the average pedestrian walking speed in Equations 3.26 and Equation 3.27 are discussed later in this section.

In scenario 2, the interference starts as the pedestrian or group of pedestrians enters the crosswalk. Unlike scenario 1, the critical walking time is increased. Therefore, the leading platoon vehicle slows and then comes to a full stop. The stopped delay is the difference in time between the critical pedestrian walking time and the time for the vehicle to slow down. The critical length of the midblock crosswalk is the longest distance vehicles are required to be stopped for a pedestrian or group of pedestrians to

cross. According to the New Jersey State law, the average walking distance in crosswalks on two- lane urban street segments is the critical length (actual length) of the crosswalk. The average walking distance on four -lane urban street segment is the critical walking distance, which is three-fourth the actual length of the crosswalk. Therefore, for scenario 2, the delay incurred by the leading platoon vehicle during interference is given as follows:

For two-lane urban street segment

:

$$d_{scenario2} = \frac{1.47S_f}{2}\left(\frac{1}{r_d} + \frac{1}{r_a}\right) + \left(\frac{L_W}{S_{Ped}} - \frac{1.47S_f}{r_d}\right) \tag{3.28}$$

For four-lane (two lanes in each direction) urban street segment:

$$d_{scenario2} = \frac{1.47S_f}{2}\left(\frac{1}{r_d} + \frac{1}{r_a}\right) + \left(\frac{3L_W}{4S_{Ped}} - \frac{1.47S_f}{r_d}\right) \tag{3.29}$$

where $\frac{L_W}{S_{Ped}} \geq \frac{1.47S_f}{r_d}$ and $\frac{3L_W}{4S_{Ped}} \geq \frac{1.47S_f}{r_d}$.

All variables are as previous defined. The steps in computing the average pedestrian walking distances $L_w/2$ and $3L_w/4$, and the average pedestrian walking speed in Equations 3.28 and 3.29 are discussed later in this section.

***Step 3**: Compute Delay to the Second and Subsequent Platoon Vehicles.* Once the delay the delay to the leading platoon vehicle is computed, the next step is to compute the delays to second and subsequent platoon vehicles. The delay to the second and subsequent vehicles is incurred indirectly due to a shock wave that propagates upward in the platoon once the leading platoon vehicle is interrupted by a pedestrian crossing. Typically on urban street segments, a platoon travelling from an upstream signalized intersection to a downstream signalized intersection disperses as it travels downstream due to drivers` desire to increase their speeds. This phenomenon, as defined previously, is called platoon dispersion. As a platoon disperses, the headways between vehicles increase. Therefore, the delay incurred by a leading platoon vehicle at a midblock pedestrian crosswalk on urban street segment would be greater than the second and subsequent following platoon vehicles. Therefore the delay to second platoon vehicle is the delay to the leading platoon vehicle less a critical headway between platoon vehicles. The HCM 2010 computes the delay to second and subsequent platoon vehicles as follows:

$$d_i = d_{i-1} - (h_{\phi<h<H_i} - \phi) \tag{3.30}$$

where:

$$h_{\phi<h<H_i} = \frac{1}{\mu} + \frac{\phi - H_i e^{-\mu(H_i-\phi)}}{1-e^{-\mu(H_i-\phi)}}$$

$$H_i = d_{i-1} + \phi$$

$$\mu = \frac{1}{1/q_n - \phi}$$

where:

d_{i-1} = delay to the previous platoon vehicle(s/veh)
d_i = the delay to vehicle i (i =3,4,.., n).
$h_{1\phi<h<H_1}$ = average headway of those headways between ϕ and H_1,
H_i =maximum headway that a following p vehicle can have and still incur delay(s/veh).
ϕ =headway of bunched vehicle stream=1.5(s/veh)(HCM 2010) ,
μ =flow parameter (veh/s),
q_n =flow rate per lane = v_n / 3600 (veh/s),
v_n = flow rate per lane (veh/h/ln)

Step 4*: Compute the Delay in Second Per Vehicle.* Once the delay to each platoon vehicle per interference is computed, the next step is to compute the delay in second per vehicle during interference. This delay is computed by first estimating the number of interference based on the pedestrian volume and traffic volume at the midblock crosswalk. Subsequently, the delay in second per vehicle at a midblock crosswalk on urban street segment is computed for a typical analysis period. This delay is computed as follows: by dividing the total delay per interference, $d_{ped/\text{int}}$, by the expected number of vehicles per midblock pedestrian interference, $n_{ped/\text{int}}$ during an hour . This is given as follows:

$$d_{ped} = \frac{d_{ped/\text{int}}}{n_{ped/\text{int}}} \tag{3.31}$$

where:

d_{ped} = midblock delay in seconds per vehicle;
$d_{ped/\text{int}}$ = total delay per interference(s);
$n_{ped/\text{int}}$ = number of vehicles per midblock interference per analysis period (veh)

$n_{ped/\text{int}}$ in Equation 3.31 is computed by dividing the total number of platoon vehicles per hour by the number of interference per analysis period . The equation incorporates a Poisson probability model that calculates the probability of a midblock interference occurring per second of analysis period. It is given as follows:

$$n_{ped/\text{int}} = \frac{nN_c}{\left(1 - e^{-\frac{\lambda}{N_s}}\right) N_s} \tag{3.32}$$

where:

N_s = analysis period in seconds.

N_c = number of cycles at the upstream signal during an analysis period;

$d_{ped/\text{int}}$ in Equation 3.31 is the sum of delay incurred by each platoon vehicle during a midblock interference. It is given as follows:

$$d_{ped/\text{int}} = \sum_{i=1}^{n} d_i \tag{3.33}$$

Therefore, the delay in second per vehicle during an analysis period is given as follows:

$$d_{ped} = \frac{\left(\sum_{i=1}^{n} d_i\right) * \left(1 - e^{-\frac{\lambda}{N_s}}\right) N_s}{nN_c} \tag{3.34}$$

The mean number of midblock pedestrian interference is estimated as an exponential function of traffic volume per hour and the pedestrian volume per hour. It is given as follows:

$$\lambda = e^{\gamma + \alpha_1 v + \alpha_2 pv} \tag{3.35}$$

where:

λ = estimated mean of midblock pedestrian interference per hour;
γ = model intercept
v = traffic volume at the midblock crosswalk (veh/hr.);
pv = pedestrian volume at midblock crosswalk (peds/hr);
α_1 and α_2 = coefficients of the variables of v and pv ,respectively

The final step in accounting for midblock pedestrian activity urban street segments in the HCM 2010 methodology is to modify segment running time in s/veh. The current form of the HCM 2010 segment running time equation estimates the running time of vehicles on the segment based on the geometric, operational and traffic control characteristics of both the segment and traffic signals. Therefore, for urban street segments with midblock pedestrian activity, the HCM 2010 segment running time is modified to account for this friction condition by adding Equation 3.34 to Equation 3.1.

This gives the modified segment running time equation for an urban street segment with midblock pedestrian activity as follows:

$$R_T = \frac{6.0 - l_1}{0.0025L} f_x + \frac{3,600L}{5,280S_f} f_v + \sum_{i=1}^{N_{ap}} d_{ap,i} + d_{ped} + d_{other} \tag{3.36}$$

3.3.1.2 Average Pedestrian Walking Distance. The following is the step involved in computing the average pedestrian walking distances during a midblock interference on two-lane and four-lane urban street segments as shown in Equations 3.18, 3.19, 3.23 and 3.24, 3.26, 3.27, 3.28, 3.29 Figure 3.3 and Figure 3.4 below show the outlines of the pedestrian crosswalks at the study sites on Warren Street and Martin Luther King Blvd in Newark, New Jersey, respectively. Figure 3.3 is a two-lane urban street segment and Figure 3.4 is a four-lane urban street segment. On urban street segments, pedestrians cross in two directions. The points of entry into the crosswalks are indicated as point A and point B in Figure 3.3 and Figure 3.4

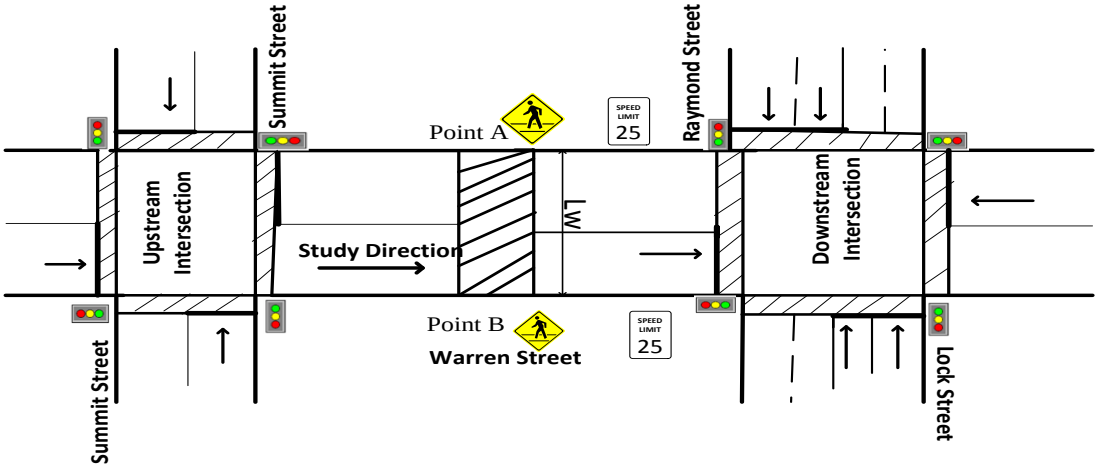

Figure 3.3 Outline of midblock pedestrian crosswalk at Site 1.

For scenario 1 on a two-lane urban street segment, the pedestrian is assumed to have walked one-half the critical walking distance before the start of the interference. The critical walking distance is defined as the distance a pedestrian would have to walk during interference. Let L_w equal the length of the entire pedestrian crosswalk. Based on the previous assumption, field observation and driver behavior; for platoon vehicles in the study direction in Figure 3.3:

- The longest pedestrian walking distance during interference is $L_w/2$. That is the driver of the leading platoon vehicle slows down for a pedestrian crossing from point A to point B, but has already walked one-half of the critical walking distance, which in this case is the length of the crosswalk.
  .
- The shortest pedestrian walking distance during interference is $L_w/4$. That is the driver of the leading platoon vehicle slows for a pedestrian crossing from point B to point A, but has already walked one-fourth of the critical walking distance (length of cross walk) or one-half of the length of lane in the study direction.

- The average pedestrian walking distance during an interference is $3L_w/8$

For scenario 2 on two-lane urban street segments the critical walking distance in the study direction is equal to the entire length of the crosswalk. In other words, vehicles in the study direction are interrupted by pedestrians just as they enter the crosswalk Therefore,

- The longest walking distance during interference is a pedestrian crossing from point A to point B, and is equal to L_w .

- The shortest pedestrian walking distance is for a pedestrian crossing from point B to point A. Based on field observation, for a pedestrian crossing from point B to point A, the driver of the leading platoon vehicle will start to accelerate once the pedestrian crosses one- half the length of the crosswalk. Therefore, the shortest walking distance during an interference is $L_w/2$

- The average pedestrian walking distance during an interference is $3L_w/4$

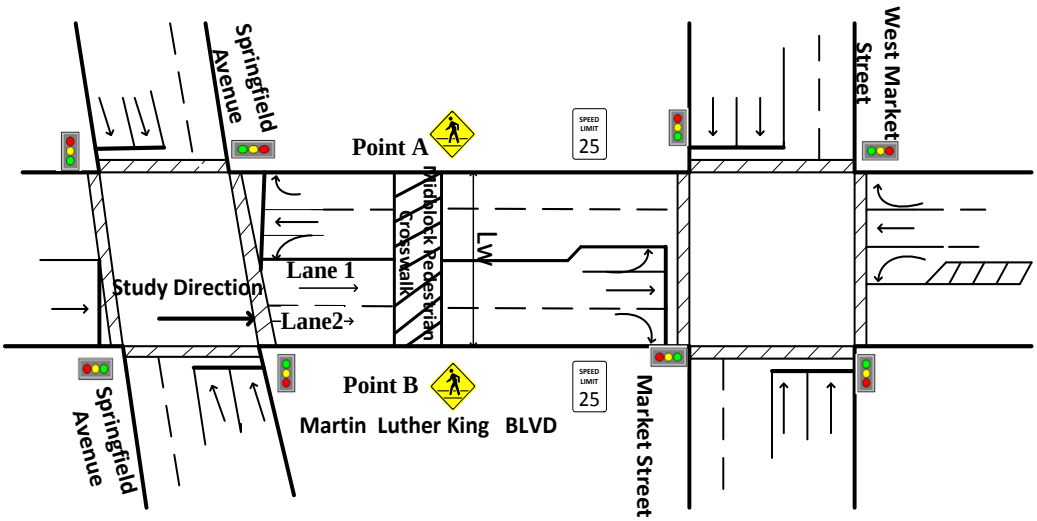

Figure 3.4 Outline of midblock pedestrian crosswalk at Site 2.

For scenario 1 on a four-lane urban street, the pedestrian is assumed to have walked one-half the critical walking distance before the start of the interference For four-lane urban street segments the critical length of the crosswalk is one-half of the entire length of crosswalk. Therefore,

- The longest pedestrian walking distance (point B to point A) during interference for vehicles in lane 1 is $L_w/4$. This is because the pedestrian would have walked one-half of the critical length of the crosswalk or the entire length of lane 2 before the start of the interference.

- The shortest pedestrian walking distance during interference for vehicles in lane 1 is $L_w/8$. This is because the pedestrian would have walked one-half of the lane width of lane1 or one-fourth of the critical length of the crosswalk.

- The average pedestrian walking distance during an interference for vehicles in lane 1 is $3L_w/16$
- The same procedure yields the average pedestrian walking distance during an interference for vehicles in lane 2 as $3L_w/16$

For scenario 2 on four-lane (two lanes in each direction) urban street segment:

- The longest pedestrian walking distance (point B to point A) during interference for vehicles in Lane 1 is $L_w/2$. That is the leading platoon vehicle in lane 1 yields to a pedestrian that has just entered the crosswalk from point B.
- The shortest pedestrian walking distance (point A to point B) during an interference for vehicles in Lane 1 is, $L_w/4$. That is the driver of the leading platoon starts to accelerate once the pedestrian crosses the entire length of lane 1 or one-half of the critical distance.
- The average pedestrian walking distance during an interference for vehicles in Lane 1 $3L_w/8$.
- The same procedure yields the average pedestrian walking distance during an interference for vehicles in lane 2 as $3L_w/8$.

Based on the New Jersey Law, "The driver of a vehicle shall stop and remain stopped to all allow a pedestrian to cross the roadway within a marked crosswalk, when the pedestrian is upon, or within one lane of, the half of the roadway, upon which the vehicle is traveling or onto which it is turning. ***Half of roadway*** means all traffic lanes conveying traffic in one direction of travel".

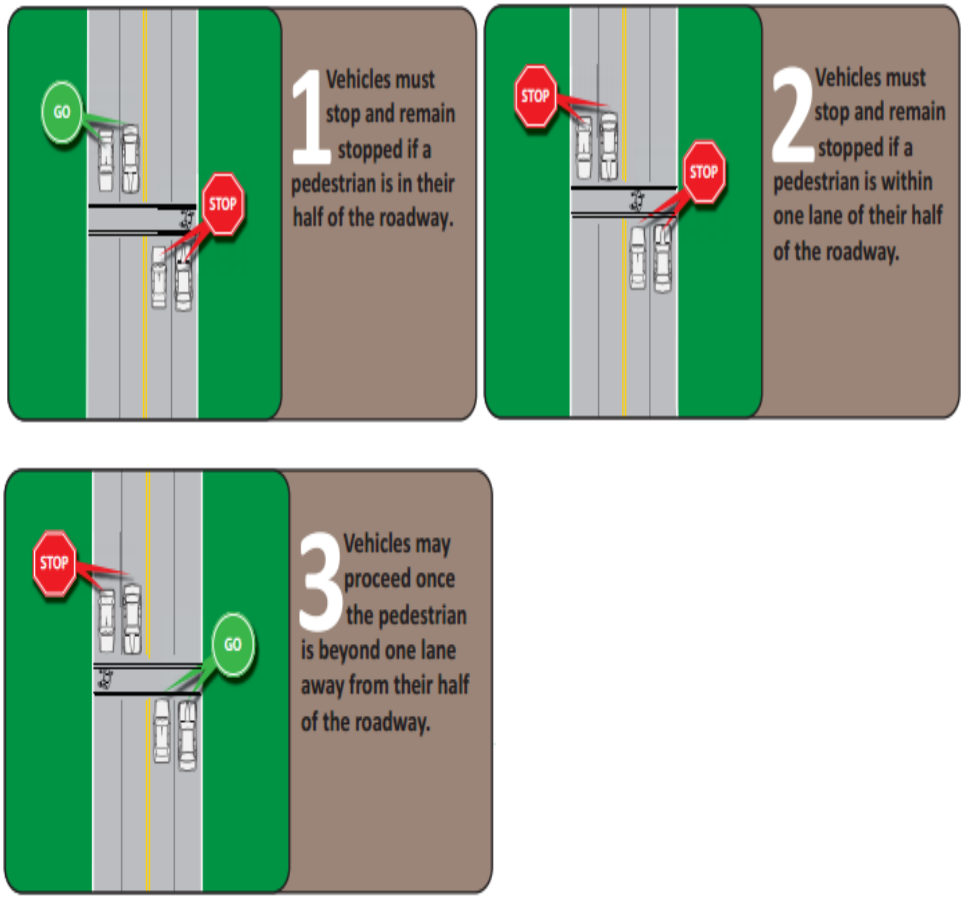

Figure 3.5 Illustration of the New Jersey law on pedestrian crossing within midblock crosswalks on four –lane urban street segment.

Based on the New Jersey Law, "The driver of a vehicle shall stop and remain stopped to all allow a pedestrian to cross the roadway within a marked crosswalk, when the pedestrian is upon, or within one lane of, the half of the roadway, upon which the vehicle is traveling or onto which it is turning. ***Half of roadway*** means all traffic lanes conveying traffic in one direction of travel". Based on this Law, there is increase in the pedestrian walking time and therefore on scenario 2 holds true as all interrupted platoon vehicles will come to a full stop. From the graphics in Figure 3.6, on crosswalks on four-lane (two lanes in each direction) urban street segments, the pedestrian walking distance is three-fourth the length of the midblock crosswalk, i.e. $3L_w/4$.

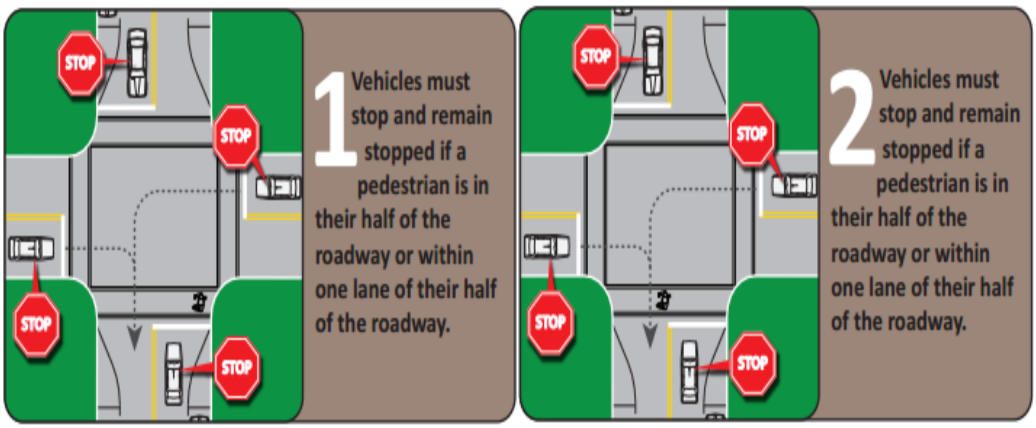

Figure 3.6 Illustration of the New Jersey law on pedestrian crossing within pedestrian crosswalks on two –lane urban street segment.

On midblock crosswalks on two-lane (single lane in each direction) urban street segments, the critical walking distance is the same as the actual length of the crosswalk. This is because vehicles must stop and remain stopped until a pedestrian or group of pedestrians cross the entire crosswalk.

3.3.1.3 Average Pedestrian Walking Speed. At signalized intersections on dense urban street segments, pedestrians sometimes cross in groups within midblock crosswalks. In such situation, the pedestrian walking time will be greater than that for a single pedestrian. This, therefore, increases the delay incurred by platoon vehicles; especially at midblock crosswalks. The HCM 2010 Urban Street methodology describes a procedure for computing the average walking speed of pedestrians crossing at crosswalks on urban street segments. The HCM 2010 average walking speed is computed as a function of the pedestrian flow per unit of sidewalk and the free-flow pedestrian walking speed. According to the HCM 2010, the free-flow speed reflects the speed at which pedestrians walk under conditions of negligible pedestrian -to-pedestrian conflicts and negligible adjustments in a pedestrian`s desired walking path to avoid other pedestrians. The HCM

2010 average pedestrian walking speed equation has been modified in this research to account for the average speed per midblock interference. The HCM 2010 computes the pedestrian flow per unit width of sidewalk as follows:

$$v_p = \frac{v_{ped}}{60W_E} \tag{3.36}$$

where:

v_p = Pedestrian flow per unit width of sidewalk (p/ft/min),
v_{ped} = Pedestrian flow rate in the subject sidewalk (in both directions) (p/hr),
W_E = effective width of sidewalk

The above equation has been modified to compute the pedestrian flow rate per unit width of midblock crosswalk per interference. The modified equation is given as follows.

$$v_{p/\text{int}} = \frac{v_{ped}}{N_{\text{int}}W} \tag{3.37}$$

where:

$v_{p/\text{int}}$ =pedestrian flow per unit width of midblock crosswalk per interference p/ft/interference)
v_{ped} = pedestrian flow rate in the midblock crosswalk (walking in both directions) (p/hr),
N_{int} = number of interference per analysis period,
W = width of midblock crosswalk (ft)

$$N_{\text{int}} = \left(1 - e^{-\frac{\lambda}{3600}}\right) N_s \tag{3.38}$$

The average pedestrian walking speed is therefore given as follows:

$$s_{ped} = (1 - 0.00078 v_{p/\text{int}}^2) s_{pf} \geq 0.5 s_{pf} \tag{3.39}$$

where:

s_{ped} = average walking speed (ft/s);
s_{pf} = free-flow pedestrian walking speed (ft/s);

The HCM 2010 recommends a free-flow speed of 4.4 ft/s for segment evaluation if 0% to 20% of pedestrians traveling along the segment subject direction are elderly(i.e., 65 years of age or older). However, if more than 20% of pedestrians are elderly, an average free-flow walking speed of 3.3 ft/s is recommended. These values are the free-flow walking speeds for sidewalk, and maybe different from those for midblock crosswalk. This research has measured pedestrian walking speeds at midblock crosswalk for various age groups. This data are presented and discussed in the following chapter.

3.3.2 Application of the Developed Midblock Delay Model

This subsection presents the application of the developed midblock pedestrian delay model in evaluating the performance of automobile on urban street segments. The 2010 HCM segment running time equation in its present form, as shown in Equation 3.1, estimates the running time based on the segment`s operational, geometric and traffic control characteristics. The equation incorporates a component that accounts for other

delays, d_{other}, which is described in the 2010 HCM as delay due to other sources along the segment(e.g. curb parking, pedestrian etc) in s/veh . It does not, however, provide specific values to adjust the segment running time. In addition, these delay values cannot be easily measured or estimated by users of the model. On urban street segments with midblock pedestrian activity, there are interruptions to vehicular traffic which in turn increase in the vehicle running times between the upstream stream and downstream signalized intersections. As a consequence of vehicular interruptions and delays, the speed at which vehicles travel on the segment increases.

The first step in applying the developed midblock delay model is to determine the platoon size based on signal timings at upstream signalized intersection. Once the platoon size (veh.) is determined, the next step is to determine whether there is midblock pedestrian activity on the segment. If there is no midblock pedestrian activity, the segment running time, platoon arrival time, proportion of arrivals on green, control delay and travel speed are computed as presented in the HCM 2010. Otherwise, the segment travel speed is computed as shown in the flow chart in Figure 3.7.

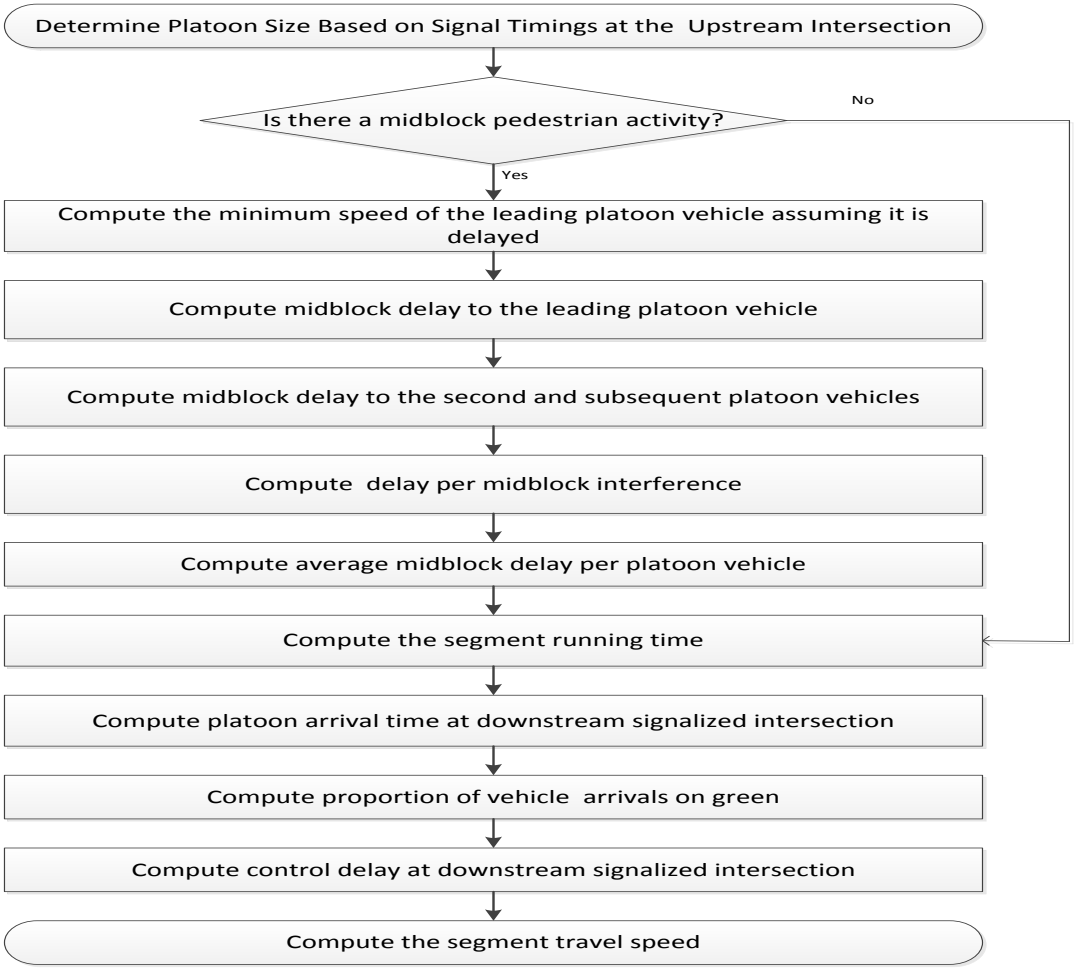

Figure 3.7 Application of the developed midblock pedestrian delay model.

3.3.1.4 Statistical Evaluation Approach. This subsection describes the statistical approach for evaluating the HCM 2010 platoon dispersion model and validating the developed midblock delay model. The approach is presented in two parts. The first part involves measures of performances to quantify the difference between the observed (measured) and predicted (or estimated) variables. This is referred to as quantitative technique. The second part involves the use of statistical plots to compare the set of variables. This is referred to as qualitative technique.

Quantitative techniques, also known as objective, numerical or formal techniques on some other occasions, quantify the difference between the observed and predicted (estimated). Quantitative validation techniques include, but not limited to

- Goodness-of-fit measures
- Hypothesis testing and confidence intervals

Goodness-of-Fit Measures: A number of goodness-of-fit measures can be used to evaluate the overall performance of the measures of performance (MOPs). Three frequently used goodness-of-fit measures are the root-mean-square error (RMSE), the root-mean-square percent error (RMSPE) and the mean absolute percent error (MAPE). These statistics quantify the overall error of the MOPs. Percent error measure provides information on the magnitude of the error relative to the average measurement. These measures as presented by Ni et al. (2004) are given below:

Suppose there are two processes X (the predicted or measured) and Y (the observed): $X_1, X_2, \ldots, X_n$ and $Y_1, Y_2, \ldots, Y_n$, where n is the sample size. Let residuals Z be the paired difference between the two processes: $Z_i = Y_i - X_i,\ i = 1, 2, ..., n$.

- The root- mean- square error (RMSE) is calculated as follows:

$$RMSE = \sqrt{\frac{1}{n}\sum_{i=1}^{n} Z_i^{\,2}} \tag{3.40}$$

- Root- mean- square percentage error (RMSPE):

$$RMSPE = \sqrt{\frac{1}{n}\sum_{i=1}^{n}\left(\frac{Z_i}{Y_i}\right)^2} \tag{3.41}$$

- Mean absolute percent error(MAPE):

$$MAPE = \frac{1}{n}\sum_{i=1}^{n}\left|\left(\frac{Z_i}{Y_i}\right)\times 100\right| \tag{3.42}$$

Another Goodness-of-fit measure is the Chi- square Test. The Chi-square distribution is used to decide whether or not a set of data fits a specified theoretical probability model. The chi-square test can also be used to decide whether several samples came from the same population. This type of test is called *chi-square test of homogeneity* (Dowdy et al, 2003). The test statistic used to test the null hypothesis is the chi-square statistic which is calculated as follows:

$$\chi_c^{\,2} = \sum_{i=1}^{n}\frac{(Y_i - X_i)^2}{X_i} \tag{3.42}$$

where:

χ_c^2 = chi-square statistic;

With a degree of freedom *df= n-1-r*. Where *r* number of estimated parameters. The null hypothesis states there is no significant difference between the observed (or measured) and predicted values. Significant difference is determined if the computed chi-square statistic (χ_c^2) is greater than or equal to the critical chi-square statistic ($\chi_{df,\alpha}^2$). The decision criteria are represented as follows:

- If $\chi_c^2 \geq \chi_{df,\alpha}^2$, then the difference is significant. Therefore the null hypothesis is rejected.
- If $\chi_c^2 < \chi_{df,\alpha}^2$, then the difference is not significant. Therefore, we fail to reject the null hypothesis

Hypothesis Testing and Confidence Intervals: In addition to the Goodness-of-fit tests, hypothesis tests and confidence interval tests can be performed in model validation. Hypothesis tests include but not limited to, two-sample t-test, Mann-Whitney test, and two –sample Kolmogorov-Smirnov test. The two-sample tests assume that both sets of outputs are independent draws from identical distributions (IID). Therefore, these tests should be performed separately for each time-space measurement point. If the number of observations at each time-space point is not sufficient to obtain significant results, observations from appropriate time intervals (such that the IID assumption holds, at least approximately) maybe grouped together. The two-sample t-test further assumes that the two distributions (observed and predicted) are normal and share a common variance. This assumption of variance equality may be unrealistic (Toledo and Koutsopoulos, 2004). Law and Kelton(2000) proposed an approximate t-solution procedure which relaxes the variance equality assumption. The two- sample t-test for equality of mean is performed based on the following hypothesis:

$$H_0 : M^{pred} = M^{obs,\text{measured}}$$
$$H_1 : M^{pred} \neq M^{obs,measured}$$

where M^{pred}, M^{obs} are the mean of the predicted and observed(measured) values, respectively. At α significance level, we reject H_0 if:

$$\frac{\left|M^{pred} - M^{obs,measured}\right|}{\sqrt{\frac{\left(s^{pred}\right)^2}{N^{pred}} + \frac{\left(s^{obs,measured}\right)^2}{N^{obs,measured}}}} \geq t_{\alpha,\hat{f}} \tag{3.43}$$

$$\hat{f} = \frac{\left(\frac{s_n^{pred}}{N^{pred}} + \frac{s_n^{obs,measured}}{N^{obs}}\right)^2}{\frac{\left(s_n^{pred}\right)^4}{\left(N^{pred}\right)^2\left(N^{pred}-1\right)} + \frac{\left(s_n^{obs,measured}\right)^4}{\left(N^{obs,measured}\right)^2\left(N^{obs,measured}-1\right)}} \tag{3.44}$$

where s_n^{pred} and s_n^{obs} are the sample standard deviations of the predicted and observed values, respectively. N^{pred} and N^{obs} are the corresponding sample sizes. $\hat{f}$ is the modified number of degrees of freedom

Qualitative techniques, also known as subjective, visual or informal techniques on some other occasions, are typically performed on the basis of visual comparison of the predicted and observed data in various graphs and plots. It is generally accepted and fairly reliable means to evaluate model performance and identify problems. However, the

downside of this approach is also obvious: its result is also qualitative and fuzzy. That is also the reason it is necessary to employ quantitative techniques to provide complementary information. According to Ni et al.(2004), qualitative techniques generally include, but not limited to the following:

- Diagonal plot, where observed values are plotted against predicted values and an ideal fit would be a 45 degree line. Sometimes a transformation might be necessary to stretch or squeeze data points so that they are aligned evenly along the line.

- Histogram, where the frequency of residuals is displayed and a favorable outcome generally a bell shape with most residuals centered around 0.

CHAPTER 4

DATA COLLECTION AND SUMMARY

4.1 Introduction

This chapter describes the data collection and summary procedure used in this research. The chapter is divided into two sections. Section 4.2 describes the procedures for collecting and measuring data in the field. This section is further divided into two subsections: Subsection 4.2.1 describes the data collection and measurement sites; subsection; Subsection 4.2.2 describes the procedure for measuring proportion of vehicle arrivals on green and platoon arrival time in the field. Section 4.3 describes the procedure field data collection and summary procedure of midblock pedestrian activity data. This section is further divided into three subsections: Subsection 4.3.1 describes the sites where data on midblock pedestrian activity were collected. Subsection 4.3.2 describes midblock pedestrian activity on urban street segments; while Subsection 4.3.3 describes the procedure used in this research to measure midblock pedestrian activity variables in the field.

4.2 Platoon Dispersion Field Data Collection

4.2.1 Description of Data Collection Sites

Data on platoon dispersion were collected on urban street segments at four sites in New Jersey. The platoon dispersion study involved collecting data of the queue discharge flow profile at an upstream signalized intersection and the corresponding arrival flow profile at the downstream intersection at each site. All four sites have no parking lanes. A summary

of the site characteristics are shown in Table 4.1. The distances in the Table 4.1 were recorded using a DMW-0621 Kintrex measuring wheel.

Table 4.1 Summary of Study Site Characteristics

Site	Location	Corridor	From	To
1	Newark, NJ	M.LK. Blvd	Springfield Ave.	Market St.
2	Saddle Brook, NJ	US 46	Fifth St.	Sixth St.
3	Newark, NJ	Hwy 21	Center St.	Lombardy St.
4	Elizabeth, NJ	US 1	E. Grand St.	Bond St.

Table 4.2 Continuation of Table 4.1

Site	Distance Between Intersection(ft)	Speed Limit(mph)	Friction Condition
1	560	25	Midblock Pedestrian Activity(220 pedestrian/hr)
2	700	50	No Friction
3	1,245	35	Medium to High Truck Volume(90 trucks/hr)
4	925	40	No Friction

Site 1 is shown in Figure 4.1. It is a three - lane (2 lanes in the study direction and a single lane in the opposite direction) urban collector street segment in downtown Newark, New Jersey. The site has an hourly volume of 457vph in the study direction, 9% of which are left turning vehicles and 12% are right turning vehicles. It has pedestrian crosswalks at the upstream and downstream signalized intersections, and also at mid-segment; approximately 300ft from the upstream signalized intersection. The pedestrian

volume at this site is approximately 435 pedestrians per hour during the peak hour, with about 220 pedestrians per hour crossing at the midblock crosswalk.

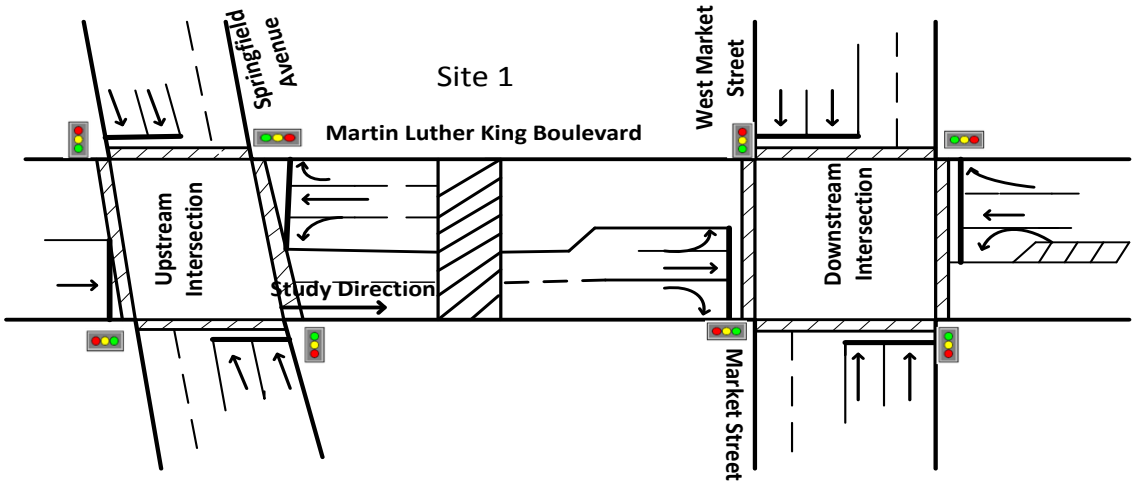

Figure 4.1 Geometric layout of Site 1.

Site 2 is shown in Figure 4.2. It is a four lane urban principal arterial in the city of Saddle brook, New Jersey. The site has a traffic volume of 1129 vph in the study direction, all of which are through vehicles as left turns are prohibited in the study direction. There is a mid-segment access point presented at this site, but with minimal access demand of approximately 10veh/hr. The roadway has a restrictive median on 80% of its segment. A restrictive median is defined as a portion of a roadway physically separating vehicular traffic traveling in opposite directions.

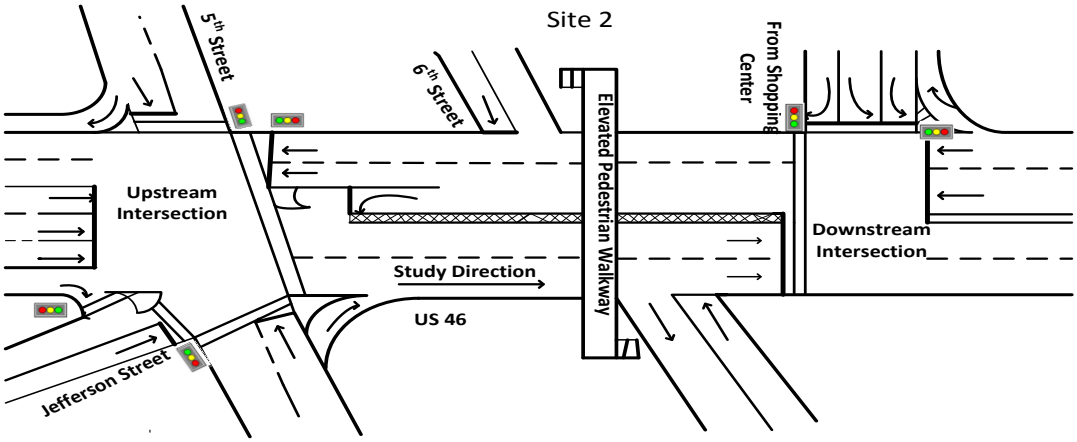

Figure 4.2 Geometric layout of Site 2.

Site 3 is a six lane urban principal arterial street segment located in downtown Newark, New Jersey. The roadway carries a through traffic volume of 1343vph, of which 7% are trucks. It has restrictive median on 100% of its segment.

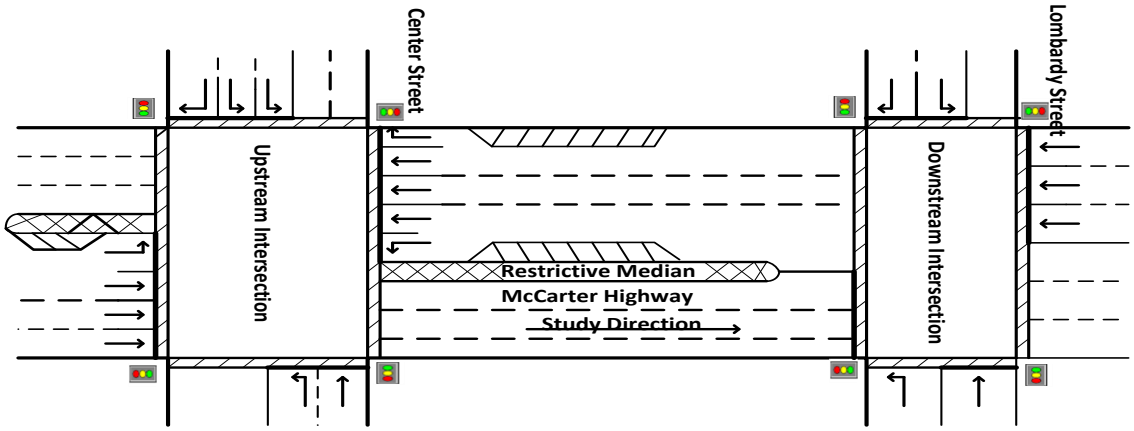

Figure 4.3 Geometric layouts of Site 3.

Site 4 is a six-lane urban principal arterial in the city of Elizabeth, New Jersey. The roadway has a through traffic volume of 1979vph in the study direction. Left turn is

prohibited in the study direction at this site. A restrictive median is presented on 100% of the segment at the site as shown in Figure 4.4

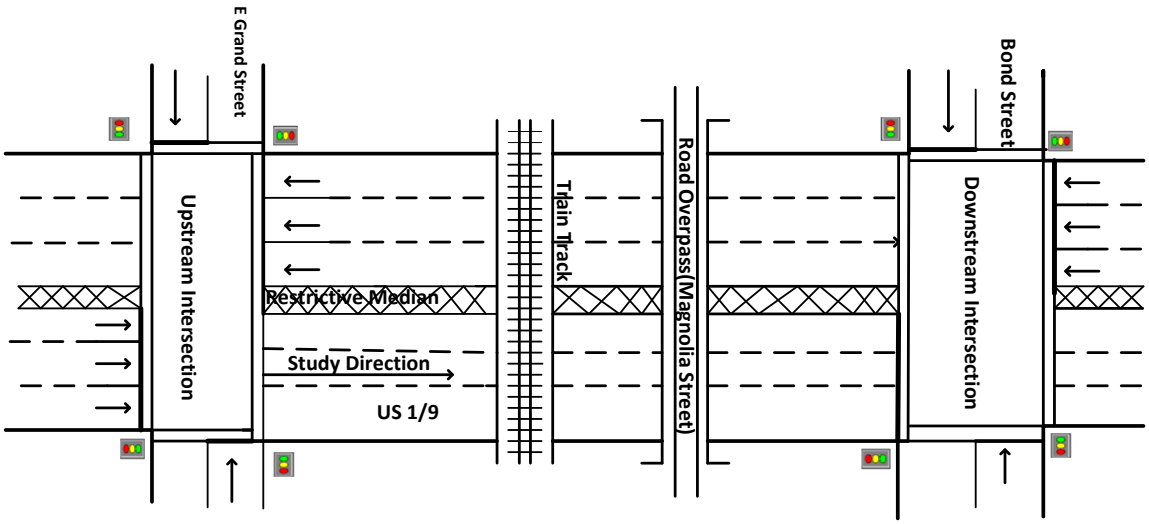

Figure 4.4 Geometric layout of Site 4.

4.2.2 Field Measurement of Proportion of Arrivals on Green and Platoon Arrival Flow Profiles

This subsection presents a procedure for collecting platoon dispersion data and for measuring proportion of vehicle arrivals on green in the field. Several studies including, Robertson (1969) and Seddon (1972) have studied platoon dispersion in the field by recording the platoon discharge flow at an upstream signalized intersection and the corresponding arrival flow at a specified downstream location. A similar procedure is used in this research to collect platoon dispersion data in the field. Platoon dispersion occurs due to fluctuation in vehicle speeds. Therefore, depending on the rate of platoon dispersion, the arrival flow at a downstream location would be lower than that recorded at the stop-line of the upstream signalized intersection.

Collecting platoon dispersion data in the field can be complex and challenging, requiring data to be collected in both space and time. Data were collected by using two Sony DCR SR 100 video cameras. One camera recorded the discharge of vehicles from the stop line of the upstream signalized intersection and the second camera recorded the arrival times of vehicles at the stop line of the downstream intersection. The discharge time in this research is defined as the time at which the back bumper of a vehicle crosses the upstream stop line. While the vehicle arrival time is defined as the time at which the back bumper of the vehicle crosses the downstream stop line. Platoon arrival time was measured by recording the arrival time of the leading platoon vehicle at the downstream stop-line. This process of recording the discharge and arrival times was repeated for every vehicle in the platoon during the data collection period. To ensure accuracy in the platoon discharge and arrival times, the time on both cameras was synchronized. Data were collected for a total of 6hrs at site 1, 2 hours at site 2, and one hour at sites 3 and 4.

Once the platoon dispersion data was recorded in the field, the data was summarized using a "stop and play" technique, where vehicles in a platoon were tracked on the video as they traveled between the upstream and downstream signals; their respective discharge and arrival times were recorded. Platoons that were partially degraded by platoon vehicles turning left or right were eliminated from the final data set. Additionally, platoons interrupted by queued vehicles at the downstream location were also eliminated. This process of data summary and reduction was repeated until a final data set was obtained. The data set included a total of 144 platoons from four sites. The platoon size ranged from 6 to 18 vehicles.

The second set of field data was obtained by measuring the proportion of vehicle arrivals on green. This was obtained by counting the number of vehicles in the platoon crossing the downstream stop line during green. Table 4.3 shows the signal timings at the respective study locations. The effective green was assumed to be equal to the total duration of the green and yellow times. That is total time vehicles were permitted to go through the downstream intersection. The effect green time, however, does not exclude the startup lost time. This is because the startup lost time only impacts discharging vehicles not arriving vehicles. The offset was recorded as the difference in time between the start of green at the upstream signal and the downstream signal. The 2010 HCM predicted proportions of arrivals on green were estimated with respect to these timings.

Table 4.3 Signal Timings Recorded at the Downstream Signalized Intersections

Site	Number of Lanes in Study Direction(ln)	Cycle Length(s)	Effective Green Time(s)	Offset(s)
1	2	100	35	5
2	2	120	40	4
3	3	60	25	10
4	3	110	50	3

4.3 Field Data Collection on Midblock Pedestrian Activity

This section presents the procedure and technique used in collecting data at midblock of the study site. This section is divided into three subsections: the first subsection describes midblock pedestrian activity on urban street segments. The second subsection describes the procedure and technique used in collecting the following data: traffic volume, midblock pedestrian volume, number of midblock pedestrian crossings and the number of

midblock interference. Subsection three describes the measurement of free-flow of vehicles based on the steps and requirements provided in the HCM 2010.

4.3.1 Description of Study Sites

Site 1 is shown in Figure 3.3. It is a two - lane (1 lane in each direction) urban street segment in downtown Newark, New Jersey. It is location on the campus of the New Jersey Institute of Technology (N.J.I.T). The midblock pedestrian crosswalk is approximately 31ft long. The average pedestrian volume crossing at midblock during the data collection period was 182 pedestrians per hour and an average hourly volume of 186 vph for the study period. It has pedestrian crosswalks at the upstream and downstream signalized intersections, and also at mid-segment; approximately 300ft from the upstream signalized intersection

Site 2 is shown in Figure 3.4. It is a four - lane (2 lanes in each direction) urban collector street segment in downtown Newark, New Jersey. It has pedestrian crosswalks at the upstream and downstream signalized intersections, and also at mid-segment; approximately 300ft from the upstream signalized intersection. The midblock pedestrian crosswalk is approximately 57ft long. The average pedestrian volume crossing at midblock during the data collection period was 135 pedestrians per hour. The site had an average hourly volume of 313 vph recorded during the study period.

4.3.2 Description of Midblock Pedestrian Activity

Pedestrian crosswalks, whether marked or unmarked, provide connections between pedestrian facilities across sections of roadway used by automobiles, bicycles, and transit vehicles. Depending on the type of control used for the crosswalk, local laws, and driver adherence of those laws, pedestrians will experience varying levels of delay, safety, and comfort while waiting to use the crosswalk (HCM 2010). Conversely, depending on the type of control used for the crosswalk, the pedestrian volume and the pedestrian walking speed, vehicles in a platoon will experience varying levels of delay as pedestrians cross at midblock crosswalks. Platoon delays due to midblock pedestrian crossings increase the segment running time and the platoon arrival time at a downstream signalized intersection. An increase in segment running time consequently decreases the segment travel speed. Field study of midblock pedestrian activity involved measuring and quantifying several variables including: a) the number of pedestrians per hour crossing at midblock..; b) the number of midblock pedestrian crossings per hour; c) the traffic volume corresponding to the pedestrian volume/crossings and midblock interference; d) the number of midblock interference. For this research, a midblock pedestrian interference is defined as the slowing down or stopping of a platoon due to a pedestrian or group of pedestrians making a midblock crossing. The duration of a pedestrian midblock interference is defined as the difference between the time the leading vehicle of an interrupted platoon comes to a full stop as a result of crossing pedestrians and the start time of that same vehicle.

4.3.3 Field Measurement and Summary of Midblock Pedestrian Activity Variables

This subsection presents a description of the data collection and summary of the traffic flow (vph), pedestrian volume (pedestrian/hr), number of pedestrian crossings per hour and number of midblock interference per hour recorded at the midblock crosswalk of the study site.

At Site 1, a portable video camera was tied to a post at an altitude of about 12 ft. overlooking the midblock pedestrian crosswalk. The camera was set to continuously record pedestrian and vehicular activities for three days. At Site 2, the data collection involved using Sony video camcorder to record vehicular and pedestrian activities for a total 22 hours, but on different days of the week and during peak and off peak periods. The 22-hr video data was later reduced to 17 hours after 5hrs of video data were eliminated from the data set due to frequent traffic congestion at the downstream signalized intersection, causing vehicles to queue beyond the midblock crosswalk. Therefore it was not possible to record midblock interference under such traffic condition.

Upon completion of the field data collection, the videos were then summarized in the Transportation lab. The data summary involved manually viewing of the videos to record the traffic and pedestrian variables. For each hour, the traffic and pedestrian flows per hour at midblock were counted using a manual counter and the data recorded on a data summary sheet. The recorded data was later input into an excel spreadsheet. The number of midblock interference was recorded by dividing each one hour video into sixty one minute intervals. The number of interference was recorded for each minute. Interference was determined to have occurred if a vehicle or group of vehicles slowed

down or came to a full stop as pedestrian or group of pedestrians crossed the midblock crosswalk. For Site 1, a total of 5hrs of data was extracted from the 3-day worth of recorded data. The 5-hr data includes peak and off-peak vehicular-pedestrian activity, but excludes all activity during the dark. For Site 2, the 22-hr video data was reduced to 17 hours after 5hrs of video data were eliminated from the data set due to frequent traffic congestion at the downstream signalized intersection, causing vehicles to queue beyond the midblock crosswalk. Therefore it was not possible to record midblock interference under such traffic condition

A summary of the data for Site 1 shows the hourly traffic flow at the midblock crosswalk ranged from 76 to 327 vehicles per hour. Pedestrian volume ranged from 31 to 337 pedestrian per hour. The number of pedestrian crossings ranged from 30 to 260 crossings per hour, while the number of midblock interference ranged from 1 to 49 per hour. The data summary for Site 2 shows the hourly traffic flow at the midblock crosswalk ranged from 241 to 441 vehicles per hour at Site 2. Pedestrian volume ranged from 24 to 212 pedestrian per hour. The number of pedestrian crossings ranged from 27 crossings per hour to 185 crossings per hour, while the number of midblock interference ranged from 3 to 58 per hour.

4.3.3.1 Pedestrian Walking Speed. This subsection describes the technique used to compute pedestrian walking speeds using field data recorded at the midblock crosswalk. The subsection also presents a summary of the collected data. During data summary and based on careful observation, pedestrians were assigned to one of the following age groups based on gender.

- Child (ages 0 – 12)
- Teen (ages 13 – 18)
- Young adult (ages 19 – 30)
- Middle (ages 19 -30)
- Older (age older than 60 but not classified as "elderly or physically disabled")
- Elderly or physically disabled (e.g., using crutches, a self-propelled wheelchair, etc.)
- Age Uncertain

Using a stop watch and the video recordings, the walking time was recorded for each pedestrian. The walking time was recorded as the time for each pedestrian to walk from end to end in the crosswalk. Based on the measured distance of the crosswalk of 31 feet at Site 1 and 57 feet at Site 2, the pedestrian walking speed was calculated for each pedestrian.

At Site 2, total of 913 pedestrians were recorded during the study. Of these, 310(34%) were female and 603(66%) were male. In addition, of the total number of pedestrians, none were children, teenagers, older and elderly or physically disabled. A total of 841(92%) pedestrians were young, 40(4%) were middle age and 32(4%) were those whose age could not be determined.

A total of 2,540 pedestrians were recorded during the study at Site 2. A total of 2,491 pedestrians (98%) were observed to be "walking". The remaining 49 pedestrians (2%) were observed to be running, both walking and running during the crossing. These 49 data points were not included in the analyses of pedestrian walking speed. Of the 2,491 pedestrians that were observed as walking, 1,416(57%) were female and

1,075(43%) were male. In addition, of the 2,491 pedestrians, 2(0.08%) were children, 267(10.7%) were teenagers, 294(11.8%) were young adults, 1594(64%) were middle age, 186(7.5%) were older, 60(2.4%) were elderly or physically disabled and 88(3.5%) pedestrians whose age could not be determined.

4.3.3.2 Free-Flow Speed. This subsection describes the technique used in this research to measure free-flow speed of vehicles at the study Site 2. The HCM 2010 presents steps for determining the free-flow speed for vehicle traffic on urban street segments. The first step involves conducting a spot-speed study at a mid-segment location during low-volume conditions. The Manual stipulates recording the speeds of 100 or more free-flowing passenger cars. According to the HCM 2010, a car is free-flowing when it has headway of 8 seconds or more to the vehicle ahead and 5 seconds or more to the vehicle behind in the same traffic lane. The second step in determining the free-flow speed involves computing the average of the spot speeds, S_{spot}, and their standard deviation σ_{spot}. The third step involves computing the segment free-flow speed S_f, as a space-mean speed as follows:

$$S_f = S_{spot} - \frac{\sigma_{spot}^2}{S_{spot}} \tag{4.1}$$

In this research, the free-flow speed at the study site was measured based on the conditions and requirements stipulated in the HCM 2010 as stated above. The study was conducted under low traffic and, when no pedestrians were crossing at the midblock crosswalk. However, unlike the HCM 2010 procedure that uses a spot speed technique to

compute the free-flow speed, the technique used in this research involved measuring the speeds of vehicles based on their travel times between two specified points on the segment. The first point was 144 feet from the stop line of the upstream signalized intersection, while the second point was the stop line of the downstream signalized intersection. The distance between these two points was measured to be 416 feet. The first point was selected to provide sufficient distance for drivers to accelerate to their desired speeds after the start of green. This technique of measuring the free-flow speed was used for two reasons: a) no radar device was available to record spot-speeds of vehicles; b) the study site had enough point of elevation from where the entire length of the segment was visible. To ensure that vehicles were traveling under free-flow conditions, the flowing measures were taken: a) majority of the vehicles recorded were leading platoon vehicles because the segment was almost always cleared of vehicles from the previous platoon due to the start of green at the downstream signalized intersection before the start of green at the upstream signalized intersection; b) only vehicles that entered and exited the segment while no pedestrian(s) was presented were recorded ; c) the travel time of vehicles were recorded only when the signal was green at the downstream intersection to ensure that the downstream signal did not influence drivers` travel speeds. The travel times were recorded for 420 passenger cars. Based on the individual travel times of vehicles and the measured distance between the two reference points on the segment, the travel speeds were calculated for each vehicle. The segment free-flow speed was then calculated using a modified form of Equation 4.1

CHAPTER 5

DATA ANALYSIS AND RESULTS

5.1 Introduction

The previous chapter presents the procedure used in this research to collect data in the field and the technique used to summarize and reduce the data. In Chapter 5, the collected and summarized data are analyzed and the results of performing regression analysis are presented. The data analysis section is presented in two parts: the first part analyzes the data used in evaluating the performance of the HCM platoon dispersion model for non-friction and friction traffic conditions. The second part analyses the data collected on pedestrian activity at midblock crosswalks on urban street segments.

5.2 Data Analysis

This section presents an analysis of the research data. The analysis is presented in two subsections: Subsection 5.2.1 analyzes the data used in evaluating the HCM 2010 platoon dispersion model. This subsection is analyzes the procedure used in this research to obtain the observed and estimated variables under non-friction and friction conditions. Subsection 5.2.2 analyzes the data on midblock pedestrian activity on urban street segments. The subsection is presented in two parts: the first part analyses the data on midblock pedestrian interference and measured free-flow speed. This part also presents

figures of hourly distributions of the measured data. The second part of this subsection analyzes the data on pedestrian walking speed by both age group and gender, including figures of percentile walking speeds and cumulative distribution of walking speeds.

5.2.1 Evaluation of the HCM 2010 Platoon Dispersion Model

This subsection is presented in two parts. The first part discusses the statistical approach to evaluate the HCM platoon dispersion model. The second part discusses how the observed proportion of arrivals on green was obtained in the field and estimated using the HCM2010.

5.2.1.1 Observed and Estimated Platoon Variables. In applying the HCM 2010 procedure in computing the proportion of arrivals, several geometric features and operational characteristics are taken into account. Some of these features and characteristics such as segment length, distance between the upstream and downstream intersections, posted speed limits were measured and recorded in the field, and were used as input values in estimating the 2010 HCM free flow speed, segment running time, platoon arrival time and smoothing factor . Table 5.1 shows the input variables used in computing the platoon arrival time and smoothing factor for each site using the HCM 2010 procedure.

Table 5.1 Platoon Dispersion Model Variables for Each Study Site

Variable	Site 1	Site 2	Site 3	Site 4
Distance Between Intersection, L_s (ft)	560	700	1,245	925
Segment Length, L (ft)	425	605	1,100	800
Mid Segment Demand Flow Rate(v_m) (veh/hr)	0	10	0	0
Number of Lanes in Study Direction, N_{th} (ln)	2	2	3	3
Free Flow Speed, S_o (mph)	32.1	38	39.4	37.9
Start Up Lost Time, l_1 (sec)	2	2	2	2
Segment Running Time, t_R (sec)	12.7	12.9	19.2	16.4
Time Step Duration, d_t (sec)	1	1	1	1
Estimated Platoon Arrival Time, t_p (sec)	10.80	11.00	16.50	14.10
Smoothing Factor, F	0.33	0.32	0.25	0.28

Based on the variables in Table 5.1, the estimated proportion of arrival on green for each platoon was computed for each site using the HCM 2010 procedure. The first step involved in estimating the proportion of arrivals on green was to compute the segment running time, smoothing factor, and platoon arrival time using Equations 3.1, 3.6 and 3.7, respectively. The second step involved estimating the arrival flow for 1 second time step using the recurrence model in Equation 3.8. Once the arrival flows were estimated, the next step involved computing the proportion of arrivals on green using Equation 3.10.

The observed proportion of arrivals on green was obtained for each site by recording the proportion of through platoon vehicles arriving on green at the downstream signal. Both the observed and estimated proportions of arrivals on green were obtained based on the same time duration. At Sites 1 and 3, the effective green at the downstream signal was not sufficient to serve all the platoon vehicles, therefore the observed

proportion of arrivals was obtained based on the actual cycle length. At Site 2 and Site 4, however, the effective green times at the downstream signals were always sufficient to serve the entire through platoon vehicles. In such situations the observed proportion of arrivals on green was always 100% (1) because all the vehicles in the platoon would go through the intersection on green. Therefore it was deemed inappropriate to use the actual cycle lengths in computing the estimating the proportion of arrivals on green. With a very long duration of effective timings, both the measured and estimated proportion of arrivals on green for each platoon were 100 %(or 1). That is all the vehicles in the platoon arrived on green. Therefore, at Site 2 and Site 4, a reasonable duration of effective green time and cycle length less than the actual durations recorded at the sites were assumed and used to compute the proportion of arrivals on green based on the arrivals flow profiles estimated using the HCM 2010 procedure and the arrival flow profiles observed in the field. With these assumed effective green times and cycle lengths, and the estimated and observed arrival flow profiles, not all platoon vehicles "arrived" on green at the downstream signal. Using this technique, a set of observed and estimated proportion of arrivals on green was obtained for Sites 2 and 4.

Table 5.2 shows a summary of the platoon data for each site. The table shows the parameter values (range, mean and standard deviation) for each platoon variable (platoon size, estimated arrivals on green, observed arrivals on green) for each site. As shown in Table 5.2 the average of the mean values of the observed number of vehicle arrivals on green for Sites 2 and 4, the sites with non-friction traffic conditions, is approximately10 vehicles. This value is one-half the average of the mean values of the number of vehicle arrivals on green of the approximate 5 vehicles for Sites 1 and 3, the sites with friction

traffic conditions. In addition, the average of the mean values of the estimated number of vehicle arrivals on green for Sites 2 and 4 is 8 vehicles. The average of the mean values of the estimated number of vehicle arrivals on green for Sites 1 and 3 is approximately 7 vehicles.

Table 5.2 Summary of Platoon Data

Variable	Parameter	Site 1	Site 2	Site 3	Site 4
Platoon Size(veh)	Range	7 - 16	5 - 19	5 - 12	7 - 23
	Mean	12	11	8	14
	Standard Deviation	2	4	2	5
Observed Arrivals on Green(veh)	Range	2 - 8	5 - 13	2 - 6	5 - 13
	Mean	5	10	4	9
	Standard Deviation	1	3	1	2
Estimated Arrivals on Green(veh)	Range	3 -9	5 - 12	4 -7	7-11
	Mean	7	9	6	8
	Standard Deviation	1	3	1	1

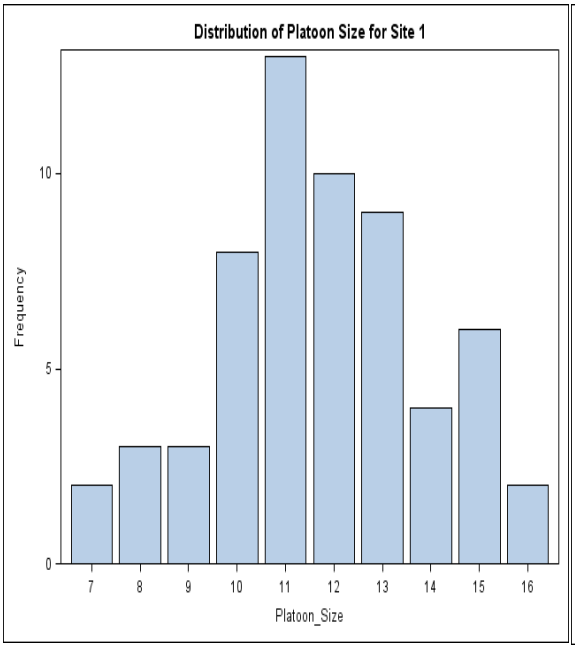

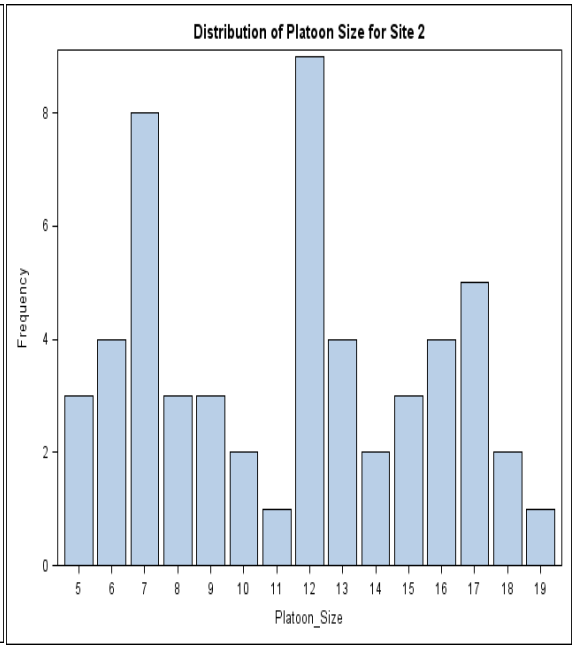

Figures 5.1 - 5.2 Distribution of platoon size for Site 1 and Site 2, respectively.

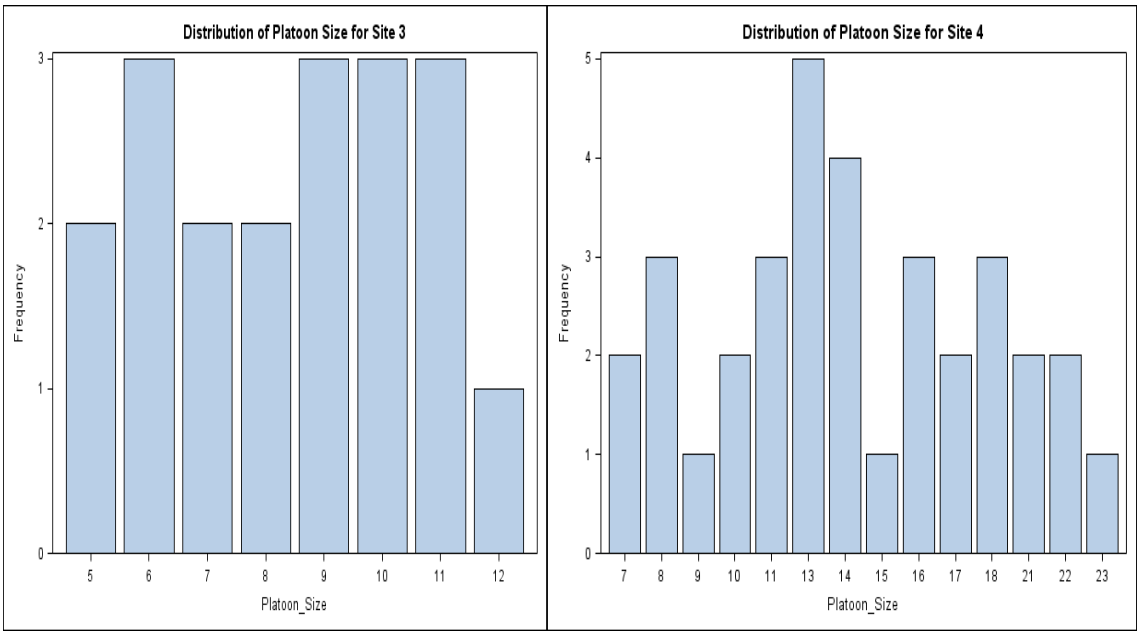

Figure 5.3 – 5.4 Distribution of platoon size for Site 3 and Site 4, respectively.

Table 5.3 shows the mean, standard error, and standard deviation values of the observed and estimated proportion of arrivals on green. The purpose was to analyze the mean and variability of the data and estimates of each variable. As shown in Table 5.3 the average of the mean values of the observed proportion of arrivals on green for Sites 2 and 4, the sites with non-friction traffic conditions, is 79%. This value is far greater than average of the mean values of proportion of arrivals on green of 52% for Sites 1 and 3, the sites with friction traffic conditions. In addition, the average of the mean values of the estimated proportion of arrivals on green for Sites 2 and 4 is 75%. The average of the mean values of the estimated proportion of arrivals on green for Sites 1 and 3 is 67%. Based on these figures, there is a difference of 4% between the observed and estimated proportion of arrivals on green for Sites 2 and 4; and a difference of 15% between the observed and estimated proportion of arrivals on green for Sites 1 and 3.

Table 5.3 Summary of Proportion of Vehicle Arrivals On Green

Variable	Parameter	Site 1	Site 2	Site 3	Site 4
Measured Proportion of Arrivals on Green (%)	Mean	47.4	90.1	55.4	67.9
	Standard Error	1.752	2.128	5.731	4.385
	Standard Deviation	13.57	14.27	23.63	19.61
Predicted Proportion of Arrivals on Green (%)	Mean	59.6	86.5	74.7	63.4
	Standard Error	1.633	2.412	3.771	4.032
	Standard Deviation	12.65	16.18	15.55	18.03

In addition, Table 5.4 shows the range, the mean, the standard error and standard deviation of the measured and estimated platoon arrival time for all four sites. The average values of the segment length and post speed limit for Sites 2 and 4, sites with non-friction traffic conditions, are 813 ft and 45 mph. While the average values of the segment length and post speed limit for Sites 1 and 3, sites with friction traffic conditions, are 903 ft. and 30 mph. From Table 5.4, the average value of the measured platoon arrival times for Sites 2 and 4 and for Sites 1 and 3, are 13 seconds and 20 seconds, respectively. While the average value of the HCM 2010 estimated platoon arrival times for Sites 2 and 4 and for Sites 1 and 3, are 13 seconds and 12 seconds, respectively. The data show no difference between the average of the mean values of measured and estimated platoon arrivals times for Sites 2 and 4. However, the data shows difference of 6 seconds between the averages of the mean values of measured and estimated platoon arrivals times for Sites 1 and 3.

Table 5.4 Summary of Platoon Arrival Time Data

Variable	Parameter	Site 1	Site 2	Site 3	Site 4
Measured Platoon Arrival Time(sec)	Range	10 - 21	7 - 16	21 - 28	11 -17
	Mean	16.57	10.80	24.2	14.47
	Standard Error	0.32	0.28	0.47	0.37
	Standard Deviation	2.75	1.87	2.06	1.75
Predicted Platoon Arrival Time(sec)	Range	n/a	n/a	n/a	n/a
	Estimated Value	10.8	11.0	16.5	14.10
	Standard Error	n/a	n/a	n/a	n/a
	Standard Deviation	n/a	n/a	n/a	n/a

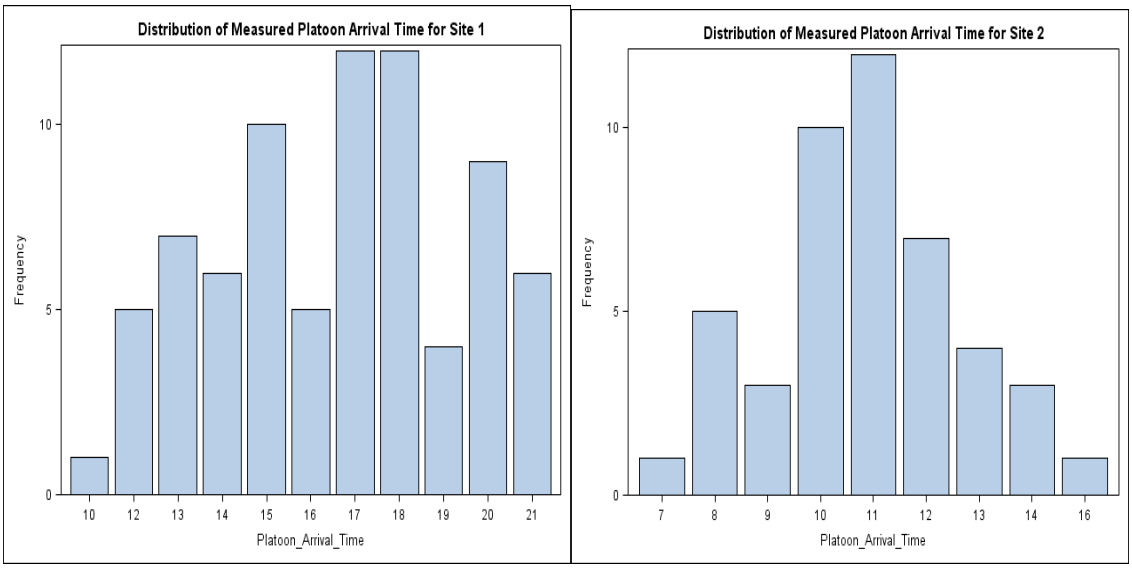

Figure 5.5 – 5.6 Distribution of platoon arrival time for Site 1 and Site 2, respectively.

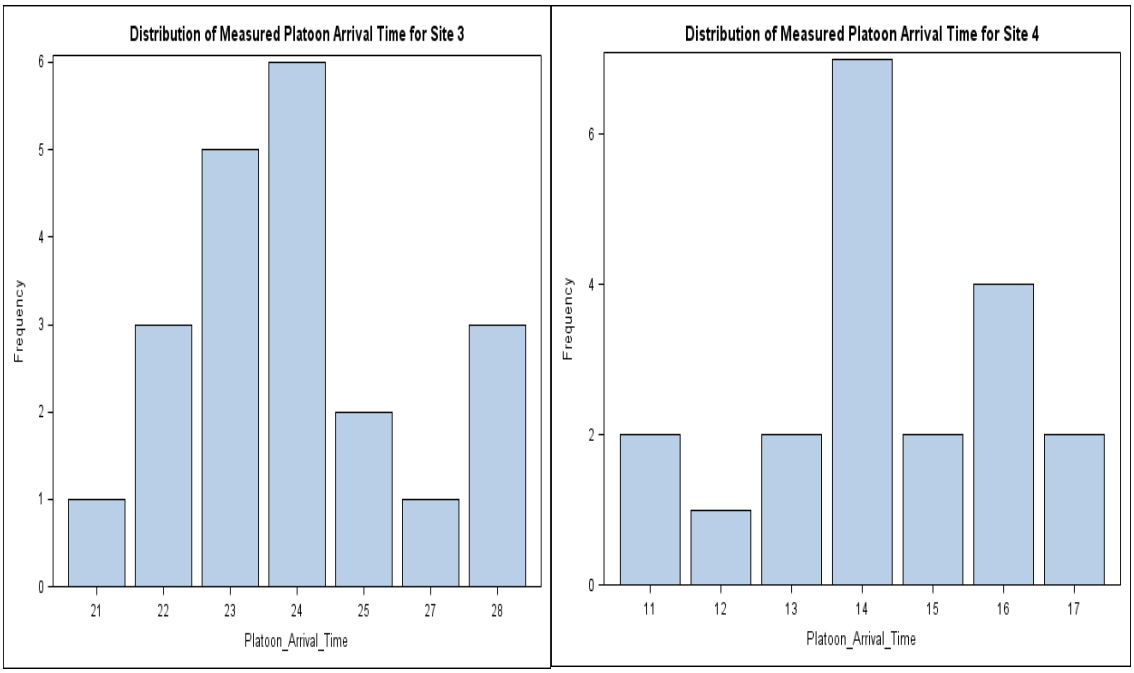

Figure 5.7 – 5.8 Distribution of platoon arrival time for Site 3 and Site 4, respectively.

5.2.2 Midblock Pedestrian Activity on Urban Street Segments

This subsection presents the analysis of the data collected on midblock pedestrian activity at crosswalks on urban street segments. The following data are presented and analyzed: traffic volume per hour, pedestrian volume per hour, number of midblock pedestrian crossings per hour, the number of midblock interference per hour, measured free-flow speed in mile per hour and the pedestrian walking speed in feet per second, obtained at the two study sites.

Table 5.5 shows the traffic volume, pedestrian volume, number of pedestrian crossings and the number of midblock interference obtained for 22 of the 27 hours of video data summarized for both sites with midblock crosswalks. The 22-hr data represent the number of hours during which there was no traffic congestion causing queue backing

up to the midblock cross walk. Therefore, all midblock interferences were due to vehicular and pedestrian interactions at the midblock crosswalks.

A summary of the data for Site 1 shows the hourly traffic flow at the midblock crosswalk ranged from 76 to 327 vehicles per hour. Pedestrian volume ranged from 31 to 337 pedestrians per hour. The number of pedestrian crossings ranged from 30 to 260 crossings per hour, while the number of midblock interference ranged from 1 to 49 per hour. The data summary for Site 2 shows the hourly traffic flow at the midblock crosswalk ranged from 241 to 441 vehicles per hour at Site 2. Pedestrian volume ranged from 24 to 212 pedestrians per hour. The number of pedestrian crossings ranged from 27 crossings per hour to 185 crossings per hour, while the number of midblock interference ranged from 3 to 58 per hour.

Table 5.5 Summarized Data of Midblock Pedestrian Activity Variables

Traffic Volume(Veh/hr)	Pedestrian volume(Ped/hr)	Number of Crossings(Crossings/hr)	Number of Interference(Interference/hr)
441	212	185	32
351	143	119	26
410	203	167	37
409	149	146	32
324	152	132	23
241	93	27	3
319	24	27	6
375	106	118	29
323	30	30	4
349	52	56	13
351	67	62	19
345	194	156	58
357	86	37	7
330	100	80	13
389	204	160	38
302	68	61	9
367	182	156	50
327	337	260	49
76	31	30	1
80	168	149	5
238	242	188	25
210	135	88	19

Figure 5.9 shows the plot of the data in Table 5.5. The figure explains the relationship between the midblock interference and, traffic volume, pedestrian volume and the number of pedestrian crossings at midblock crosswalks. The figure shows midblock interference tends to increase with increasing in traffic volume, pedestrian volume and the number of pedestrian crossings. However, the figure also shows there is no direct correlation between the midblock interference and traffic volume, pedestrian volume and number of pedestrian crossings. As shown by the 1st hour, with a traffic volume of 441, pedestrian volume of 212 and number of crossings of 185, the number of midblock interference is 58. While for the 12th hour, with a traffic volume of 345, pedestrian volume of 194, number of crossings of 156, the number of midblock interference is 32.

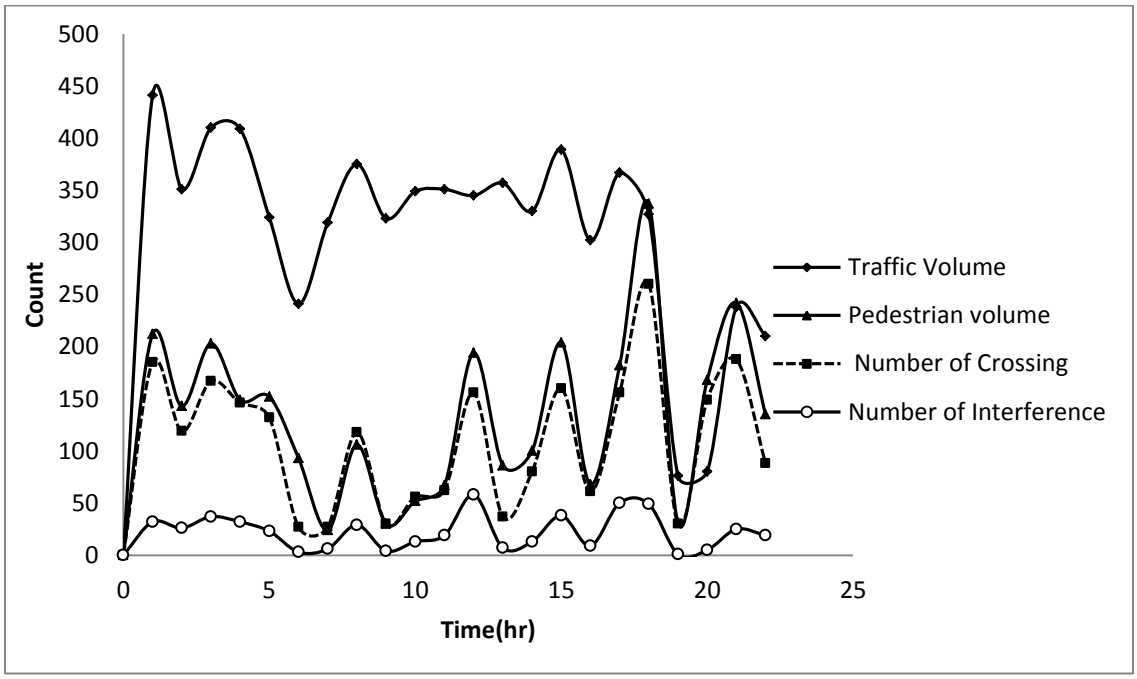

Figure 5.9 Hourly distributions of midblock pedestrian activity variables.

Table 5.6 shows a further summary of the data in Table 5.5 also shows a mean free-flow speed of 28 mph recorded between two points along the segment. This value is 3mph greater than the posted speed limit of 25mph at the study site. Using the equation and procedure in the HCM 2010, the free-flow speed was estimated to be 32.1 mph.

Table 5.6 Statistical Summary of Midblock Pedestrian Activity Variables

Variable	N	Mean	Standard deviation	Minimum value	Maximum value
Free Flow Speed(mph)	440	28.2764	3.6412	21.8182	40.5195
Traffic Volume(veh/hr)	22	314	94.464	76	441
Pedestrian Volume(peds/hr)	22	135	79.0681	24	337
Number of Crossings(crossings/hr)	22	110	64.9319	27	260
Number of Interference(Interference/hr)	22	22	16.6205	1	58

Table 5.7 shows the hourly and total midblock pedestrian volumes by age group obtained for all 27 hours of data collected. At Site 1, a total of 913 pedestrians were recorded for the 5-hr of video data summarized. Of these, 310(34%) were female and 603(66%) were male. In addition, of the total number of pedestrians, none were children, teenagers, older and elderly or physically disabled. A total of 841(92%) pedestrians were young, 40(4%) were middle age and 32(4%) were those whose age could not be determined.

At Site 2, a total of 2,491 pedestrians (98%) were observed to be "walking". About 49 pedestrians (2%) were observed to be running, both walking and running during the crossing. These 49 data points were not included in the analyses of pedestrian walking speed. Of the 2,491 pedestrians that were observed as walking, 1,416(57%) were female and 1,075(43%) were male. In addition, of the 2,491 pedestrians, 2(0.08%) were

children, 267(10.7%) were teenagers, 294(11.8%) were young adults, 1594(64%) were middle age, 186(7.5%) were older, 60(2.4%) were elderly or physically disabled and 88(3.5%) pedestrians whose age could not be determined.

Table 5.7 Hourly Distribution Midblock Pedestrian Volumes by Age Group

	Age Group						
	0 - 12	13 - 18	19 - 30	31 -60	> 60, but not elderly or disabled	Elderly or Disabled	Age Uncertain
	0	17	22	133	34	1	5
	0	5	11	165	12	2	8
	0	33	26	81	2	3	4
	0	3	12	66	9	3	0
	0	1	1	17	5	0	0
	0	5	0	18	4	2	1
	0	9	8	27	6	0	2
	0	22	8	26	4	2	5
	0	25	13	33	4	8	3
	0	41	13	41	1	1	3
	0	26	17	21	3	0	1
	2	1	7	114	4	3	12
	0	0	1	53	2	0	8
	0	6	10	129	2	1	4
	0	6	3	13	2	3	0
	0	0	17	75	11	3	0
	0	2	22	121	5	4	5
	0	7	33	110	12	5	9
	0	15	23	129	10	8	9
	0	0	0	0	0	0	0
	0	18	24	111	45	4	2
	0	25	23	111	9	7	7
	0	0	317	12	0	0	8
	0	0	16	9	0	0	6
	0	0	161	5	0	0	2
	0	0	227	3	0	0	10
	0	0	120	11	0	0	4
Total	2	267	1135	1634	186	60	118

Figure 5.10 shows the hourly distribution of midblock pedestrian volume for children, teen, young adults and middle age groups. Figure 5.11 is a continuation of Figure 5.10. It shows the hourly distribution of midblock pedestrian volumes for

pedestrians classified as older 60, but not elderly or disabled, elderly and disabled and those pedestrians whose ages could not be determined. The data points for the first 22 hours represent the data for Site 2; while the remaining 5 hours data points represent the data for Site 1. As shown in Figure 5.10 and Figure 5.11, a total of 2 children were recorded at both sites. The Figures also show hourly distribution of pedestrian volumes less than 50 pedestrian per hour for teen (13-18), young adults (19-30), older than 60 but not elderly or disabled, elder and disabled, and Age uncertain age group for site 2. Only middle age (31-60) age group has hourly distribution of midblock pedestrian volumes greater than 50 for Site 2. However, for Site 1, only young adults (19-30) age group has hourly distribution of pedestrian volume greater than 50 pedestrians per hour. This is because Site 1 is located on the campus of N.J.I.T, a University, with majority of its students being young adults.

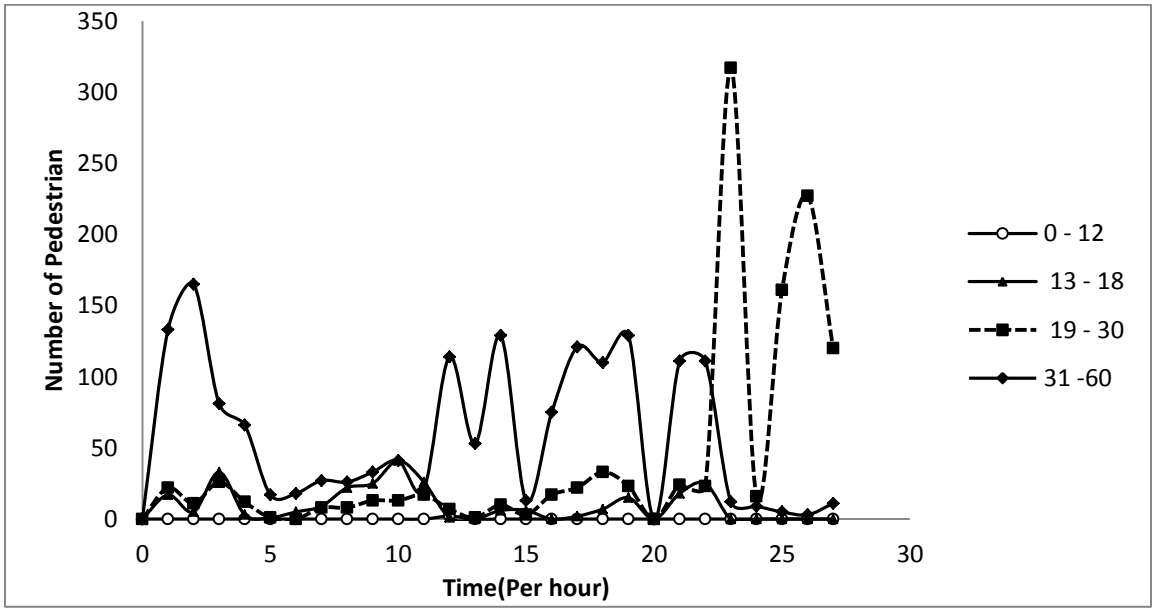

Figure 5.10 Hourly distributions of midblock pedestrian volumes by age group.

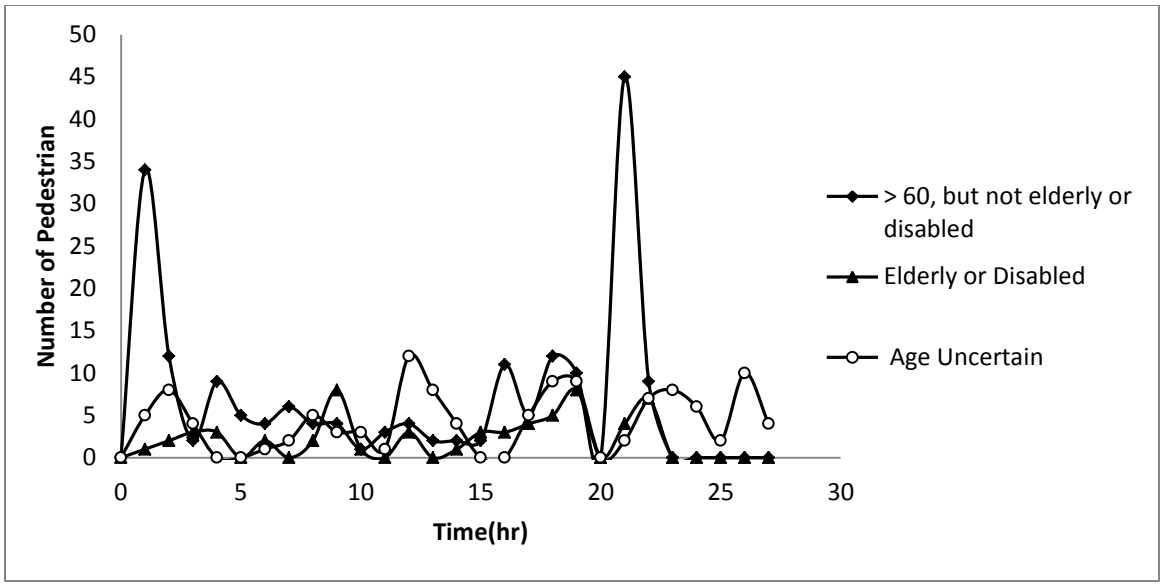

Figure 5.11 Continuation of Figure 5.10.

5.2.2.1 Pedestrian Walking Speed. This subsection presents analysis of the midblock pedestrian walking speeds by age group and gender. The walking speeds are analyzed based on percentiles. Percentiles are often used in traffic engineering in speed-related studies. In pedestrian speed studies, the 15th percentile speed represents the walking speed which can be exceeded by 85 percent of pedestrian population. The 15th percentile walking speed is used in pedestrian signal design.

Table 5.8 presents the 15th and 50th percentile walking speeds calculated for those pedestrians walking during the crossing by age group. The walking speed values in parentheses are those obtained in a previous project TCRP-08-NCHRP 3-71 and presented in a previous by Fitspatrick et al. (2006). As shown in Table 5.8, older and elder or physically disabled pedestrians walked the slowest with 15th percentile walking speeds of 3.56(ft/s) and 3.0(ft/s), respectively. Pedestrians belonging to the young age group walked the fastest at 15th percentile speed of 4.43(ft/s). Teenagers and middle age pedestrians were determined to walk at the same speed of 4.07(ft/s). The 50th percentile

speeds also show older and elder or physically disabled pedestrians walked the slowest at average speeds of 4.07(ft/s) and 3.35(ft/s), respectively. Unlike the 15th percentile speed which shows pedestrians belonging to the young age group walked the fastest at an average speed of 4.43(ft/s), the 50th percentile speed shows young pedestrians walked the fastest at an average speed of 5.17(ft/s). Teenagers walked at 50th percentile speed of 4.71(ft/s). This speed is slightly slower than the 50th percentile walking speed of young and middle age pedestrians, but faster than the 50th percentile walking speed of old and elder or physically disabled pedestrians.

Table 5.8 Percentile Walking Speed by Age Group

		Walking Speed(ft/s)	
Age Group	Sample Size	15th Percentile	50th Percentile
Elderly or Physically disabled	60(15)	3.0(2.75)	3.35(3.38)
Older(more than 60 but not classified as elderly)	149(92)	3.56(3.19)	4.07(4.38)
Middle(ages 31 -60)	1685(1464)	4.07(3.82)	4.75(4.75)
Young(ages 19 - 30)	653(789)	4.43(3.83)	5.17(4.78)
Teen (ages 13 - 18)	268(76)	4.07(3.79)	4.71(4.64)
Age Uncertain	89	4.13	4.75
All Pedestrian	2,904(2,445)	4.07(3.82)	4.75(4.78)

( ) are the walking speeds obtained in a TCRP-08-NCHRP 3-71 project

Figure 5.12 shows the distribution of 15th and 50th percentile walking speeds by age group presented in Table 5.8. All walking speeds are previously discussed.

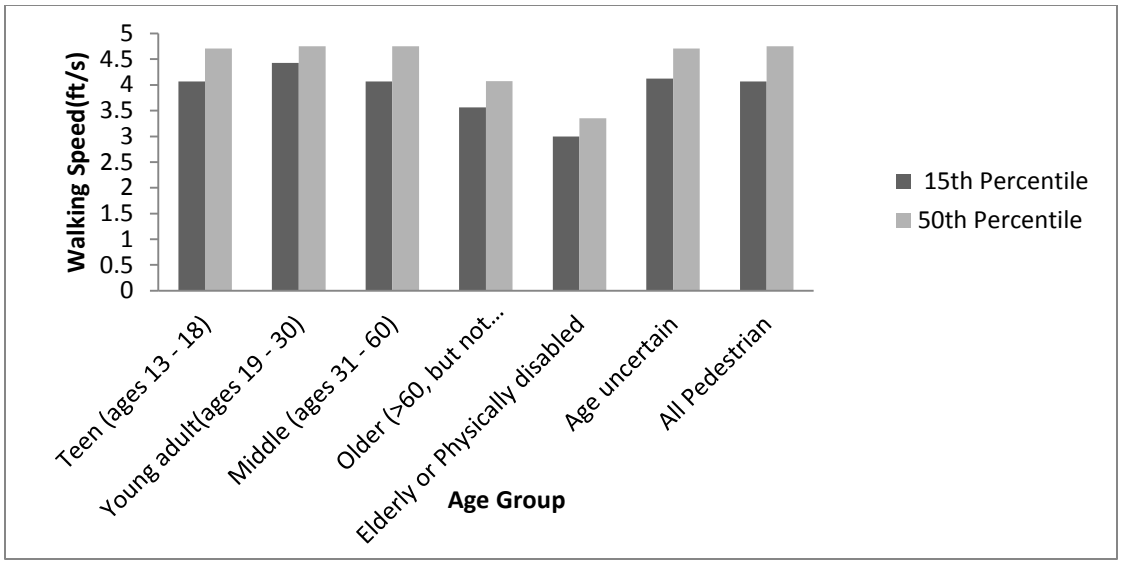

Figure 5.12 Percentile walking speed by age group.

Table 5.9 presents the 15th and 50th percentile walking speeds by age group and gender. To compare the results in this study with a study conducted by Fitspatrick et al. (2006), the data were regrouped to reflect the following:

- Age 60 or younger(ages 13 -60)
- Older than 60

The walking speeds for younger pedestrians are greater than those of older pedestrians. The 15th percentile walking speed for younger pedestrians is 4.71(ft/s), while the 15th percentile walking speed for older pedestrians was 3.35(ft/s). Younger and older pedestrians have the same 50th percentile speed of 3.8 ft/s. In addition, the walking speeds for male pedestrians are greater than those for female pedestrians. The 15th percentile speed for all male pedestrian is 4.13(ft/s) and the 15th percentile walking speed for female is 4.00(ft/s). The 50th percentile walking speeds for male and female are 4.75(ft/s) and 4.71(ft/s), respectively.

Table 5.9 Percentile Walking Speed by Age Group and Gender

Age Group	Sample Size	Walking Speed(ft/s) 15th Percentile	Walking Speed(ft/s) 50th Percentile
Male			
Young	1212(1,434)	4.38(3.75)	4.75(4.78)
Old	89(75)	3.43(3.11)	4.07(4.19)
All	1,301(1,509)	4.13(3.67)	4.75(4.75)
Female			
Young	1,390(890)	4.07(3.79)	4.71(4.67)
Old	120(31)	3.30(2.82)	3.67(4.41)
All	1,510(921)	4.00(3.75)	4.71(4.67)
Both genders			
Young	2,602(2,324)	4.71(3.77)	3.8(4.74)
Old	209(106)	3.35(3.03)	3.8(4.25)
All	2,811(2,430)	4.07(3.70)	4.75(4.72)

( ) are the walking speeds obtained in the TCRP-NCHRP 3-71 project and presented by Fitspatrick et al. (2006).

Figures 5.13 and 5.14 show the distribution of the 15th walking speeds obtained in this study and those obtained in the TCRP-08-NCHRP 3-71 project, by both age group and gender as presented in Table 5.9. The figures show the 15th percentile walking speeds obtained in this study are greater than those obtained in the TCRP-08-NCHRP 3-71 project. This difference is walking speed could be because pedestrians tend to walk faster at un-signalized midblock crosswalks than at crosswalks at signalized intersections with pedestrian signals.

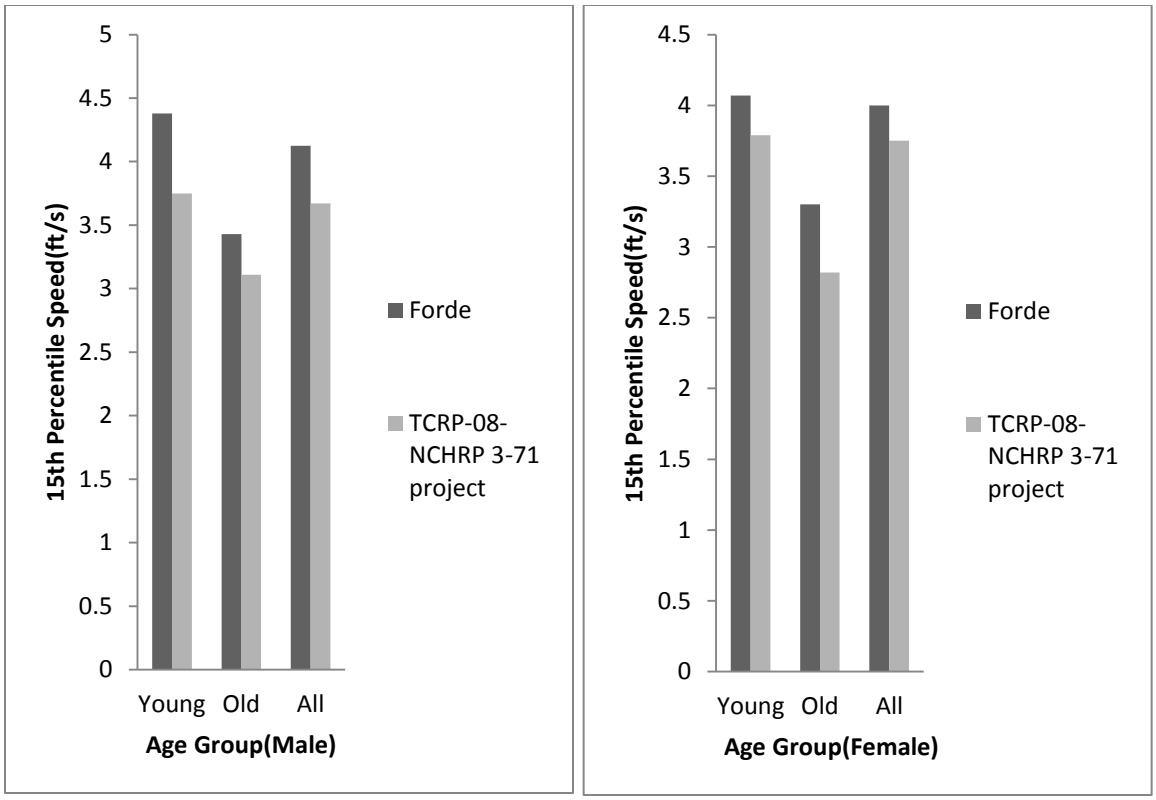

Figures 5.13 – 5.14 15th percentile walking speed by age group and gender.

Figures 5.15 and 5.16 show the distribution of the 50th walking speeds obtained in this study and those obtained in the TCRP-08-NCHRP 3-71 project and presented by Fitspatrick et al. (2006), by both age group and gender as presented in Table 5.9. Unlike Figures 5.13 and 5.14 that show the 15th percentile walking speeds obtained in this study for all age groups and gender being greater than those obtained in the TCRP-08-NCHRP 3-71 project Figure 5.15 shows the 50th percentile walking speeds obtained in this study for young and old male pedestrians are less than those obtained in the TCRP-08-NCHRP 3-71 project. The 50th percentile walking speeds for all male pedestrians, however, are the same for both studies.

In addition, Figure 5.16 shows the 50th percentile walking speeds for young and all female pedestrians obtained in this study are greater than those obtained in the TCRP-

08-NCHRP 3-71 project. However, the 50th percentile walking speed for older female pedestrians obtained in this study is less than those obtained in the TCRP-08-NCHRP 3-71 project.

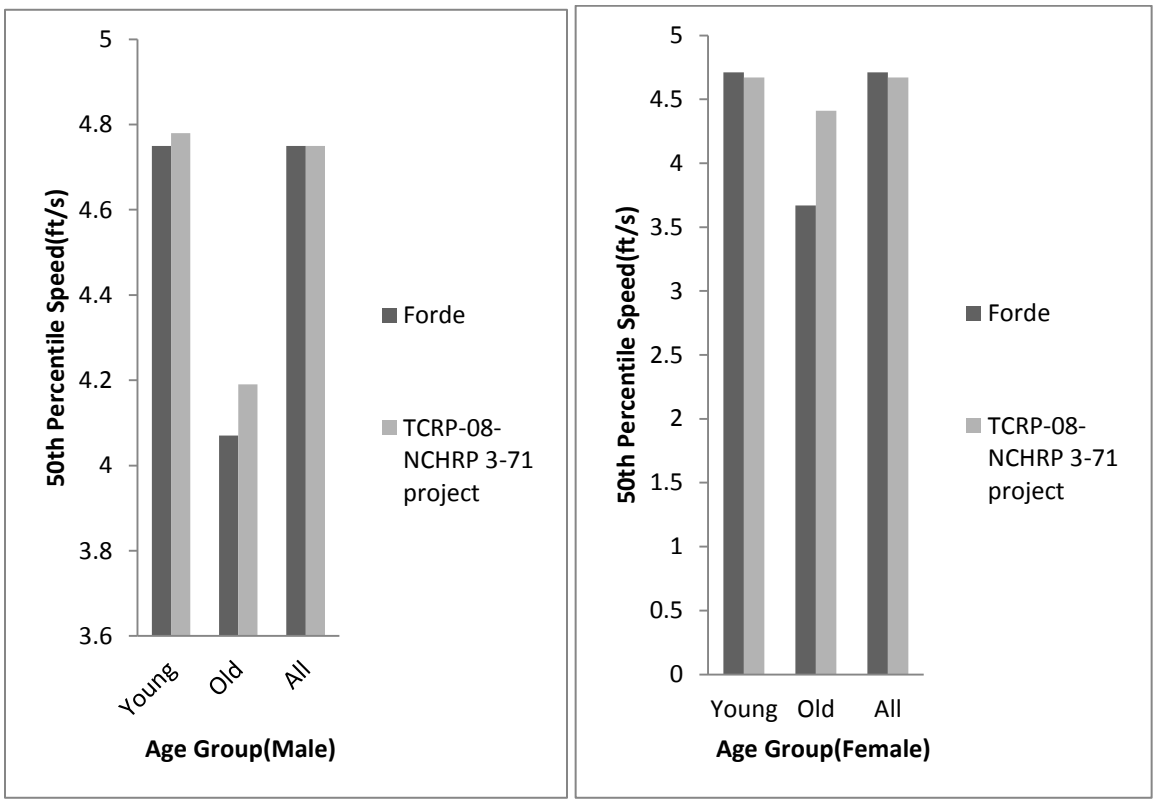

Figures 5.15- 5.16 50th percentile walking speed by age group and gender.

Figure 5.17 shows the distribution of the 15th walking speeds obtained in this study and those obtained in the TCRP-08-NCHRP 3-71 projects by age group for both gender combined. Figure 5.18 shows the distribution of the 50th walking speeds obtained in this study and those obtained in the TCRP-08-NCHRP 3-71 project by age group and both genders combined. Figure 5.17 shows the 15th percentile walking speeds obtained in this study for all age groups and gender combined are greater than those obtained in the TCRP-08-NCHRP 3-71 project. Figure 5.18 shows the 50th percentile walking speeds obtained in this study for young and old pedestrians is less than those obtained in the

TCRP-08-NCHRP 3-71 project. The 50th percentile walking speed obtained in this study for all pedestrians of both genders combined is greater than those obtained in the TCRP-08-NCHRP 3-71 project.

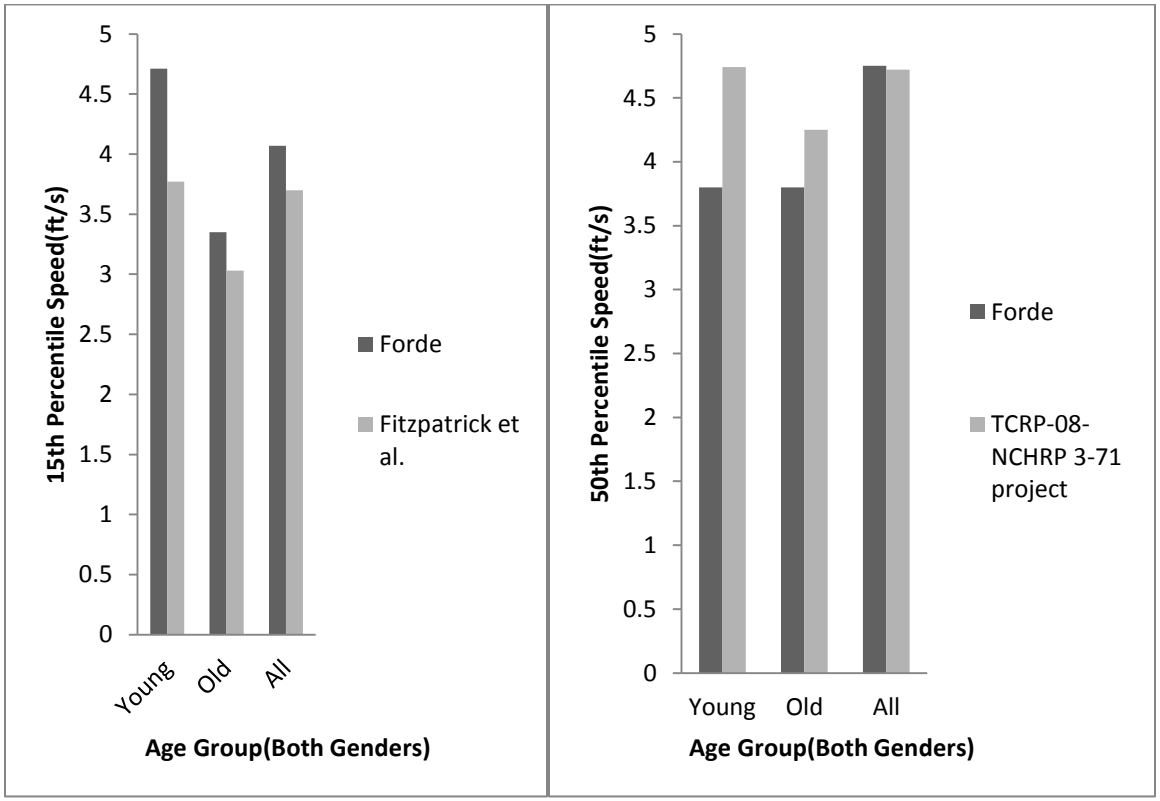

Figures 5.17 - 5.18 15th and 50th percentile walking speed by age group and gender.

Table 5.10 shows the result of an *F* test conducted to determine whether the walking speeds by gender and age group were statistically different. The results show no statically significant difference between the 15th percentile walking speeds for both age group and gender categories as shown by the p-values greater than 0.05. However, the results show statistically significant difference between the 50th percentile walking speeds for two groups: a) older and younger female pedestrians, b) younger male and female pedestrians.

Table 5.10 Results of F-Test for Gender and Age Group Walking Speed Comparison

Comparison	15th Percentile Walking Speed(ft/s)	*P-value*	50th Percentile Walking Speed(ft/s)	*P-value*
Male				
Older	3.43(3.11)	0.4950	4.75(4.19)	0.4158
Younger	4.38(3.75)		4.07(4.78)	
Female				
Older	3.35(2.82)	0.2882	4.71(4.41)	*0.0543*
Younger	4.07(3.79)		4.07(4.67)	
Both genders				
Older	3.80(3.03)	0.0681	4.75(4.25)	***0.0001***
Younger	4.07(3.77)		3.3(4.74)	
Older				
Male	3.43(3.11)	0.3645	4.07(4.19)	0.2224
Female	3.35(2.82)		4.07(4.41)	
Younger				
Male	4.38(3.75)	0.4553	4.75(4.78)	***0.0248***
Female	4.07(3.79)		4.71(4.67)	
Both age groups				
Male	4.13(3.67)	0.1951	4.75(4.75)	0.2316
Female	4.00(3.75)		4.71(4.67)	

Table 5.11 shows the sample size (N), the average walking speed, standard deviation of walking speed, minimum and maximum speed values by age group obtained in this study. As shown in Table 5.11, elder or physically disabled pedestrian walked the slowest at average speed of 3.42(ft/s). Pedestrians belonging to the young age group walked the fastest with average walking speed of 5.07(ft/s). Middle age and teenagers walked the same with average speeds of 4.75(ft/s) and 4.75(ft/s), respectively.

Table 5.11 Statistical Summary of Walking Speed by Age Group

Age Group	N	Mean	Standard deviation	Minimum value	Maximum value
Elderly or Physically disabled	60	3.4153	0.4616	2.1923	4.7143
Older(more than 60 but not classified as elderly)	149	4.1356	0.6474	2.850	7.1250
Middle(ages 31 -60)	1685	4.7564	0.6453	2.850	8.1429
Young(ages 19 - 30)	654	5.0677	0.7726	3.0000	8.2500
Teen (ages 13 - 18)	268	4.7465	0.7625	2.6667	11.0000
Age Uncertain	89	4.8224	0.496	3.4444	6.2000

Figure 5.19 shows distribution of average pedestrian walking speeds by age groups. As shown, younger pedestrians walked the fastest. While elderly or disabled pedestrians walked the slowest.

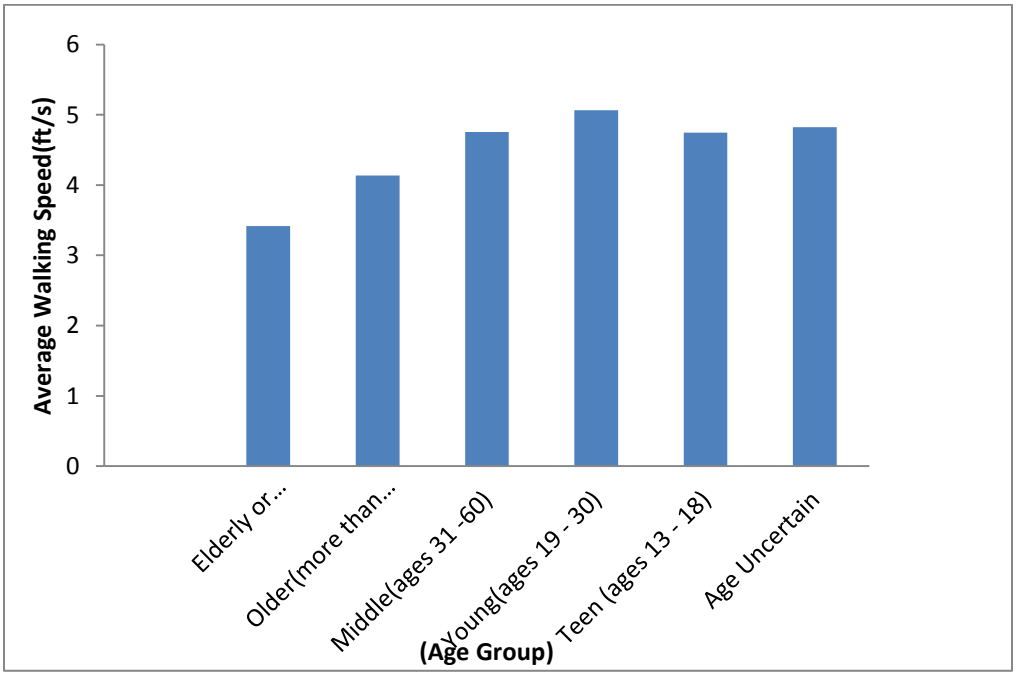

Figure 5.19 Average walking speeds by age group.

5.2.2.2 Cumulative Frequency Distribution. This subsection presents the cumulative frequency curves of pedestrian walking speeds (ft/s) for each age group and the cumulative frequency curve for free flow speeds (mph). The cumulative frequency is important when analyzing data, where the value of the cumulative frequency indicates the number of elements in the data set that lie below a specified value. As discussed previously, percentiles are often used in traffic engineering in speed-related studies. In pedestrian speed studies, the 15th percentile speed represents the walking speed which can be exceeded by 85 percent of pedestrian population.

Figure 5.20 shows the cumulative curve plotted for all walking speed values calculated for teenagers (ages 13-18). As shown in the figure, the cumulative frequency curve confirms the 15th percentile walking speed of 4.07 ft/s and 50th percentile speed of 4.71ft/s. The curve also shows an 85th percentile walking speed of 5.5 ft/s. for teenagers

Figure 5.20 Cumulative frequency distribution curve for teen age group.

Figure 5.21 shows the cumulative curve of all walking speed values calculated for young adults (ages 19-30). The figure shows a 15th percentile walking speed of 4.43 ft/s

and 50th percentile speed of 5.17 ft/s. The 85th percentile walking speed is shown as 6.2 ft/s.

Figure 5.21 Cumulative frequency distribution curve for young adults.

Figure 5.22 shows the cumulative curve for all walking speed values calculated for middle age (ages 31-60) pedestrians. The figure shows a 15th percentile walking speed of 4.07 ft/s and 50th percentile speed of 4.75 ft/s. The figure shows the 85th percentile walking speed as 5.5 ft/s.

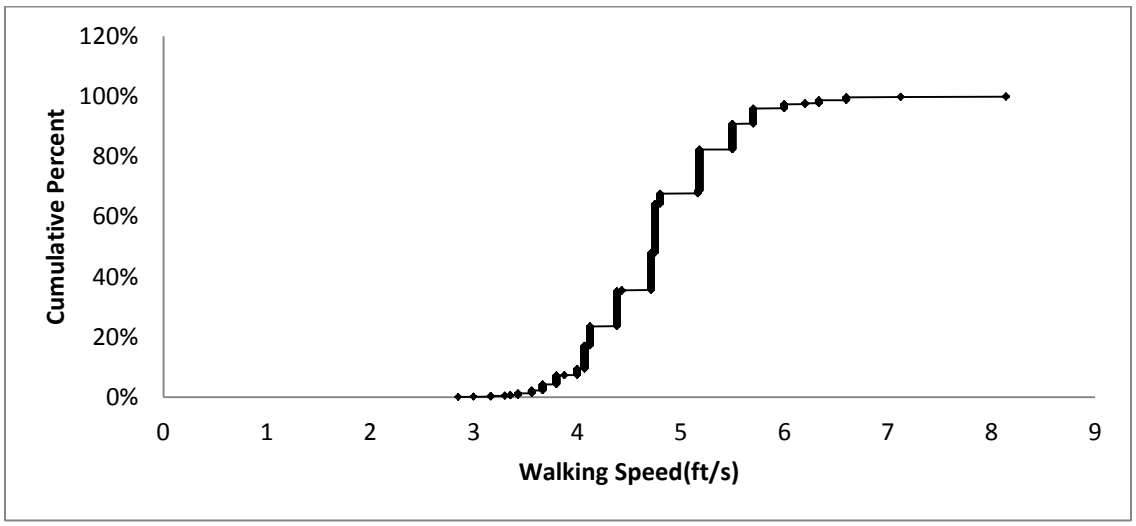

Figure 5.22 Cumulative frequency distribution curve for middle age pedestrians

Figure 5.23 shows the cumulative curve plotted for all walking speed values calculated for pedestrians older than 60, but not classified as elder or disabled. The figure shows a 15th percentile walking speed of 3.56 ft/s and 50th percentile speed of 4.07 ft/s. The figure shows an 85th percentile walking speed of 4.71 ft/s. The figure also shows 95% of older pedestrians walked at speeds below 5 ft/s.

Figure 5.23 Cumulative frequency distribution curve for older pedestrians**.**

Figure 5.24 shows the cumulative curve of all walking speed values calculated for elder or disabled pedestrian. The figure shows a 15th percentile walking speed of 3.0 ft/s and 50th percentile speed of 3.35 ft/s. The figure also shows an 85th percentile walking speed of 4.0 ft/s. The figure also shows 100% of elderly or disabled pedestrians walked at speeds below 5 ft/s.

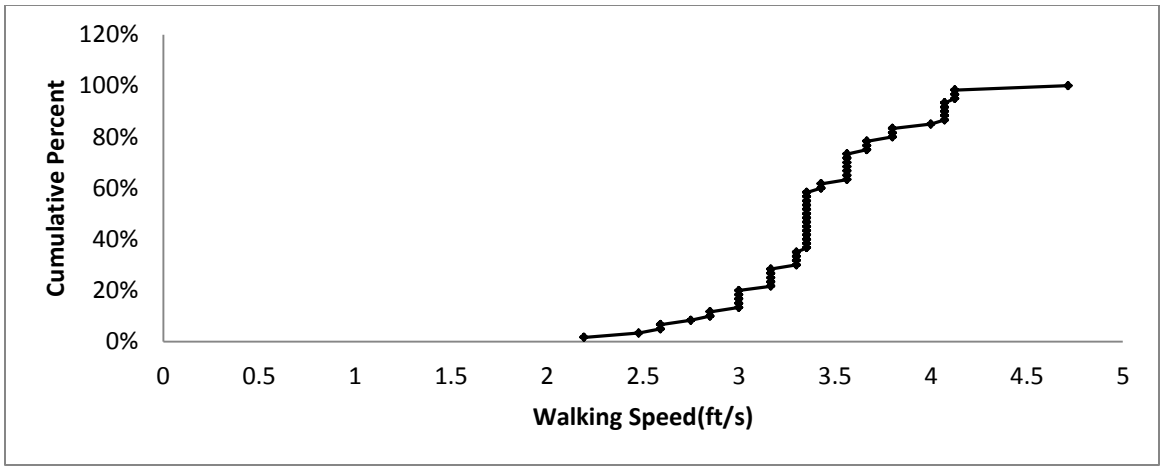

Figure 5.24 Cumulative frequency distribution curve for elder or disabled pedestrians.

Figure 5.25 shows the cumulative curve of all walking speed values calculated for pedestrians whose age groups could not be determined. The figure shows a 15th percentile walking speed of 4.125 ft/s and 50th percentile speed of 4.75 ft/s. The figure shows an 85th percentile walking speed of 5.5 ft/s.

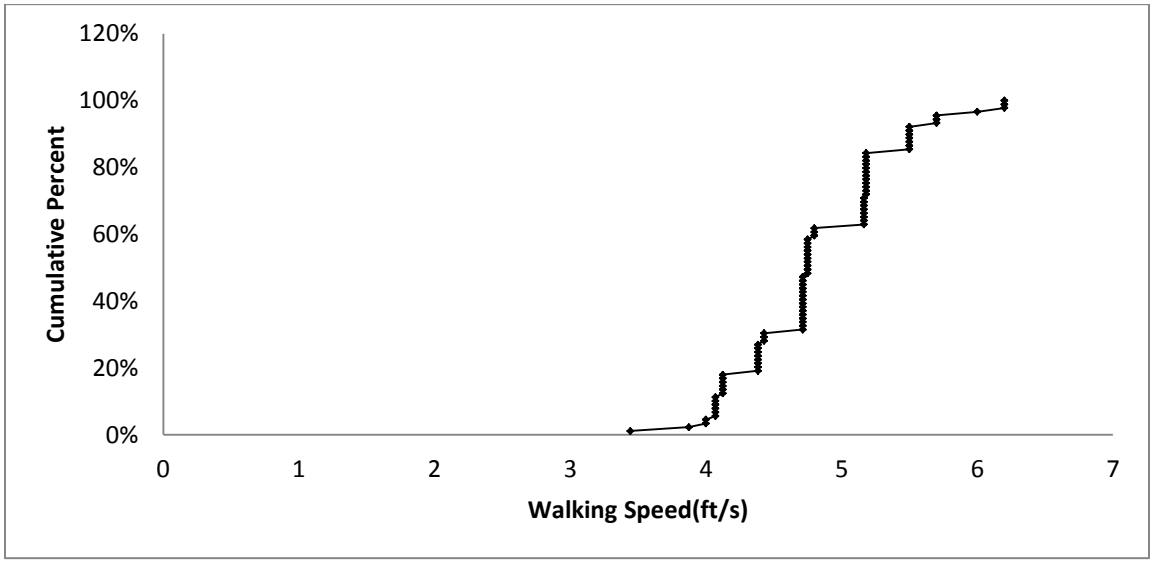

Figure 5.25 Cumulative frequency distribution curve for uncertain age group.

Figure 5.26 shows the cumulative curve of all walking speed values calculated for pedestrians of all age groups and for both genders. The figure shows a 15th percentile

walking speed of 4.07 ft/s and 50th percentile speed of 4.75 ft/s. The figure shows an 85th percentile walking speed of 5.5 ft/s.

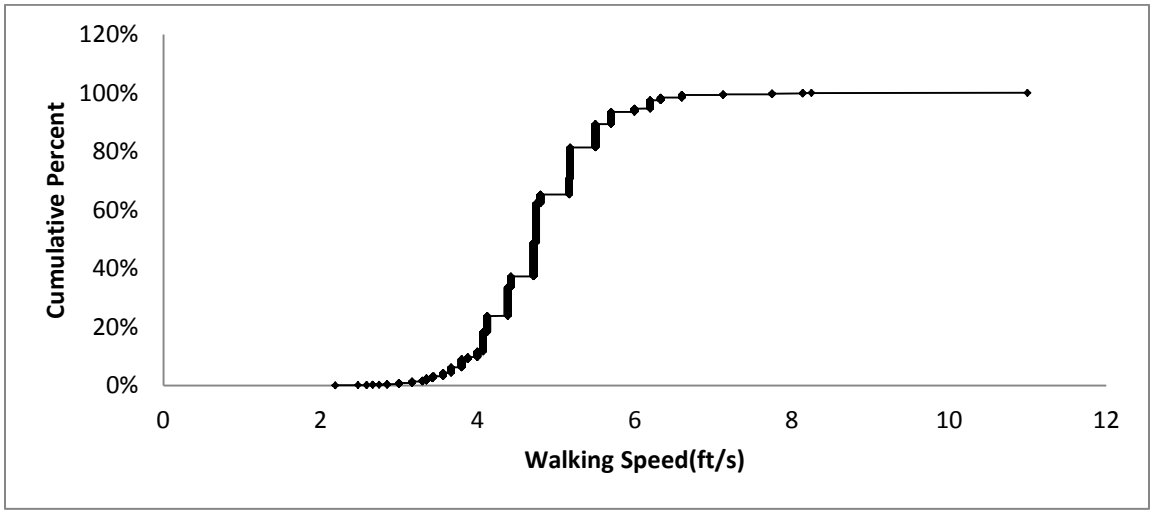

Figure 5.26 Cumulative frequency distribution curve for all age groups and both genders.

Figure 5.27 shows the cumulative curve of measured free-flow speeds. The figure shows a 15th percentile free-flow speed of 23.64 mph and 50th percentile speed of 28.3 mph. The figure shows an 85th percentile walking speed of 31.5 mph.

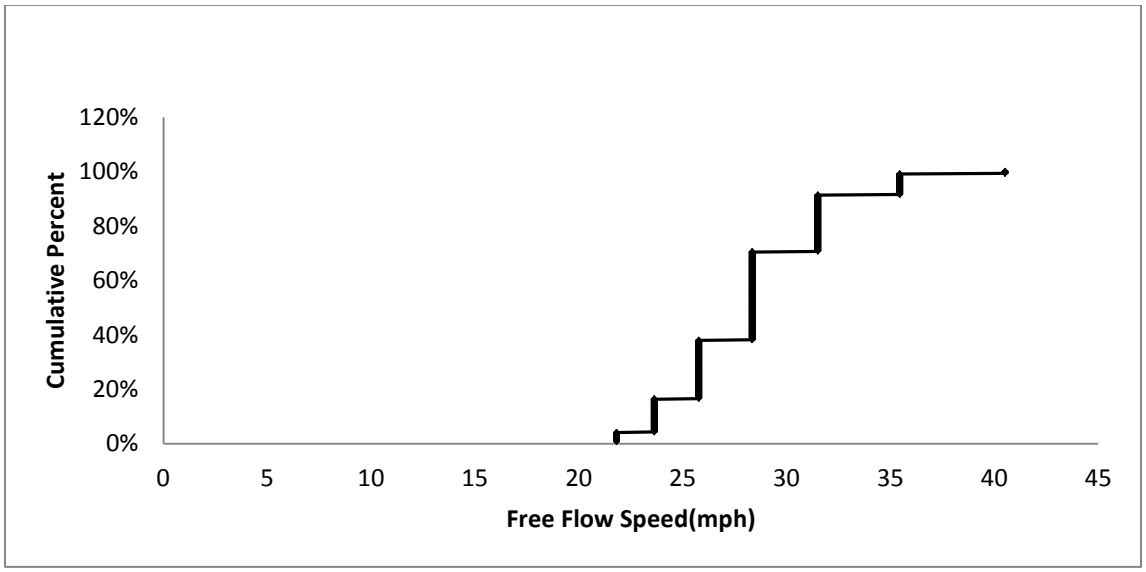

Figure 5.27 Cumulative frequency distribution curve for free-flow speed.

5.3 Results

The section presents the results obtained in this research. The section is subdivided into two subsections: Subsection 5.3.1 presents the statistical procedure and results obtained in evaluating the HCM 2010 platoon dispersion model. This subsection is presented in two parts: the first part compares the platoon arrival times measured in the field to those estimated using the HCM 2010 platoon arrival time equation. The second part of Subsection 5.3.1 compares the proportion of arrivals on green measured in the field to those estimated using the HCM 2010 platoon dispersion model and procedure. Subsection 5.3.2 presents the result of conducting study on midblock pedestrian activity on urban street segments. This subsection is presented in two parts: part one presents the results of performing Poisson regression analysis. Parts two validates both the deterministic midblock delay model developed and the probability Poisson model. .

5.3.1 Statistical Evaluation of the HCM 2010 Platoon Dispersion Model.

The statistical approach used in this research to evaluate the HCM 2010 platoon dispersion model involved applying two different groups of statistical tests to evaluate the performance of the HCM 2010 platoon dispersion model under non-friction and friction traffic conditions. These groups include: Hypothesis testing and Goodness-of-fit tests. The hypothesis test performed is the Independent two-sample t-test. The Goodness-of-fit tests include the Chi-square test, the root-mean-square error (RMSE), the root-mean-square percent error (RMSPE) and the mean absolute percentage error (MAPE). These statistics quantify the overall error of the MOPs. Percent error measure provides information on the magnitude of the error relative to the average measurement. These

statistical tests were performed to compare the observed and estimated platoon variables for both non-friction and friction traffic conditions.

The Independent two-sample t-test compares the difference of means of the compared variables, while taking into account the difference in variance of the data set. Depending on the assumption that both population of the sample of data are equal or not equal, the standard error of the mean of the difference between the groups and the degree of freedom are computed differently. That yields two possible different t-statistics and two different p-values. In performing the independent samples t-test, there is a need to test the hypothesis on equal variance. Two methods are applied in computing the standard error of the difference of means; the Pooled and the Satterthwaite`s methods. The pooled variance estimator is used if it assumed that the two populations have equal variance. The Satterthwaite`s method is used when the variances are not assumed to be equal. Several statistics are obtained from the Independent two-sample t-test as follows: ***Num DF*** **is** the degree of freedom for the F-distribution. The F distribution is the ratio of two estimates of variances. It therefore has two parameters, the degrees of freedom of the numerator and the degrees of freedom of the denominator. The folded form of the F statistic, F', tests the hypothesis that variances are equal. ***Pr>F*** is the two-tailed significance probability. The null hypothesis states that there is no statistically significant difference between the means of the compared variables. The null hypothesis is rejected if the p-value is less than or equal to the significance level of 0.05. If the p-value is greater than 0.05, however, the null hypothesis is not rejected. Similarly, the null hypothesis for the Chi-square test is rejected if the calculated chi-square is greater than the critical chi-square statistic. Otherwise it is not rejected.

5.3.1.1 Comparison of Measured and Estimated Platoon Arrival Time. The measured and estimated platoon arrival times were compared to determine how well the platoon arrival time equation, a key component of the HCM 2010 platoon dispersion model, can estimate the time in seconds a platoon will arrive at downstream signalized intersection after departing the upstream signal. To increase the sample sizes, the data set for Sites 2 and 4(sites with no friction conditions) were grouped. Similarly, the data set for Sites 1 and 3 were grouped. Table 5.12 shows a statistical summary of platoon arrival time validation. The variable column represents the measured and estimated variables; the ***N*** column represents the validation sample sizes. The ***Mean*** column shows the mean value of the measured and estimated platoon arrival time data sets. ***Std.Dev.*** is the standard deviation of the compared variables. ***Std. Err*** is the standard error of the mean. It is a measure of how the sample mean deviates from the actual population mean. The 95% Confidence Level of the mean is a range of values (interval) of the measured and estimated platoon arrival time that acts as a good estimate of the unknown population mean of platoon arrival times.

Table 5.12 Summary of Platoon Arrival Time Validation Data

Variable		N	Mean	Std Dev	Std Err	Min.	Max.	95% CL Mean	
Platoon Arrival Time Under No-Friction Condition(sec)	Estimated	66	11.05	1.39	0.17	11	14	11.57	12.25
	Measured	66	11.91	2.42	0.30	7	17	11.32	12.5
Platoon Arrival Time Under Friction Condition(sec)	Estimated	98	12.29	2.47	0.25	11	17	11.79	12.78
	Measured	98	18.2	4.07	0.41	10	28	17.39	19.02

Table 5.13 shows the results of t-test statistics of platoon arrival time for both non-friction and friction traffic conditions. Using the grouped data sets, the Independent two-sample t-test in SAS 9.2 was performed to compare the difference between the measured and estimated platoon arrival times. It tests whether the difference in means for these two variables is zero. Based on the Pooled and Satterthwaite method, the p-value is 1.00 for non-friction traffic conditions. This value is greater than 0.05 and it is therefore concluded that the difference in mean between the estimated and measured platoon arrival time is not significantly different from zero. However, the p-value of 0.001 for both methods for friction condition is less than the significant level of 0.05. It is therefore concluded that the difference in mean between the measured and estimated platoon arrival time is significantly different from zero. The test results confirm the statistical summary of the validation data. The HCM 2010 platoon arrival time equation performs well in estimating the platoon arrival times on urban street segments with minimal or no traffic friction condition. The equation, however, does not under performs on urban street segments with friction traffic conditions. The results show the platoon arrival time over-estimates the platoon arrival time under traffic friction conditions. On dense urban arterial street segments with moderate to high friction conditions, there is an increase in segment running time, which consequently increases the platoon arrival time at the downstream signal. Under friction traffic condition, the HCM 2010 platoon arrival time equation under-estimates the arrival time of the platoon (i.e. platoon arrives earlier at the downstream signal than observed in the field). On urban street segment with friction conditions, likelihood of a being interrupted is greater.

Table 5.13 Results of T-test Statistics of Platoon Arrival Time Data

Variable	Method	Equality of Variances			Variances	DF	t Value	Pr > |t|
		Num DF	F Value	Pr > F				
Platoon Arrival Time Under No-Friction Condition(sec)	Folded F	65	3.02	<.0001				
	Pooled				Equal	130	0.00	1.0000
	Satterthwaite				Unequal	103.8	0.00	1.0000
Platoon Arrival Time Under Friction Condition(sec)	Folded F	97	2.7	<.0001				
	Pooled				Equal	194	-12.31	<.0001
	Satterthwaite				Unequal	160.2	-12.31	<.0001

Table 5.14 shows the results of Chi-square test. As shown in the table, the calculated chi-square statistic is less than the critical chi-square value for platoon arrival time under no-friction traffic condition. This indicates no statistically significant difference between the platoon arrival times measured at urban street segments with no-friction condition and those estimated using the HCM 2010 platoon arrival time equation. The result, however, shows the calculated chi-square statistic is greater than the critical chi-square value for platoon arrival time under friction traffic condition indicating statistically significant difference between the measured and estimated values. These results confirm the test results obtained in the Independent two-sample t-test.

Table 5.14 Results of Chi-square Test Statistics of Platoon Arrival Time Data

Variable	df	χ^2	$\chi^2_{df,\alpha}$	$\chi^2 > \chi^2_{df,\alpha}$	Difference Statistically Significant?
Platoon Arrival Time Under No-Friction Condition(sec)	65	18.65	84.82	No	No
Platoon Arrival Time Under Friction Condition(sec)	97	**338.73**	120.99	Yes	Yes

Table 5.15 shows the results of the mean errors calculated for each group of data and for each traffic condition. The results show relatively small root mean square error, root mean square percent error, and mean absolute percent error for the comparison of measured and estimated platoon arrival time under no traffic conditions. However, the mean errors for the comparison of measured and estimated platoon arrival time under traffic friction condition are relative large. These mean error values support the conclusions of the t-test and chi-square tests.

Table 5.15 Mean errors of platoon arrival time data

Variable	RMSE	RMSPE	MAPE(%)
Platoon Arrival Time Under No-Friction Condition(sec)	1.8174	0.1731	12.3012
Platoon Arrival Time No-Friction Condition(sec)	6.4949	0.3344	31.3446

In addition to performing quantitative evaluation tests to compare the measured and estimated platoon arrival times, qualitative evaluation tests are also performed. One of these qualitative tests in the histogram plots showing the percent distribution of the residuals. The residual values are the difference of the measured and estimated platoon

arrival times. Figure 5.28 shows the residual plots of the measured and estimated platoon arrival time under no-friction condition, while Figure 5.29 residual values are the difference of the measured and estimated platoon arrival times under traffic friction condition. Normally, the residuals should be distributed in a bell shape (i.e., more points around 0 and the rest balanced at both sides). Only Figure 5.28 shows a nearly bell shape with more than 40% of the residual values are distributed around 0 (i.e. between 0 and less than +/- 2 second residual value). Unlike Figure 5.28, in Figure 5.29, only about 6% of the residual values are distributed around 0(i.e. 0 and less +/-2 second of residual value). This shows the HCM 2010 Platoon arrival time equation underestimates the platoon arrival time under friction condition.

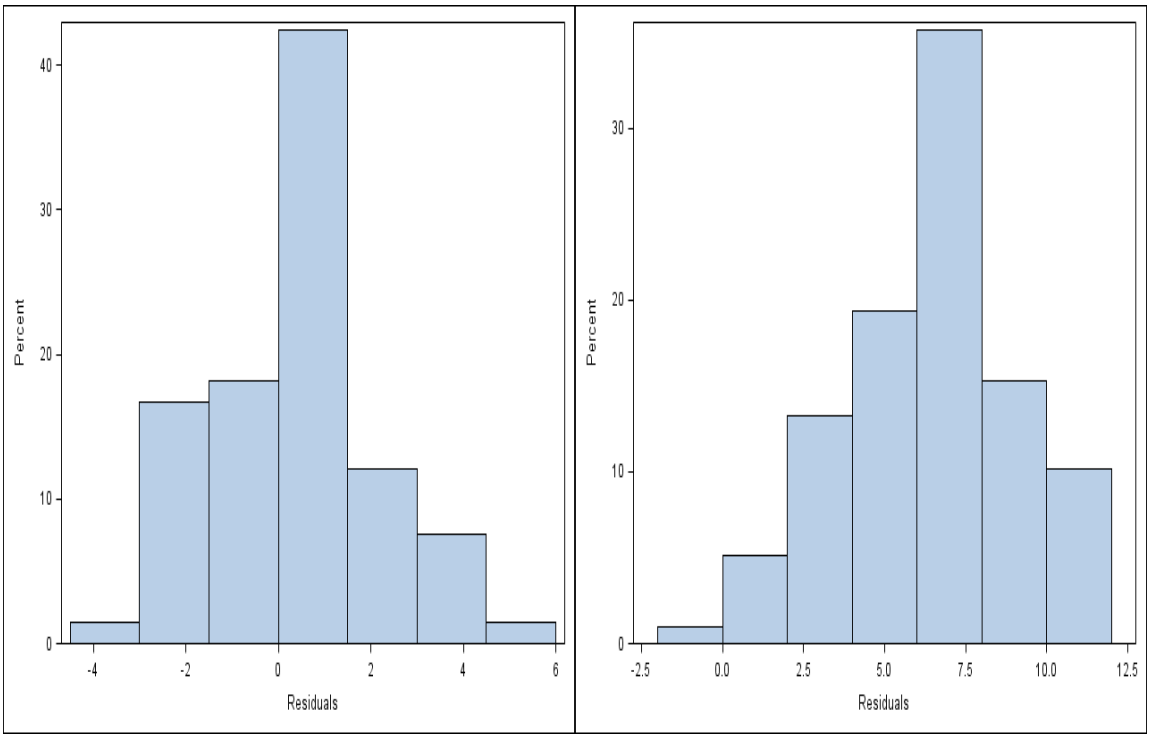

Figures 5.28-5.29 Residuals of platoon arrival time for non-friction and friction traffic conditions, respectively.

5.3.1.2 Comparison of Observed and Estimated Proportion of Arrivals on Green. This subsection compares the observed and estimated proportion of arrivals on green under non-friction and friction conditions. The same statistical tests were performed to compare the proportion of arrivals on green. Table 5.16 shows the statistical summary of proportion of arrivals of green data for both traffic conditions.

Table 5.16 Summary of Proportion of Arrivals on Green Validation Data

Variable		N	Mean	Std Dev	Std Err	Min.	Max.	95% CL Mean	
Proportion of Arrivals on Green Under No-Friction Condition (%)	Estimated	88	76.83	19.87	2.12	32.00	100.00	72.62	81.04
	Observed	88	81.08	19.43	2.07	32.00	100.00	76.96	85.20
Proportion of Arrivals on Green Under Friction Condition (%)	Estimated	79	63.19	14.52	1.63	29.00	100.00	59.94	66.44
	Observed	79	49.19	16.33	1.84	18.00	100.00	45.53	52.85

Table 5.17 shows the results of t-test statistics of proportion of arrivals on green for both non-friction and friction traffic conditions. Based on the Pooled and Satterthwaite method, the p-value is 0.1533 for non-friction traffic conditions. This value is greater than 0.05. Therefore it is concluded that the difference in mean between the observed and estimated proportion of arrivals is not significantly different from zero. However, the p-value of 0.001 for both methods for friction traffic condition is less than the significant level of 0.05. It is therefore concluded that the difference in mean of the observed and estimated values is significantly different from zero. This significant difference in the mean is due to the platoon arrival time equation of the HCM platoon dispersion model under-estimating the platoon arrival time(platoon arriving earlier than

observed in the field) and subsequently over-estimating the proportion of arrivals on green at the downstream signal(i.e. more vehicle arrivals than observed in the field).

Table 5.17 Results of T-test Statistics of Proportion of Arrivals on Green Validation

Variable	Method	Equality of Variances			Variances	DF	t Value	Pr > |t|
		Num DF	F Value	Pr > F				
Proportion of Arrivals on Green Under No-Friction Condition (%)	Folded F	87	1.05	0.834				
	Pooled				Equal	174	-1.43	0.1533
	Satterthwaite				Unequal	173.9	-1.43	0.1533
Proportion of Arrivals on Green Under Friction Condition (%)	Folded F	78	1.27	0.301				
	Pooled				Equal	156	5.7	<.0001
	Satterthwaite				Unequal	153.9	5.7	<.0001

Table 5.18 shows the results of Chi-square test. As shown in the table, the calculated chi-square statistic is less than the critical chi-square value for proportion of arrivals on green under no-friction traffic condition. This indicates no statistically significant difference between the proportion of arrivals on green measured at the urban street segments with no-friction condition and those estimated using the HCM 2010 procedure. The result, however, shows the calculated chi-square statistic is greater than the critical chi-square value for proportion of arrivals on green under friction traffic condition indicating statistically significant difference between the measured and estimated values. These results confirm the test results obtained in the Independent two-sample t-test

Table 5.18 Results of Chi-square Test Statistics of Proportion of Arrivals on Green

Variable	df	χ^2	$\chi^2_{df,\alpha}$	$\chi^2 > \chi^2_{df,\alpha}$	Difference Statistically Significant?
Proportion of arrivals on green under non-friction condition(%)	87	93.58	109.77	No	No
Proportion of arrivals on green under friction condition(%)	78	596.62	99.62	Yes	Yes

Table 5.19 shows the results of the mean errors calculated for each group of data and for each traffic condition. The results show relatively small root mean square error, root mean square percent error, and mean absolute percent error for the comparison of measured and estimated proportion of arrivals on green under no traffic conditions. However, the mean errors for the comparison of measured and estimated proportion of arrivals on green under traffic friction condition are relative large. These mean error values support the conclusions of the t-test and chi-square tests.

Table 5.19 Mean Errors of Proportion of Arrivals on Green

Variable	RMSE	RMSPE	MAPE(%)
Proportion of Arrivals Under No-Friction Condition (%)	8.4315	0.1211	8.2638
Proportion of Arrivals Under Friction Condition(%)	17.2428	0.2705	22.8679

Figures 5.30 and 5.31 show the residual plots of the observed and estimated for proportion of arrivals on green under no-friction and friction conditions, respectively. Figure 5.30 shows a nearly bell shape with about 80% of the residual values are distributed around 0 (i.e. between 0 and less than +/- 10% residual value). Figure 5.31 on the other shows about 41% of the residual values are distributed around 0(i.e. between. 0 and less +/10residual value). This figure shows majority of the residual values are less than 0. This indicates the HCM 2010 platoon dispersion model over-estimates the proportion of arrivals on green under friction condition.

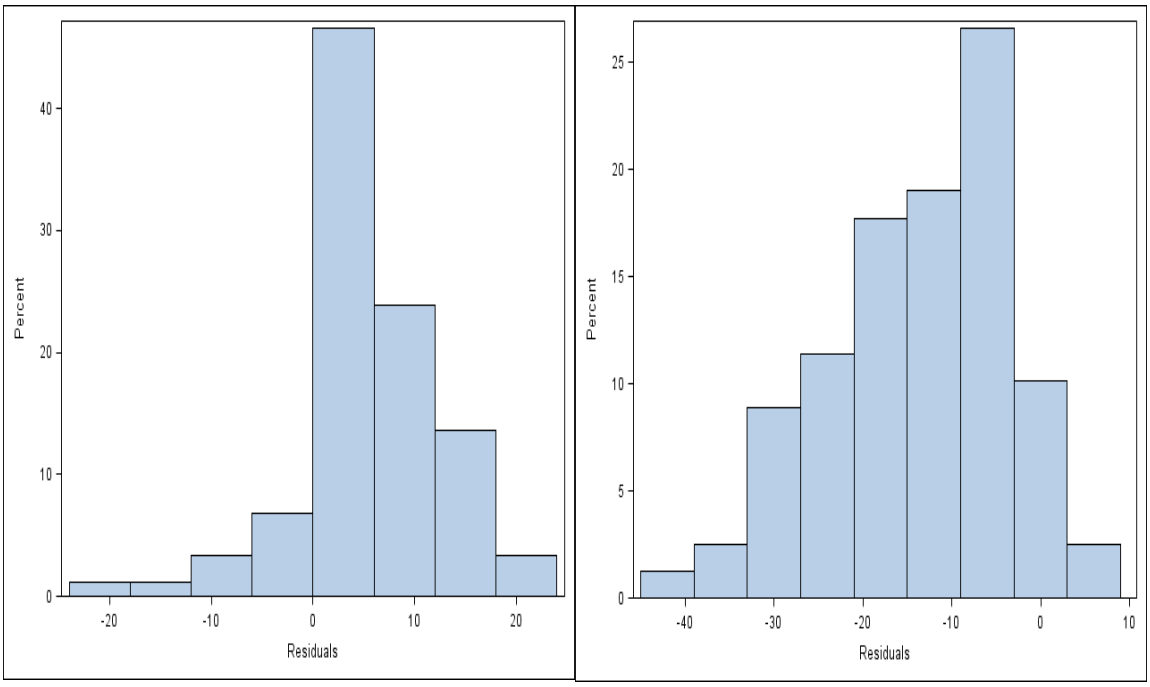

Figures 5.30 - 5.31 Residuals of proportion of arrivals on green for non-friction and friction traffic conditions, respectively.

Another qualitative model evaluation technique used in this research is the use of diagonal plots to compare the observed and estimated values. Figures 5.32 and 5.33 below show diagonal plots obtained for each traffic condition. The observed proportion of arrivals on green is plotted against the estimated proportion of arrivals on green, with

the mean shown as a large bold symbol. A diagonal line with zero slope and y-intercept of 1 is overlaid. The location of the points with respect to the diagonal line reveals the strength and direction of the difference of the observed and estimated proportion of arrivals. Tight clustering along the line indicates positive correlation of the two variables. The ideal fit would be a 45 degree line than runs from the bottom left to the upper right.

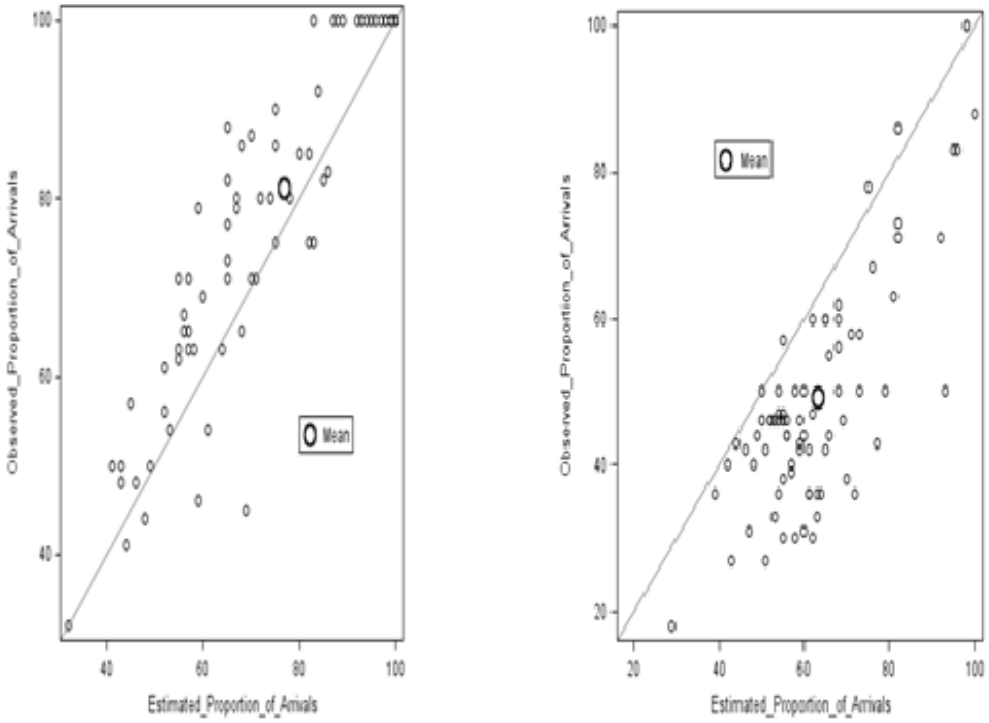

Figures 5.32 - 5.33 Diagonal plots of proportion of arrivals on green for non-friction and friction traffic conditions, respectively.

5.3.2 Development and Validation of Midblock Delay Model

This subsection is divided into two parts. The first present a detailed description of the regression procedure used in developing the Poisson regression model and a discussion of the results obtained. The second part of this subsection presents the technique used in

this research to validate both the deterministic midblock delay and the stochastic Poisson regression model.

5.3.2.1 Development of Poisson Regression Model. The midblock delay model developed in this research comprised of a Poisson probability model. This probability model is applied to calculate the probability of a number of midblock interference occurring during a specified time period at midblock crosswalks on urban street segments.

A Poisson regression analysis was performed to estimate the model coefficients for the following independent variables: traffic volume per hour, pedestrian volume per hour and number of pedestrian crossing per hour. The GENMOD (Generalized Linear Model) procedure in SAS 9.2 was applied in the model development. The GENMOD procedure fits generalized linear models, as defined by Nelder and Wedderburn (1972). The class of generalized linear models is an extension of traditional linear models that allows the mean of a population to depend on a *linear predictor* through a nonlinear *link function* and allows the response probability distribution to be any member of an exponential family of distributions.

The regression analysis was performed for two sets of variables: The first set includes the number of midblock interference per hour as the response variable, while traffic volume per hour and the pedestrian volume per hour were used as predictor variables. The second set of data included the number of midblock interference per hour as the response variable, while traffic volume per hour and the number of pedestrian crossing per hour were used as predictor variables. The goal was to determine which of the two data sets fits the model better. Using the generalized linear model procedure in

SAS 9.2 and specifying the Poisson distribution, the model parameters were estimated for both sets of data as shown in Tables 5.20 and 5.21.

In Tables 5.20 and 5.21 below, ***Parameter*** shows the predictor variables and the scale parameters. ***DF*** is the degrees of freedom (DF) spent on each of the respective parameter estimates. The ***Estimate*** is the estimated Poisson regression coefficients for the model. The response variable (number of interference per hour) in this analysis is a count variable. Poisson regression models the log of the number of interference per hour as a linear function of the predictor variables (traffic volume per hour, pedestrian volume per hour and the number of crossings per hour). ***Standard Error*** is the standard errors of the individual regression coefficients. They are used in both the Wald 95% Confidence Limits and the Chi-square test statistic. ***Wald 95% Confidence Limits*** is the Wald Confidence Interval (CI) of an individual Poisson regression coefficient, given the other predictors are in the model. That is, for a given predictor variable with a level of 95% confidence, we are 95% confident that upon repeated trials, 95% of the confidence intervals will include the true population Poisson regression coefficient. ***Wald Chi-Square and Pr>ChiSq*** are the test statistics and p-values, respectively. They test the null hypothesis that the regression coefficient is zero, given that the rest of the predictors are in the model.

As shown in Table 5.20, the p-values for the model parameters are less than 0.05. This indicates the model coefficients are significantly different from zero. Therefore the null hypothesis that the regression coefficients are zero is rejected. In Table 5.21, the p-values of the model parameters are also far less than 0.05. Therefore the null hypothesis that the regression coefficients are zero is rejected. The results also show that

combinations of traffic volume per hour and any of the two variables: the pedestrian volume per hour or the number of pedestrian crossing, are good predictors of the number of midblock pedestrian interference per hour on urban street segments.

Table 5.20 Analysis of Maximum Likelihood Parameter Estimates for Traffic volume and Pedestrian Volume

Parameter	DF	Estimate	Standard Error	Wald Chi-Square	Pr >ChiSq
Intercept	1	0.6753	0.2464	7.51	0.0061
Traffic_Volume	1	0.0046	0.0007	48.41	<.0001
Pedestrian_volume	1	0.0058	0.0005	112.09	<.0001
Scale	0	1.0000	0.0000		

Table 5.21 Analysis of Maximum Likelihood Parameter Estimates for Traffic Volume and Number of Pedestrian Crossings

Parameter	DF	Estimate	Standard Error	Wald Chi-Square	Pr>ChiSq
Intercept	1	0.8136	0.2359	11.90	0.0006
Traffic_Volume	1	0.0039	0.0006	36.46	<.0001
Number_of_Crossings	1	0.0078	0.0007	115.08	<.0001
Scale	0	1.0000	0.0000		

5.2.3.2 Validation of the Developed Midblock Delay Model. This subsection presents the results obtained in validating both the deterministic midblock delay model and the stochastic Poisson regression model. The model validation was aimed at determining if the models would perform successfully when applied in real world traffic conditions.

5.2.3.2.1 Validation of the Deterministic Midblock Delay Model. The first step involved in validating the developed midblock delay model was to measure a data set of the midblock delay in seconds per vehicle incurred by platoon vehicles due to pedestrian crossings at midblock crosswalks on urban street segments. HCM 2010 describes a

technique for measuring control delay at a signalized intersection called the queue-count technique and it is based on direct observation of vehicle-in-queue counts for a subject lane group. According to the Manual, the measurement technique normally requires: a) two field personnel for each lane group surveyed; (b) a multifunction digital watch that includes a countdown repeater timer, with the countdown interval in seconds, and (c) a volume-count board with at least two tally count makers. In this research, a similar but different technique was used to measured midblock delay due to pedestrian interference. In addition, instead of using the measuring equipment stated in the HCM 2010, this research made use of a video camera positioned at an elevation to capture an aerial view of midblock vehicular and pedestrian activities at the study street segment. The use of video cameras provided an opportunity for replays and reviews. This approach was to ensure that accurate measurements were obtained. The midblock delay measurement procedure involved using an electronic stop watch to record several delay variables for both single vehicles and more than one vehicle platoon size.

For single vehicles, four delay variables were measured: the pedestrian(s) walking time(s); the time for the vehicle to decelerate to a full stop or to slow down depending on the scenario; the stopped or slowing time; the time for the vehicle to accelerate back to the normal speed after the interference ended. For more than one -vehicle platoon size, five platoon variables were measured: the pedestrian(s) walking time(s); the time for the leading platoon vehicle to decelerate to a full stop or to slows down; the stopped time for the leading platoon vehicle; the time for the leading platoon vehicle to accelerate back to the normal speed after the interference ended and finally, the time for all the following platoon vehicles to cross a reference point, where the leading platoon vehicle came to a

full stop. Based on very careful observations, the start of pedestrian walking time was recorded from the point when it was deemed the driver of the leading platoon vehicle had seen the pedestrian or group of pedestrians, perceived the potential interference and therefore stepped on his/her brake. The elapse time from the start of the interference and the leading platoon vehicle coming to a full stop or slowing down was measured as the "deceleration time". If the vehicle came to a full stop, the stopped time was recorded as the elapsed time from the vehicle coming to a full stop and the start-up time. The vehicle start-up, based on careful observations, corresponded to the end of the pedestrian walking time. The acceleration time was recorded as the elapsed time between the vehicle starting-up and attaining normal speed.

For more than one vehicle platoon sizes, the previous measurement steps were repeated for the leading platoon vehicle plus the time for all the following platoon vehicles to cross a reference point where the leading platoon came to a full stop. This procedure used in measuring midblock delay was repeated for several platoon sizes. The midblock delay in second per vehicle was obtained by dividing the total midblock delay per platoon by the platoon size. A total validation data set of 226 samples of measured midblock delay in second per vehicle was obtained. This included a range of 1 to 9 platoon sizes.

The second step in validating the deterministic midblock delay model involved using field measured variables and parameters, including those variables and parameters obtained in this research and those provided in the HCM 2010, to estimate the midblock delay to each platoon vehicle and subsequently the total delay per platoon. The field measured variables and parameters include but not limited to: the field measured free-

flow speed, pedestrian walking time, traffic volume per hour, and rate of deceleration, rate of acceleration. Using excel spreadsheet and the input variables and parameters, the delay to the leading and following platoon vehicles were computed using equations of the developed deterministic delay model. The computation involved iterations for more than one platoon vehicle; with one iteration for each platoon vehicle. Based on the computation, midblock delay per to each subsequent platoon vehicle decreased with increase in platoon size. At the seventh iteration, the estimated delay to the seventh platoon vehicle was computed as zero for all the 226 data points. This indicated a point of convergence. Therefore, the total delay per platoon size was computed as the sum of the delay per vehicle. Because of the convergence at the seventh platoon vehicle, all delay (measured and estimated) values for seven or more platoon sizes were eliminated from data set. A final validation data set was therefore reduced from 226 to 209.

Table 5.22 below shows a summary of the midblock delay model validation data. The statistical summary was performed for three data sets as follows: for combined single vehicle and multiple vehicle platoons data set of sample size 209; single vehicle data set of sample size of 80; and multiple vehicle platoon data set of sample size of 129. The results show the difference in mean between the measured and estimated midblock delays as follows: 1.20 sec/veh for all data set, 3.23 sec/veh for single vehicle data set, and -0.0521 sec/veh for multiple vehicle platoon data set.

Table 5.22 Summary of Midblock Delay Model Validation Data

Variable		N	Mean	Std. Dev	Std. Err	Min.	Max.	95% CL Mean	
Midblock delay for all data set(s/veh)	Estimated	209	7.9033	3.7261	0.2577	1.8499	22.8684	7.3952	8.4114
	Measured	209	9.108	4.4034	0.3046	3.2563	24.962	8.5076	9.7085
Midblock delay for single Vehicle data set(s/veh)	Estimated	80	10.187	3.5342	0.3951	5.1784	22.8684	9.401	10.974
	Measured	80	13.419	3.7313	0.4172	7.1473	24.962	12.59	14.249
Midblock delay for multiple vehicle platoon data Set(s/veh)	Estimated	129	6.487	3.0937	0.2724	1.8499	21.1774	5.948	7.026
	Measured	129	6.4349	2.0252	0.1783	3.2563	13.31	6.082	6.7877

Table 5.23 shows a summary of the Independent two-sample t-test statistics for both measured and estimated midblock delay for the three data sets. The independent two- sample t-test was performed to compare means of the measured and estimated midblock delay. The goal was test whether the difference in mean of the measured and estimated midblock delay are significantly different from zero. As discussed in a previous section, depending on the assumption that both population of the sample of data are equal or not equal, the standard error of the mean of the difference between the groups and the degree of freedom are computed differently. That yields two possible different t-statistic and two different p-values. In performing the independent samples t-test, there is a need to test the hypothesis on equal variance. Two methods are applied in computing the standard error of the difference of means; the Pooled and the Satterthwaite`s methods. The pooled variance estimator is used if it assumed that the two populations have equal variance. The Satterthwaite`s method is used when the variances are not assumed to be equal. ***Num DF*** **is** the degree of freedom for the F-distribution. The F distribution is the

ratio of two estimates of variances. Because this value is less than 0.05, then it is concluded that the variances for both the estimated and measured delays are different; therefore the Satterthwaite method is used to interpreter the p-value. ***Pr>|t|,*** also known as p-value, is the two-tailed probability computed using the t-distribution. It is the probability of observing a t-value of equal or greater absolute value and the Null hypothesis. If the p-value is less than the pre-specified alpha value of 0.05, it is concluded that the difference is significant from zero. From Table 5.23, the ***Pr>|t|*** is greater than the significant level of 0.05 for all data set and multiple vehicles data set. It is therefore concluded that difference in mean between the measured and estimated midblock delay is not significantly different from zero. However, for single vehicle data set, the ***Pr>|t|*** value is less than 0.05. It is therefore concluded that the difference in mean between the measured and estimated midblock delay is significantly different from zero.

Table 5.23 Summary of Independent Two-Sample T-test Statistics of Midblock Delay Validation Data

		Equality of Variances						
Variable	Method	Num DF	F Value	Pr > F	Variances	DF	t Value	Pr > |t|
Midblock delay for all data set(s/veh)	Folded F	208	1.4	0.0164				
	Pooled				Equal	416	-3.02	0.270
	Satterthwaite				Unequal	404.91	-3.02	0.256
Midblock delay for single vehicle data set(s/veh)	Folded F	79	1.11	0.6308				
	Pooled				Equal	158	-5.62	<.0001
	Satterthwaite				Unequal	157.54	-5.62	<.0001
Midblock delay for multiple vehicle platoon data set(s/veh)	Folded F	128	2.33	<.0001				
	Pooled				Equal	256	0.16	0.8729
	Satterthwaite				Unequal	220.68	0.16	0.873

Table 5.24 shows the results of chi-square validation test. The table shows the calculated and critical chi-square statistics for the three data sets. As shown in the table, the calculated chi-square statistic is less than the critical chi-square value for all data set and multiple vehicle platoon data set. This indicates no statistically significant difference between the measured and estimated midblock delays for all data set and for multiple vehicle platoon data set. The results, however, shows the calculated chi-square statistic is greater than the critical chi-square statistic for single vehicle data set; indicating statistical difference between the measured and estimated midblock delay. These results confirm the test results obtained in the Independent two-sample t-test in Table 5.23

Table 5.24 Results of Chi-square Test of Midblock Delay Validation Data

Data Set	df	χ^2	$\chi^2_{df,\alpha}$	$\chi^2 > \chi^2_{df,\alpha}$	Difference Statistically Significant?
Midblock delay for all data set(s/veh)	208	147.77	242.65	No	No
Midblock delay for single vehicle data set(s/veh	79	103.05	100.75	Yes	Yes
Midblock delay for multiple vehicle platoon data set(s/veh)	128	41.11	155.40	No	No

Table 5.25 shows the results of the mean errors calculated for each data set. The results show relatively smaller root mean square error, root mean square percent error, and mean absolute percent error for multiple vehicle platoon data relative to all data set

and single vehicle data set. Based on the results, there is 35%, 9% and 15% decrease in the respective mean error for multiple vehicle data set relative to all data set. Conversely, the results show 39%, 13% and 24% increase in the respective mean error for single vehicle data set relative to all data set. These tests confirm the conclusion from the previous t-test and chi-square test.

Table 5.25 Mean Errors of Midblock Delay Validation Data

Variable	RMSE	RMSPE	MAPE (%)
Midblock delay for all data set(s/veh)	2.4788	0.2357	20.10054
Midblock delay for single vehicle data set(s/veh	3.4524	0.2661	24.8988
Midblock delay for multiple vehicle platoon data set(s/veh)	1.6010	0.2147	17.1248

Figures 5.34 and 5.36 below show the diagonal plot for the measured midblock delay plotted against the estimated midblock delay, with the mean shown as a large bold symbol. A diagonal line with zero slope and y-intercept of 1 is overlaid. The location of the points with respect to the diagonal line reveals the strength and direction of the difference of the measured and estimated midblock delay. Tight clustering along the diagonal line indicates positive correlation of the two variables. The ideal fit would be a 45 degree line than runs from the bottom left to the upper right. In Figure 5.34, the midblock delays measured in the field are plotted against the midblock delays estimated using the developed model. As shown in the figure, there is clustering along the diagonal line for majority of the 209 data points. There are, however, a few data points that are farther away from the diagonal line. These points represent the measure-estimated delay

values plotted for single vehicles as shown in Figure 5.35. The figure shows the developed model consistently underestimates the midblock delays when compared to the measured midblock delays, and therefore the data points are pulled away from the diagonal line toward the area of the measured midblock delay. This underestimation may be due to the parameters, especially the deceleration and accelerations rates, used in estimating the midblock delays. However, when compared to the measured midblock delays, model performs far better in estimating midblock delays for multiple vehicle platoons as shown by the tight clustering of the data points in Figure 5.36

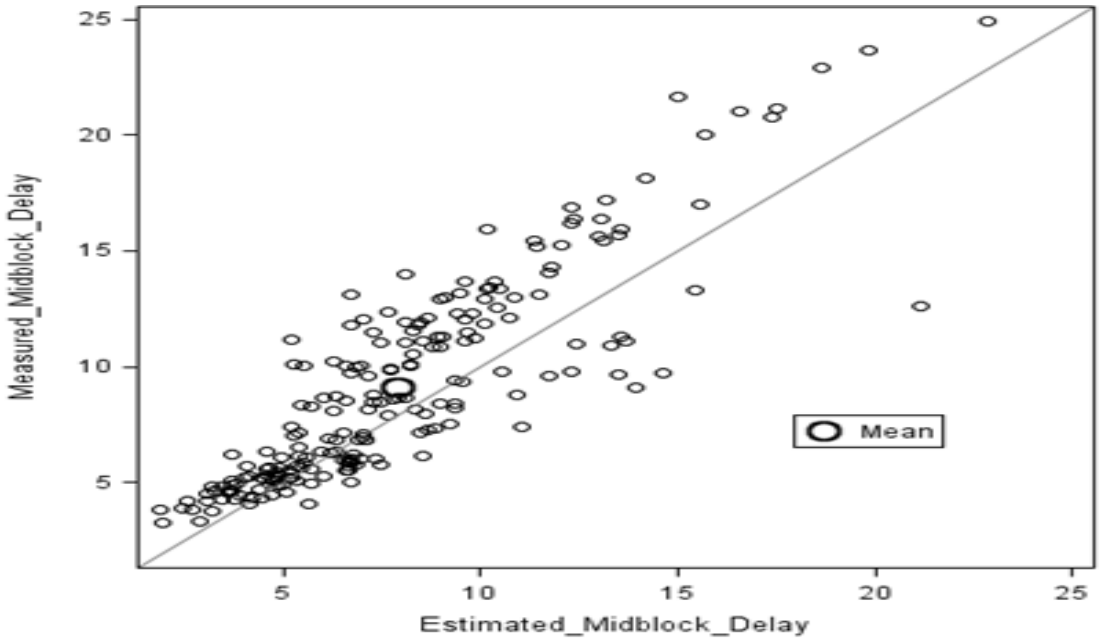

Figure 5.34 Diagonal plot of measured versus estimated midblock delay in seconds per vehicle for both single and multiple vehicle platoons.

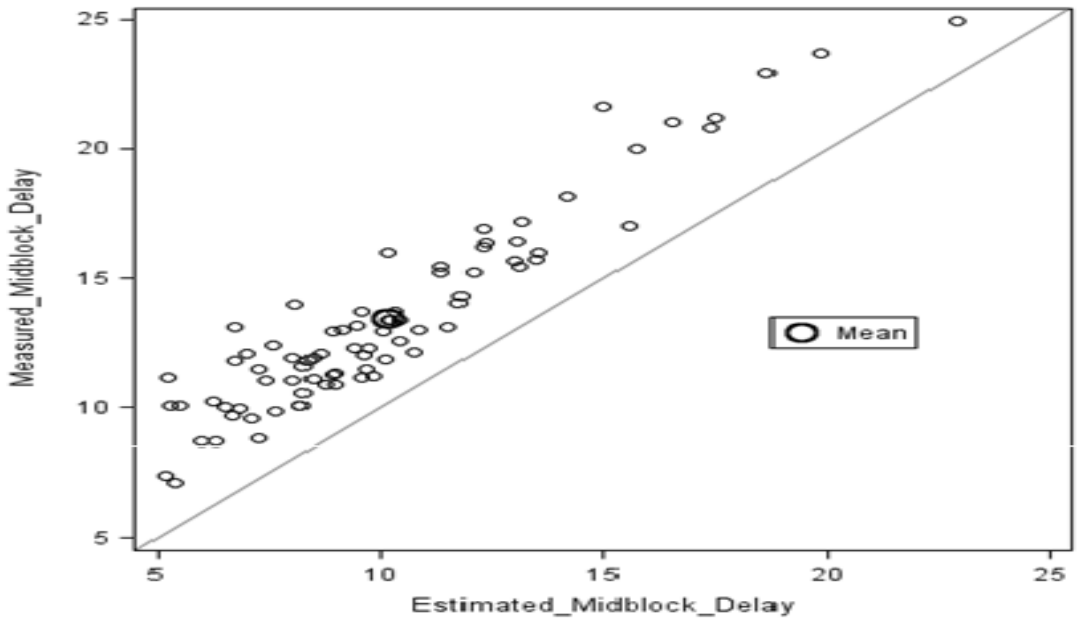

Figure 5.35 Diagonal plot of measured versus estimated midblock delay in seconds per vehicle for single vehicles.

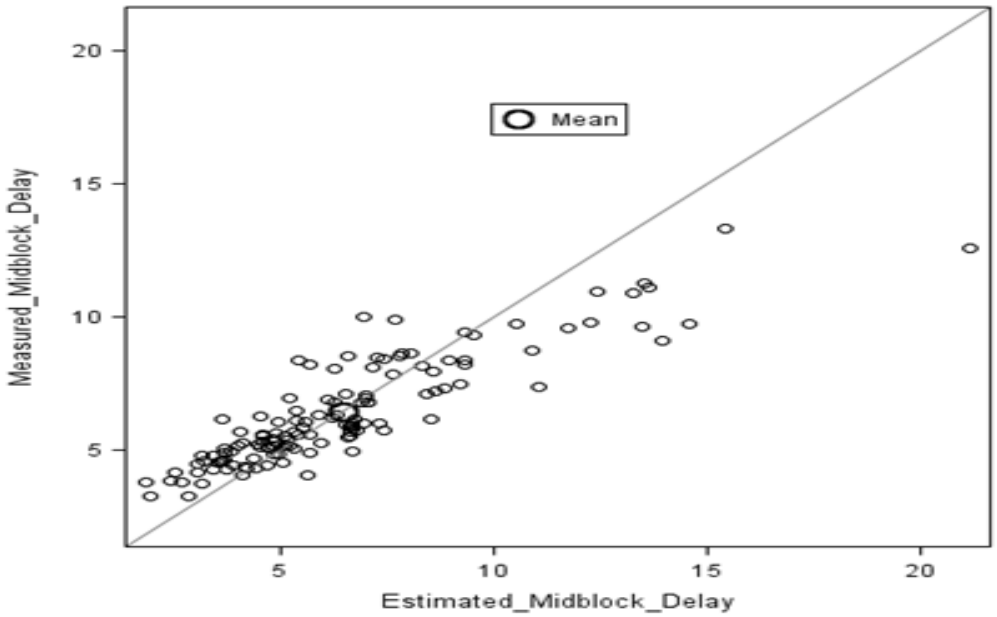

Figure 5.36 Agreement plot of measured versus estimated midblock delay in seconds per vehicle for multiple vehicle platoons.

Figures 5.37 and 5.39 show the normal quantile-quantile (Q-Q) plots for both measured and estimated midblock delay for all three data sets. A quantile-quantile plot compares ordered values with quantiles of a specific theoretical distribution. If the data

are from the theoretical distribution, the points on the Q-Q plot lie approximately on a straight line. The Q-Q plot of the residual is useful for diagnosing violations of normality. If the data in a Q-Q plot come from a normal distribution, the points will cluster tightly around the reference line. A normal density is overlaid on the residual histogram to help in detecting departures from normality. If the data are normally distributed with mean and standard deviation, the points on the plot should lie approximately on a straight line.

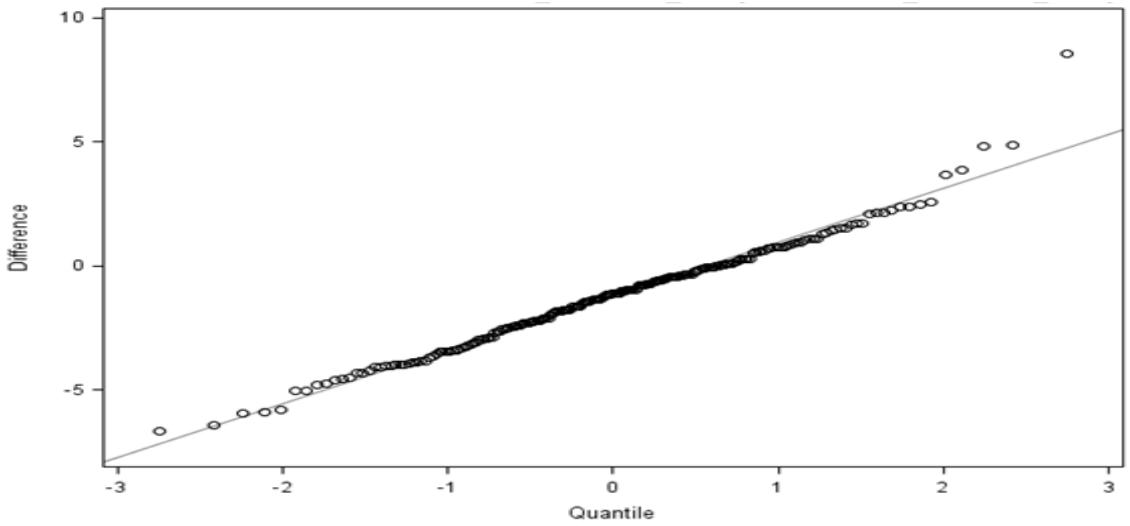

Figure 5.37 Q-Q plot for measured and estimated midblock delay for both single and multiple vehicle platoon data set.

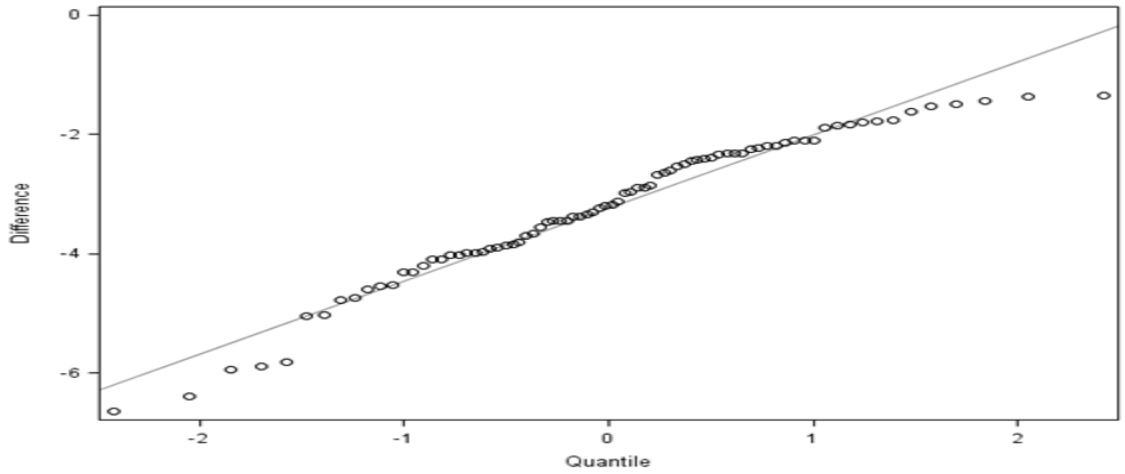

Figure 5.38 Q-Q plot for measured and estimated midblock delay for single vehicle data set.

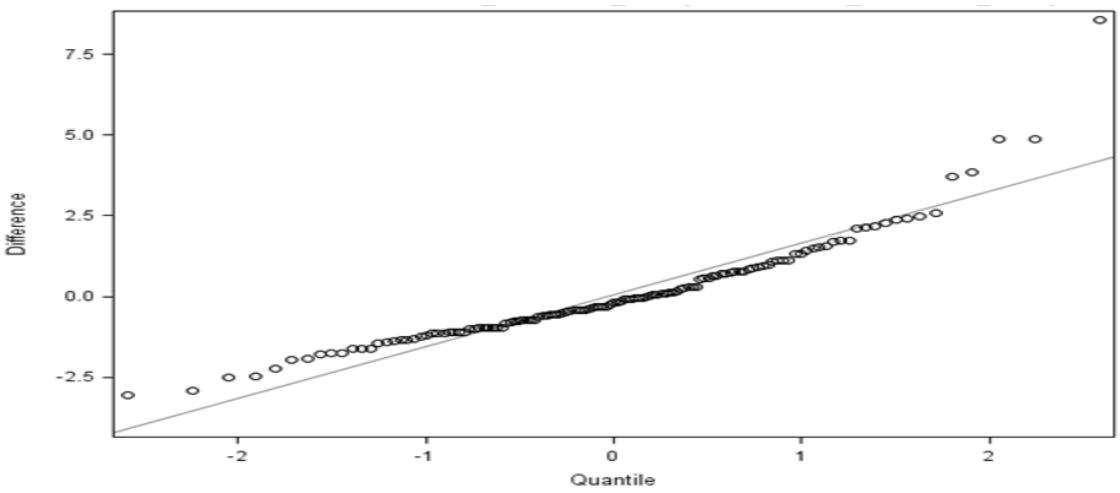

Figure 5.39 Q-Q plot for measured and estimated midblock delay for multiple vehicle platoon data set.

Figures 5.40 and 5.41 show the residual plots of measured and estimated midblock delay for single vehicle and multiple vehicle platoon data set, respectively. Normally, the residuals should be distributed in a bell shape (i.e., more points around 0 and the rest balanced at both sides). As shown Figure 5.40, the residual plot of single vehicle data set, about 40% of the residual values are distributed around 0 (i.e. between 0 and less than +/- 2.5 sec/veh). In Figure 5.41, however, about 90% of the residual values are distributed around 0(i.e. between. 0 and less +/- 2.5 sec/veh).

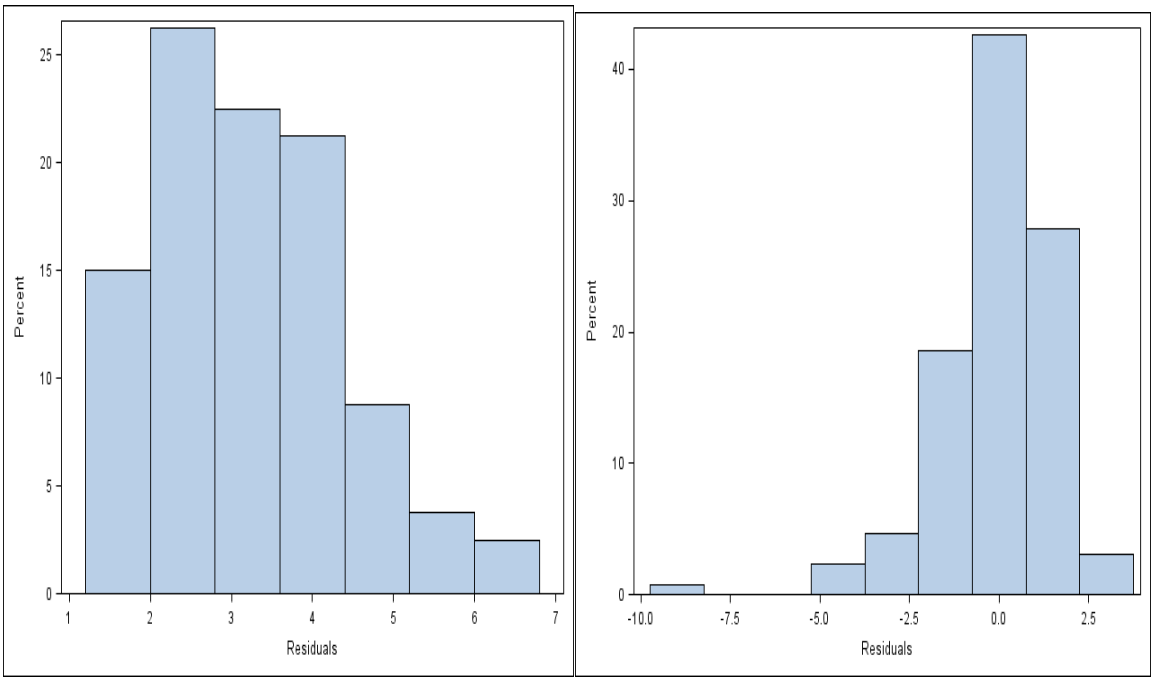

Figures 5.40 - 5.41 Residuals of measured and estimated midblock delay for single vehicle and multiple vehicles platoon data set, respectively.

Figure 5.42 shows a distribution of platoon size of the measured validation data. The figure show of the total of 226 measured values, of which 209 were used for the model validation, 35% of the data represent single vehicle platoon, 17% represent two-vehicle platoons, 16% represent 3-vehicle platoons, 11% represent 4-vehicle platoon, 9% represent 5-vehicle platoons, 4% represent 6-vehicle platoons, 4% represent 7-vehicle platoons, 2% represent 8-vehicle platoons, 1% represent 9-vehicle platoons.

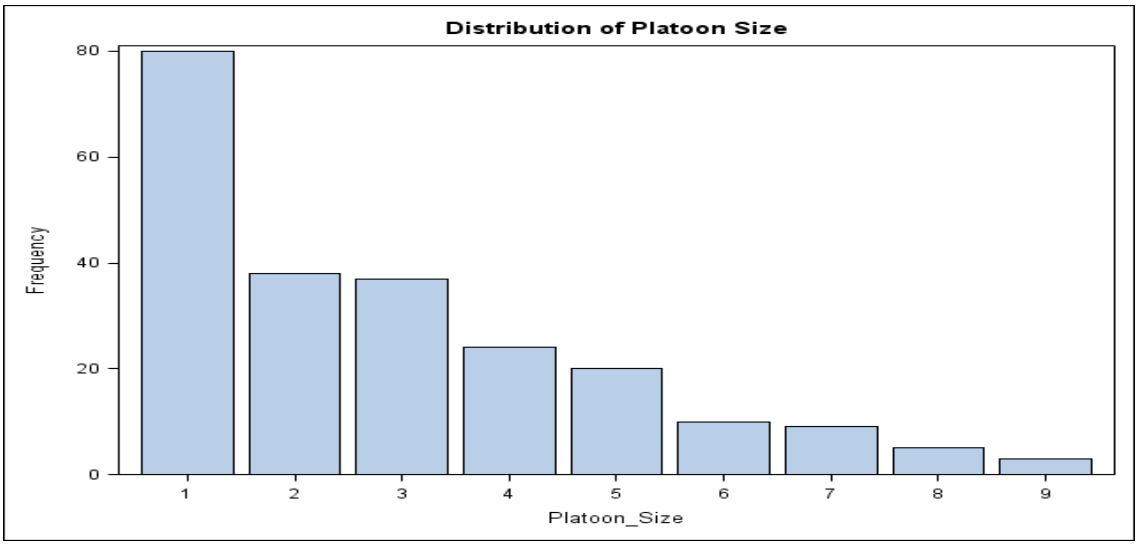

Figure 5.42 Distribution of platoon size for midblock delay model validation data.

5.2.3.2.2 Validation of Poisson Regression Model. This subsection is presented in two parts. The first part validates the assumption of equality between the mean and variance of the number of midblock interference. The second part validates the developed Poisson regression model above in Table 5.20 and Table 5.21.

The main limitation of the Poisson regression model is that the variance is constrained to be equal to its mean. However, as traffic flows become heavily congested or when traffic signals cause cyclical traffic stream disturbances, other distribution of traffic flow become more appropriate (Mannering et al., 2005). If the variance is significantly greater than the mean, the data are said to be over dispersed, and if the variance is significantly less than the mean, the data are said to be under-dispersed. In either case the Poisson distribution is no longer appropriate. Therefore, there is a need to compare the means and variances of the measured number of midblock interferences. The data for the statistical test was obtained by first recording the number of midblock interference occurring per minute for each of the 17 hours of the data set. A total of 60

samples of midblock interference were obtained for each hour. The means and variances were then calculated for each hour to obtain a data set of 17 paired samples of mean and variance.

The second part of the Poisson model validation involved performing statistical tests to see how well the developed Poisson regression model estimates midblock interference based on the model variables. Because of insufficient data points for model development and validation, the technique used in validating the Poisson regression model involved using the measured values of the independent variables to estimate the number of the interference per hour based on the estimated regression coefficients in Table 5.20 and Table 5.21. The Independent two-sample t-test, the chi-square test and mean error tests were used to compare the data sets. The results are shown below

Table 5.26 shows a summary of the validation data for three different data sets. The first data set represents the data used to validate the assumption of equality between the mean and variance. All statistics are as previous defined and explained. The descriptive statistic values in Table 5.26 show little difference between the means and variances. This is confirmed by the t-test results in Table 5.27. The Table shows p-values far greater than 0.05, confirming no statistically significant difference between the two parameters. Therefore the assumption of Poisson distribution seems reasonable.

In addition, Table 5.26 also shows a summary of the validation data used to compare the measured and estimated number of interference. All statistics are as previous defined and explained. The descriptive statistic values in Table 5.26 show minimal difference between the estimated and measured number of interference per hour for both category of data sets. This is confirmed by the t-test results in Table 5.21. The Table

shows p-values far greater than 0.05, confirming no statistically significant difference between the measured and estimated number of interference for both category of data.

Table 5.26 Summary of Poisson Regression Validation Data

Variable/Test		N	Mean	Std Dev	Std Err	Min.	Max.	95% CL Mean	
Test of Poisson Distribution	Mean	17	0.4	0.273	0.0662	0.05	0.96	0.261	0.542
	Variance	17	0.48	0.454	0.1102	0.05	2	0.242	0.71
No. of Interference Per Hour(Traffic-Pedestrian Volume)	Estimated	22	22.6	15.05	3.2078	3.34	62.43	15.94	29.28
	Measured	22	22.6	16.62	3.5435	1	58	15.27	30.01
No. of Interference Per Hour(Traffic Volume-Pedestrian Crossings)	Estimated	22	22.7	15.293	3.2605	3.83	61.37	15.91	29.47
	Measured	22	22.6	16.621	3.5435	1	58	15.27	30.01

Table 5.27 Summary of Poisson Regression Validation T-test Statistics

		Equality of Variances					t	
Variable	Method	Num DF	F Value	Pr > F	Variances	DF	Value	Pr > |t|
Test of Poisson Distribution	Folded F	16	2.77	0.0494				
	Pooled				Equal	32	-0.58	0.5683
	Satterthwaite				Unequal	26.22	-0.58	0.5692
No. of Interference Per Hour(Traffic-Pedestrian Volume)	Folded F	21	1.22	0.6525				
	Pooled				Equal	42	-0.01	0.9951
	Satterthwaite				Unequal	41.59	-0.01	0.9951
No. of Interference Per Hour(Traffic Volume-Pedestrian Crossings)	Folded F	21	1.18	0.7063				
	Pooled				Equal	42	0.01	0.9905
	Satterthwaite				Unequal	41.712	0.01	0.9905

Table 5.28 shows the Chi-square statistics for the number of interference estimated using traffic volume and pedestrian volume and also the number of midblock interference estimated using traffic volume and number of pedestrian crossings as independent variables. The result shows the calculated chi-square statistic is greater than the critical chi-square statistics for both data sets. This indicates significant difference between the measured and estimated values. This result is contrary to the t-test results. This discrepancy in the test results may be due to small sample sizes used in the statistically tests.

Table 5.28 Results of Chi-square Test of Poisson Regression Validation Data

Data Set	df	χ^2	$\chi^2_{df,\alpha}$	$\chi^2 > \chi^2_{df,\alpha}$	Difference Statistically Significant?
No. of Interference Per Hour(Traffic-Pedestrian Volume)	21	92.20219	32.67	Yes	Yes
No. of Interference Per Hour(Traffic Volume-Pedestrian Crossings)	21	85.47445	32.67	Yes	Yes

Table 5.29 shows the results of the mean errors calculated for each data set. The results show relatively small root mean square error, root mean square percent error, and mean absolute percent error for number of interference per hour(Traffic Volume-Pedestrian crossings) data set as compared to the mean error for number of interference per hour(Traffic Volume-Pedestrian volume) data set. This shows the model performs

better in estimating the number of interference per hour using traffic volume and the number of pedestrian crossings as independent variables.

Table 5.29 Mean Errors of Poisson Regression Validation Data

Variable	RMSE	RMSPE	MAPE(%)
Test of Poisson Distribution	0.2655	0.3809	24.3654
No. of Interference Per Hour(Traffic-Pedestrian Volume)	10.3509	0.8968	57.2091
No. of Interference Per Hour(Traffic Volume-Pedestrian Crossings)	10.0753	0.8385	53.1092

Figure 5.43 shows the SAS 9.2 diagonal plot of variance versus mean of midblock interference per minutes. Tight clustering along the diagonal line indicates positive correlation of the two parameters.

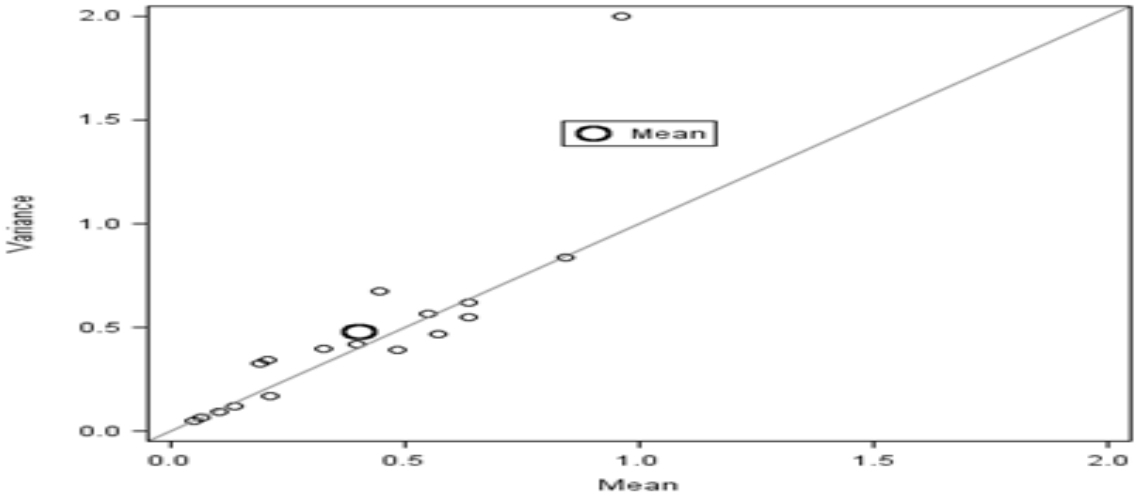

Figure 5.43 Diagonal plot of mean and variance of number of midblock interference.

Figure 5.44 shows the diagonal plot of estimated number of interference versus the measured of interference for a combination of traffic volume and pedestrian volume. The Figure shows the data points are evenly distributed on both sides of the diagonal line,

with majority of the data points closer to the line. However, the model over and under estimated for a few data points.

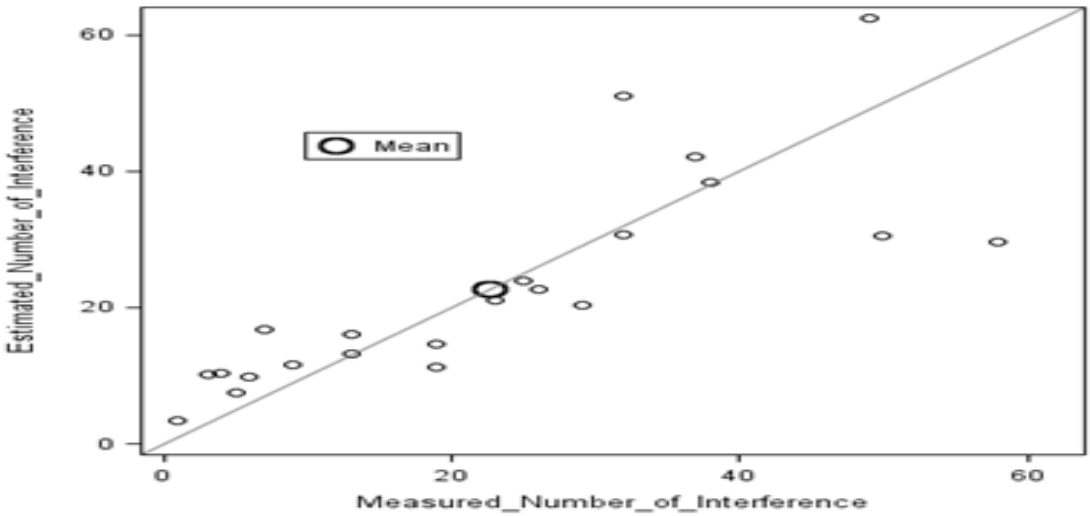

Figure 5.44 Diagonal plot of number of interference for traffic volume- pedestrian *volume*

Figure 5.45 shows the diagonal plot of estimated number of interference versus the measured of interference for a combination of traffic volume and number of pedestrian crossings per hour. Like Figure 5.44, Figure 5.45 shows the data points are evenly distributed on both sides of the diagonal line, with majority of the data points closer to the line. However, the model over and under estimated for a few data points.

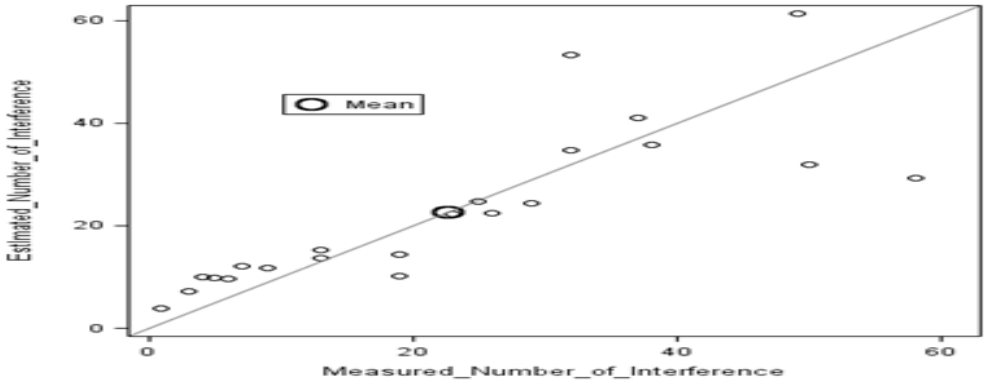

Figure 5.45 Diagonal plot of number of interference for traffic volume- pedestrian crossings.

CHAPTER 6

SENSITIVITY ANALYSIS

6.1 Introduction

The following tasks were performed in the previous chapter: the data collected in this research have been analyzed; the results of the regression analysis were presented and discussed; the developed midblock delay model was validated using field data. In this chapter, sensitivity analyses are performed to analyze the performance of the developed midblock delay model by varying four model parameters and one model variable above and below their baseline values. Baseline values are defined in tis research as the initial values used in the model development and validation. The four parameters and one variable are: deceleration rate, acceleration rate, free-flow speed, the headway of bunched vehicles and pedestrian walking time. For each of the parameters and variable, their baseline values were increased and decreased by 50%, while keeping all other parameters and variables constant. Different data sets of estimated midblock delay were computed. Tables and figures are presented to compare the baseline estimated midblock delay values to the estimated midblock delay based on the varied parameter and variable values. In addition, the measured midblock delay values are compared to the estimated midblock delay based on the varied parameter values.

6.2 Sensitivity Analysis of Deceleration and Acceleration Rates

This section presents the sensitivity analyses of varying both the deceleration and acceleration values. The task was performed in two parts: the first part involved

Increasing and decreasing the value of the baseline deceleration rate of 6.7 ft/s^2 by 50 %, while keeping all other parameters and variables constant. The estimated midblock delay values were then computed for the increased and decreased deceleration value. In the second part, the midblock delay was estimated for 50% increase and decrease in the baseline acceleration rate of 3.5 ft/s^2 , while keeping all other parameters and variables constant.

The results are presented in tabular and graphical forms as shown below. Table 6.1 shows the statistical summary of increase and decrease in baseline deceleration and acceleration rates. The table shows the mean, standard deviation, standard error and the minimum and maximum values for the respective data set. The values in the dash row shows the statistics of the baseline estimated midblock delay values. The rows above the dash row show the statistics of the increase parameters, while the rows below the dash row show the decreased statistics of the decreased parameters. The results show for 50% increase in deceleration rate, there is 10.5% increase in the mean, 3.5% increase in the standard deviation and 3.5% increase in the standard error. Conversely, the results show for 50% decrease in deceleration rate, there is 30.9% decrease in the mean, 9.7% decrease in the standard deviation and 9.7% decrease in the standard error.

In addition, the results show for 50% increase in acceleration rate, there is 19.8% decrease in the mean, 6.4% decrease in the standard deviation and 6.4% decrease in the standard error. Conversely, the results show for 50% decrease in acceleration rate, there is 61.6% increase in the mean, 20.3% increase in the standard deviation and 20.3% increase in the standard error.

Table 6.1 Statistical Summary of Increasing and Decreasing the Baseline Deceleration and Acceleration rates

Variable	Mean	Std. Dev	Std. Error	Min.	Max
Estimated midblock delay for 50% increase in baseline deceleration(s/veh)	8.7404	3.8538	0.2666	2.2863	23.9033
Estimated midblock delay for 50% increase in baseline acceleration(s/veh)	6.3375	3.4872	0.2412	1.1489	20.8874
Baseline estimated midblock delay (s/veh)	7.9089	3.7246	0.2576	1.8848	22.8684
Estimated midblock delay for 50% decrease in baseline deceleration(s/veh)	5.4582	3.3615	0.2325	0.7498	19.7639
Estimated midblock delay for 50% decrease in baseline acceleration(s/veh)	12.7826	4.4795	0.3099	4.3604	28.8114

Table 6.2 shows the results of the mean errors calculated for each set of data. The error values in the dash row are those obtained by comparing the measured midblock delay to those delay values estimated using the baseline parameters and variables. The error values in the rows above and below the dash row show the error values obtained by comparing the measured midblock delay to those delays estimated for increase and decrease in the deceleration rate and acceleration rate, respectively.

The results show for 50% increase in deceleration rate, there is 14.9% decrease in the root mean square error, 8.01% decrease in the root mean square percent error and 12.8% decrease in the mean absolute percent error of the compared measured-estimated midblock delay values. Conversely, the results show for 50% decrease in deceleration rate, there is 79.5% increase in the root mean square error, 93.7% increase in the root mean square percent error and 109.1% increase in the mean absolute percent error of the

compared measured-estimated midblock delay. The results indicate increasing the deceleration rate pulls the estimated midblock delay values toward the measured midblock delay values. Hence, the increase in the mean and decrease in the error delay values.

Furthermore, Table 6.2 shows for 50% increase in acceleration rate, there is 47.7 %, 54.1% and 61.8% increase in the root mean square error, root mean square percent error and mean absolute percent error of the compared measured-estimated midblock delay values, respectively. Conversely, the results show for 50% decrease in deceleration rate, there is 66.9%, 144.0% and 147.0% increase in the root mean square error, root mean square percent error and mean absolute percent error of the compared measured-estimated midblock delay values, respectively. The results indicate increasing and decreasing the acceleration rate increases the mean errors of the compared measured-estimated midblock delay.

Table 6.2 Comparison of measured-estimated midblock delay for increase and decrease in the baseline deceleration and acceleration rates

Variable	RMSE	RMSPE	MAPE(%)
Comparison of measured and estimated midblock delay for 50% increase in the baseline deceleration rate (s/veh)	2.1100	0.2168	17.5232
Comparison of measured and estimated midblock delay for 50% increase in the baseline acceleration(s/veh)	3.6616	0.3633	32.5267
Comparison of measured and estimated midblock delay for the baseline deceleration-acceleration rates(s/veh)	2.4788	0.2357	20.1005
Comparison of measured and estimated midblock delay for 50% decrease in baseline deceleration rate (s/veh)	4.4510	0.4566	42.0352
Comparison of measured and estimated midblock delay for 50% decrease in baseline acceleration rate (s/veh)	4.1370	0.5752	49.6484

Figure 6.1 shows the diagonal plot of baseline estimated midblock delay in s/veh versus the estimated midblock delay for 50% increase in deceleration rate. Figure 6.2 shows the diagonal plot of baseline estimated midblock delay in s/veh versus the estimated midblock delay for 50% decrease in deceleration. As shown in Figure 6.1, increase in the deceleration rate increases the estimated midblock delay. Hence, pulls the delay values away from the baseline estimated delay. Conversely, decrease in the deceleration rate decreases the estimated midblock delay. Hence, pulls the delay values toward the baseline estimated midblock delays. Both figures confirm the results in Tables 6.1 and 6.2. As shown in the figures, a 50% decrease in deceleration rate pulls the estimated midblock delay values farther away from the diagonal line than a 50% increase in deceleration rate. This confirms the 10.5% and 30.9% increase and decrease in the mean values.

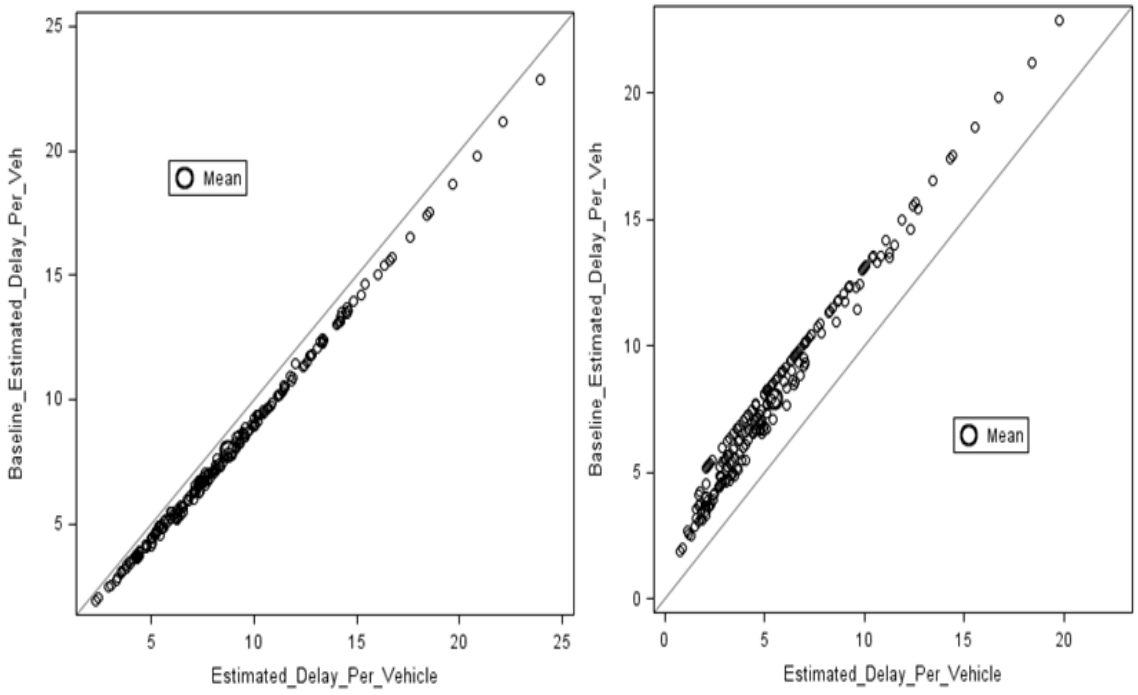

Figures 6.1 – 6.2 Estimated midblock delay for 50% increase and decrease in the baseline deceleration rates, respectively.

Figure 6.3 shows the diagonal plot of baseline estimated midblock delay in s/veh versus the estimated midblock delay for 50% increase in acceleration rate. Figure 6.2 shows the diagonal plot of baseline estimated midblock delay in s/veh versus the estimated midblock delay for 50% decrease in acceleration. As shown in Figure 6.1, increase in the deceleration rate decreases the estimated midblock delay. Hence, pulls the delay values toward the baseline estimated delays. Conversely, decrease in the acceleration rate increases the estimated midblock delay. Hence, pulls the delay away from the baseline estimated delays. Both figures confirm the results in Tables 6.1 and 6.2. As shown in the figures, a 50% decrease in acceleration rate pulls the estimated midblock delay values farther away from the diagonal line than a 50% increase in acceleration rate. This confirms the 19.8%, and 61.6% increase and decrease in the mean values of

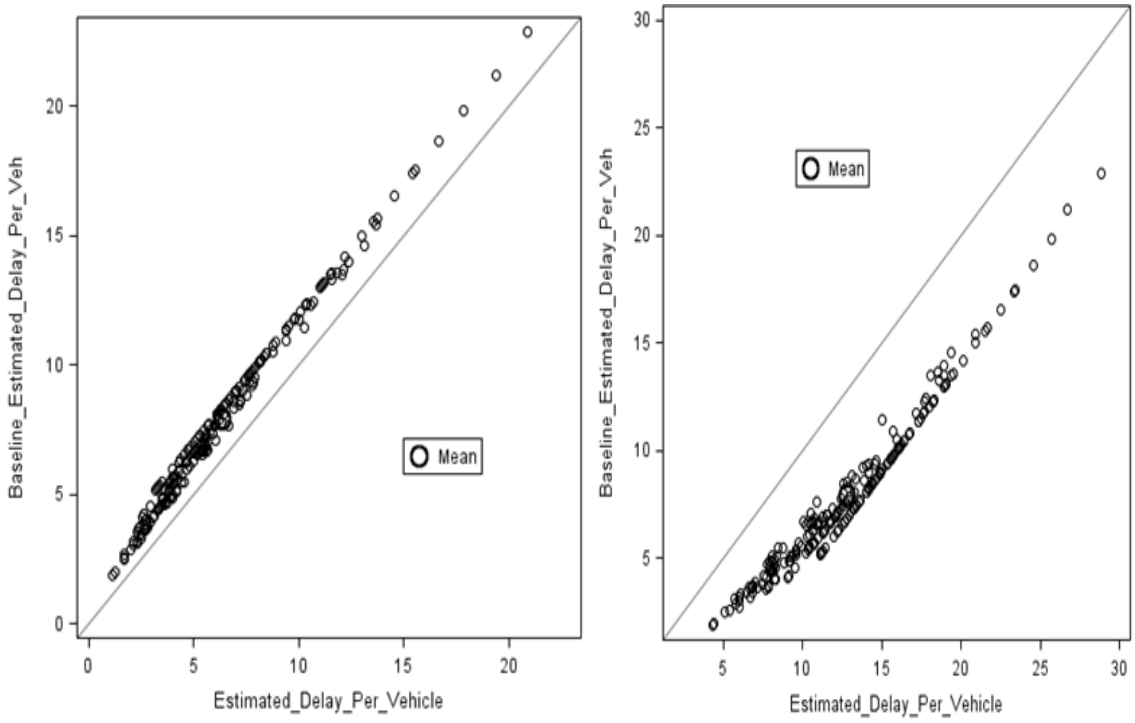

Figures 6. 3 – 6.4 Estimated midblock delay for 50% increase and 50% decrease in the baseline acceleration rate, respectively**.**

Figure 6.5 shows the diagonal plot of the measured midblock delay versus the estimated midblock delay for 50% increase in deceleration rate. Figure 6.5 shows the diagonal plot of measured midblock delay versus the estimated midblock delay for 50% decrease in deceleration rate. Figure 6.6 shows for a 50% increase in deceleration rate, there is increase in the estimated midblock delay. This, therefore, pulls the new estimated midblock delay values toward the measured midblock delay values. This is shown by the almost evenly distributed delay data points around on both sides of the diagonal line. However, for a 50% decrease in deceleration rate, there is a decrease in the new estimated midblock delay values. The model tends to underestimate the new midblock delays relative to the measured midblock delays. Therefore, the delay values are pulled away from the diagonal line toward the measured midblock delays.

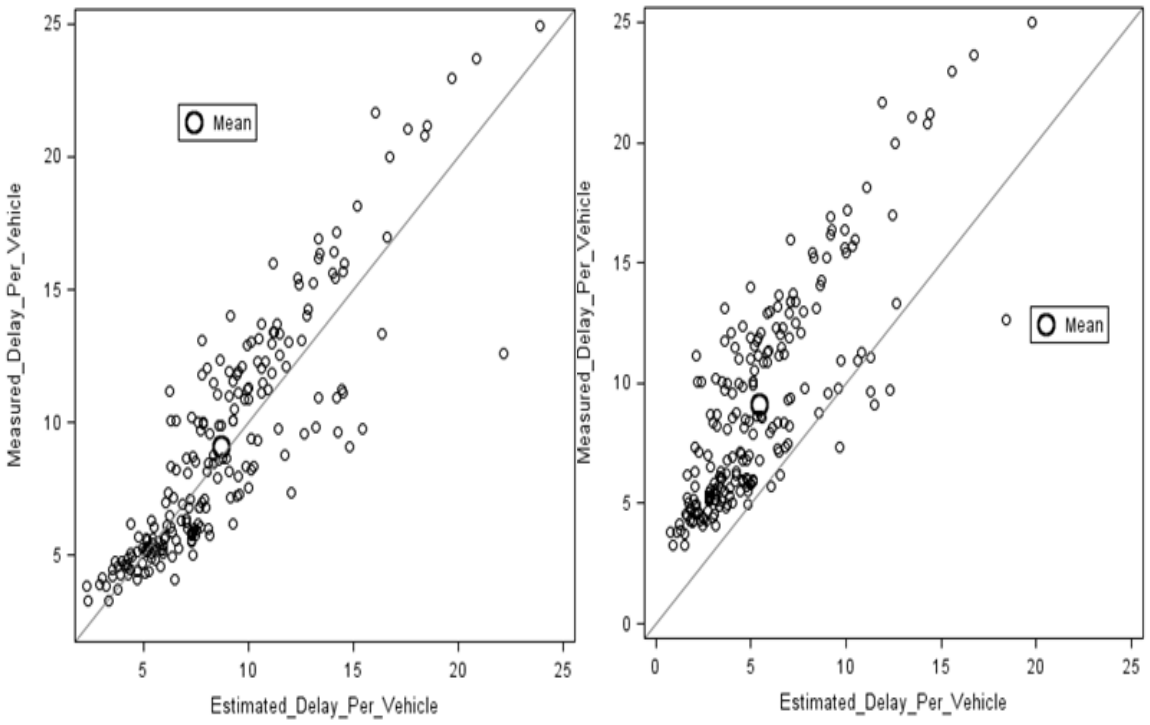

Figures 6.5 – 6.6 Measured-estimated midblock delays for 50% increase and 50% decrease in the baseline deceleration rates, respectively.

Figure 6.7 shows the diagonal plot of the measured midblock delay versus the estimated midblock delay for 50% increase in acceleration rate. Figure 6.8 shows the diagonal plot of measured midblock delay versus the estimated midblock delay for 50% decrease in acceleration rate. Figure 6.7 shows for a 50% increase in acceleration rate, there is decrease in the new estimated midblock delays. The model therefore tends to underestimate the midblock delay. Therefore, this pulls the midblock delay values little bit toward the measured midblock delay values. However, for a 50% decrease in acceleration rate, there is an exponential increase in the new estimated midblock delay values. The model tends to overestimate the delay relative the measured midblock delays Therefore, the delay values are pulled away from the diagonal line and measured midblock delay toward the new estimated midblock delay. This exponential increase in the midblock delays is due to the fact that it takes longer time for a stopped vehicle to accelerate to the normal speed (i.e. the speed prior to the interference)

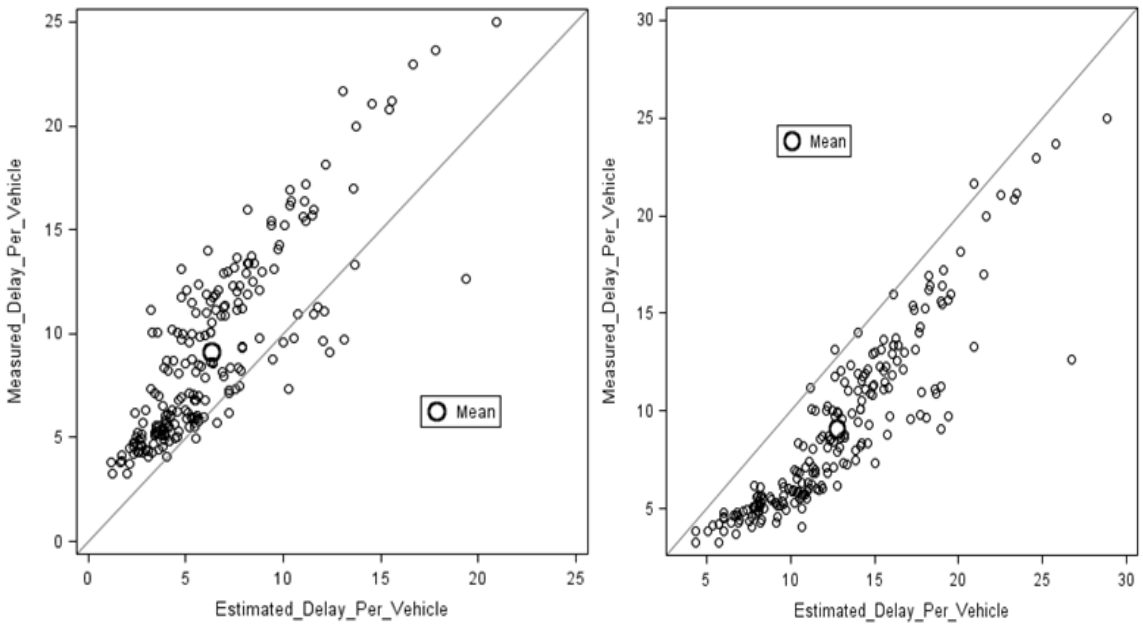

Figures 6.7 – 6.8 Measured-estimated midblock delays for 50% increase and 50% decrease in the baseline acceleration rate, respectively.

6.3 Sensitivity Analysis of Free-Flow Speed

This presents the results of performing sensitivity analyses by varying the free-flow speed 50% above and below the baseline value of 28.3 mph. Table 6.3 shows the statistical summary of increase and decrease in baseline free-flow speed. The table shows the mean, standard deviation, standard error and the minimum and maximum values for the respective data set. The values in the dash row show the statistics of the baseline estimated midblock delay values. The row above the dash row shows the statistics of the increase in baseline free-flow speed, while the row below the dash row shows the statistics of the decrease in free-flow speed. The results show for 50% increase in the free-flow speed, there is 14.4%, 4.8% and 4.8% increase in the mean, standard deviation and standard error of the estimated midblock delay values, respectively. Conversely, the results show for 50% decrease in free-flow speed, there is 14.3%, 4.6% and 4.6% decrease in the mean, standard deviation and standard error of the estimated midblock delay values, respectively. The result shows free-flow speed has a direct effect on estimated midblock delay. This is because when vehicles travel at reduced speeds on urban street segments, there is decrease in time for drivers to slow or come to s full stop during braking; and a decrease in time for drivers to accelerate from slowing down or from a stop back to their normal speed. Additionally, there is a linear relationship between increase and decrease in free-flow speed and increase and decrease in estimated midblock delay.

Table 6.3 Statistical Summary of Increase and Decrease in the Baseline Free-Flow Speed

Variable	Mean	Std. Dev	Std. Error	Min.	Max
Estimated midblock delay for 50% increase in the baseline free-flow speed(s/veh)	9.0511	3.9024	0.2699	2.4384	24.2877
Baseline estimated midblock delay (s/veh)	7.9089	3.7246	0.2576	1.8848	22.8684
Estimated midblock delay for 50% decrease in the baseline free-flow speed(s/veh)	6.7804	3.5528	0.2457	1.3534	21.4492

Table 6.4 shows the results of the mean errors calculated for each set of data. The error values in the dash row are those obtained by comparing the measured midblock delay to those delay values estimated using the baseline free-flow speed and variables. The error values in the rows above and below the dash row show the error values obtained by comparing the measured midblock delay to those delays estimated for 50% increase and decrease in the baseline free-flow speed, respectively.

The results show for 50% increase in free-flow speed, there is 17.3%, 5.6% and 13.2% decrease in the root mean square error, root mean square percent error and mean absolute percent error of the compared measured-estimated midblock delay values, respectively. Conversely, the results show for 50% decrease in deceleration rate, there is 32.7%, 35.8% and 40.8% increase in the root mean square error, root mean square percent error and mean absolute percent error of the compared measured-estimated midblock delay values, respectively.

Table 6.4 Comparison of Measured-Estimated Midblock Delay for Increase and Decrease in Baseline Free-Flow Speed

Variable	RMSE	RMSPE	MAPE(%)
Comparison of measured and estimated midblock delay for 50% increase in the baseline free-flow speed(s/veh)	2.0492	0.2226	17.4373
Comparison of measured and baseline estimated midblock delay (s/veh)	2.4788	0.2357	20.1005
Comparison of measured and estimated midblock delay for 50% decrease in the baseline free-flow speed(s/veh)	3.2893	0.3202	28.2974

Figure 6.9 shows the diagonal plot of baseline estimated midblock delay in s/veh versus the estimated midblock delay for 50% increase in free-flow speed. Figure 6.10 shows the diagonal plot of baseline estimated midblock delay in s/veh versus the estimated midblock delay for 50% decrease in free-flow speed. As shown in Figure 6.9, increase in the free-flow speed increases the estimated midblock delay. Hence, pulls the delay values away from the diagonal line toward the estimated delay for increase in free-flow speed. Conversely, decrease in the free-flow speed decreases the estimated midblock delay. Hence, pulls the delay values toward the baseline estimated midblock delays.

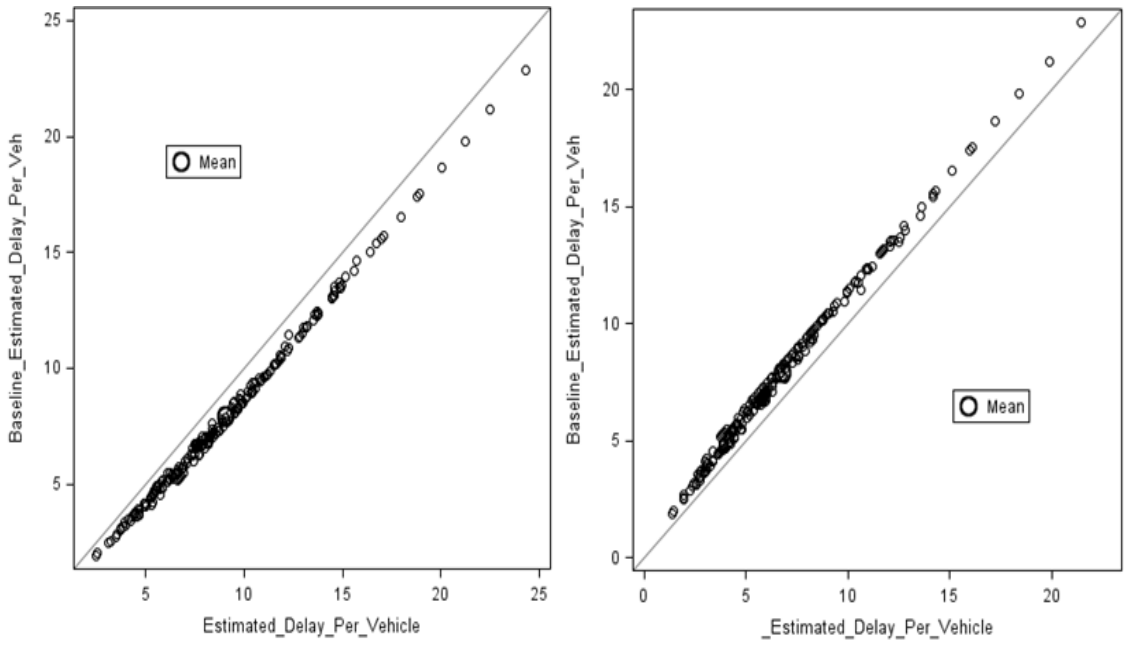

Figures 6. 9 – 6.10 Estimated midblock delay for 50% increase and 50% decrease in the baseline free-flow speed, respectively.

Figure 6.11 shows the diagonal plot of the measured midblock delay versus the estimated midblock delay for 50% increase in free-flow. Figure 6.12 shows the diagonal plot of measured midblock delay versus the estimated midblock delay for 50% decrease in free-flow speed. Figure 6.11 shows for a 50% increase in free-flow speed, there is increase in the estimated midblock delay. This, therefore, pulls the estimated midblock delay values toward the measured midblock delay values. Hence, the almost evenly distributed delay data points around on both sides of the diagonal line. However, for a 50% decrease in free-flow speed, there is a decrease in estimated midblock delay values. Therefore, the delay values are pulled away from the diagonal line toward the measured midblock delay.

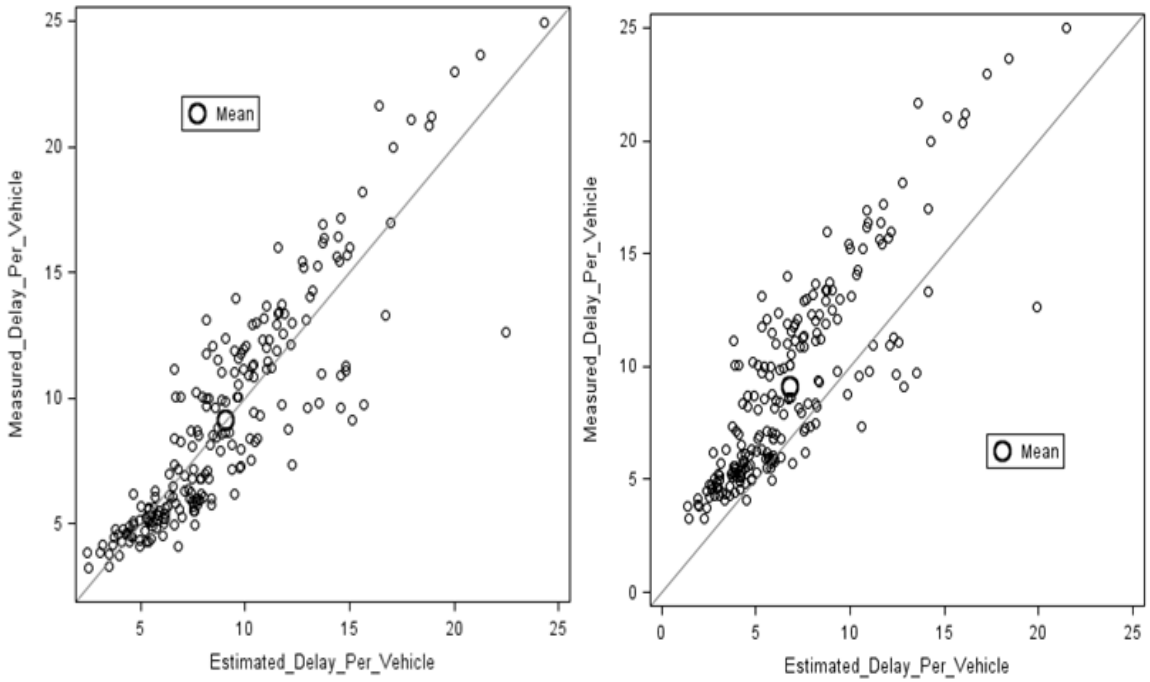

Figures 6.11 – 6.12 Measured-estimated midblock delays for 50% increase and 50% decrease in the baseline free-flow speed, respectively.

6.4 Sensitivity Analysis of Headway of Bunched Vehicles

In this section, sensitivity analyses are performed to evaluate the effect on the estimated midblock delay due to 50% increase and decrease in baseline value of 1.5 sec in the headway of bunched vehicles. Table 6.5 shows the statistical summary of increase and decrease in the baseline value of the headway of bunched vehicles. The results show for 50% increase in the baseline value of the headway of bunched vehicles, there is 1.1%, 1.6% and 2.4% increase in the mean, standard deviation and standard error of the estimated midblock delay values, respectively. Conversely, the results show for 50% decrease in the baseline value of the headway of bunched vehicles, there is 0.9%, 1.4% and 1.4% decrease in the mean, standard deviation and standard error of the estimated

midblock delay values, respectively. The result shows free-flow speed has direct and minimal effect on estimated midblock delay.

Table 6.5 Statistical Summary of Increase and Decrease in the Baseline Value of Headway of Bunched Vehicles

Variable	Mean	Std. Dev	Std. Error	Min.	Max
Estimated midblock delay for 50% increase in the baseline value of headway of bunched vehicles (s/veh)	6.5652686	3.1449584	0.2789182	1.9011315	21.616145
Baseline estimated midblock delay (s/veh)	6.4960383	3.0948017	0.2724821	1.8848443	21.177428
Estimated midblock delay for 50% decrease in the baseline value of headway of bunched vehicles (s/veh)	6.4380884	3.0519692	0.2687109	1.8716261	20.793038

Table 6.6 shows the results of the mean errors calculated for each set of data. The results show for 50% increase in the baseline value of the headway, there is 3.7%, 2.2% and 1.5% increase in the root mean square error, root mean square percent error and mean absolute percent error of the compared measured-estimated midblock delay values, respectively. Conversely, the results show for 50% decrease in the baseline value of the headway, there is 3%, 1.7% and 1.1% decrease in the root mean square error, root mean square percent error and mean absolute percent error of the compared measured-estimated midblock delay values, respectively.

Table 6.6 Comparison of Measured-Estimated Midblock Delay for Increase and Decrease in Baseline Value of Headway of Bunched Vehicles

Variable	RMSE	RMSPE	MAPE(%)
Comparison of measured-estimated midblock delay for 50% increase in the baseline value of headway of bunched vehicles(s/veh)	1.6602697	0.2194312	17.387694
Comparison of measured and baseline estimated midblock delay (s/veh)	1.6010167	0.2146598	17.124863
Comparison of measured-estimated midblock delay for 50% decrease in the baseline value of headway of bunched vehicles(s/veh)	1.553102	0.2111165	16.930257

Figure 6.13 shows the diagonal plot of baseline estimated midblock delay in s/veh versus the estimated midblock delay for 50% increase in the baseline value of the headway of bunched vehicles. Figure 6.14 shows the diagonal plot of baseline estimated midblock delay in s/veh versus the estimated midblock delay for 50% decrease in the baseline value of the headway of bunched vehicles. As shown in both figures, the delay values for both variables lie on the diagonal line. This indicates increase or decrease in the baseline value of the headway of bunched vehicles has little or no effect on midblock delay. Similarly, there is no difference between measured-estimated midblock delay for 50% increase and 50% decrease in baseline value of headway of bunched vehicles as shown in Figures 6.15 and 6.16, indicating no significant effects.

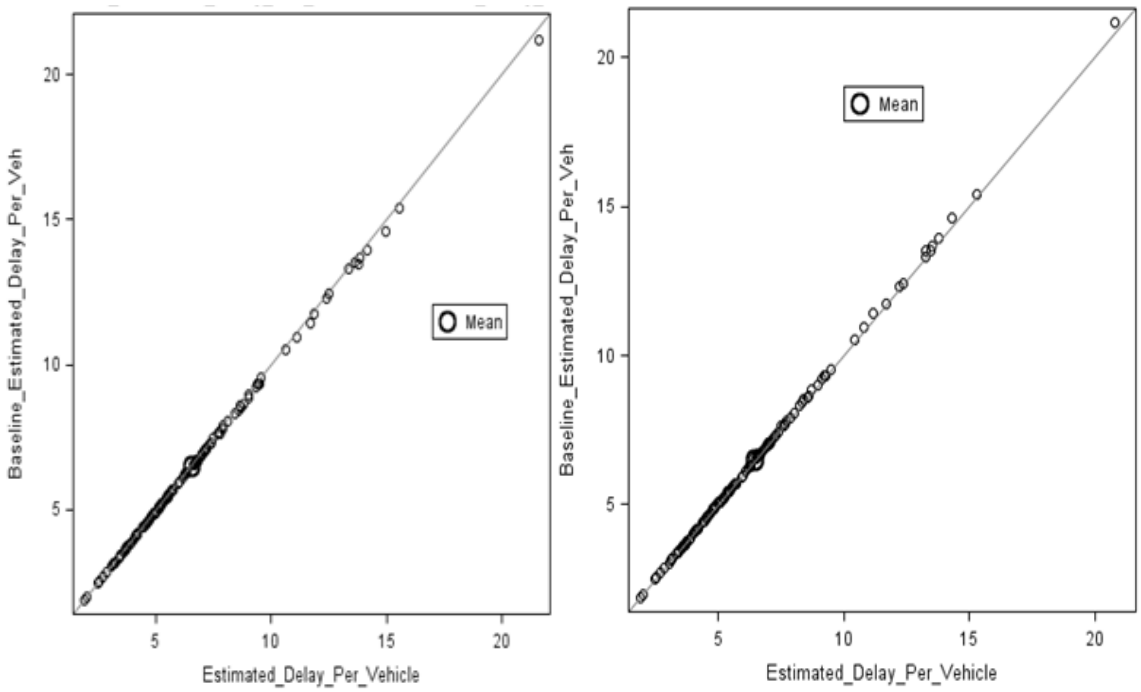

Figures 6.13 – 6.14 Estimated midblock delay for 50% increase and 50% decrease in the baseline value of headway of bunched vehicles, respectively.

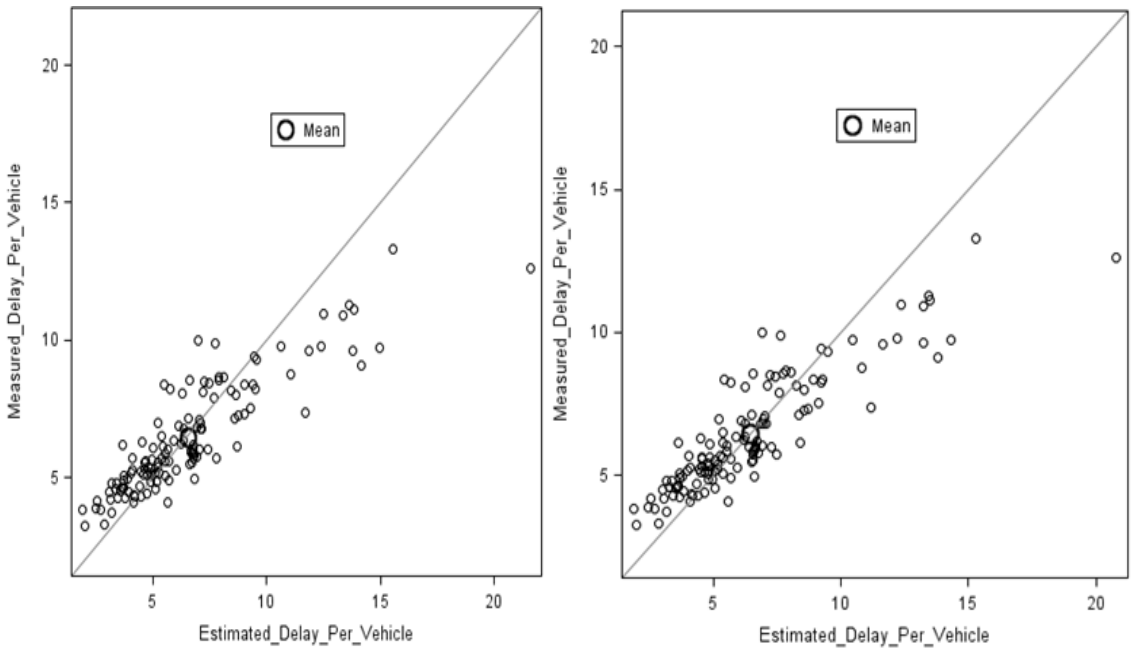

Figures 6.15 -6.16 Measured-estimated midblock delays for 50% increase and 50% decrease in the baseline value of headway of bunched vehicles, respectively.

6.5 Sensitivity Analysis of Pedestrian Walking Time

This section presents the sensitivity analyses for varying both the measured pedestrian walking times 50% above and below the baseline values. The results are presented in Tables 6.7 and 6.8 and in Figures 6.17 - 6.20. Table 6.7 shows the statistical summary of increasing and decreasing the baseline pedestrian walking times. The table shows the mean, standard deviation, standard error and the minimum and maximum values for the respective data set. The results show for 50% increase in pedestrian walking times, there is 39.1% increase in mean, 47.8% increase the standard deviation and 47.8% standard error of the estimated midblock delay values. Conversely, the results show for 50% decrease in pedestrian walking times, there is 37.6% increase in mean, 45.0% increase the standard deviation and 45.0% standard error of the estimated midblock delay values.

Table 6.7 Statistical Summary of Increase and Decrease in the Baseline Value of Pedestrian Walking Time

Variable	Mean	Std. Dev	Std. Error	Min.	Max
Estimated midblock delay for 50% increase in the baseline value of pedestrian walking time(s/veh)	11.004959	5.5063563	0.3808826	2.367284	32.981876
Baseline estimated midblock delay (s/veh)	7.9089	3.7246	0.2576	1.8848	21.177428
Estimated midblock delay for 50% decrease in the baseline value of pedestrian walking time(s/veh)	4.9372276	2.047784	0.1416482	1.4193101	12.853448

Table 6.8 shows the results of the mean errors calculated for each set of data. The error values in the dash row are those obtained by comparing the measured midblock delay to those delay values estimated using the baseline values of pedestrian walking time. The rows above and below the dash row show the error values obtained by comparing the measured midblock delay to those delays estimated for 50% increase and 50% decrease in the baseline pedestrian walking time, respectively.

The results show for 50% increase in pedestrian walking time, there is 47.2% increase root mean square error, 81.4% increase in the root mean square percent error and 51.3% increase in the mean absolute percent error of the compared measured-estimated midblock delay values. Conversely, results show for 50% decrease in pedestrian walking time, there is 98.5% increase root mean square error, 90.3% increase in the root mean square percent error and 117.6% increase in the mean absolute percent error of the compared measured-estimated midblock delay values.

Table 6.8 Comparison of Measured-Estimated Midblock Delay for Increase and Decrease in the Baseline Value of Pedestrian Walking Time

Variable	RMSE	RMSPE	MAPE(%)
Comparison of measured and estimated midblock delay for 50% increase in the baseline value of pedestrian walking time(s/veh)	3.6490805	0.4275763	30.41328
Comparison of measured and baseline estimated midblock delay (s/veh)	2.4788	0.2357	20.1005
Comparison of measured and estimated midblock delay for 50% decrease in the baseline value of pedestrian walking time(s/veh)	4.921146	0.4484814	43.746467

Figure 6.17 shows the diagonal plot of the baseline estimated midblock delay in s/veh versus the estimated midblock delay for 50% increase in the baseline value of pedestrian walking time. Figure 6.18 shows the diagonal plot of baseline estimated midblock delay in s/veh versus the estimated midblock delay for 50% decrease in the baseline values of pedestrian waiting time. As shown in Figure 6.17, increases the midblock block delay and therefore pulls the delay values away from the baseline estimated midblock delays. Figure 6.18 shows that for an increase in pedestrian walking time, there is decrease in the midblock delays. Figure 6.17 and Figure 6.18, however, show different patterns in the data points unlike similar plots in the previous sections. As shown in both figures, the data points tend to pull away from the diagonal line as the delay increases. This is because as the pedestrian walking times increase, the vehicle stopped time increases. However, as pedestrian walking times decrease, the vehicle stopped time decreases and tends to zero. Therefore, scenario 2(vehicle coming to full stop) tends to scenario1 (vehicle slowing but not coming to full stop)

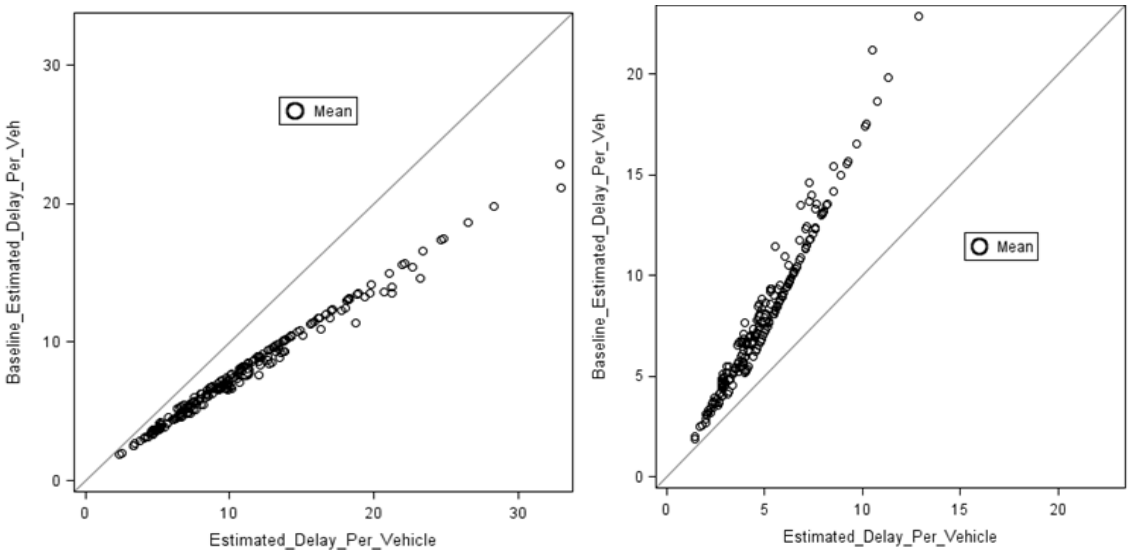

Figures 6.17 – 6.18 Estimated midblock delay for 50% increase and 50% decrease in the baseline value of Pedestrian Walking Time, respectively.

Figure 6.19 shows the diagonal plot of the measured midblock delay versus the estimated midblock delay for 50% increase in the baseline values of pedestrian walking time. Figure 6.20 shows the diagonal plot of measured midblock delay versus the estimated midblock delay for 50% decrease in the baseline pedestrian walking time. Figure 6.19 shows for a 50% increase in pedestrian walking time there is increase in the delay. This increase pulls the new estimated midblock delays away from both the baseline estimated midblock delay and the diagonal line, but towards both the measured midblock delays and the diagonal line. However, 50% decrease in pedestrian walking times decreases the new estimated midblock delays. Therefore, the model underestimates the midblock delays relative to the measured midblock delays. This decrease pulls the new estimated midblock delay away from the baseline estimated midblock delay and the diagonal line.

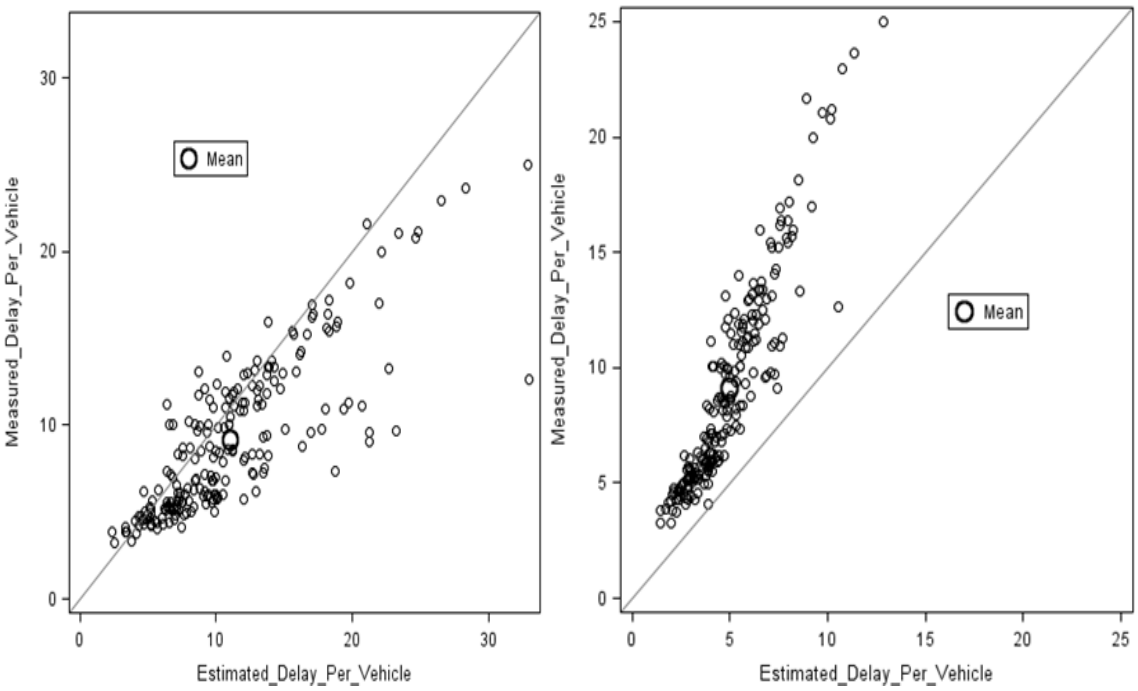

Figures 6.19 -6.20 Measured-estimated midblock delay for 50% increase and 50% decrease in the baseline value of Pedestrian Walking Time, respectively.

CHAPTER 7

CONCLUSIONS AND FUTURE RESEARCH

7.1 Conclusions

This research has achieved the following: a) evaluated the predictive capability of the 2010 HCM platoon dispersion model in predicting the proportion of vehicle arrivals on green at downstream signalized intersections under non-friction and friction traffic conditions, b) developed an integrated deterministic and stochastic model that estimates the delay incurred by platoon vehicles due to midblock pedestrian activity on urban street segments; c) measured pedestrian walking speeds based on age groups for over three thousand pedestrians walking within midblock crosswalks on urban street segments; d) used field measured data to validate the deterministic midblock delay model; e) performed sensitivity analysis to study the relationship between midblock delay and several model variables and parameters. The two sample independent t-test, Chi-square test and mean error statistical tests were performed to evaluate the HCM 2010 platoon dispersion model and the developed midblock delay model. The results of the statistical tests show no statically significant difference and relatively small mean errors between the observed and estimated proportion of vehicle arrivals on green under no-friction traffic condition. The results of the statistical tests, however, show statistically significant difference and relatively high mean errors between the observed and estimated proportion of arrivals on green under friction traffic conditions. In addition, results of the three statistical tests show no statistically significant difference and relatively small mean

errors between the midblock delays measured in the field and the midblock delays estimated using the developed model.

Finally, sensitivity analysis was performed by increasing and decreasing the following variables and parameters by 50% of their baseline values: deceleration rate, acceleration rate, free-flow speed, the headway of bunched vehicles, and pedestrian walking time. The results show increasing the deceleration rate increases the estimated midblock delay(s/veh), and increasing the acceleration rate decreases the estimated midblock delay(s/veh). Conversely, decreasing the deceleration rate decreases the estimated midblock delay, and decreasing the acceleration rate increases the estimated midblock delay. The results of the sensitivity analysis also show increasing the free-flow speed increases the estimated midblock, while decreasing the free-flow speed decreases the estimated midblock delay. The results show very little or no significant relationship between the estimated midblock delay and the headway of bunched vehicles. Pedestrian walking time was determined to impact the estimated midblock delay more than other variables and parameters. Increasing the pedestrian walking time increases the estimated midblock delay. Conversely, decreasing the pedestrian walking time decreases the estimated midblock delay. The results show the estimated stopped delay converges to zero with significant decrease in pedestrian walking time.

Based on the results obtained in this research, the following conclusions are made:

- The HCM 2010 platoon dispersion model can be reliably applied to estimate the proportion of vehicle arrivals on green on urban street segments with no friction traffic conditions. The HCM 2010 platoon dispersion model, however, cannot be reliably applied to estimate the proportion of vehicle arrivals on green on urban

street segments with friction traffic conditions. It is therefore recommended that the HCM 2010 platoon dispersion model, specifically the segment running time and smoothing factor, be modified to directly account for traffic friction conditions;

- The developed deterministic midblock delay model can be reliably applied to estimate the delay incurred by platoon vehicles due to pedestrian activities at midblock crosswalks on urban street segments. It is, however, recommended that additional hours of data on midblock interference be collected to modify and further improve the predictive ability of the developed probability model.
- Pedestrians walk faster at midblock crosswalks than crosswalks at signalized intersections. Overall, young (ages 19 - 30) pedestrians walk fastest compared to other age groups. Middle (ages 31 -60) walk faster when compared to Teenagers (ages 13 - 18). Elderly or physically disabled pedestrian walk the slowest. Furthermore, based on the 15^{th} percentile speed, young pedestrians walk fastest and elder or disabled pedestrian walk the slowest. However, based on the 15^{th} percentile speeds, middle age pedestrians and teenagers walk at the same speed.
- The time it takes for a pedestrian or group of pedestrians to walk across a midblock crosswalk significantly impacts the delay incurred by platoon vehicles traveling on urban street segments. Typically on urban street segments vehicles decelerate at a faster rate than the rate at which they accelerate. The delay associated with deceleration is therefore lower than the delay associated with acceleration. However, in situations wherein there is increased pedestrian walking time, a vehicle decelerating at a rate far greater rate than the ideal rate

will incur an increased delay because the vehicle will come to a stop faster and therefore will increased its stopped time for all the pedestrians to cross.

7.2 Future Research

This section presents future research to be conducted based on the findings of this research. As discussed in the previous section, the limitation of the HCM 2010 platoon dispersion model is it inability to predict vehicle arrival flow profiles of platoon vehicles at downstream signalized intersections. Therefore to account for this limitation, extensive research should be conducted to study the arrival flow profiles of platoon vehicles after being interrupted and reformed at mid-segment. Two significant mid-segment platoon interruptions on urban street segment include pedestrian crossings at midblock crosswalks and on-street parking maneuvers. Furthermore, the HCM 2010 platoon dispersion model was evaluated using field data collected at four urban street segments in New Jersey. Even though the model may have performed very well in predicting the proportion of vehicle arrivals on green on urban street segments under no friction condition, the result may be different if the model was evaluated using data collected on urban street segments from different states with different operational, geometric and driver behavior and pattern. In addition, the midblock delay model developed in this research estimates the delay incurred by platoon vehicles(s/veh) when the lead platoon is interrupted by pedestrians crossing at midblock crosswalks. Therefore, the delay incurred by the following platoon vehicles is estimated based on the delay incurred by the leading platoon vehicle. However, on dense urban streets with high pedestrian volume and high pedestrian flow, the following vehicles in a platoon maybe delayed by successive

pedestrian interruptions. That is, the leading and following platoon vehicles are interrupted by a pedestrian or a group of pedestrians. Once this interference ends, the leading and/or the second, third, etc. platoon vehicle(s) starts to accelerate beyond the crosswalk before the second interference due to a second pedestrian or group of pedestrians crossing. This second interference incurs additional delay to the remaining platoon vehicles. A future research would be to develop a probability model that would account for such limitation, and then incorporated into the midblock delay model developed in this research.

This research developed an integrated deterministic-stochastic midblock delay model. The deterministic delay model estimates the delay incurred by vehicles due to pedestrian interference at midblock crosswalk on urban street segment. The stochastic part of the delay model calculates the probability of occurrence of a number of midblock interference per time interval. The deterministic midblock delay model is applied in two parts. First, the delay is estimated for a leading platoon. In the second part, the delay is estimated to second and subsequent platoon vehicles. Based on these applications, the deterministic model was validated using three data. The first data set included the measured and estimated midblock delays in sec/veh for single vehicles. The second data set included the measured and estimated midblock delays in sec/veh for more than one vehicle-platoon. And a third data set included a combination of data set 1 and data set 2. The statistical results show the developed deterministic model consistently underestimates the midblock delays when compared to the measured midblock delays for data set 1. The statistical results, however, show that the model performs better for data set 2 and data set 3.The midblock delay underestimation for data set 1 may be due to the

model parameters used in the validation, especially the deceleration and accelerations rates. This assertion is based on the results of the sensitivity analysis.

The sensitivity analysis shows for a 50% increase in the baseline deceleration rate, there is increase in the estimated midblock delay. This, therefore, pulls the new estimated midblock delay values toward the measured midblock delay values. The results of sensitivity analysis show the estimated midblock delay for a 50% decrease in the baseline acceleration rate, there is an exponential increase in the estimated midblock delay values. The model therefore tends to overestimate the delay relative the measured midblock delay values. The delay values are pulled away from the diagonal line and measured midblock delay toward the new estimated midblock delay. This exponential increase in the estimated midblock delay values is due to the fact that it takes longer time for a stopped vehicle to accelerate to the normal speed or desired speed (i.e. the vehicle speed prior to the interference). What this indicates is that the value of decelerate rate and the value of the accelerate rate as recommended by the HCM 2010, may be less than the decelerate rate of vehicles on the study segment where midblock delay validation data were measured. It also shows that value of acceleration rate as recommended by the HCM 2010, may be greater than the rate at which vehicles decelerate on the study segment. A future research would be to perform a second validation of the deterministic model using field data collected on other urban street segments.

In addition, another limitation of the HCM 2010 Urban Street methodology is that it does not account for midblock on-street maneuver. Similar to pedestrian activity on urban street segments, drivers executing parallel parking maneuvers or pulling away from on-street parking spaces interrupt oncoming platoon vehicles and consequently incurring

delay. A future research would be to conduct a field study on the relationship between on-street parking activity and midblock delay. A midblock delay model maybe developed to estimate the delay incurred by platoon vehicles due to midblock on-street parking maneuvers.

Another future research would be to study the impact of midblock pedestrian activity on platoon arrival flow profiles at downstream signalized intersections. Typically on urban street segments, a platoon travelling from an upstream signalized intersection to a downstream signalized intersection disperses as it travels downstream due to drivers` desire to increase their speeds. This phenomenon, as defined previously, is called platoon dispersion. As a platoon disperses, the headways between the platoon vehicles increase. Therefore, the profile of a dense platoon discharging from an upstream signal would be different from the arrival flow profile at the downstream signal. On urban street segments with midblock pedestrian crosswalks, platoon vehicles are sometimes interrupted as the travel between upstream and downstream signals due to pedestrian crossings at midblock. This interruption sends shock wave that propagates upward in the platoon once the leading platoon vehicle is interrupted by a pedestrian crossing. Depending on the number of pedestrians crossing during the interference (i.e. duration of interference), a dispersed platoon may or may not completely reform at midblock. Therefore platoon arrival flow profiles should be analyzed for three scenarios:

In scenario 1, the platoon discharges from the upstream signal, progresses downstream without any midblock interference. As it progresses downstream, it disperses due to a variation in speeds and assumed to arrive on green at the downstream signal. An arrival flow profile in veh/time step is obtained. In scenario 2, the platoon discharges

from the upstream signal and progresses to the downstream signal. Unlike scenario 1, it is interrupted by a pedestrian or a group of pedestrians that is already within the critical length of the crosswalk. The critical length of the crosswalk is the length of the crosswalk pedestrians have to walk for platoon vehicles to be interrupted. In this scenario, the driver of the leading platoon vehicle slows down but does not come to a full stop. Because this vehicle does not come to a full stop, the drivers of the first few following platoon vehicles would slow down to avoid collision. However, the impact of the interference on vehicles in the back of the platoon would be minimal. The arrival flow profile in this scenario would be different from that in scenario 1. Furthermore, in scenario 3, the leading vehicle of the dispersed is interrupted at midblock by a pedestrian or a group of pedestrian who is just about to enter or just entered the critical length of the crosswalk. Unlike scenario 2 wherein the pedestrian or pedestrians was already within the critical length of the crosswalk and therefore the duration of the interference is smaller, in scenario 3, the pedestrian or pedestrians would have to would the entire critical length of the crosswalk. Therefore, in scenario 3, the leading and following platoon vehicles come to a full stop and reforms at midblock due to the increase in the duration of interference. The shape of the reformed platoon therefore tends towards the initial shape of the dense platoon on red at the stop line of the upstream signal. Once the interference ends, the drivers will start to accelerate to their desired speeds. Because of the delay due to acceleration and decrease in the segment travel distance (between midblock crosswalk and stop line of downstream signal), there is decrease in the rate of platoon dispersion and subsequently increase in the vehicle arrival rate assumed to be on green at the stop line of the downstream signal.

APPENDIX A

PLATOON DISPERSION ON URBAN ARTERIAL STREET SEGMENT

Platoon dispersion is the spreading of group of vehicles called platoon as they travel from an upstream signalized intersection to a downstream signalized intersection due to drivers` desire to increase their speeds. Figure A.1 shows two dense platoons of vehicles at the stop-line of the upstream signal during the red signal indication at one of the study sites. Figure A.2 shows the dispersed platoons further downstream after departing the upstream signal.

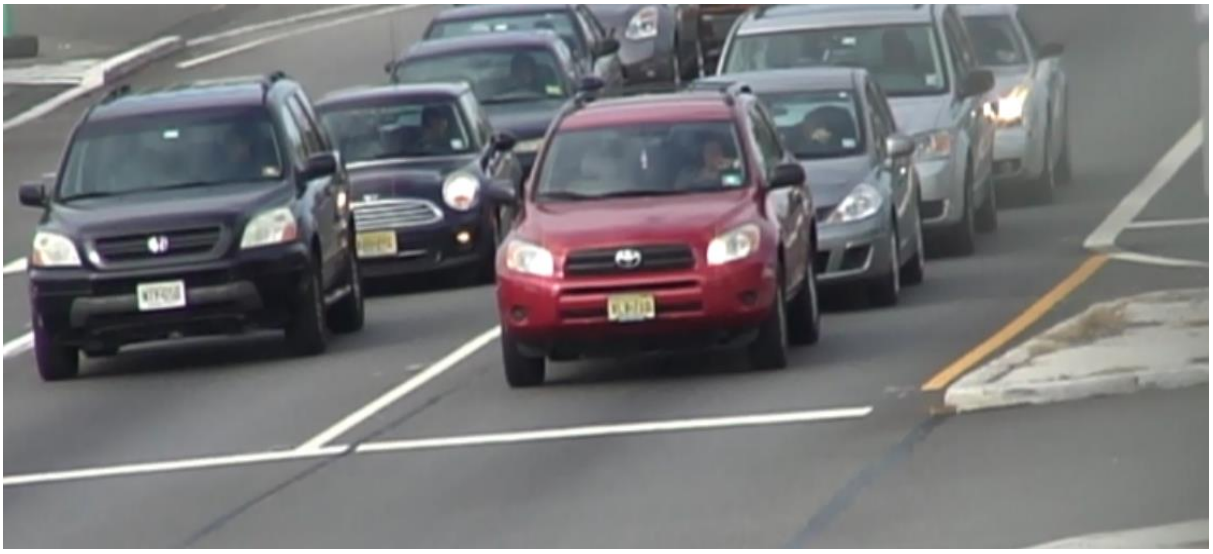

Figure A.1 Dense platoons at stop line of upstream intersection on red.

Figure A.2 Dispersed platoons at the downstream intersection.

APPENDIX B

MIDBLOCK PEDESTRIAN ACTIVITY AND INTERFERENCE ON URBAN STREET SEGMENT

On urban street segments with midblock crosswalks, platoon vehicles typically get interrupted as they travel between the upstream and downstream signalized intersections due to pedestrian crossings. Platoon vehicles therefore incur delays as they slow down and/or stop to allow pedestrians to cross. The number of interference and the quantity of delay incurred depend on the pedestrian volume at the crosswalk and traffic volume along the segment. Figure B.1 shows a group of pedestrians crossing in a midblock crosswalk on an urban street segment in Newark, New Jersey. Figure B.2 shows a midblock interference at one of the study sites. The figure shows a platoon of vehicles stopped as a group of pedestrians cross at midblock. Figure B.3 shows the midblock crosswalk at site 1. This site is on the campus of New Jersey Institute of Technology (N.J.I.T).

Figure B.1 Pedestrian crossings at midblock crosswalk at Study Site 2.

Figure B.2 Midblock pedestrian interference at Study Site 2.

Figure B.3 Midblock crosswalk at Study Site 1(Warren Street, Newark, New Jersey).

Figure B 4. VISSIM 3D animation of midblock pedestrian activity.

APPENDIX C

DATA COLLECTION DEVICE AND INSTRUMENTS

The Figures C.1 – C.4 show the data collection device and instruments used in this research. Figure C.1 shows a Sony DCR-SR 100 video camera used to record platoon discharge and arrival flow profiles and midblock pedestrian activity on urban street segments. Figure C. 1 shows a tripod used to hold the Sony video camera. Figure C. 3 shows a Kintrex measuring wheel used to measure distances.

Figure C.1 Sony DCR-SR 100 video camera

Figure C.2 Tripod for Sony DCR-SR 100 video camera

Figure C.3 Kintrex measuring wheel.

Figure C.4 Accusplit stopwatch.

APPENDIX D

NEW JERSEY STATE LAW ON PEDESTRIAN CROSSING WITHIN A MARKED CROSSWALK

The New Jersey State Law on pedestrian crossing within a marked crosswalk states "*…the driver of a vehicle shall stop and remain stopped to all allow a pedestrian to cross the roadway within a marked crosswalk, when the pedestrian is upon, or within one lane of, the half of the roadway, upon which the vehicle is traveling or onto which it is turning.* ***Half of roadway*** *means all traffic lanes conveying traffic in one direction of travel"*

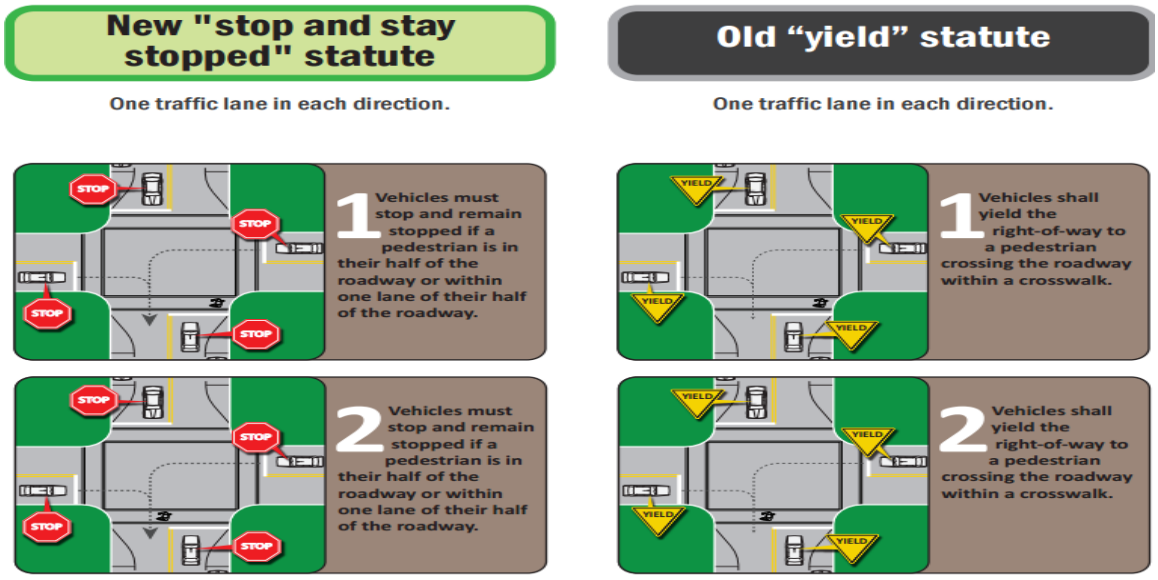

Figure D.1 Graphics of the New Jersey State Law on pedestrian crossings in crosswalks on two-lane urban street segments.

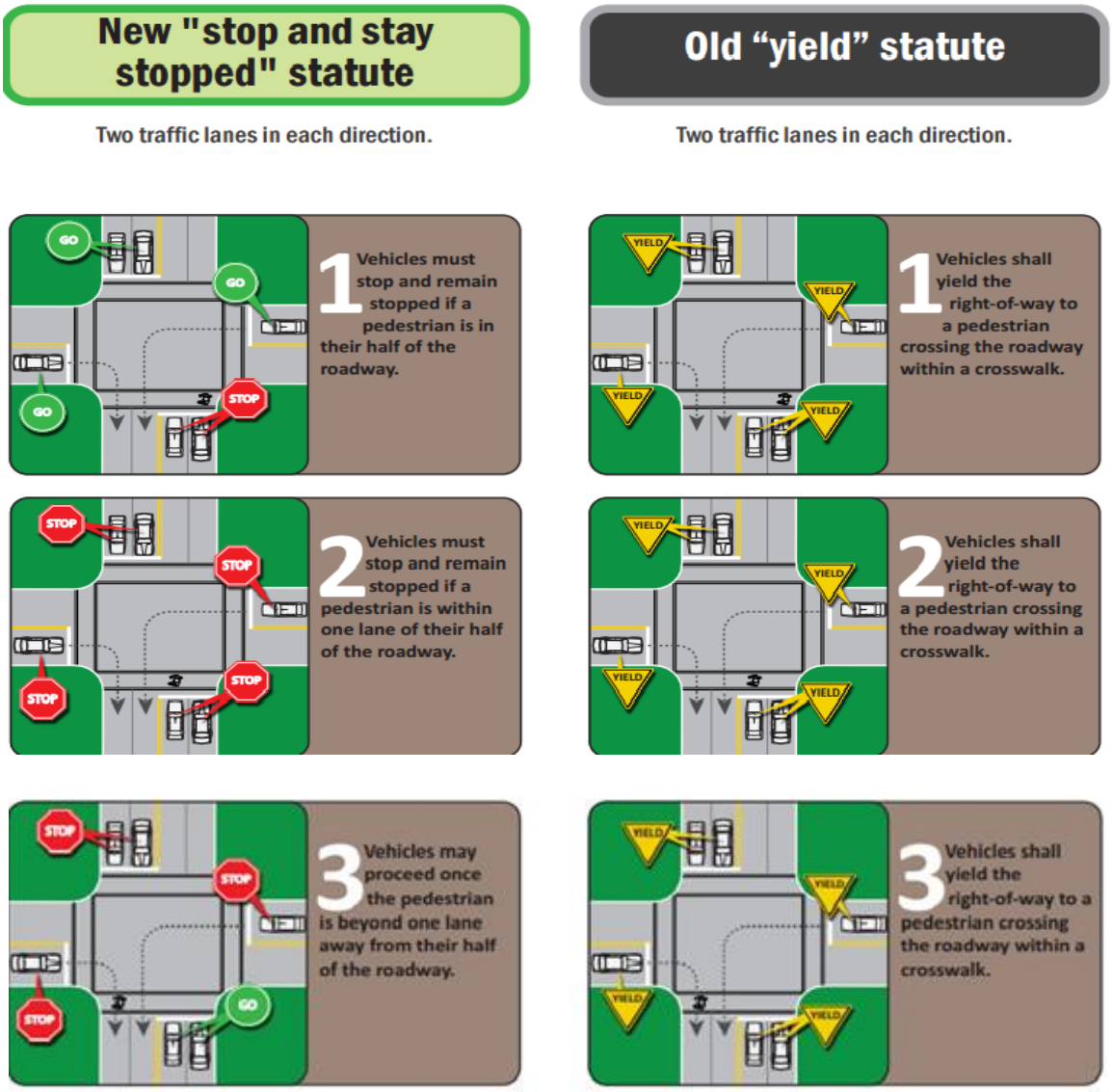

Figure D.2. Graphics of the New Jersey State Law on pedestrian crossings in crosswalks on four-lane urban street segments.

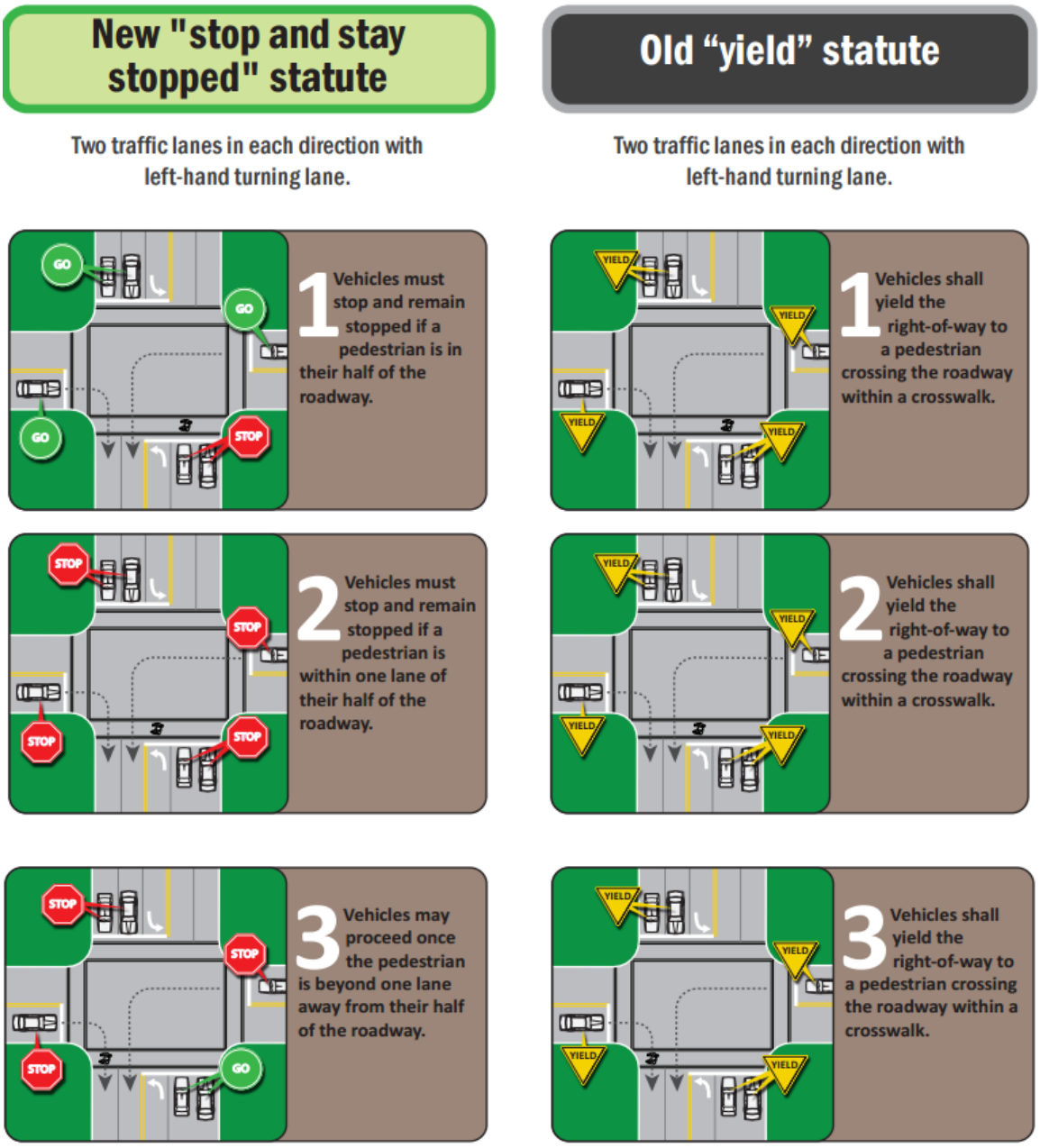

Figure D.3. Graphics of the New Jersey State Law on pedestrian crossings in crosswalks on four-lane urban street segments with exclusive left turn lanes.

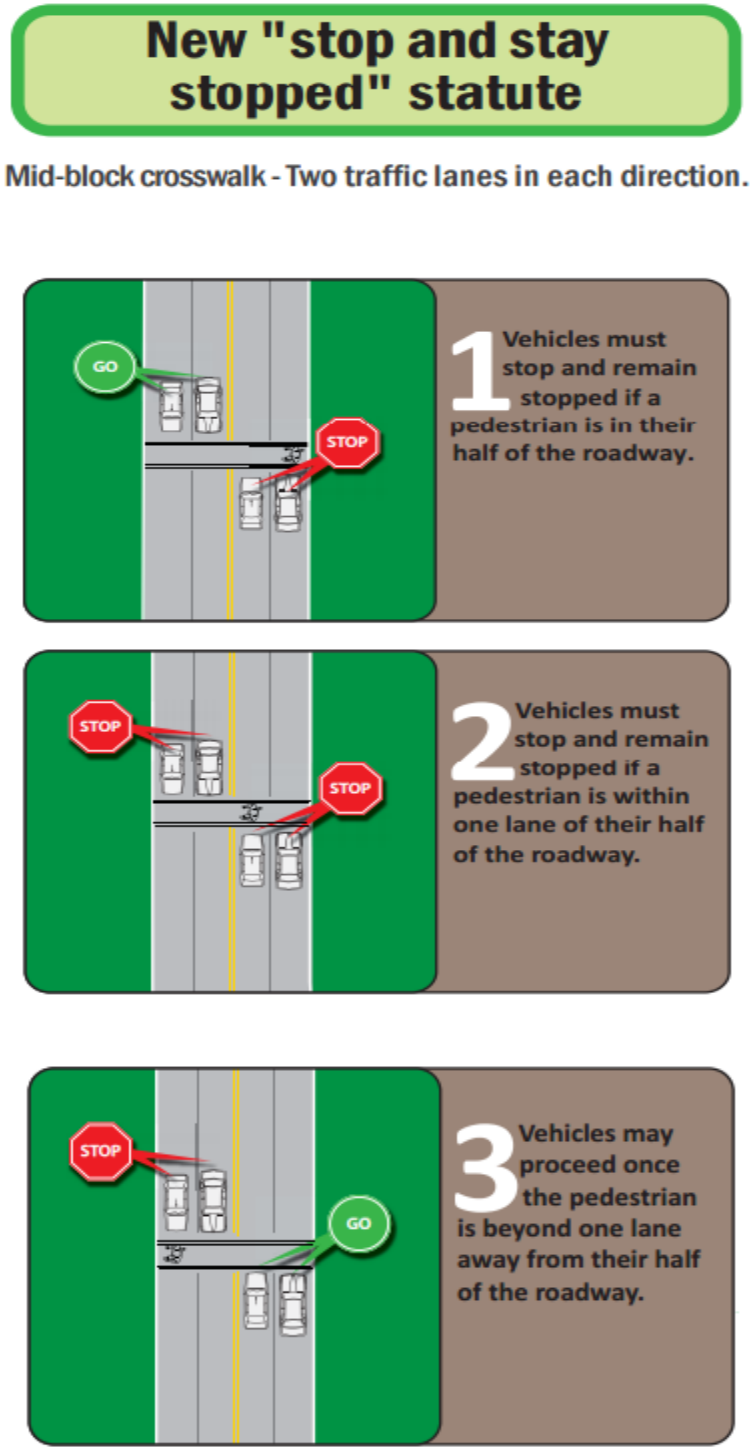

Figure D.4 Graphics of the New Jersey State Law on pedestrian crossings at midblock crosswalks on four-lane urban street segments.

APPENDIX E

RESULT of POISSON REGRESSION ANALYSIS FOR MIDBLOCK PEDESTRIAN INTERFERENCE

The results of the generalized linear model (GENMOD) regression procedure in SAS 9.2 are presented. The results show the estimated coefficients of the model variables. Two different regression analyses were performed. The first analysis was performed with the number of midblock pedestrian interference as the dependent variable and traffic volume and pedestrian volume as independent variables. The second regression analysis was performed with the number of midblock pedestrian interference as the dependent variable and traffic volume and number of pedestrian crossings as independent variables.

The SAS System

The GENMOD Procedure

Model Information

Data Set	SASDATA.PEDESTRIAN5
Distribution	Poisson
Link Function	Log
Dependent Variable	Number_of_Interference

Number of Observations Read	22
Number of Observations Used	22

Criteria For Assessing Goodness Of Fit

Criterion	DF	Value	Value/DF
Deviance	19	78.7731	4.1460
Scaled Deviance	19	78.7731	4.1460
Pearson Chi-Square	19	80.9904	4.2627
Scaled Pearson X2	19	80.9904	4.2627
Log Likelihood		1152.6217	
Full Log Likelihood		-89.8695	
AIC (smaller is better)		185.7390	
AICC (smaller is better)		187.0723	
BIC (smaller is better)		189.0121	

Algorithm converged.

Analysis Of Maximum Likelihood Parameter Estimates

Parameter	DF	Estimate	Standard Error	Wald 95% Confidence Limits		Wald Chi-Square	Pr > ChiSq
Intercept	1	0.6753	0.2464	0.1924	1.1581	7.51	0.0061
Traffic_Volume	1	0.0046	0.0007	0.0033	0.0059	48.41	<.0001
Pedestrian_volume	1	0.0058	0.0005	0.0047	0.0069	112.09	<.0001

Scale	0	1.0000	0.0000	1.0000	1.0000

NOTE: The scale parameter was held fixed.

The GENMOD Procedure

Model Information

Data Set	SASDATA.CROSSING5
Distribution	Poisson
Link Function	Log
Dependent Variable	Number_of_Interference

Number of Observations Read	22
Number of Observations Used	22

Criteria For Assessing Goodness Of Fit

Criterion	DF	Value	Value/DF
Deviance	19	71.8478	3.7815
Scaled Deviance	19	71.8478	3.7815
Pearson Chi-Square	19	76.1961	4.0103
Scaled Pearson X2	19	76.1961	4.0103
Log Likelihood		1156.0843	
Full Log Likelihood		-86.4068	
AIC (smaller is better)		178.8137	
AICC (smaller is better)		180.1470	
BIC (smaller is better)		182.0868	

Algorithm converged.

Analysis Of Maximum Likelihood Parameter Estimates

Parameter	DF	Estimate	Standard Error	Wald 95% Confidence Limits		Wald Chi-Square	Pr > ChiSq
Intercept	1	0.8136	0.2359	0.3513	1.2760	11.90	0.0006
Traffic_Volume	1	0.0039	0.0006	0.0026	0.0052	36.46	<.0001
_Number_of_Crossings	1	0.0078	0.0007	0.0064	0.0092	115.08	<.0001
Scale	0	1.0000	0.0000	1.0000	1.0000		

NOTE: The scale parameter was held fixed.

APPENDIX F

DERIVATIONS OF POISSON PROBABILITY MODEL

The derivation of Poisson probability model is presented in the subsection. The Poisson distribution is applicable to populations having the following properties:

- The probability of occurrence of individuals having particular characteristics is low.
- The characteristic is a discrete variable.

According to Gerlough and Barnes (1971), the Poisson distribution can be derived as a limiting case of the binomial distribution. This is most commonly seen derivation. It is possible, however, to derive the Poisson distribution directly from fundamental considerations of probability.

Deriving the Poisson distribution as a Limiting Case of the Binomial Distribution

Let n =number of items in sample
p = probability of occurrence of a particular characteristic E
$q = (1 - p)$ = probability of non-occurrence of characteristic E
x = number of items in sample having characteristic E

Then, from the binomial distribution:

$$P(x) = C_x^n p^x q^{n-x} = C_x^n p^x (1-p)^{n-x}$$

Where $x = 0, 1, 2, ...n$
Now let:

p be made indefinitely small
n be very large

$pn = m$,
Where m is finite and not necessarily small
Then:

$$p = \frac{m}{n}$$

$$P(x) = C_x^n \left(\frac{m}{n}\right)^x \left(1-\frac{m}{n}\right)^{n-x} \; ; x = 0,1,2,...n$$

$$= \frac{n!}{x!(n-x)!}\left(\frac{m}{n}\right)^x \left(1-\frac{m}{n}\right)^{n-x}$$

$$= \frac{n!}{x!(n-x)!}\left(\frac{m}{n}\right)^x \left(1-\frac{m}{n}\right)^{n} \left(1-\frac{m}{n}\right)^{-x}$$

$$P(x) = \left[\frac{m^x}{x!}\right]\left[\left(1-\frac{m}{n}\right)^n\right]\left[\frac{n!}{(n-x)!n^x\left(1-\frac{m}{n}\right)^x}\right]$$

$$= [A][B][C]$$

Where A, B, and C represent the individual terms in brackets.

Now, if $n \to \infty$

$$\lim_{n\to\infty} P(x) = \lim_{n\to\infty}\{[A][B][C]\}$$

$$= \left[\lim_{n\to\infty} A\right]\left[\lim_{n\to\infty} B\right]\left[\lim_{n\to\infty} C\right]$$

$$A = \frac{m^x}{x!}$$

$$\lim_{n\to\infty} A = \frac{m^x}{x!}$$

$$B = \left(1-\frac{m}{n}\right)^n$$

$$\lim_{n\to\infty} B = e^{-m}$$ (Proof of this relationship is presented by Gerlough and Barnes,1971)

$$C = \frac{n!}{(n-x)!n^x\left(1-\frac{m}{n}\right)^x}$$

When n is very large, negligible error is introduced by representing $n!$ by one term of Sterling's formula. The same statement holds for $(n-x)!$

Therefore,

$$C = \frac{\sqrt{2\pi n} \times n^n e^{-n}}{\sqrt{2\pi(n-x)}(n-x)^{n-x} e^{-(n-x)} \left(1-\frac{m}{n}\right)^x n^x}$$

$$C = \frac{\sqrt{2\pi} \times n^{\frac{1}{2}} \times n^n \times e^{-n}}{\sqrt{2\pi}(n-x)^{\frac{1}{2}}(n-x)^{n-x} e^{-(n-x)} \left(1-\frac{m}{n}\right)^x n^x}$$

$$= e^{-x} \left(1-\frac{x}{n}\right)^{-\frac{1}{2}} \frac{n^{n-x}}{(n-x)^{n-x}} \frac{1}{\left(1-\frac{m}{n}\right)^x}$$

$$= e^{-x} \left(1-\frac{x}{n}\right)^{-\frac{1}{2}} \frac{1}{\left(\frac{n-x}{n}\right)^{n-x}} \frac{1}{\left(1-\frac{m}{n}\right)^x}$$

$$C = \left[e^{-x}\right] \left[1-\frac{x}{n}\right]^{-\frac{1}{2}} \frac{1}{\left(1-\frac{x}{n}\right)^{n-x}} \frac{1}{\left(1-\frac{m}{n}\right)^x}$$

$$C = \left[e^{-x}\right] \left[1-\frac{x}{n}\right]^{x-\frac{1}{2}} \left[\frac{1}{\left(1-\frac{x}{n}\right)^n}\right] \left[\frac{1}{\left(1-\frac{m}{n}\right)^x}\right]$$

$$= [C_1][C_2][C_3][C_4]$$

Where C_1, C_2, C_3, and C_4 represent the individual terms in brackets

$$C_1 = e^{-x}$$

$$\lim_{n \to \infty} C_1 = e^{-x}$$

$$C_2 = \left(1 - \frac{x}{n}\right)^{x-\frac{1}{2}}$$

$$\lim_{n \to \infty} C_2 = 1$$

$$C_3 = \frac{1}{\left(1 - \frac{x}{n}\right)^{n}}$$

$$\lim_{n \to \infty} C_3 = \frac{1}{e^{-x}}$$

$$C_4 = \frac{1}{\left(1 - \frac{m}{n}\right)^{x}}$$

$$\lim_{n \to \infty} C_4 = 1$$

$$\lim_{n \to \infty} C = \left[\lim_{n \to \infty} C_1\right]\left[\lim_{n \to \infty} C_2\right]\left[\lim_{n \to \infty} C_3\right]\left[\lim_{n \to \infty} C_4\right]$$

$$= \left[e^{-x}\right][1]\left[\frac{1}{e^{-x}}\right][1]$$

$$= 1$$

$$\lim_{n \to \infty} P(x) = \frac{m^x}{x!} e^{-m}$$

Since the main body of this discussion assumes the existence of the conditions for the Poisson distribution,(i.e., $n \to \infty$) the above equation may be written simply:

$$P(x) = \frac{m^x}{x!} e^{-m} \qquad \text{Q.E.D}$$

Direct Derivation of the Poisson distribution

Consider a process in which the average or expected rate of arrival is μ arrivals per unit time.

Let

$P_i(t)$ =the probability of i arrivals up to the time t.

μdt =the probability of one arrival in the incremental period dt.

Note: It is assumed that dt is of such a short duration that the probability of more than one arrival is dt is negligible.

Therefore, $(1-\mu dt)$ = the probability of no arrival in dt

Then:

$P_i(t+dt)$ =the probability that i arrivals have taken place up to the time $(t+dt)$

= [Probability (i - 1 arrivals in t). Probability (1 arrival in dt)

+ [Probability (i arrivals in t).Probability (0 arrivals in dt)]

$$P_i(t+dt) = P_{i-1}(t)\times P_1(dt) + P_i(t)\times P_0(dt)$$

$$= P_{i-1}(t)\mu dt + P_i(t)(1-\mu dt)$$

$$= [P_{i-1}(t) - P_i(t)](\mu dt) + P_i(t)$$

$$\frac{P_i(t+dt) - P_i(t)}{dt} = \mu[P_{i-1}(t) - P_i(t)]$$

Or

$$\frac{dP_i(t)}{dt} = \mu[P_{i-1}(t) - P_i(t)] \qquad (2)$$

Now,

$P_{-1}(t) = 0$ (i.e., impossible to have less than zero)

$P_0(t) = 1$ (i.e., no arrivals up to time $t = 0$)

$P_i(0) = 1$ for $i \geq 1$ (zero probability of $i \geq 1$ arrivals at time $t = 0$)

Setting $i = 0$ in Equation (2)

$$\frac{dP_0(t)}{dt} = \mu[0 - P_0(t)]$$

$$\frac{dP_0(t)}{P_0(t)} = -\mu dt$$

$$\ln P_0(t) = -\mu t + c$$

$$P_0(t) = e^{-\mu t + c}$$

Since

$$P_0(0) = 1$$

$$1 = e^0$$

Therefore $c = 0$

Setting $i = 1$ in Equation (2) and inserting the above value for $P_0(t)$

$$\frac{dP_1(t)}{dt} = \mu[e^{-\lambda t} - P_1(t)]$$

$$\frac{dP_1(t)}{dt} + \mu P_1(t) = \mu e^{-\mu t}$$

Using method of operators for solving this differential equation

$$(D + \mu)P_1(t) = \mu e^{-\mu t}$$

$$P_1(t) = \frac{1}{D + \mu} \mu e^{-\mu t}$$

$$= (\mu t)e^{-\mu t} + C_2 e^{-\mu t}$$

But $P_1(0) = 0; \ \therefore C_2 = 0$

$$\therefore P_1(t) = (\mu t)e^{-\mu t}$$

$$\frac{dP_2(t)}{dt} = \mu[P_1(t) - P_2(t)]$$

$$\frac{dP_2(t)}{dt} + \mu P_2(t) = \mu P_1(t) = \mu(\mu t)e^{-\mu t}$$

$$P_2(t) = \frac{1}{D+\mu}\mu(\mu t)e^{-\mu t}$$

Based on the method of operators, the form

$$y = \frac{1}{D+A}w(x)$$

Results in a solution

$$y = e^{-Ax}\int e^{Ax}w(x)dx + ce^{-Ax}$$

Therefore

$$P_2(t) = \frac{\mu^2 t^2}{2}e^{-\mu t} + C_3 e^{-\mu t}$$

But $P_2(0) = 0;\ \therefore C_3 = 0$

$$P_2(t) = \frac{(\mu t)^2 e^{-\mu t}}{2}$$

Similarly

$$P_3(t) = \frac{(\mu t)^3 e^{-\mu t}}{3!}$$

$$P_4(t) = \frac{(\mu t)^4 e^{-\mu t}}{4!}$$

$$P_x(t) = \frac{(\mu t)^x e^{-\mu t}}{x!}$$ Q.E.D

APPENDIX G

EQUATIONS OF THE INDEPENDENT TWO-SAMPLE T-TEST PARAMTERS AND STATISTICS

The following is a detailed description of the two-sample t-test parameters and statistics. The equations provided form part of the SAS T-test procedure for Independent two-sample T-test. Definition of the key notations is given as follows:

n_1^* = number of observation at first class level

n_2^* = number of observation at second class level

y_{1i} =value of *ith* observation at first class level, $i \in \{1,....,n_1^*\}$

y_{2i} =value of *ith* observation at first class level, $i \in \{1,....,n_2^*\}$

f_{1i} =frequency of *ith* observation at first class level, $i \in \{1,....,n_1^*\}$

f_{2i} =frequency of *ith* observation at second class level, $i \in \{1,....,n_2^*\}$

w_{1i} =frequency of *ith* observation at first class level, $i \in \{1,....,n_1^*\}$

w_{2i} =frequency of *ith* observation at second class level, $i \in \{1,....,n_2^*\}$

n_1 = sample size for first class level= $\sum_{i}^{n_1^*} f_{1i}$

n_2 = sample size for first class level= $\sum_{i}^{n_1^*} f_{2i}$

Observations at the first class level are assumed to be distributed as $N(\mu_1, \sigma_1^2)$, and the observation at the second class level are assumed to be distributed as $N(\mu_2, \sigma_2^2)$, where $\mu_1, \mu_1, \sigma_1, \sigma_2$ are unknown. The within-class-level mean estimates $\left(\bar{y}_1 \text{and} \bar{y}_2\right)$ are computed as follows:

$$\bar{y}_1 = \frac{\sum_{1i}^{n^*} f_{1i} w_{1i} y_{1i}}{\sum_{1i}^{n^*} f_{1i} w_{1i}}$$

$$\bar{y}_2 = \frac{\sum_{2i}^{n^*} f_{2i} w_{2i} y_{2i}}{\sum_{2i}^{n^*} f_{2i} w_{2i}}$$

The within-class-level standard deviation estimates $\left(s_1 \text{ and} s_2\right)$ are computed as follows:

$$s_1 = \left(\frac{\sum_{1i}^{n^*} f_{1i} w_{1i} (y_{1i} - \bar{y}_1)}{n_1 - 1} \right)^{\frac{1}{2}}$$

$$s_2 = \left(\frac{\sum_{2i}^{n^*} f_{2i} w_{2i} (y_{2i} - \bar{y}_2)}{n_2 - 1} \right)^{\frac{1}{2}}$$

The within-class-level standard error estimates $\left(SE_1 \text{ and} \text{SE}_2\right)$ are computed as follows:

$$SE_1 = \frac{s_1}{\sum_{1i}^{n^*} f_{1i} w_{1i}}$$

$$SE_2 = \frac{s_2}{\sum_{2i}^{n^*} f_{2i} w_{2i}}$$

The mean difference $\mu_1 - \mu_2 = \mu_d$ is estimated by $\bar{y}_d = \bar{y}_1 - \bar{y}_2$

Under the assumption of equal variances ($\sigma_1^2 = \sigma_2^2$), the pooled estimate of the common standard deviation is computed as follows:

$$s_p = \left(\frac{(n_1 - 1)\text{s}_1^2 + (n_2 - 1)\text{s}_2^2}{n_1 + n_2 - 2} \right)^{\frac{1}{2}}$$

The pooled estimate of the standard error of $\bar{y}_d$ assuming equal variances is computed as follows:

$$SE_p = s_p \left(\frac{1}{\sum_{1i}^{n^*} f_{1i} w_{1i}} + \frac{1}{\sum_{2i}^{n^*} f_{2i} w_{2i}} \right)^{\frac{1}{2}}$$

The pooled $100(1-\alpha)\%$ confidence interval for the mean difference μ_d is

$$\left(\bar{y}_d - t_{1-\frac{\alpha}{2}, n_1+n_2-2} SE_p, \bar{y}_d + t_{1-\frac{\alpha}{2}, n_1+n_2-2} SE_p \right) \quad , \quad \text{2-Sided}$$

$$\left(-\infty, \bar{y}_d + t_{1-\alpha, n_1+n_2-2} SE_p \right) \quad , \quad \text{Sides=L}$$

$$\left(\bar{y}_d - t_{1-\alpha, n_1+n_2-2} SE_p, \infty \right) \quad , \quad \text{Sides=U}$$

The t value for the pooled test is computed as follows:

$$t_p = \frac{\bar{y}_d - \mu_0}{SE_p}$$

The $p-value$ for the test is computed as follows:

$$p-value = \begin{cases} P(t_p^2 > F_{1-\alpha,1,n_1+n_2-2}) \text{.....} 2-\text{sided} \\ P(t_p < t_{\alpha, n_1+n_2-2}) \text{.....lower} 1-\text{sided} \\ P(t_p > t_{1-\alpha,1,n_1+n_2-2}) \text{.....Upper} 1-\text{sided} \end{cases}$$

Under the assumption of unequal variances (the Behrens-Fisher problem), the unpooled standard error is computed as follows:

$$SE_u = \left(\frac{s_1^2}{\sum_{i=1}^{n_1^*} f_{1i} w_{1i}} + \frac{s_2^2}{\sum_{i=1}^{n_2^*} f_{2i} w_{2i}} \right)^{\frac{1}{2}}$$

Satterthwaite`s(1946) approximation for the degrees of freedom, extended to accommodate weights, is computed as follows:

$$df_u = \frac{SE_u^4}{\frac{s_1^4}{(n_1-1)\left(\sum_{i=1}^{n_1^*} f_{1i}w_{1i}\right)^2} + \frac{s_2^4}{(n_2-1)\left(\sum_{i=1}^{n_2^*} f_{2i}w_{2i}\right)^2}}$$

The unpooled Satterthwaite $100(1-\alpha)\%$ confidence interval for the mean difference μ_d is

$$\left(\bar{y}_d - t_{1-\frac{\alpha}{2},\mathrm{df}_u} SE_u, \bar{y}_d + t_{1-\frac{\alpha}{2},\mathrm{df}_u} SE_u\right) \quad , \quad \text{2-Sided}$$

$$\left(-\infty, \bar{y}_d + t_{1-\alpha,\mathrm{df}_u} SE_u\right) \quad \text{, Sides=L}$$

$$\left(\bar{y}_d - t_{1-\alpha,\mathrm{df}_u} SE_u, \infty\right) \quad , \quad \text{Sides=U}$$

The t value for the unpooled Satterthwaite test is computed as follows:

$$t_p = \frac{\bar{y}_d - \mu_0}{SE_u}$$

The $p-value$ for the test is computed as follows:

$$p-value = \begin{cases} P(t_p^2 > F_{1-\alpha,1,\mathrm{df}_u}) \ldots\ldots\ldots\ldots 2-\text{sided} \\ P(t_p < t_{\alpha,\mathrm{df}_u}) \ldots\ldots\ldots\ldots\ldots \text{Lower} 1-\text{sided} \\ P(t_p > t_{1-\alpha,\mathrm{df}_u}) \ldots\ldots\ldots\ldots\ldots \text{Upper} 1-\text{sided} \end{cases}$$

The folded form of the F statistic, F', tests the hypothesis that variances are equal (Steel and Torrie,1980), where

$$F' = \frac{\max(s_1^2, s_1^2)}{\min(s_1^2, s_1^2)}$$

A test of F' is a two-tailed F test because you do not specify which variance you expect to be larger. The p-value gives the probability of a greater F value under the null hypothesis that $\sigma_1^2 = \sigma_2^2$.

REFERENCES

Abbas, M., D. Bullock, and A. Rhodes. Comparative Study of Theoretical, Simulation, and Field Platoon Data. *Traffic Engineering and Control*. Vol. 42, No.7, 2001, pp. 232-236.

Aiken, L.S., and S. G. West. *Multiple Regression: Testing and Interpreting Interactions*. Sage Publications, Inc, 1991.

Arasan,V.T., and S.H. Kashani. Modeling Platoon Dispersal Pattern of Heterogeneous Road Traffic .In *Transportation Research Record 1852*, TRB, National Research Council, Washington, D.C., 2003, pp. 175-182.

Axhausen, K. W., and H. G. Korling. Some Measurements of Robertson`s Platoon Dispersion Factor. In *Transportation Research Record 1112*, TRB, National Research Council, Washington, D.C., 1987, pp. 71-77.

Baass, K.G., and S. Lefebvre .Analysis of Platoon Dispersion with Respect to Traffic Volume. In *Transportation Research Record 1194*, TRB, National Research Council, Washington, D.C., 1988, pp. 42-43.

Bonesson, J. A. and McCoy, P. T. Capacity and Operational Effects of Midblock Left-Turn Lanes, Appendix B. *Transportation Research Board*, National Research Council, Washington, DC, 1997.

Bonneson, J. A., M. P. Pratt and M. A. Vandehey. Predicting the Performance of Automobile Traffic on Urban Streets. Final report. NCHRP Project 3-79. TRB, *Texas Transportation Institute*, College Station, Texas, 2008.

Bonneson, J. A., M. P. Pratt, and M. A. Vandehey. Predicting Arrival Flow Profiles and Platoon Dispersion for Urban Street Segments. In *Transportation Research Record 2173*, TRB, National Research Council, Washington D.C., 2010, pp. 28-35.

Bonneson, J. and Fitts, J. W. Delay to Major Street Through Vehicles At Two-Way Stop-Controlled Intersections. Prepared for 3rd *International Symposium on Intersections Without Traffic Signals*, Portland, Oregon, 1997.

Bonneson, J. Delay to Major Street Through Vehicles due to Right-Turn Activity. Transportation Research : Part A-Administrative, Vol. 32, No.2. Elsevier Science Ltd., Great Britain, 1998, pp. 139-148.

Bowman, B.L., and R.L. Vecellio. Pedestrian Walking Speeds and Conflicts at Urban Median Locations. In *Transportation Research Record 1438*, TRB, National Research Council, Washington, D.C., 1994, pp. 67-73.

Brewer, M.A., K. Fitzpatrick, J.A. Whitacre, and D. Lord. Exploration of Pedestrian Gap-Acceptance Behavior at Selected Locations. In *Transportation Research Record 1982*, TRB, National Research Council, Washington, D.C., 2006, pp. 132- 140.

Castle,D.E., and J.W. Bonneville. Platoon Dispersion Over Long Road Links. In *Transportation Research Record 1021*, TRB, National Research Council, Washington, D.C., 1985, pp. 42 - 43.

Coffin, A, and J. Morrall. Walking Speeds of Elderly Pedestrians at Cross Walks. In *Transportation Research Record 1487*, TRB, National Research Council, Washington D.C., 1995, pp. 63-67.

Collins,J. F., and P.Gower. Dispersion of Traffic Platoons on A4 in Hounslow. Supplementary Report 29 UC. In *Transport and Road Research Laboratory*.

CORSIM User`s Manual. FHWA, *U.S. Department of Transportation*, 2003.

Courage, K., and C.E. Wallace. TRANSYT-7F Users Guide. Office of Traffic Operations and Intelligent Vehicle/Highway Systems, *U.S. Department of Transportation*, Dec. 1991.

Cui, Z. and S. Nambisan. Methodology for Evaluating the Safety of Midblock Pedestrian Crossings. In *Transportation Research Record 1828*, TRB, National Research Council, Washington, D.C., 2003, pp.75-22.

Denny, R.W.,Jr. Traffic Platoon Dispersion Modeling. *Journal of Transportation Engineering*, ASCE, Vol. 115, No.2, 1989, pp. 193-207.

Deshpande, R., N. H. Gartner, and M. L. Zarrilo. Urban Street Performance: Level of Service and Quality of Progression Analysis. In *Transportation Research Record 2173*, TRB, National Research Council, Washington D.C., 2010, pp. 57-63.

Dowdy, S., S.Wearden, and C. Daniel. *Statistics for Research*. John Wiley and Sons, Inc., New York, 2003.

El-Reedy, T.Y., and R. Ashworth. Platoon Dispersion along a Major Road in Sheffield. *Traffic Engineering and Control*, April 1978, pp. 186-189.

Fitzpatrick, K., M.A. Brewer, and T. Shawn. Another Look at Pedestrian Walking Speed..In *Transportation Research Record 1982*, TRB, National Research Council, Washington, D.C., 2006, pp. 21- 29.

Fleiss, J.L., B. Levin, M. C. Paik. *Statistical Methods for Rates and Proportions* .Third Edition. .John Wiley and Sons, Inc., New York, 2003.

Freund, J. R., R.C. Littell. *SAS System for Regression*. Third Edition. John Wiley and Sons, Inc., New York, 2000.

Gartner, H. G., and P. Wagner. Analysis of Traffic Flow Characteristics on Signalized Arterials. *In Transportation Research Record*, No. 1883,TRB, National Research Council,Washington,D.C.,2004, pp. 94-100.

Geroliminis , N., and A. Skabardonis. Prediction of Arrival Profiles and Queue Lengths along Signalized Arterial by Using a Markov Decision. In *Transportation Research Record 1934*, TRB, National Research Council, Washington, D.C., 2005, pp 116-124.

Grace, M. J. and R.B. Potts. A Theory of the Diffusion of Traffic Platoons. *Operation Research* 12, 1964, pp. 255-285.

Guar, A., and P. Mirchandan. Method for Real-Time Recognition of Vehicle Platoons. In *Transportation Research Record 1748*, TRB, National Research Council, Washington, D.C., 2001, pp. 8-17.

Guebert, A. A., and G. Sparks. Timing Plan Sensitivity to Changes in Platoon Setting. *University of Saskatoon*, 1989.

Herman, R., R.B. Potts, and W.R. Rothery. Behavior of Traffic Leaving a Signalized Intersection. *Traffic Engineering Control*, Vol. 5, No. 9, pp. 529-533.

Highway Capacity Manual. TRB, *National Research Council*, Washington D.C., 2010.

Jaccard, J., and R. Turrisi. *Interaction Effects in Multiple Regression*. Second Edition. Sara Miller McCune, Sage Publications, Inc, 2003.

Jost, D., K. Nagel. Probabilistic Traffic Flow Breakdown in Stochastic Car-Following Models. In *Transportation Research Record 1852*,TRB,National Research Council,Washington, D.C., 2003, pp.152 -166.

Knoblauch, R. L., M.T. Pietrucha, and M. Nitzburg. Field Studies of Pedestrian Walking Speed and Start-Up Time .In *Transportation Research Record 1538*, TRB, National Research Council, Washington, D.C., 1996, pp. 27- 38.

Lam, J.K. Studies of Platoon Model and Its Practical Application. Proc., *Seventh International Symposium on Transportation and Traffic Theory*, Kyoto, Japan, 1977, pp. 119-144.

Lighthill, M. J., and G.B. Witham. On Kinematic Waves II- A Theory of Traffic Flow on Long Crowded Roads. Proc. of the *Royal Society*, A229, London, England, pp. 317-345.

Manar, A., and K.G., Baass. Traffic Platoon Dispersion Modeling on Arterial Street. In *Transportation Research Record 1566*, TRB, National Research Council, Washington, D.C., 1996, pp. 49-53.

McCoy, P. T., E. A. Balderson, R. T. Hsueh, and A.K. Mohaddas. Calibration of TRANSYT Platoon Dispersion Model for Passenger Cars under Low-Friction Traffic Flow Conditions. In *Transportation Research Record 905*,TRB, National Research Council,Washington, D.C.,1983, pp. 48-52.

McShane, W. R. Access Management and the Relationship to Highway Capacity and Level of Service. *Technical Memorandum on Activity 4; final report, RS&H Project No. 992 1062 001*, Florida Intrastate Highway System, Florida, 1995.

Montgomery, D.C., and E.A. Peck. *Introduction to Linear Regression Analysis*. John Wiley and Sons, Inc., New York, New York, 1992.

Multimodal Level of Service Analysis for Urban Streets. *NCHRP* report 616.

Myers, R.H., D.C. Montgomery, and G.G. Vining. *Generalized Linear Models*. John Wiley and Sons, Inc., New York New York, 2002.

Pacey, G. M. The Progression of a Bunch of Vehicles Released From a Traffic Signal. Research Note Rn/2665/GMP. *Road Research Laboratory*, London, 1956.

Rakha, H., and M. Farzaneh. Calibration of TRANSYT-7F Traffic Dispersion Model: Issues and Proposed Solutions. *Virginia Tech Transportation Institute*, 2004

Rakha, H., and M. Farzaneh. Macroscopic Modeling of Traffic Dispersion: Issues and Proposed Solutions. 84th *Transportation Research Board* Annual Meeting, Washington, D.C., 2005.

Rakha, H., and M. Farzaneh. Procedure for Calibrating TRANSYST Platoon Dispersion Model. In *Journal of Transportation Engineering*, ASCE, Vol. 132, No. 7, 2006, pp. 548 - 554.

Robertson. I. TRANSYT: A Traffic Network Study Tool. RRL Report LR 253.*Road Research Laboratory*, Crowthorne, Berkshire, United Kingdom, 1969.

Roger, P.R., S.P. Elena, and M.R. Wlliam. *Traffic Engineering* , Fourth Edition.

Rouphail, N.M. Analysis of TRANSYT Platoon –Dispersion Algorithm. In *Transportation Research Record 905*, TRB, National Research Council, Washington, D.C.,1983 ,pp.72-80.

Seddon, P. A. A Program for Simulating the Dispersion of Platoon of Road Traffic Simulation. Vol. 18, No. 3, 1972, pp. 81-90.

Seddon, P. A. Another Look at Platoon Dispersion Program:1. The Kinematic Wave Theory . *Traffic Engineering and Control*, Vol. 13, No. 8, December 8, 1971, pp. 332-336.

Seddon, P. A. Another Look at Platoon Dispersion Program:2. The Diffusion Theory . *Traffic Engineering and Control*, Vol. 13, No. 9, January 1972, pp 388-390.

Seddon, P. A. Another Look at Platoon Dispersion Program:3. The Recurrence Relationship . *Traffic Engineering and Control*, Vol. 13, No. 10, February 1972, pp. 442-444.

Seddon, P.A. Prediction of Platoon Dispersion In Combination Methods of Linking Traffic Signals. *Transportation Research*, U.K. Vol. 6, No. 2, 1972, pp. 125-130.

Shin, M.S., B. Ran, R.R., He, and K. Choi. Introducing Platoon Dispersion into an Analytical Dynamic Assignment Process. In *Transportation Research Record 1733*, TRB, National Research Council, Washington, D.C., 2000, pp.96-104.

Smelt J. M. Platoon Dispersion Data Collection and Analysis. Proc., Annual Meeting of the *Australian Road Board*, Vol. 12, part 5, 1986, pp. 71-86.

Statistical Analysis System (SAS) User`s Guide 9.2.

Stover, V.G., Adkins, W.G., and Goodknight, J.C. NCHRP Report 93: Guidelines for Medial and Marginal Access Control on Major Roadways. *Highway Research Board*, National Research Council, Washington, DC, 1970.

Tarko, P. A., K. Choocharukul, A. Bhargava, and K. C. Sinha. Simple Method of Predicting Travel Speed on Urban Arterial Streets for Planning Applications. In *Transportation Research Record 1988*,TRB,National Research Council,Washington,D.C.,2006, pp.48-54.

Tarnoff, P.J., and P.S. Parsonson. NCHRP Report 233: Selecting Traffic Signal Control at Individual Intersections .*Transportation Research Board*, National Research Council, Washington, D.C., June, 1981.

Thamizh A and Shiraj H K. Modeling Platoon Dispersal Pattern of Heterogeneous Road Traffic. In *Transportation Research Record*, No. 1852, TRB, National Research Council, Washington, D.C., 2008, pp. 175 - 182.

Todd,K. Effect of Arterial Platoon Progression on Capacity. *Traffic Engineering and Control*, Vol. 29, No. 9, 1988.

Tracz, M. The Prediction of Platoon Dispersion Based on Rectangular Distribution of Journey Time. *Traffic Engineering and Control*, November 1975, pp. 490-492.

Vecellio, R. L. Platoon Dispersion Characteristics on One-Way Signalized Arterials. In *Transportation Research Record* 597, TRB, National Research Council, Washington, D.C.,1976,pp.42-43.

Walpole, R. E., M. H. Meyers. *Probability and Statistics for Engineers and Scientists*. Macmillan Publishing Co., Inc. New York, New York, 1978.

Walpole, R. E., M. H. Meyers. *Probability and Statistics for Engineers and Scientists.* Macmillan Publishing Co., Inc., New York, New York, 1989.

Washburn, S.S., K. G. Courage, T. Nguyen. Integrated Simulation-Based Method for Estimating Arrival Type for Signalized Arterial Planning Applications. In *Transportation Research Record*, No. 1852,TRB,National Research Council,Washington,D.C.,2003, pp. 69 - 76.

Wassan, J., M. Abass,D. Bullock, A. Rhodes, and C.K., Zhu. Reconciled Platoon Accommodations at Traffic Signals. Final Report, FHWA Project No. C-36-17VV. *National Technical Information Services*, 1999.

Wey., and R. Jayakrishnan. A Network Traffic Signal Optimization Formulation with Embedded Platoon Dispersion Simulation. Presented at the 76th Annual Meeting of the *Transportation Research Board*, Washington, D.C., 1997.

Yiming, B., W. Dianhai, M. Dongfang, and D. Yuzhou. Calibration of Platoon Dispersion Parameter Considering the Impact of Number of Lanes. *Transportation Research Board* 91st Annual Meeting, Washington, D.C., 2012.

Yu, L. Calibration of Platoon Dispersion Parameters on the Basis of Link Travel Time Statistics. In *Transportation Research Record* 1727, TRB, National Research Council, Washington, D.C., 2000, pp. 89-94.

Yu,L, and M. Van Aerde. Implementing TRANSYT`s Macroscopic Platoon Dispersion In Microscopic Traffic Simulation Models. Presented at the 74th Annual Meeting of the *Transportation Research Board*, Washington, D.C., 1995.